USGS
science for a changing world

Simulation of Water Levels and Salinity in the Rivers and Tidal Marshes in the Vicinity of the Savannah National Wildlife Refuge, Coastal South Carolina and Georgia

Prepared in cooperation with the Georgia Ports Authority

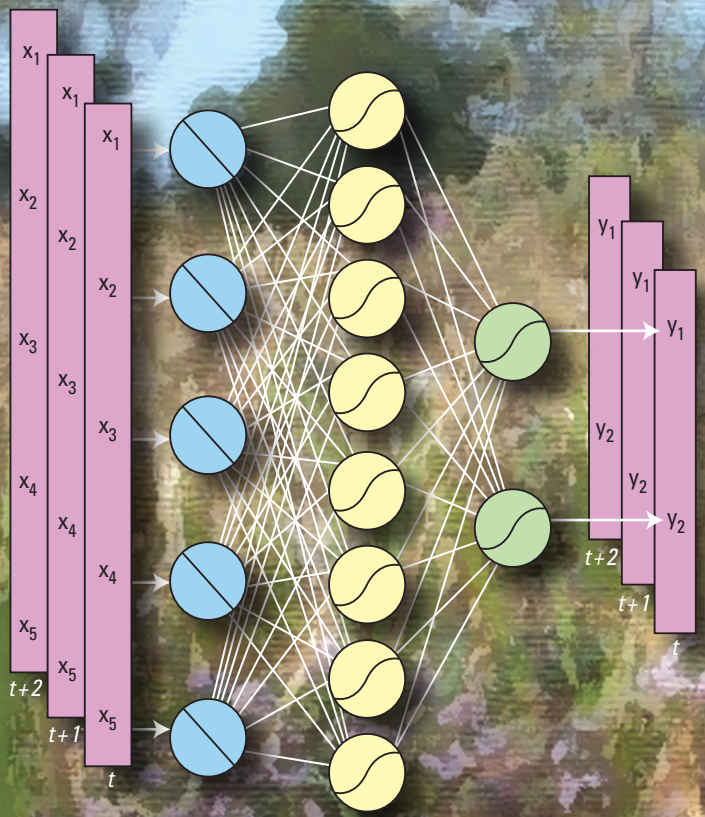

Scientific Investigations Report 2006–5187

U.S. Department of the Interior
U.S. Geological Survey

Simulation of Water Levels and Salinity in the Rivers and Tidal Marshes in the Vicinity of the Savannah National Wildlife Refuge, Coastal South Carolina and Georgia

By Paul A. Conrads, Edwin A. Roehl, Ruby C. Daamen, and Wiley M. Kitchens

Prepared in cooperation with the Georgia Ports Authority

Scientific Investigations Report 2006–5187

U.S. Department of the Interior
U.S. Geological Survey

U.S. Department of the Interior
DIRK A. KEMPTHORNE, Secretary

U.S. Geological Survey
Mark Myers, Director

U.S. Geological Survey, Reston, Virginia: 2006

For product and ordering information:
World Wide Web: *http://www.usgs.gov/pubprod*
Telephone: 1-888-ASK-USGS

For more information on the USGS—the Federal source for science about the Earth, its natural and living resources, natural hazards, and the environment:
World Wide Web: *http://www.usgs.gov*
Telephone: 1-888-ASK-USGS

Suggested citation:
Conrads, P.A., Roehl, E.A., Daamen, R.C., and Kitchens, W.M., 2006, Simulation of water levels and salinity in the rivers and tidal marshes in the vicinity of the Savannah National Wildlife Refuge, coastal South Carolina and Georgia: U.S. Geological Survey Scientific Investigations Report 2006–5187, 134 p.; available online at *http://pubs.usgs.gov/sir/2006/5187/*

Contents

Figures

Figures—continued

Figures—continued

Figures—continued

Tables

Conversion Factors

Inch/Pound to SI

Multiply	By	To obtain
	Length	
inch (in.)	2.54	centimeter (cm)
inch (in.)	25.4	millimeter (mm)
foot (ft)	0.3048	meter (m)
mile (mi)	1.609	kilometer (km)
	Area	
square foot (ft^2)	0.09290	square meter (m^2)
square mile (mi^2)	2.590	square kilometer (km^2)
	Volume	
cubic foot (ft^3)	0.02832	cubic meter (m^3)
	Flow rate	
cubic foot per second (ft^3/s)	0.02832	cubic meter per second (m^3/s)
picocurie per liter (pCi/L)	0.037	becquerel per liter (Bq/L)

SI to Inch/Pound

Multiply	By	To obtain
	Area	
square meter (m^2)	10.76	square foot (ft^2)

Horizontal coordinate information is referenced to the North American Datum of 1983 (NAD 83).

Acronyms and Abbreviations Used in the Report

AI	artificial intelligence
ANN	artificial neural network
ASA	Applied Science Associates
ATM	Applied Technology and Management
BEP	back error propagation
BFHYDRO	Boundary Fitted Hydrodynamic Model
CRADA	Cooperative Research and Development Agreement
DSS	decision support system
EFDC	Environmental Fluid Dynamics Code
EIS	Environmental Impact Statement
FCFWRU	Florida Cooperative Fish and Wildlife Unit
GaEPD	Georgia Environmental Protection Division
GPA	Georgia Ports Authority
GUI	Graphical User Interface
LMS	Lawler, Matusky, and Skelly
ME	mean error
MLP	multilayer perceptron
MSE	mean square error
M2M	Model-to-Marsh application
NWIS	National Water Information System
OLS	ordinary least squares
PME	percent model error
psu	practical salinity units
Q	streamflow
RMSE	root mean square error
R^2	coefficient of determination
SISO	single input single output
SNWR	Savannah National Wildlife Refuge
SSE	sum of square error
SSR	state space reconstruction
USACOE	U.S. Army Corps of Engineers
USFW	U.S. Fish and Wildlife Service
USGS	U.S. Geological Survey
WASP7	Water Assessment and Simulation Program–Version 7
WES	Waterways Experiment Station–U.S. Army Corps of Engineers
WL	water level
XWL	tidal range

Simulation of Water Levels and Salinity in the Rivers and Tidal Marshes in the Vicinity of the Savannah National Wildlife Refuge, Coastal South Carolina and Georgia

By Paul A. Conrads, Edwin A. Roehl, Ruby C. Daamen, and Wiley M. Kitchens

Abstract

The Savannah Harbor is one of the busiest ports on the East Coast of the United States and is located downstream from the Savannah National Wildlife Refuge, which is one of the Nation's largest freshwater tidal marshes. The Georgia Ports Authority and the U.S. Army Corps of Engineers funded hydrodynamic and ecological studies to evaluate the potential effects of a proposed deepening of Savannah Harbor as part of the Environmental Impact Statement. These studies included a three-dimensional (3D) model of the Savannah River estuary system, which was developed to simulate changes in water levels and salinity in the system in response to geometry changes as a result of the deepening of Savannah Harbor, and a marsh-succession model that predicts plant distribution in the tidal marshes in response to changes in the water-level and salinity conditions in the marsh. Beginning in May 2001, the U.S. Geological Survey entered into cooperative agreements with the Georgia Ports Authority to develop empirical models to simulate the water level and salinity of the rivers and tidal marshes in the vicinity of the Savannah National Wildlife Refuge and to link the 3D hydrodynamic river-estuary model and the marsh-succession model.

For the development of these models, many different databases were created that describe the complexity and behaviors of the estuary. The U.S. Geological Survey has maintained a network of continuous streamflow, water-level, and specific-conductance (field measurement to compute salinity) river gages in the study area since the 1980s and a network of water-level and salinity marsh gages in the study area since 1999. The Georgia Ports Authority collected water-level and salinity data during summer 1997 and 1999 and collected continuous water-level and salinity data in the marsh and connecting tidal creeks from 1999 to 2002. Most of the databases comprise time series that differ by variable type, periods of record, measurement frequency, location, and reliability.

Understanding freshwater inflows, tidal water levels, and specific conductance in the rivers and marshes is critical to enhancing the predictive capabilities of a successful marsh succession model. Data-mining techniques, including artificial neural network (ANN) models, were applied to address various needs of the ecology study and to integrate the riverine predictions from the 3D model to the marsh-succession model. ANN models were developed to simulate riverine water levels and specific conductance in the vicinity of the tidal marshes for the full range of historical conditions using data from the river gaging networks. ANN models were also developed to simulate the marsh water levels and pore-water salinities using data from the marsh gaging networks. Using the marsh ANN models, the continuous marsh network was hindcasted to be concurrent with the long-term riverine network. The hindcasted data allow ecologists to compute hydrologic parameters—such as hydroperiods and exposure frequency—to help analyze historical vegetation data.

To integrate the 3D hydrodynamic model, the marsh-succession model, and various time-series databases, a decision support system (DSS) was developed to support the various needs of regulatory and scientific stakeholders. The DSS required the development of a spreadsheet application that integrates the database, 3D hydrodynamic model output, and ANN riverine and marsh models into a single package that is easy to use and can be readily disseminated. The DSS allows users to evaluate water-level and salinity response for different hydrologic conditions. Savannah River streamflows can be controlled by the user as constant flow, a percentage of historical flows, a percentile daily flow hydrograph, or as a user-specified hydrograph. The DSS can also use output from the 3D model at stream gages near the Savannah National Wildlife Refuge to simulate the effects in the tidal marshes. The DSS is distributed with a two-dimensional (plan view), color-gradient visualization routine that interpolates and extrapolates model output to fill and color a grid of the study area. Grid cell size is either 10 or 100 meters (100.76 or 1,076 square feet). Interpolation is performed using a simple ratio of linear distance between nearest marsh gages and actual distance from each cell between nearest marsh gages. The salinity values and grid parameter, and corner coordinates, can be exported as an ASCII file for input into a mapping package such as ArcView™.

Introduction

The Savannah Harbor, as with many major estuarine systems, meets many local and regional water-resource needs. The tidal parts of the Savannah River provide water supply for coastal South Carolina and Georgia, provide habitat for the extensive freshwater marsh, provide assimilative capacity for municipal and industrial dischargers, and provide navigation for a major shipping terminal on the East Coast (fig. 1). With increases in industrial and residential development in Georgia and South Carolina, there are competing, and often conflicting, interests in the water resources of the Savannah River. As part of a proposed deepening of Savannah Harbor and modification of the navigation channel geometry, the environmental effect on many of the ecological and economic resources in Savannah, including the freshwater tidal marshes, are being evaluated.

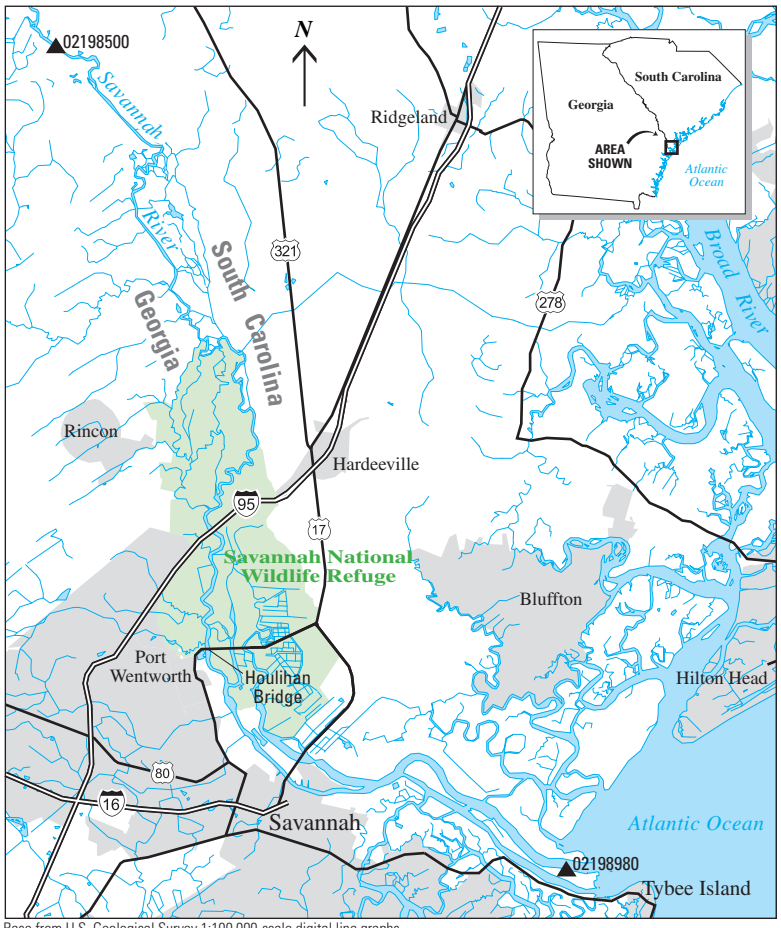

Figure 1. Study area in the vicinity of the Savannah National Wildlife Refuge, coastal South Carolina and Georgia. Savannah Harbor is located in the lower 21 miles of the Savannah River. The U.S. Geological Survey gaging stations at Savannah River near Clyo, Ga. (02198500) and Savannah River at Fort Pulaski (02198980) also are shown.

The freshwater-dominated parts of the tidal marsh may be the most sensitive of the tidal marshes to alterations of environmental gradients. Freshwater tidal marshes generally have a greater diversity of plant communities compared to saltwater tidal marshes. As numerous studies have shown (Odum and others, 1984; Latham, 1990; Gough and Grace, 1998; Howard and Mendelsson, 1999), the salinity gradient is a driving force in shaping the vegetative communities of a tidal marsh. A study by Odum and others (1984) estimated that there were 405,000 acres of tidal freshwater marshes along the Atlantic Coast, of which 28 percent were in coastal South Carolina and Georgia. In the late 1960s, the tidal freshwater wetlands of the lower Savannah River were estimated at 24,000 acres (Tiner, 1977), with approximately one-fifth of the tidal freshwater marsh in South Carolina and Georgia. Since that time, the amount of tidal freshwater marsh in the Savannah Estuary has been greatly reduced due to salinity intrusion. The remaining tidal freshwater marsh is an essential part of the 28,000-acre Savannah National Wildlife Refuge (SNWR), which was established in 1927 (*http://www.fws.gov/savannah/*).

As part of the Environmental Impact Statement (EIS) for a potential deepening of the harbor, two studies were undertaken (independent from the study described in this report) by plant ecologists from the U.S. Geological Survey (USGS) and Applied Technology and Management (ATM) to study the tidal marshes of the SNWR to understand how the plant communities respond to changing hydrologic and pore-water salinity conditions in the marsh. Using data and analysis from the marsh studies, plant succession models were developed that predict plant communities based on water-level and pore-water salinity conditions. Concurrently with the marsh studies, a three-dimensional (3D) hydrodynamic and water-quality model (also independent of the study described in this report) was applied to the Savannah Harbor to simulate changing flow and water-quality conditions in the rivers surrounding the tidal marshes. The plant succession models and the 3D hydrodynamic model will be used in conjunction to evaluate the effect of the harbor deepening on the tidal marshes. The 3D model simulates only changing flow and salinity in the rivers and not in the marshes. Defining the linkage between the water level and salinity of the Savannah River and tidal marshes and simulating marsh water-level and salinity conditions was critical to developing a successful plant succession model.

The U.S. Geological Survey (USGS), in cooperation with the Georgia Ports Authority (GPA), initiated a study to (1) develop empirical models to simulate water level and pore-water salinity at river gaging stations; (2) develop empirical models to simulate water level and salinity at marsh gaging

stations; (3) develop a spreadsheet application that integrates historical databases, empirical river and marsh models, output from the 3D model of Savannah Harbor, and marsh predictions that is easy to use and can be readily disseminated; and (4) develop a visualization routine that will spatially extrapolate the model results across the marsh. The USGS collaborated with Advanced Data Mining on the study.

The USGS entered into a Cooperative Research and Development Agreement with Advanced Data Mining in 2002 to collaborate on applying data-mining techniques and artificial neural network (ANN) models to water-resources investigations. The emerging field of data mining addresses the issue of extracting information from large databases (Weiss and Indurkhya, 1998). Data mining is a powerful tool for converting large databases into knowledge to solve problems that are otherwise imponderable because of the large numbers of explanatory variables or poorly understood process physics. Data-mining methods come from different technical fields such as signal processing, statistics, artificial intelligence, and advanced visualization. Data mining uses methods for maximizing the information content of data, determining which variables have the strongest correlations to the problems of interest, and developing models that predict future outcomes. This knowledge encompasses both understanding of cause-effect relations and predicting the consequences of alternative actions. Data mining is used extensively in financial services, banking, advertising, manufacturing, and e-commerce to classify the behaviors of organizations and individuals, and to predict future outcomes.

Purpose and Scope

This report presents the results of a study that links water-level and salinity conditions of the Back River, Little Back River, Middle River, and Front River to tidal marshes in the vicinity of the SNWR (fig. 2). This report documents the development of the Model-to-Marsh application (also referred to as the M2M application) including the results of applying data mining and ANN models to the Savannah, Back, Little Back, Middle, and Front Rivers. The modeling scope of effort consisted of four phases: (1) simulating the long-term USGS water-level and salinity river data from the period 1994–2005; (2) simulating the short-term water-level and salinity river data collected by the GPA during summer 1997 and 1999 and the marsh water-level and pore-water salinity data collected by the USGS and the GPA during 1999 to 2005; (3) integrating the 3D model input into the application and spatially extrapolating the simulated salinity response across the marsh; and (4) integrating the developed models of the riverine and marsh gaging sites and historical databases into a spreadsheet application.

An important part of the USGS mission is to provide scientific information for the effective water-resources management of the Nation. To assess the quantity and quality of the Nation's surface-water, the USGS collects hydrologic and water-quality data from rivers, lakes, and estuaries using standardized methods, and maintains the data from these stations in a national database. Often these databases are under utilized and under interpreted for addressing contemporary hydrologic issues. The techniques presented in this report demonstrate how valuable information can be extracted from existing databases to assist local, State, and Federal agencies. The application of data-mining techniques, including ANN models, to the Savannah River Estuary demonstrates how empirical models of complex hydrologic systems can be developed, disparate databases and models can be integrated to support multidisciplinary research, and study results can be easily disseminated to meet the needs of a broad range of end users.

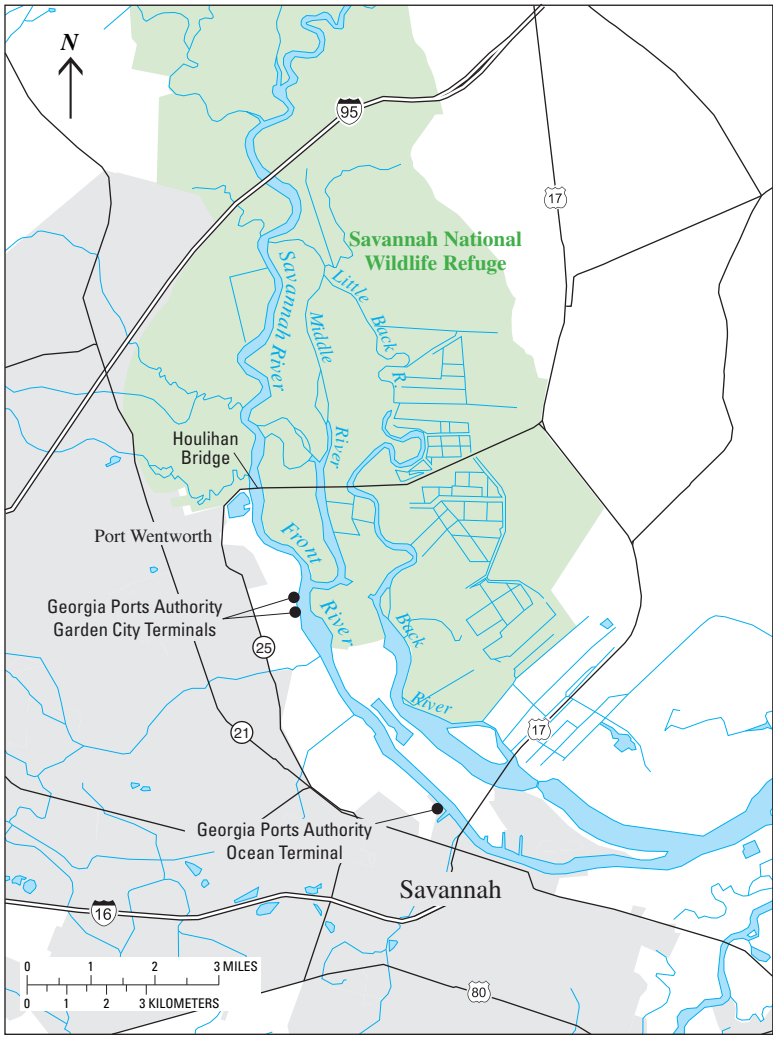

Figure 2. The Savannah, Front, Middle, Back, and Little Back Rivers in the vicinity of the Savannah National Wildlife Refuge.

Description of Study Area

The Savannah River originates at the confluence of the Seneca and Tugaloo Rivers, near Hartwell, Ga., and forms the State boundary between South Carolina and Georgia to the divergence of the Little Back River near the coast (figs. 2, 3). From Lake Hartwell, the Savannah River flows through two physiographic provinces, the Piedmont and the Coastal Plain (fig. 3). The city of Augusta, Ga., is on the Fall Line, which separates these two provinces. The slope of the river ranges from an average of about 3 feet per mile in the Piedmont to less that 1 foot per mile in the Coastal Plain. Upstream from the Fall Line, three large Federal multipurpose dams (Lake Hartwell, Richard B. Russell Lake, and J. Strom Thurmond Lake) provide hydropower, water supply, recreational facilities and a limited degree of flood control. Thurmond Dam is responsible for most of the flow regulation that affects the Savannah River at Augusta (Sanders and others, 1990).

From Augusta, Ga., the Savannah River flows 187 miles to the coast (fig. 3). The lower Savannah River is a deltaic system that branches into a series of interconnected distributary channels including the Little Back, Middle, Back, and Front Rivers (fig. 2). The hydrology of the system is dependent upon precipitation, runoff, channel configuration, streamflow, and seasonal and daily tidal fluctuations (Latham, 1990; Pearlstine and others, 1990). Savannah Harbor experiences semidiurnal tides of two high and two low tides in a 24.8-hour period with pronounced differences in tidal range between neap and spring tides occurring on a 14-day and 28-day lunar cycle. Periods of greatest tidal ranges are known as “spring” tides and the period of lowest tidal amplitude are known as “neap” tides. The tidal amplitude in the lower parts of the estuary is approximately 5 to 6 feet (ft) during neap tides and greater than 8 ft during spring tides. The resultant interaction of stream flow and tidal range allows the salinity intrusion to be detected more than 25 miles upstream and the tidal water-level signal to reach approximately 40 miles upstream, near Hardeeville (fig. 1, Bossart and others, 2001).

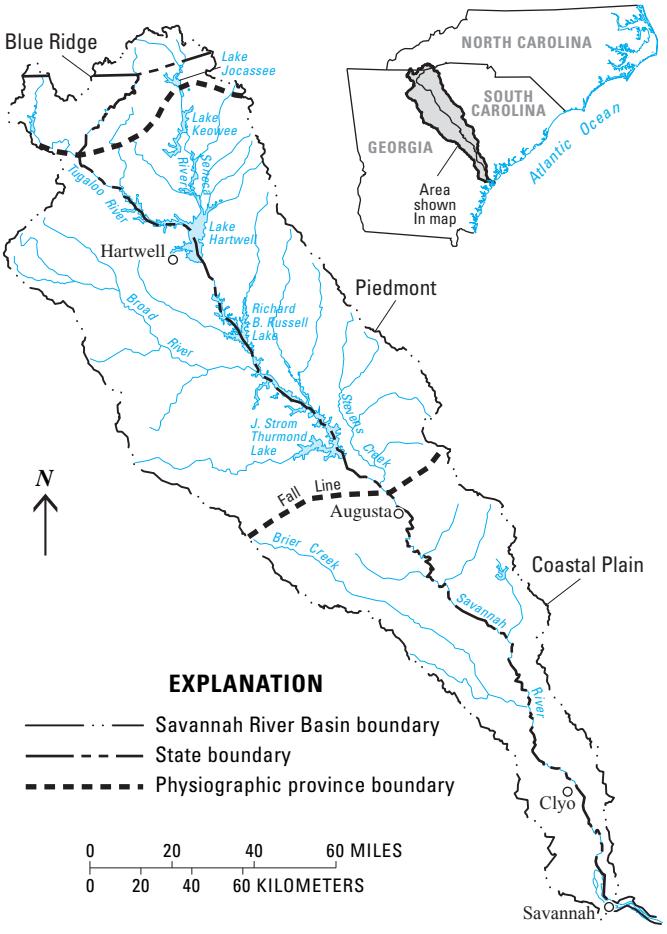

Figure 3. The physiographic provinces of the Savannah River Basin in South Carolina, Georgia, and North Carolina.

Rice plantations, with large diked fields along the banks of the Little Back, Back, Middle, and Savannah Rivers flourished in the 18th and 19th centuries. Many of the marshes and swamps were cleared, diked, impounded, and converted to rice fields during this period. With the advent of mechanized rice harvesting, rice production diminished because the heavy machinery was unsuitable for the clayey soil of the area. The rice fields were abandoned, and subsequently, many of the dikes were broken and the impoundments have reverted to tidal marshes.

Typical of coastal rivers in Georgia and South Carolina, the shallow, deltaic branches of the Savannah River did not provide natural features for a harbor, such as deep embayments or natural scouring of deep channels. Historically, the Back River had the largest channel geometry and the largest proportion of streamflow compared with the Front River (Barber and Gann, 1989). The Savannah Harbor was developed along the lower 21 miles of the Savannah River from the mid-1800s to the present (2006). The Savannah Harbor has a history of channel deepening, widening, creation of turning and sedimentation basins, and maintenance dredging and disposal as the harbor changed from a natural river system with a controlling depth of 10 ft at low tide to its currently maintained depth of 42 ft at low tide (Barber and Gann, 1989).

Two important resources are located in the Savannah River Estuary—the SNWR and the GPA (fig. 2). The tidal freshwater marsh is an essential part of the 28,000-acre SNWR. Located between river mile 18 and river mile 40, the SNWR is home to a diverse variety of wildlife and plant communities. Neighboring the SNWR, the GPA maintains two deepwater terminal facilities—Garden City Terminal and Ocean Terminal (fig. 2). To support navigation and the terminal activities of the GPA, the river channel and turning basins are maintained by dredging below U.S. Highway 17 Bridge (Houlihan Bridge) to approximately 20 miles offshore from the harbor entrance.

Substantial modifications made to the system during the past 30 years include the installation and operation of a tide gate on the Back River in 1977, deepening of the shipping channel to 38 ft (from 34 ft) in 1978, decommissioning of the tide gate in 1991, and deepening the shipping channel

to 42 ft (from 38 ft) in 1994. The tide gate was operated to facilitate the maintenance dredging of the harbor by increasing scour in the Front River and creating a sedimentation basin in the Back River that was near the dredge disposal area. The tide gate opened on flood tides (incoming) and closed on ebb tides (outgoing). The increased flows on the Front River increased scouring of the channel and minimized maintenance dredging (Latham, 1990). The operation of the tide gate had the unintended consequence of moving the saltwater wedge (salinity value of 0.5 practical salinity units, [psu]) 2 to 6 miles upstream in the Back, Little Back, and Middle Rivers (Pearlstine and others, 1990, 1993). The approximate location of the freshwater-saltwater interface for four historical periods (1875, 1940, 1965, and 1997) and their associated channel depths are shown in figure 4 (E. EuDaly, U.S. Fish and Wildlife Service, written commun., 2005). Data used in figure 4 were obtained from available historical sources, and provide a qualitative comparison of the position of the freshwater/saltwater interface and the spatial extent of the freshwater marsh.

Previous Studies

Numerous ecological and hydrodynamic studies have been conducted to support the modification and management of the harbor and the resulting changes of the flow and salinity dynamics of the Savannah River Estuary. Many of the plant ecology studies have focused on the characterization of the plant communities in freshwater tidal marshes of the SNWR and how these communities respond to changing pore-water salinity conditions. Many of the hydrodynamic and water-quality studies have focused on how modifications to the harbor (deepening, connecting rivers, creating sedimentation basin) affect flow, sedimentation, salinity, and water quality. The following sections highlight some of these studies.

Plant Ecology Studies

The operation of the tide gate had substantial effect on the saltwater intrusion into the Little Back River and ultimately on the interstitial salinity concentration in the soils of the freshwater tidal marsh of the SNWR. In 1985, a study was initiated to characterize the plant communities and environmental conditions of the tidal marsh of the lower Savannah River (Latham, 1990). That study reported that plant species are closely linked to interstitial and riverine salinity levels. The changing salinity conditions also affect the ability of freshwater species to compete with brackish species. The increased salinity corresponded to changes in the plant communities from fresh-marsh to brackish-marsh conditions.

Pearlstine and others (1990, 1993) studied vegetation responses to salinity changes in the marshes and developed a plant succession model to predict plant communities for selected environmental conditions. The study reported that if the elevated salinity levels caused by the tide gate were maintained, salt marsh cordgrass (*Spartina alterniflora*) and salt marsh bulrush (*Scirpus robustus*) would become established in the freshwater tidal marshes in the SNWR. After the removal of the tide gate and the 4-ft deepening of the harbor, Latham and Kitchens (1995) revisited transects used by Latham (1990) and Pearlstine and others (1990, 1993), and concluded that the interstitial salinities had been reduced, especially in the areas with salinities ranging between 0.5 and 3.0 psu. Loftin and others (2003) reported that although the marsh was more characteristic of a freshwater marsh than prior to removal of the tide gate, the extent of recovery was not as great as predicted by Pearlstine and others (1993). The benefits of removing the tide gate and lowering the interstitial salinity may have been limited by salinity changes caused by the 4-ft deepening of the harbor. As part of the EIS concerning the proposed deepening of the harbor to 48 ft, two studies were initiated to evaluate changes in the tidal marsh plant community in response to changing salinity conditions (Bossart and others, 2001; Dusek, 2003; Applied Technology and Management, 2003).

Hydrodynamic and Water-Quality Studies

There is a long history of scientific and engineering studies of the tides and currents of Savannah Harbor and their effects on navigation and channel maintenance (Barber and Gann, 1989). In 1940, a physical model was built at the U.S. Army Corps of Engineers, Waterway Experiment Station (WES) in Vicksburg, Miss., to analyze shoaling dynamics. This early model had a horizontal scale of 1:1,000 and a vertical scale of 1:150 and could simulate a complete tidal cycle every 18 minutes (Rhodes, 1949). In 1956, an improved physical model was built at the WES to study reducing shoaling or to control shoaling in areas where it was easy to remove the dredged material. The new model reduced the horizontal and vertical scales to 1:800 and 1:80, respectively, and covered an area of 25,000 square feet (ft^2) (U.S. Army Corps of Engineers, 1961a, 1961b, 1963). One of the solutions presented in the study was to construct a tide gate and sedimentation basin on the Back River to allow for the maximum possible rate of shoaling near the dredge disposal areas. The tide gate and sedimentation basin construction was authorized in 1965, and the project was completed in 1977 (Barber and Gann, 1989).

The application of digital computer models to the Savannah River and Savannah Harbor replaced the use of physical models in the 1970s. Huvel and others (1979) at WES developed a one-dimensional model to re-evaluate the results of the freshwater control plan, including the tide gate and increased salinities in Little Back River; the plan was based on results from physical models of the 1950s and 60s. The model was based on the long-wave equations and the convective-dispersion equation, and was calibrated to field data collected in July 1950 and September 1972 (Huvel and others, 1979).

To evaluate proposals to deepen the harbor from 38 to 42 ft, the WES initiated a study to apply a two-dimensional, laterally averaged model called LAEMSED to the estuary. The objectives of the study were to simulate how channel deepening and widening would effect salinity intrusion and shoaling

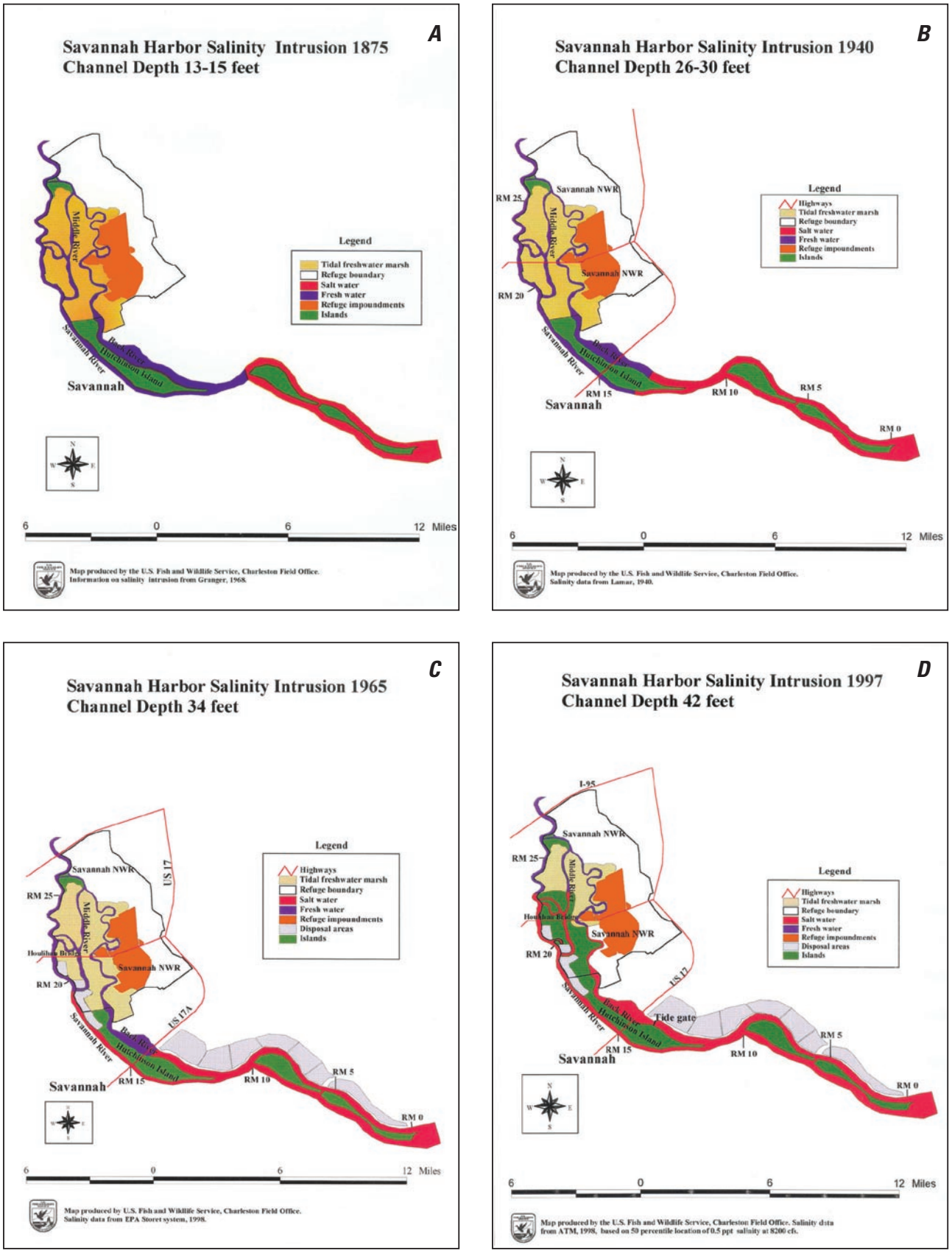

Figure 4. Location of the saltwater and freshwater interface for four channel depths: (*A*) 13–15 feet in 1875; (*B*) 26–30 feet in 1940; (*C*) 34 feet in 1965; and (*D*) 42 feet in 1997. Maps produced by the U.S. Fish and Wildlife Service, Charleston Field Office. Data references include: (*A*) Granger (1968); (*B*) Lamar (1942); (*C*) U.S. Environmental Protection Agency, STORET Database, 1998 (*http://www.epa.gov/STORET/*); and (*D*) Applied Technology and Management, 1998.

(U.S. Army Corps of Engineers, 1991). The model was verified using field data collected in 1986, 1988, and 1990. River flows ranged from 5,000 to 43,000 cubic feet per second (ft^3/s) over the sampling periods.

To evaluate a potential deepening of the harbor from 42 to 48 ft, the 3D model, Boundary Fitted Hydrodynamics (BFHYDRO) (Spaulding, 1984; Swanson, 1986; and Muin and Spaulding, 1997), was used by Applied Science Associates (ASA) and Applied Technology and Management (ATM) (Applied Science Associates and Applied Technology and Management, 1998). In addition to simulating tides, currents, and salinity, the model simulated dissolved oxygen using the Streeter-Phelps equation (Streeter and Phelps, 1925). The model was calibrated to field data collected in summer 1997 (Applied Technology and Management, 1998).

Results from the model were incorporated in the EIS regarding the potential deepening of the harbor from 42 to 48 ft (Georgia Ports Authority, 1998). After review of the EIS by State and Federal agencies, it was agreed that additional data collection was necessary to improve the water-quality model and to further refine the hydrodynamic model. To meet these goals, the 3D model, Environmental Fluid Dynamics Code (EFDC) (Hamrick, 1992) and U.S. Environmental Protection Agency (USEPA) Water Quality Assessment and Simulation Program version 7 (WASP7) (Ambrose and others, 1993; Wool and others, 2001) was applied to Savannah Harbor (Tetra Tech, 2005).

A number of mechanistic water-quality models of the river and estuary have been developed to investigate various regulatory issues of water-quality classification and assimilative capacity. A good summary of the technical history of mathematical water-quality models applied to the system from 1970 to 1988 can be found in the Georgia Environmental Protection Division (GaEPD) report, "Savannah River Classification Study" (Georgia Environmental Protection Division, 1988). Early models were either simplified steady-state calculations to estimate the assimilative capacity of the Savannah River (Olinger, 1970) or steady-state, one- and two-dimensional models to evaluate the effects of major discharges on the Savannah River (Hydroscience, Inc., 1970). The first dynamic water-quality model applied to the system was the Massachusetts Institute of Technology Transient Water Quality Network Model (Harleman, 1977). Additional field data for the model were collected in 1979 and 1980 (Pennington and Bond, 1981; Shingler, 1981). Lawler, Matusky, and Skelly Engineers (LMS) made modifications to the code and recalibrated the model in 1982 (Lawler, Matusky, and Skelly Engineers, 1983). The model was further refined by GaEPD and LMS to include more complex nutrient and algal dynamics and to validate the model with new data collected in October 1985 (Lawler, Mutusky, and Skelly Engineers, 1986; Georgia Environmental Protection Division, 1988). The USEPA has used the application of the EFDC and WASP7 codes for evaluating water-quality standards classification and Total Maximum Daily Loads for the harbor (U.S. Environmental Protection Agency, 2004).

Approach

The variability of salinity in the Savannah River is a result of many factors, including streamflow in the Savannah River and tidal conditions in the Savannah Harbor. The variability of pore-water salinity in the tidal marshes is a result of the adjacent river salinity concentration, the tidal creek connections to the river, elevation of the marsh and surrounding berms, soil type and the conditions of old abandoned rice fields and berms, and volume of water within the marsh. Although many of the plant succession models use hydrology and salinity inputs, these inputs have been derived from either field measurements or assumptions that long-term averaging from riverine-estuarine model simulations are adequate estimates of pore-water salinity in the marshes.

In order to simulate the dynamic response of the water level and salinity in the tidal marshes, empirical models were developed to simulate water levels and salinities in the river and marshes for changing hydrologic conditions (streamflow) and changing channel geometries simulated by a 3D mechanistic model (Tetra Tech, 2005). The empirical models were developed using data-mining techniques and ANN models. This is the first study in the Savannah River Estuary to integrate the dynamic water-level and salinity response of the estuary with the dynamic water-level and salinity response of the tidal marshes.

For the Savannah River and the tidal marsh, there are extensive continuous data sets of streamflow, tidal water level, and salinity in the river, harbor, and tidal marshes. Time-series data of the streamflow, salinity, and water levels in the rivers and marshes near the SNWR have been collected by various agencies during the past 20 years. The USGS has collected streamflow, water-level, and salinity data in the rivers near SNWR, and tidal conditions of the Savannah Harbor since the 1980s. The USGS Florida Cooperative Fish and Wildlife Research Unit (FCFWRU) has collected continuous water-level and pore-water salinity data in the tidal marshes since 2000. The GPA collected riverine data at more than 20 sites during summer 1997 and 1999 and marsh data for a 2-year period beginning in June 1999.

The application of data-mining techniques to simulate the water-level and pore-water response in the tidal marshes was undertaken in four phases. The first phase was to develop ANN models to simulate the riverine water-level and salinity response caused by changing streamflow condition. The second phase was to develop ANN models to simulate the marsh water-level and pore-water salinity response attributed to changing river conditions. The third phase was to incorporate the results from a 3D model of changing river conditions and a visualization module that spatially extrapolates the marsh response at selected marsh gages to the entire marsh. The final phase was the development of a Decision Support System (DSS) that integrates historical databases, model simulations, and streaming graphics with a graphical user interface (GUI) that allows a user to simulate scenarios of interest.

Acknowledgments

The complexity of this study required interagency cooperation, in addition to individual contributions. The authors thank David Schaller and Hope Moorer of the Georgia Ports Authority for their support and patience throughout the project; Larry Keegan of Lockwood Greene for his coordination of project activities with the Georgia Ports Authority; Bill Bailey, Alan Garrett, Joe Hoke, and Doug Plachy of the U.S. Army Corp of Engineers, Savannah District, for their project inputs; Ed EuDaly and John Robinette of the U.S. Fish and Wildlife Service for their support; and Steven Davie and Yuri Plis of Tetra Tech for their cooperation in integrating the 3D model output into the DSS.

Data Collection Networks

Many resource entities have been collecting data in the Savannah River Estuary, including the USGS, National Oceanic Atmospheric Administration, USEPA, GaEPD, South Carolina Department of Health and Environmental Control, the City of Savannah, the GPA, and local colleges and universities. Four existing continuous water-level and specific-conductance data sets for the harbor, river, and tidal marshes were used to build, train, and test the ANN water-level and salinity models. A description of each data set follows.

River Networks

The USGS streamflow gage near Clyo, Ga. (station 02198500; fig. 1) was established in 1929 and records streamflow on an hourly interval. The USGS has maintained a data-collection network in the Little Back River near the SNWR and in the lower Savannah River since the late 1980s. These stations collect water level and(or) specific-conductance data on a 15-minute interval (fig. 5*A*). Specific conductance is a measure of the ability of water to conduct an electrical current and is expressed in microsiemens per centimeter at 25° C. Specific conductance is related to the type and concentration of ions in solution and is a field measurement often used to compute salinity. The USGS stations are part of the USGS National Water Information System (NWIS) and are available in near real-time on the Web (*http://waterdata.usgs.gov/sc/nwis*). The USGS maintains NWIS, a distributed network of computers and fileservers for the storage and retrieval of water data collected through its activities at approximately 1.5 million sites around the country, as part of the USGS program of disseminating water data to the public. Locations of specific-conductance, water-level, and streamflow gages used in the study are listed in table 1 and shown in figures 1 and 5.

The GPA established a network of stations to support the application of the 3D hydrodynamic and water-quality model of the system (fig. 5*B*; table 1). The GPA network was maintained for the summer and fall of 1997 and 1999 by Applied Technology and Management (Applied Technology and Management, 2000). Fourteen stations were located in the vicinity of the SNWR during the two deployments. Six of the stations recorded specific-conductance values for the top and bottom of the water column.

Tidal Marsh Networks

Two continuous gaging networks were established in the tidal marshes as part of the ecological studies to evaluate potential effects to the plant communities as a result of harbor deepening (Bossart and others, 2001). The FCFWRU of the USGS has been collecting water-level and pore-water specific-conductance time-series data from a tidal-marsh gaging network since June 1999 (fig. 5*C*). The USGS network comprises four sites on the Little Back and Back Rivers, two on the Middle River, and one on the Front River. The monitoring sites consist of a pressure transducer and a specific-conductance probe just below the surface of the marsh. The locations of the USGS continuous monitors correspond to locations where the FCFWRU has been conducting plant studies since the 1980s. The GPA collected water-level and specific-conductance time-series data from June 1999 to October 2002 in tidal feeder creeks and marsh surface water, and marsh pore-water salinity at 10 locations (fig. 5*D*; table 1).

Characterization of Streamflow, Water Level, and Specific Conductance

> "The main drawback in studying estuaries is that river flow, tidal range, and sediment distribution are continually changing and this is exacerbated by the continually changing weather influences. Consequently, some estuaries may never really be steady-state systems; they may be trying to reach a balance they never achieve."
>
> *Keith Dyer*, from "Estuaries—A Physical Introduction" (1997)

Estuarine systems are complex systems that are constantly responding to changing hydrologic, tidal, and meteorological conditions. The Savannah River Estuary is constantly integrating the changing streamflow of the Savannah River, changing tidal condition of the Atlantic Ocean, and changing meteorological conditions including wind direction and speed, rainfall, low and high pressure systems, and hurricanes. The following sections characterize the streamflow and tidal water levels and how these affect the salinity intrusion in the rivers and the interstitial salinity concentrations in the marshes.

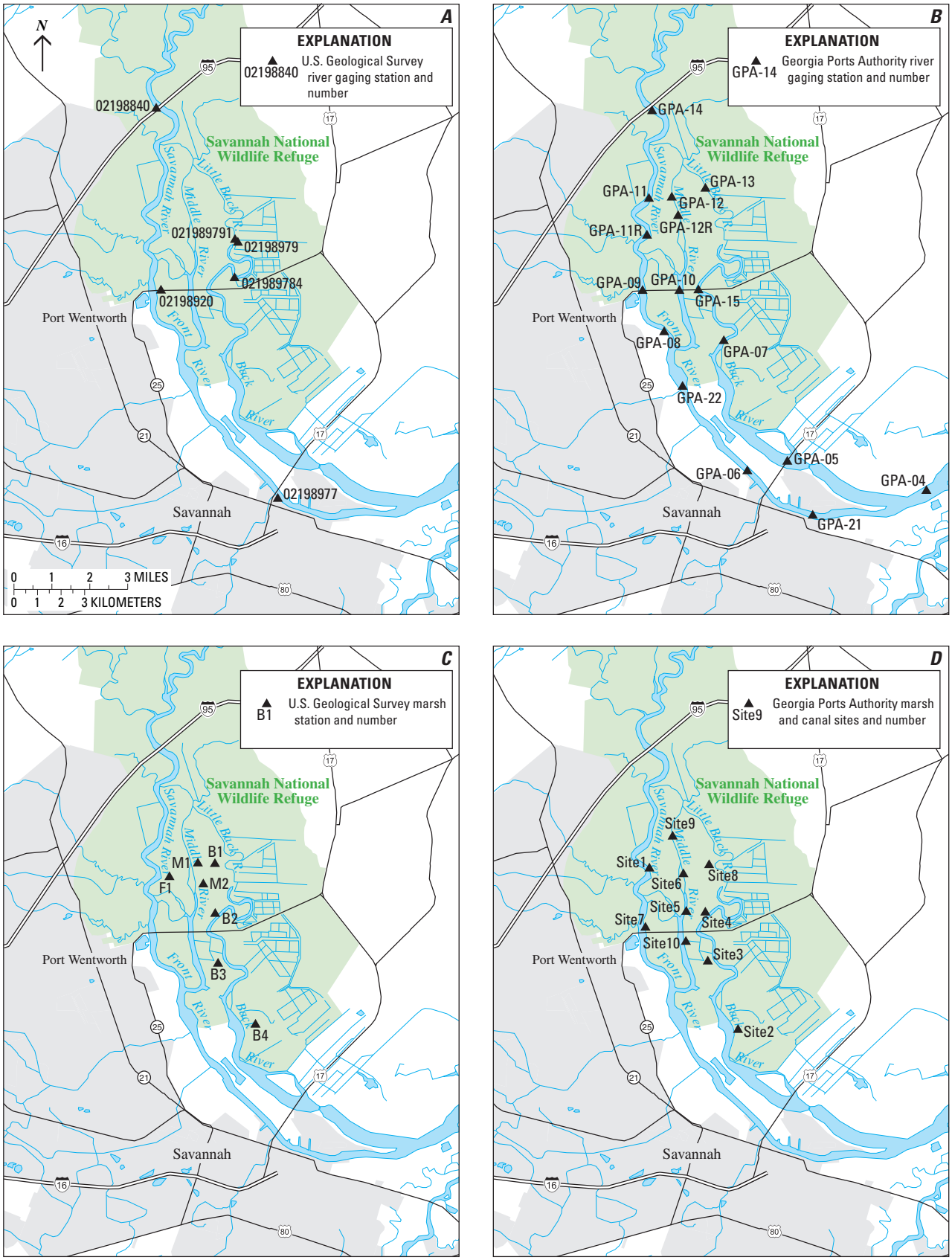

Figure 5. River and marsh continuous monitoring stations in the vicinity of the Savannah National Wildlife Refuge: (*A*) U.S. Geological Survey river stations; (*B*) Georgia Ports Authority river stations; (*C*) U.S. Geological Survey marsh stations; and (*D*) Georgia Ports Authority marsh and canal sites.

Table 1. U.S. Geological Survey and Georgia Ports Authority continuous river and marsh gaging network data used in the study.

[NAD 83, North American Datum of 1983; Q, flow; wl, water level; sc, specific conductance; scb, specific conductance-bottom probe; sbt, specific conductance-top probe]

Site identification	Station location and name used in this report	Parameters	Period of record	Longitude (decimal degrees, NAD 83)	Latitude (decimal degrees, NAD 83)
U.S. Geological Survey River Gaging Network					
02198500	Savannah River near Clyo	Q	October 1929–May 2005	81.26871649	32.52823709
02198840	Savannah River at I-95 Bridge	wl, sc	June 1987–May 2005	81.15122387	32.23575482
02198920	Front River at Houlihan Bridge	wl, sc	October 1987–May 2005	81.15122363	32.16603583
02198977	Front River at Broad Street	wl	October 1987–May 2005	81.09566748	32.18409111
021989784	Little Back River at Lucknow Canal	sc	May 1990–May 2005	81.11816773	32.17075822
02198979	Little Back River near Limehouse	wl	June 1987–May 2005	81.11705662	32.18492418
021989791	Little Back River at USFW Dock	sc	October 1989–May 2005	81.11788997	32.18575747
02198980	Savannah River at Fort Pulaski	wl	October 1987–May 2005	80.90316645	32.0341019
Georgia Ports Authority River Gaging Network					
GPA04	Savannah River near Fort Jackson	wl, scb, sct	July–September 1997 July–October 1999	81.026817	32.089001
GPA05	Back River upstream of Tide Gate	wl, scb	July–September 1997 July–October 1999	81.089816	32.100018
GPA06	Front River upstream of Broad Street	wl, scb, sct	July–September 1997 July–October 1999	81.107403	32.096371
GPA07	Back River downstream of Houlihan Bridge	wl, scb, sct	July–September 1997 July–October 1999	81.118187	32.146400
GPA08	Front River downstream of Houlihan Bridge	wl, scb, sct	July–September 1997 July–October 1999	81.144326	32.149994
GPA09	Front River at Houlihan Bridge	wl, scb, sct	July–September 1997 July–October 1999	81.155296	32.165272
GPA10	Middle River at Houlihan Bridge	wl, scb, sct	July–September 1997 July–October 1999	81.138367	32.165272
GPA11	Front River upstream of Houlihan Bridge	wl, scb	July–September 1997 July–October 1999	81.152778	32.201389
GPA11R	Front River upstream of Houlihan Bridge	wl, scb	July–September 1997 July–October 1999	81.152505	32.186568
GPA12	Middle River upstream of Houlihan Bridge	wl, sct	July–September 1997	81.141167	32.201229
GPA12R	Middle River upstream of Houlihan Bridge		July–October 1999	81.138367	32.194567
GPA13	Little Back River downstream of Union Creek	wl, scb	July–September 1997 July–October 1999	81.126183	32.204788
GPA14	Savannah River at I-95 Bridge	wl, scb	July–September 1997 July–October 1999	81.150048	32.234661
GPA15	Little Back River at Houlihan Bridge	sct	July–September 1997 July–October 1999	81.129593	32.165379
GPA21	Front River downstream of U.S. Highway 17 Bridge	wl, scb, sct	July–September 1997 July–October 1999	81.078194	32.079369
GPA22	Front River downstream of confluence with Middle River	wl, scb, sct	July–September 1997 July–October 1999	81.136643	32.128628

Table 1. U.S. Geological Survey and Georgia Ports Authority continuous river and marsh gaging network data used in the study. —Continued

[NAD 83, North American Datum of 1983; Q, flow; wl, water level; sc, specific conductance; scb, specific conductance-bottom probe; sbt, specific conductance-top probe]

Site identification	Station location and name used in this report	Parameters	Period of record	Longitude (decimal degrees, NAD 83)	Latitude (decimal degrees, NAD 83)
U.S. Geological Survey Marsh Network					
B1	Little Back River marsh	wl, sc	June 1999–May 2005	81.12750163	32.19237988
B2	Little Back River marsh	wl, sc	June 1999–May 2005	81.12707183	32.17320051
B3	Back River marsh	wl, sc	June 1999–May 2005	81.12595301	32.15408492
B4	Back River marsh	wl, sc	June 1999–May 2005	81.10885151	32.13068071
F1	Front River marsh	wl, sc	June 1999–May 2005	81.14764018	32.18721571
M1	Middle River marsh	wl, sc	June 1999–May 2005	81.13492806	32.19237218
M2	Middle River marsh	wl, sc	June 1999–May 2005	81.13266729	32.18436345
Georgia Ports Authority Marsh and Canal Network					
Site 1 marsh	Front River upstream of Houlihan Bridge	wl, sc	June 1999–October 2002	81.15105474	32.19017614
Site 1 canal	Front River upstream of Houlihan Bridge	wl, sc	June 1999–October 2002	81.15124878	32.19074944
Site 2 marsh	Back River	wl, sc	June 1999–October 2002	81.11120968	32.12842341
Site 2 canal	Back River	wl, sc	June 1999–October 2002	81.111181	32.12895093
Site 3 marsh	Back River	wl, sc	June 1999–October 2002	81.12476284	32.15492387
Site 3 canal	Back River	wl, sc	June 1999–October 2002	81.12479598	32.1545668
Site 4 marsh	Back River	wl, sc	June 1999–October 2002	81.12582291	32.1730909
Site 4 canal	Back River	wl, sc	June 1999–October 2002	81.12586215	32.17361898
Site 5 marsh	Middle River upstream of Houlihan Bridge	wl, sc	June 1999–October 2002	81.13409274	32.17312569
Site 5 canal	Middle River upstream of Houlihan Bridge	wl, sc	June 1999–October 2002	81.13404276	32.17383171
Site 6 marsh	Middle River upstream of Houlihan Bridge	wl, sc	June 1999–October 2002	81.13577841	32.18815865
Site 6 canal	Middle River upstream of Houlihan Bridge	wl, sc	June 1999–October 2002	81.13600421	32.1879131
Site 7 marsh	Front River upstream of Houlihan Bridge	wl, sc	June 1999–October 2002	81.15330879	32.16761313
Site 7 canal	Front River upstream of Houlihan Bridge	wl, sc	June 1999–October 2002	81.15307175	32.16800705
Site 8 marsh	Little Back River	wl, sc	June 1999–October 2002	81.12381219	32.19099895
Site 8 canal	Little Back River	wl, sc	June 1999–October 2002	81.12426637	32.19170637
Site 9 marsh	Middle River upstream of Houlihan Bridge	wl, sc	June 1999–October 2002	81.14075216	32.20263829
Site 9 canal	Middle River upstream of Houlihan Bridge	wl, sc	June 1999–October 2002	81.1408484	32.20241642
Site 10 marsh	Middle River downstream of Houlihan Bridge	wl, sc	June 1999–October 2002	81.13462583	32.16196182
Site 10 canal	Middle River downstream of Houlihan Bridge	wl, sc	June 1999–October 2002	81.13461947	32.16223939

Calculated Variables, Data Preparation, and Signal Processing

Tidal systems are highly dynamic and exhibit complex behaviors that evolve over multiple time scales. The complex behaviors of the variables in a natural system result from interactions between multiple physical forces. The semidiurnal tide is dominated by the lunar cycle, which is more influential than the 24-hour solar cycle; thus, a 24-hour average is inappropriate to use to reduce tidal data to daily values. For analysis and model development, the USGS data were digitally filtered to remove semidiurnal and diurnal variability. The filtering method of choice is frequency domain filtering, which is applied to a signal, or time series of data, after it has been converted into a frequency distribution by Fourier transform. This allows a signal component that lies within a window of frequencies (for example, the 12.4-hour tidal cycle lies between periods of 12.0 to 13.0 hours) to be excised, analyzed, and modeled independently of other components (Press and others, 1993). The filter for removing the high frequency tidal cycle often is referred to as a "low-pass" filter. Time series of the daily response of tidally affected signals were generated using a low-pass filter. The resulting time series represents the daily change in the tidal signal for a 30-minute time increment. Digital filtering also can diminish the effect of noise in a signal to improve the amount of useful information that a signal contains. Working from filtered signals makes the modeling process more efficient, precise, and accurate.

One variable was computed from the field measurements of the physical parameters—tidal range. Tidal dynamics are a dominant force for estuarine systems, and the tidal range is an important variable for determining the lunar phase of the tide. Tidal range is calculated from water level and is defined as the water level at high tide minus the water level at low tide for each semidiurnal tidal cycle.

Characterization of Streamflow

Streamflows at Savannah River near Clyo, Ga. (station 02198500) are regulated by releases from Lake Thurmond Dam near Augusta, Ga., and range from a minimum of 4,000 ft^3/s during periods of low flow to 50,000 ft^3/s or more during periods of high flows (fig. 6). Seasonally, the highest flows occur in late winter and early spring (February through March), and the lowest flows occur in late summer and early fall (August through October). Figure 6 shows daily duration hydrographs based on 75 years of data. Daily duration graphs characterize the state of a stream with respect to time. The plotted percentiles are best explained by an example. Suppose 75 years of daily value flow data exist for a station and the 10-percentile flow is 7,000 ft^3/s for a particular day of the year, say January 3. This means that 10 percent of all flows that occurred on January 3 of each of the 75 years of data were equal to or less than 7,000 ft^3/s. It is assumed that flows between the 0- and 10-percentiles occur during very dry hydrologic conditions and, likewise, it is assumed that flows between the 90- and 100-percentile occur during very wet hydrologic conditions. It is assumed that flows between the 25- and 75-percentiles occur during normal hydrologic conditions.

During the 11-year period from 1994 to 2004, inclusive, the Savannah River experienced extreme streamflow conditions. During the winter-spring of 1998, floods resulting from above-normal rainfall during El Niño conditions resulted in streamflows of greater than 50,000 ft^3/s (fig. 7) that were often between the 95th percentile and historical maximum daily streamflow for the period of record. After the El Niño of 1998, the southeastern United States experienced drought from 1998 to 2002, inclusive, with minimum flows of 4,500 ft^3/s. Streamflows during the drought generally ranged from the 5th percentile to the historical minimums for the period of record.

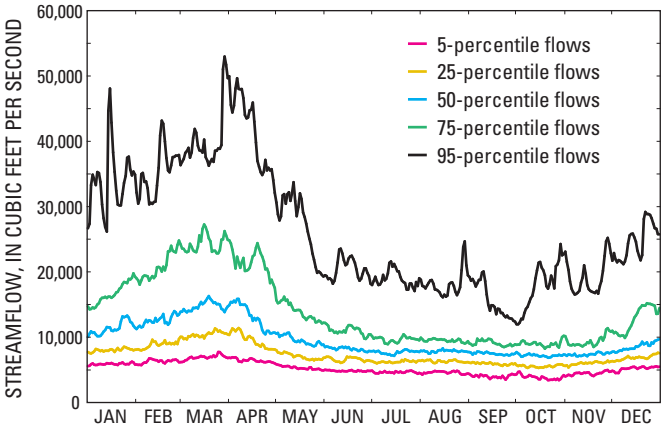

Figure 6. Duration hydrographs for Savannah River near Clyo, Ga. Percentile flows are based on streamflow data from 1929 to 2003.

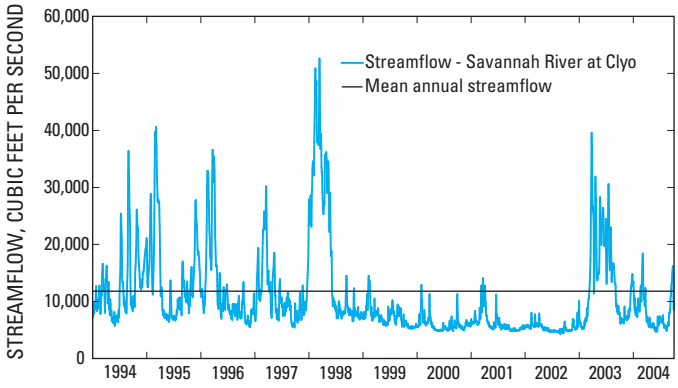

Figure 7. Daily streamflow and mean annual streamflow for Savannah River near Clyo, Ga., for the period October 1, 1994, to September 30, 2004.

Characterization of River and Marsh Water Levels

Savannah Harbor experiences semidiurnal tides of two high tides and two low tides in a 24.8-hour period. The semi-diurnal tides exhibit periodic cycles of high- and low-tidal ranges (water-level difference between high and low tide) on a 14-day cycle. The mean tidal range is 6.92 ft at Fort Pulaski (*http://Co-ops.nos.noaa.gov/tides05/tab2ec3b.html#79*). As the tidal wave propagates upstream, the tidal ranges can be larger than those in the harbor. For example, the mean tidal ranges at Fort Jackson (near the confluence of the Back and Front Rivers), Port Wentworth, and the Back River U.S. Highway 17 are 8.1, 7.0, and 7.64 ft, respectively (fig. 2). Upstream from the U.S. Highway 17 Bridge, the tidal range decreases with the increased effects of the freshwater flow of the Savannah River and decrease in channel geometry. There is approximately a 1-hour lag of the tide from Fort Pulaski to the Little Back and Back Rivers at the U.S. Highway 17 Bridge.

Figure 8 shows the water levels at three USGS stations on the Savannah River for the period during October 2002. The neap tidal period, characterized by a relatively smaller amplitude in tidal range, occurred around October 14 and 28, and the spring tidal period, characterized by a larger amplitude in tidal range, occurred around October 7 and 21. During the spring tide early in the month, the highest water levels occurred at the Broad Street water-level gage (station 02198920, fig. 5)—greater than the downstream water-level gage at Fort Pulaski (station 02198980, fig. 1). As the tidal range diminished during October, the highest water levels were experienced at the most upstream gaging station at I-95 where the high water is often affected by the streamflow of the Savannah River.

A plot of the daily tidal range clearly shows the 14-day spring-neap tidal cycles along with seasonal and semiannual cycles. The tidal range for the Fort Pulaski water-level gage (station 02198980) is shown in figure 9 for the 2002 calendar year. The 14-day spring-neap cycles are clearly shown. For example, a high spring tide (tidal range greater than 8 ft) is followed by a low spring tide (tidal range less than 8 ft). A similar pattern is apparent in the neap tides where a low neap tide (tidal range less than 5.5 ft) is followed by a high neap tide (tidal range greater than 5.5 ft).

Seasonal and semiannual cycles of minimum and maximum tidal ranges can also be seen in figure 9. The highest difference in spring and neap tides occur in the spring (March and April) and the fall (October and November) of the year. Minimum differences between the spring and neap tides occur in the summer (June and July) and in the winter (December and January) of the year.

Water-level dynamics in the tidal marshes are dependent on the height of the water levels, the surface elevation of the tidal marsh, and inertial affects. Tidal fluctuations in marsh water levels are greatest during the high spring tides and are minimal during neap tides. Marsh water-level time series for USGS gaging stations on the Back, Middle, and Front River marshes are shown in figures 10 and 11. In figure 10, hourly water levels in the Little Back River near Limehouse

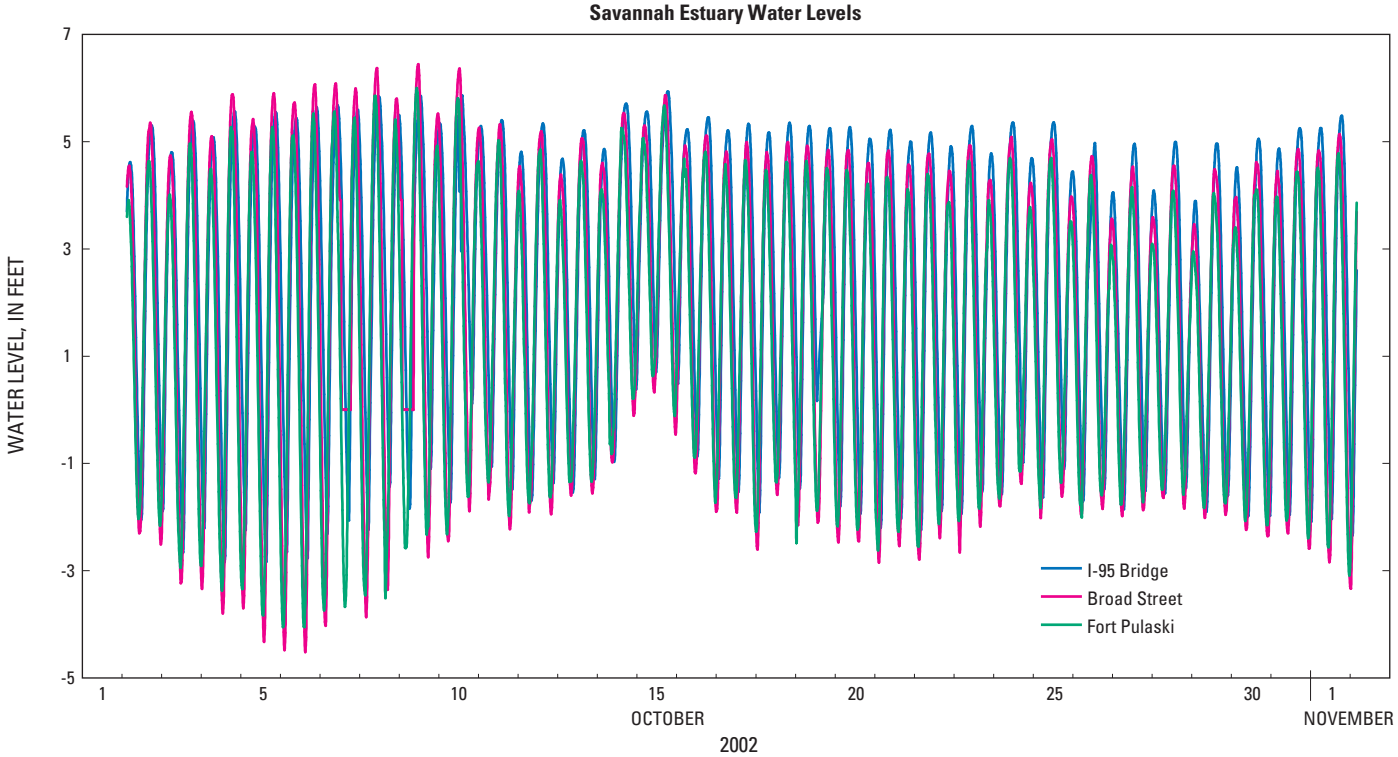

Figure 8. Hourly water levels at three gaging stations on the Savannah River for the period October 1 to October 31, 2002.

(station 02188979, left y-axis) are shown with marsh water levels (right y-axis). The Little Back River water-level time series show the periods of spring tides. Multiday periods of substantial tidal fluctuations for the four marsh sites along the Little Back and Back Rivers occur during spring tides beginning around December 15 and 29, and January 28, 2002. In figure 11, similar water-level responses are seen for the two marsh sites along the Middle River and the marsh site along the Front River. Multiday periods of substantial tidal fluctuations for the three marsh sites occur on spring tides beginning around November 10, November 29, December 10, and December 29, 2001.

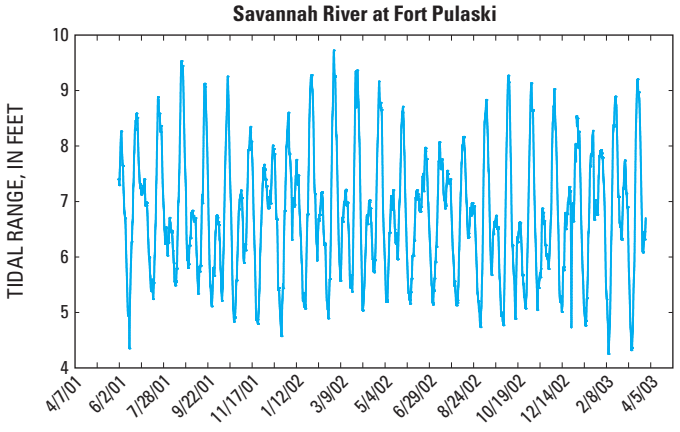

Figure 9. Daily tidal range at Savannah River at Fort Pulaski for the period June 2001 to May 2003.

Characterization of River and Marsh Specific Conductance

The location of the saltwater-freshwater interface is a balance between upstream river flows and downstream tidal forcing. During periods of high streamflow, it is difficult for salinity to intrude upstream, and thus, the saltwater-freshwater interface is moved downstream towards the ocean. During periods of low streamflow, salinity is able to intrude upstream; subsequently, the saltwater-freshwater interface is moved upstream. Historically, streamflows on the Savannah River range from 5,000 to 50,000 ft^3/s. Salinity in the Savannah River Estuary constantly responds to changing streamflow and tidal conditions. The daily mean specific conductance for the Little Back River near Limehouse (station 02198979) and daily mean streamflow for Savannah River near Clyo (station 02198500) for the 1994 to 2004 period are shown in figure 12. The period includes the full range of flows for the system from the high flows of the El Niño in 1998 to the low flows of the extended drought in the southeast from

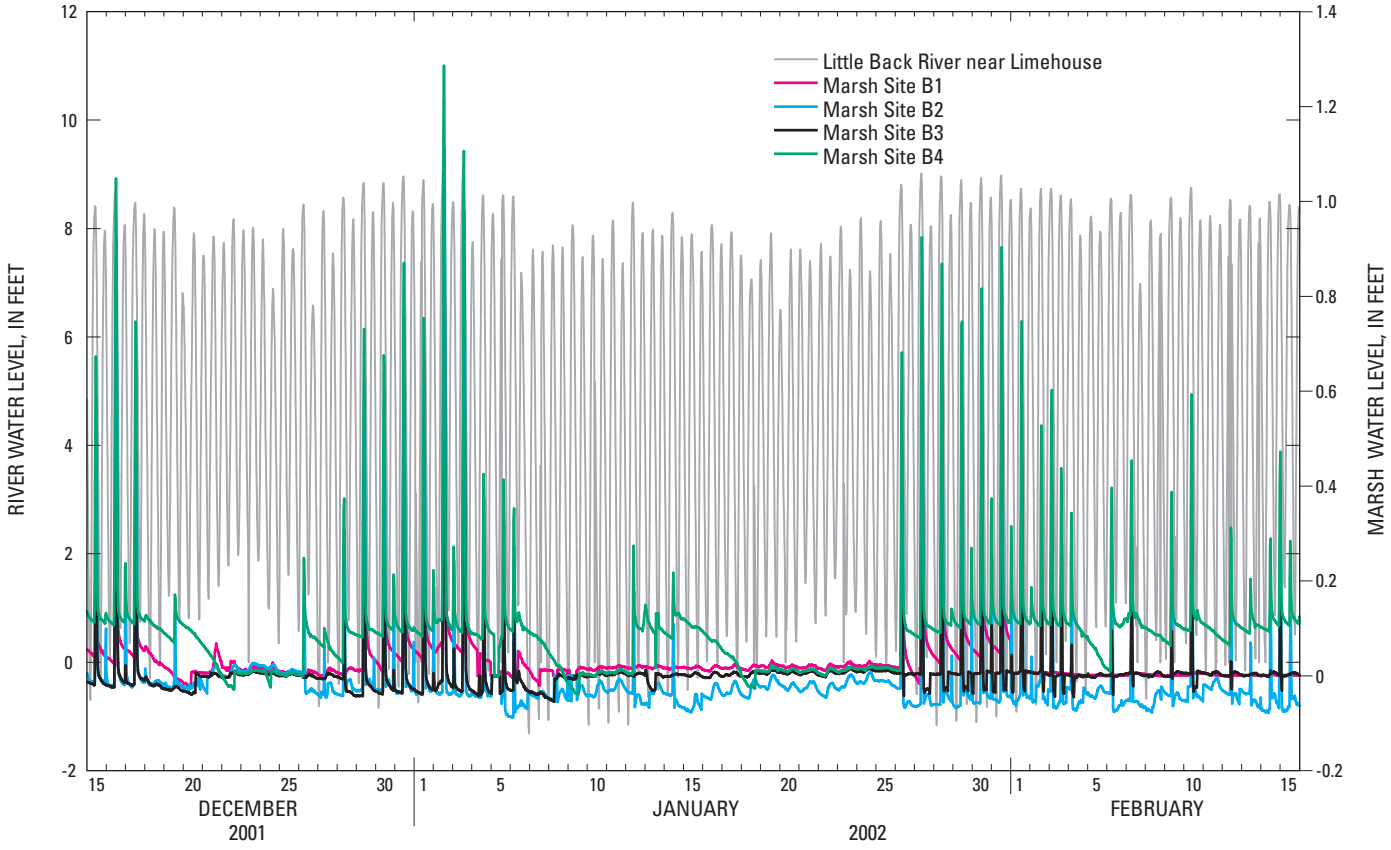

Figure 10. Hourly water-level data for the four Back River marsh gaging stations and Little Back River gaging stations for the period December 15, 2001, to February 15, 2002.

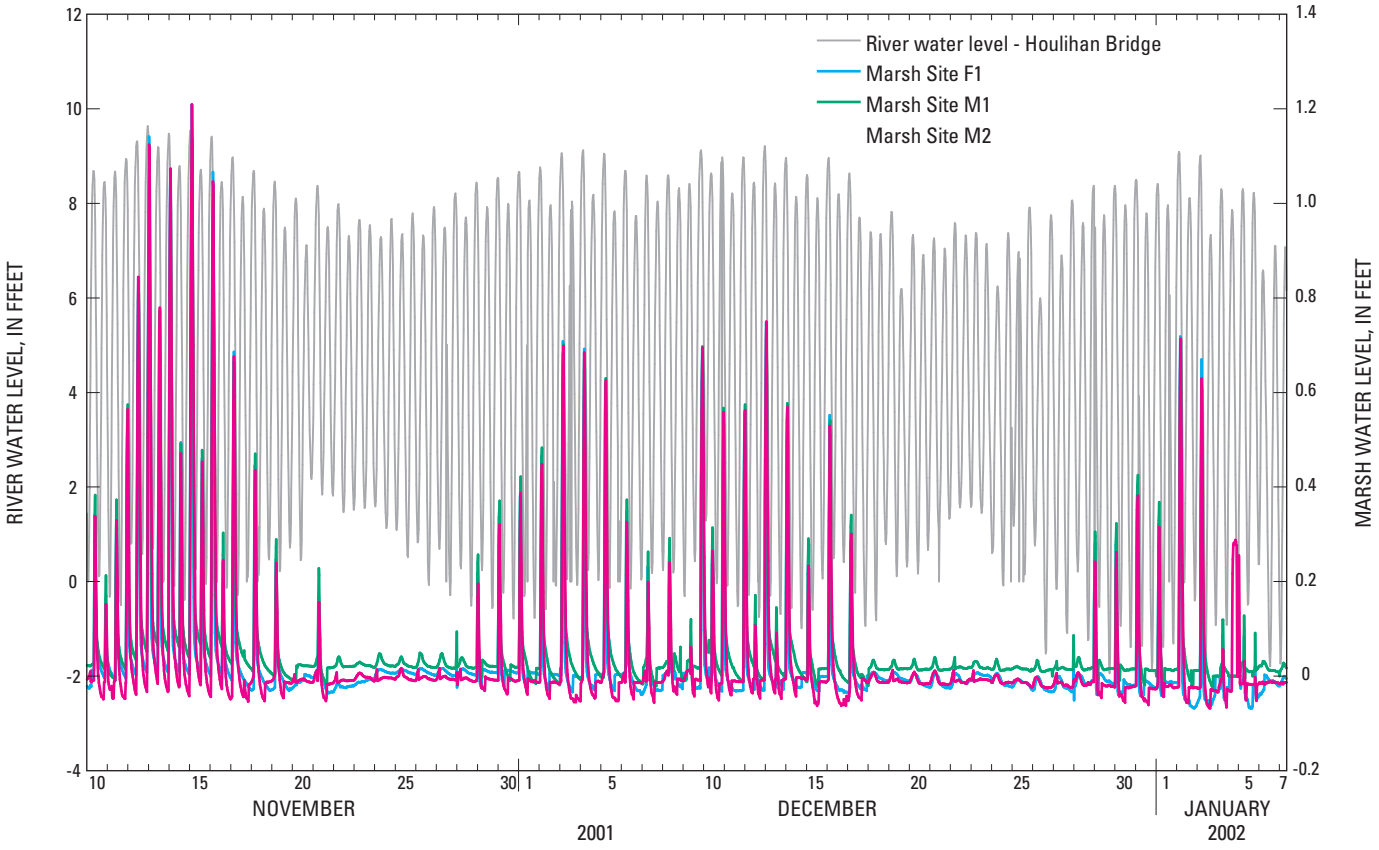

Figure 11. Hourly water-level data for three marsh gaging stations along the Middle and Front Rivers and Savannah River water level at Houlihan Bridge for the period November 10, 2001, to January 7, 2002.

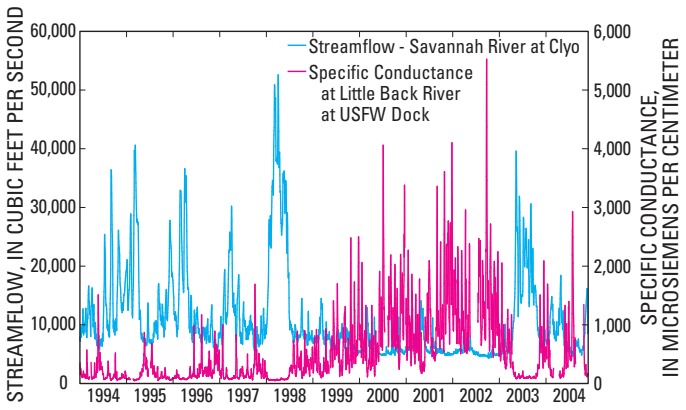

Figure 12. Daily specific conductance at Little Back River at U.S. Fish and Wildlife Service Dock gaging station and streamflow at Savannah River near Clyo, Ga., gaging station for the period January 1, 1994, to September 30, 2004.

1998 to 2002. During periods of medium streamflow and greater (streamflow greater than 10,000 ft^3/s), the specific-conductance values are low. During periods of low flow (streamflow less than 10,000 ft^3/s), specific-conductance values increase during periods of salinity intrusion. During the period prior to the high flows of El Niño in 1998, salinity intrusion with specific-conductance values of 500 to 1,000 microsiemens per centimeter (µS/cm) were not uncommon during low-flow periods. After the high flow of 1998 and the extended drought, flows were even lower and remained lower for extended periods. This resulted in greater salinity intrusions in the Little Back River with daily mean specific-conductance values as high as 4,000 µS/cm.

The Savannah River Estuary is considered a partially stratified system with large differences in surface and bottom salinities occurring during neap and spring tides over the 14- and 28-day cycles. A schematic of the largest factors that affect salinity transport along the Savannah River is shown in figure 13. During spring tides (tides with the largest tidal range), there is increased energy in the system and mixing of less dense freshwater of the river and denser saltwater of the harbor. The mixing results in smaller variation in vertical salinity concentrations. During neap tides (tides with the smallest tidal range), there is decreased energy in the system and less mixing between the freshwater and saltwater. The decreased mixing allows the freshwater to flow downstream over the saltwater intruding upstream. The decrease in mixing results in an increased salinity gradient from the surface to the bottom of the water column and increased salinity

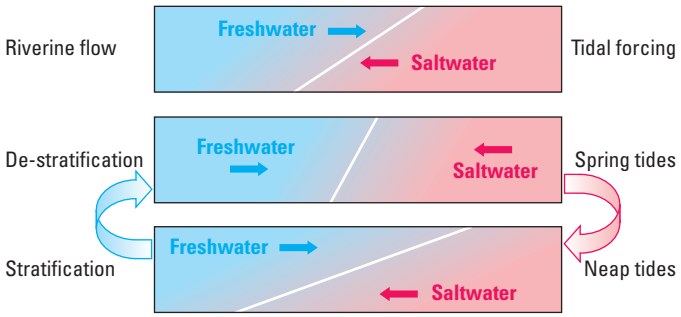

Figure 13. Conceptual model of the location of the freshwater-saltwater interface and salinity stratification-destratification cycle in estuarine rivers.

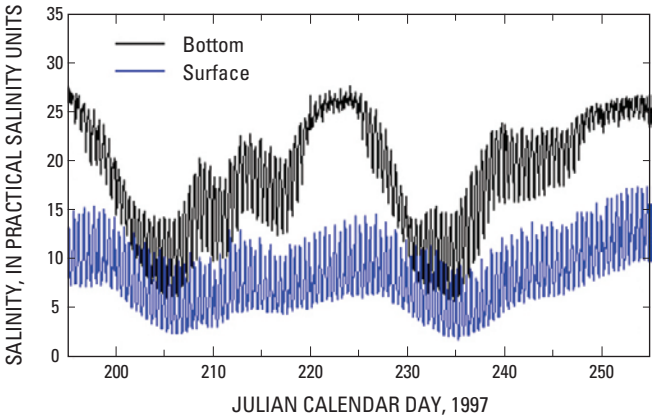

Figure 14. Surface and bottom salinities for station GPA04 for the period July 15 to September 13, 1997 (Tetra Tech, 2005). The plot shows the de-stratification of the Savannah River on about Julian days 205 and 235 and the stratification on about Julian day 225.

intrusion upstream. The stratification and de-stratification of salinity at station GPA04 for 2 months during summer 1997 is shown in figure 14. During the neap tides around Julian day 225, there is an approximate 15-psu difference between the bottom and surface salinities. During the spring tides around Julian day 205 and 235, the system de-stratifies and the differences between the bottom and surface salinities are only 3 to 5 psu.

The marsh salinities do not exhibit the semidiurnal salinity variability like the river and are dependent on the frequency and magnitude of the flooding of river water on the marsh. Tidal marshes are constantly integrating the changing river conditions in their water levels (frequency and duration of inundations) and the salinity concentration in the interstitial pore-water of the root zone. Plant distributions in the marshes are the result of the interstitial salinities. The interstitial salinities of the marshes with the surface salinities of the river, and the four marsh types and their corresponding estuarine salinity concentrations, are shown in figure 15.

Because the marshes do not flood every tide, the interstitial salinities are not the same as the river salinity. During low-flow periods and high tides, salinity intrudes farther upstream, and the surface salinities inundate the marshes. The highest salinity intrusions into the marshes occur when riverine salinity intrusions are concurrent with the spring-tide water levels. The specific-conductance time series of the four marsh gaging stations along the Little Back and Back Rivers with the specific conductance for the Front River at Houlihan Bridge (station 02198920) is shown in figure 16. The four marsh sites show a distinct gradient of increased specific-conductance values from upstream (Site B1) to downstream (Site B4). Increased specific conductance in the marsh generally occurs after increased specific conductance in the river. The specific-conductance time series of three marsh gaging stations along the Middle and Front Rivers and specific conductance for the Front River at the Houlihan Bridge water-level gage (station 02198920) are shown in figure 17.

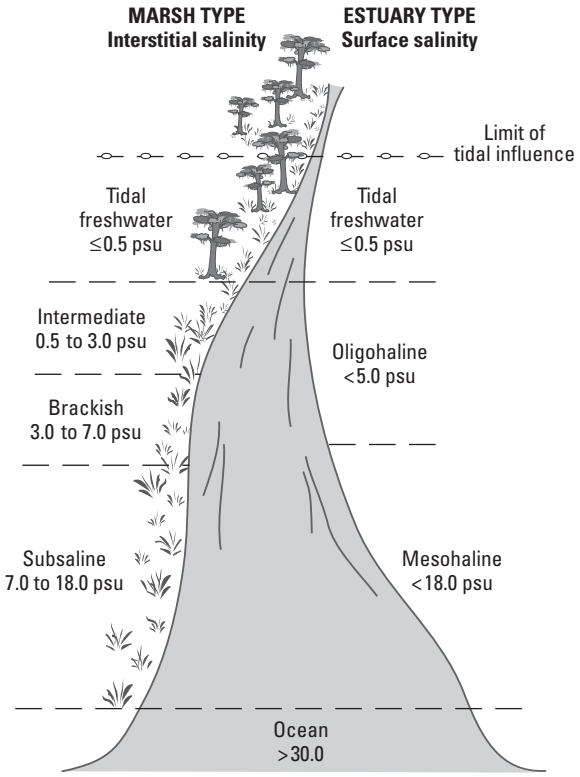

Figure 15. Tidal marsh types classified by interstitial salinity (Pearlstine and others, 1990) and average surface salinities (Cowardin and others, 1979) (modified from Odum and others, 1984).

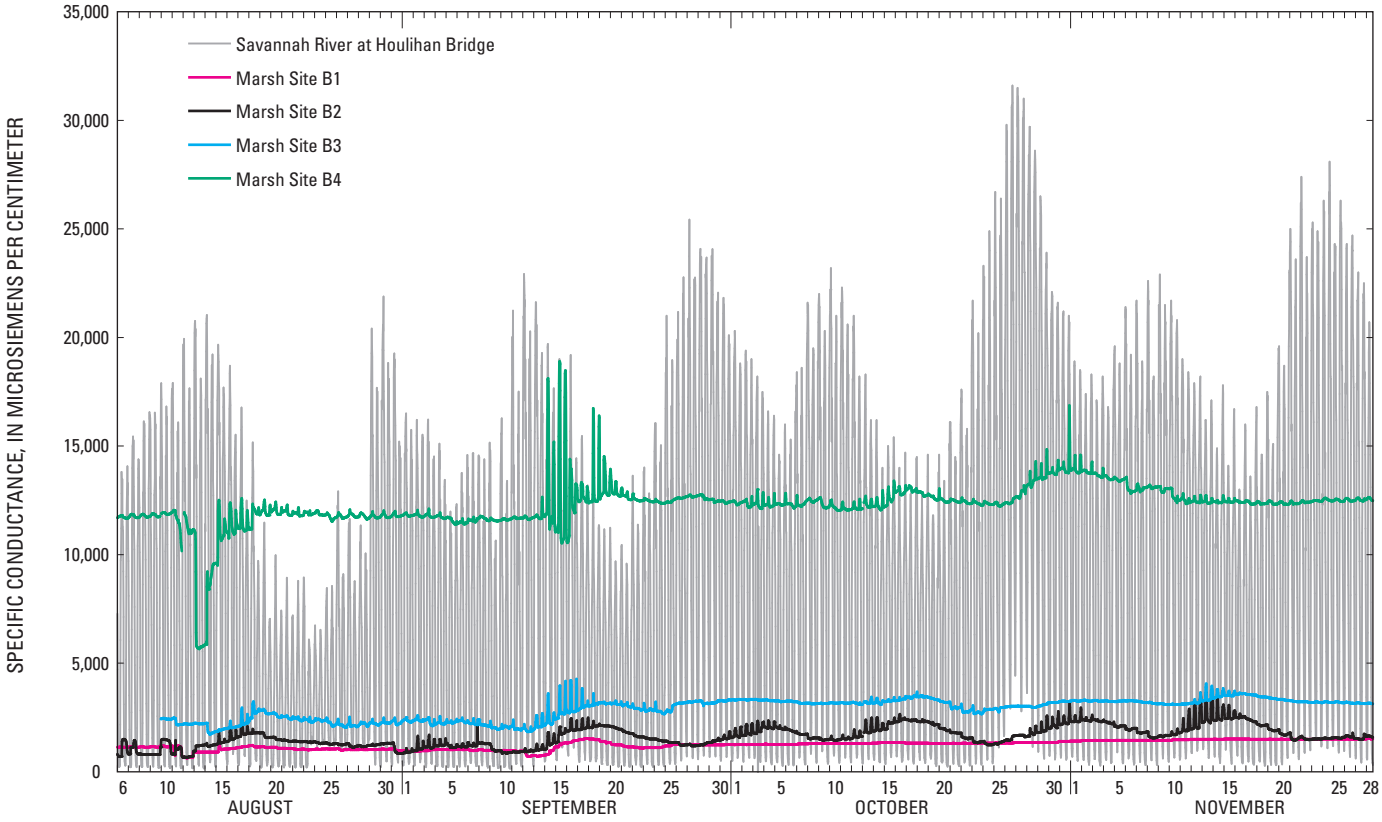

Figure 16. Hourly specific conductance at four marsh gaging stations along the Little Back and Back Rivers and specific-conductance values at the Houlihan Bridge on the Savannah River for the period August 6 to November 30, 2001.

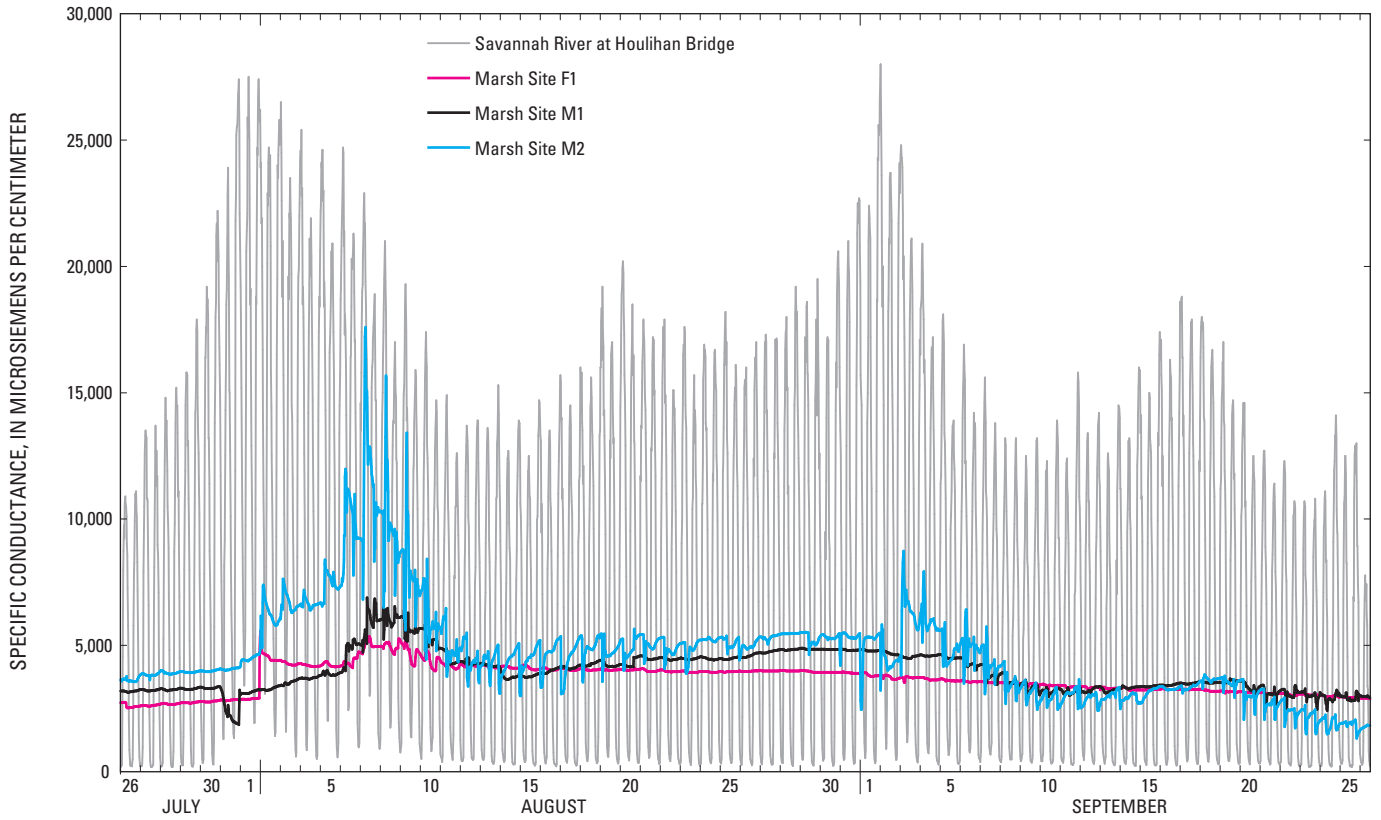

Figure 17. Hourly specific conductance for two marsh gaging stations on the Middle River, one marsh gaging station on the Front River, and at Houlihan Bridge on the Savannah River for the period July 26 to September 27, 2002.

Simulating Riverine and Marsh Water Levels and Salinity

Simulating salinity for estuarine systems typically is done using dynamic deterministic models that incorporate the mathematical descriptions of the physics of coastal hydrodynamics. These one-, two-, or three-dimensional models generally are expensive and time consuming to apply to complex coastal systems with satisfactory results. Conrads and Roehl (2005) assert that in estuaries, mechanistic model calibration is "… particularly difficult due to low watershed gradients, poorly defined drainage areas, tidal complexities, and a lack of understanding of watershed and marsh processes." Although mechanistic models have been the state of the practice for regulatory evaluations of anthropogenic effects on estuarine systems, developments in the field of advanced statistics, machine learning, and data mining offer opportunities to develop empirical ANN models that are often more accurate. Conrads and Roehl (1999) compared the application of a deterministic model and an ANN model to simulate dissolved oxygen on the tidally affected Cooper River in South Carolina. Results of their study indicated that the ANN models offer important advantages, including faster development time, use of larger amounts of data, the incorporation of optimization routines, and model dissemination in spreadsheet applications. With the real-time gaging network on the Savannah River and the availability of large databases of hydrologic and water-quality data, the GPA realized an opportunity to develop an empirical model using data-mining techniques, including ANN models, to simulate the water level and pore-water salinity of the tidal marshes in the vicinity of SNWR.

The emerging field of data mining addresses the issue of extracting information from large databases. Data mining comprises several technologies that include signal processing, advanced statistics, multidimensional visualization, chaos theory, and machine learning. Machine learning is a field of artificial intelligence (AI) in which computer programs are developed that automatically learn cause-effect relations from example cases and data. For numerical data, commonly used methods include ANN models, genetic algorithms, multivariate adaptive regression splines, and partial and ordinary least squares (OLS).

Data mining can solve complex problems that are unsolvable by any other means. Weiss and Indurkhya (1998) define data mining as "… the search for valuable information in large volumes of data. It is a cooperative effort of humans and computers." A number of previous studies by the authors and others have used data mining to simulate hydrodynamic and water-quality behaviors in the Beaufort, Cooper, and Savannah River estuaries (Roehl and Conrads, 1999; Conrads and Roehl, 1999; Roehl and others, 2000; Conrads and others, 2002a; 2002b) and stream temperatures in western Oregon (Risley and others, 2002). These studies have demonstrated the performance of data mining to simulate water level, water temperature, dissolved oxygen, and specific conductance, and for assessing the effects of reservoir releases and point and nonpoint sources on receiving streams.

The ultimate goal of this study is to produce an effective model to simulate water level and specific conductance in the tidal marsh for a given set of streamflow, water-level, and tidal range conditions. The approach taken uses all available streamflow, water-level, and specific-conductance measurements since the last major changes in channel configuration in 1994. The modeling approach uses correlation functions that were synthesized directly from data to simulate how the change in water level and specific conductance at each station location is affected by streamflow and tidal conditions over time.

Limitations of the Data Sets

As with any modeling effort, empirical or deterministic, the reliability of the model is dependent on the quality of the data and range of measured conditions used for training or calibrating the model. The available period of record for the river and marsh data-collection networks can limit the range of streamflow, water-level, tidal range, and salinity conditions that the ANN model can accurately simulate. As noted previously, substantial changes in the salinity response of the system can occur due to a small change in streamflow (fig. 12). Using the specific-conductance record for the Little Back River at USFW Dock (station 021989791) as representative of the salinity dynamics of the system, scatter plots of daily streamflow and specific-conductance data were generated for each network for the period that it was active (fig. 18). The period of record for the USGS river network (fig. 18*A*) covers the full range of historical conditions from extreme low to high flows. The GPA river network (fig. 18*A*), active during summer 1997 and 1999, covers a much smaller range of hydrologic conditions and did not measure streamflow and the corresponding salinity response for streamflows less than 5,440 ft^3/s or greater than 11,600 ft^3/s. The USGS marsh network (fig. 18*B*) was established in 2000 during the drought and measured a large range of marsh salinity conditions for streamflow ranging from 4,310 to 39,600 ft^3/s. The GPA marsh network (fig. 18*B*) also was established during the drought, but was discontinued in 2002 and only measured low-flow conditions less than 14,100 ft^3/s. Data networks and the range of flows measured for each gaging network are summarized in table 2.

Signal Decomposition, Correlation Analysis, and State-Space Reconstruction

The behavior, or dynamics, of a natural system results from interactions between multiple physical forces. For example, the specific conductance at a fixed location is subject to daily, seasonal, and annual streamflow conditions and semidiurnal, fortnightly, seasonal, and annual tidal water-level conditions. For the application of the ANN models to the

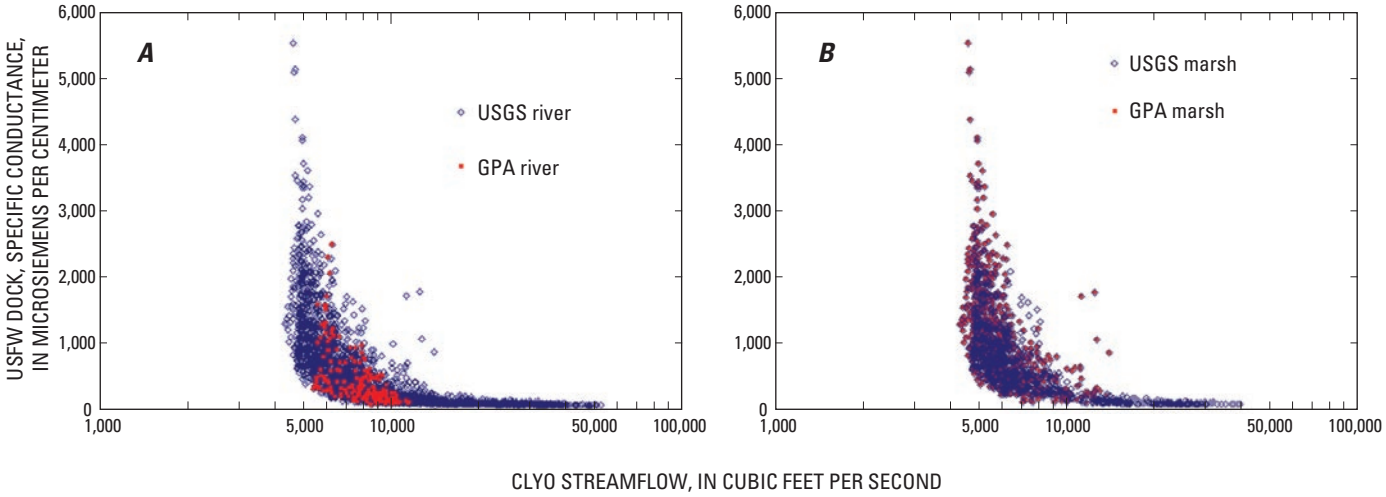

Figure 18. The daily mean streamflow at Savannah River at Clyo, Ga., and daily mean specific conductance at U.S. Fish and Wildlife Service Dock, Little Back River, for the conditions during which the gaging network was active. The two river networks are shown in the plot on the left (*A*), and two marsh networks are shown on the plot on the right (*B*).

Savannah River, data-mining methods are applied to maximize the information content in raw data while diminishing the influence of poor or missing measurements. Methods include digital filtering using fast Fourier Transforms, time derivatives, time delays, running averages, and differences between stations. Signals, or time series, manifest three types of behavior: periodic, chaotic, and noise. Periodic behavior is perfectly predictable. Examples of periodic behavior are the diurnal sunlight and temperature patterns caused by the rising and setting sun or tidal water levels attributed to orbital mechanics. Noise refers to random components, usually attributed to measurement error, and is unpredictable. Chaotic behavior neither is totally periodic nor noise, and always has a physical cause. Weather is an example of chaotic behavior. Chaotic behavior is somewhat predictable, especially for small time frames and prediction horizons.

Signal Decomposition

Signal decomposition involves splitting a signal into subsignals, called "components," which are independently attributable to different physical forces. To analyze and model these time series, the periodic and chaotic components of the signals need to be separated. Digital filtering can separate out the chaotic component in the water-level time series. Computation of the tidal range time series from the water-level time series separates out the periodic components of the water-level time series. Digital filtering can also diminish the effect of noise in a signal to improve the amount of useful information that it contains.

Time derivatives are a common analytical method used in the sciences to analyze the dynamics of a system. Time derivatives are also computed from the measured, computed, and filtered variables on the Savannah River to further understand the dynamics of the system. The 1-day derivative of the low-pass filtered water-level time series for a 90-day period was plotted with the original time series and the low-pass filtered data (fig. 19). The 1-day derivatives show the rate of change of the chaotic component of the water-level time series. For the 90-day period, the daily change in filtered water level is as high as 1.5 ft.

Often there are time delays between when an event is measured and the time that the response is observed in a system. Modeling a system is more complicated when two events of interest, a cause and an effect, do not occur simultaneously. The time between cause and effect is called the "time delay" or "delay." Each input variable of a model has its own delay. Determining the correct time delays for pulses and system response is critical to accurately simulating a dynamic system. For the Savannah River, there is a time delay between the measured streamflow at Clyo, Ga., and the response in specific conductance at the stations near the SNWF. Time delays between when the flow enters the system and the river response of the specific conductance were determined for each station by analyzing the correlation between lagged flow values for various time delays and the salinity response values at a station.

Table 2. Period of record and range of daily flow conditions measured for the river and marsh gaging networks used in the study.

[ft^3/s, cubic foot per second; USGS, U.S. Geological Survey; GPA, Georgia Ports Authority]

Gaging network	Period of record used in this study	Range of flow conditions (ft^3/s)
USGS River	Jan 1994–May 2005	4,320 – 52,600
GPA River	July–Sept 1997 July–Oct 1999	5,440 – 11,600
USGS Marsh	June 1999–May 2005	4,320 – 39,600
GPA Marsh	June 1999–Oct 2002	4,320 – 14,100

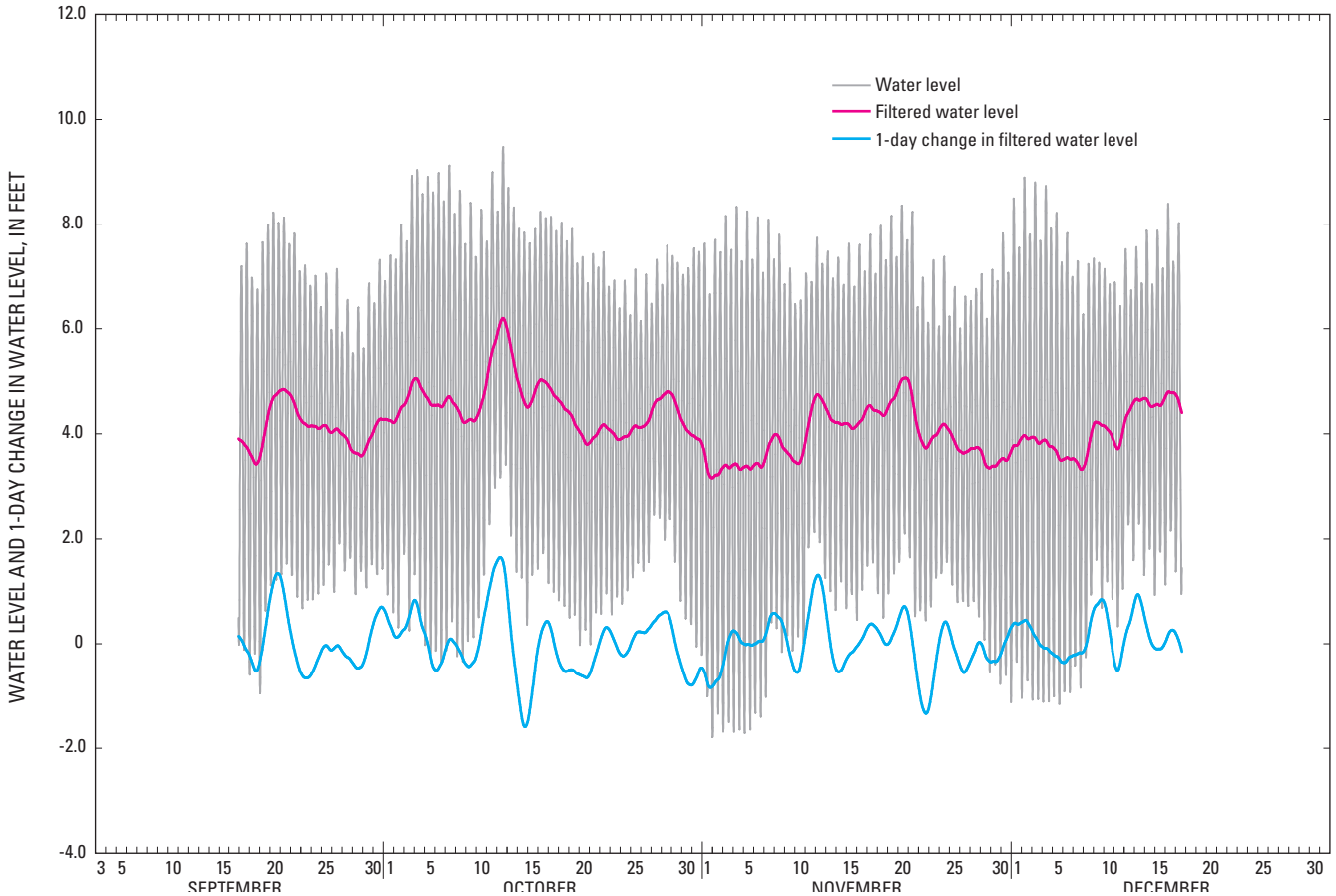

Figure 19. Hourly water levels at Fort Pulaski (station 02198980), low-pass filtered water levels, and 1-day change in filtered water levels for the 90-day period September 13 to December 13, 1994.

Averages and running averages are commonly used to remove the variability of measurements and to represent prevailing behaviors of the system. To capture the effect of the extended low-flow condition as a result of the extended drought, time derivatives of running average flow conditions were computed. The 14-day difference (time derivative) of the 14-day running average flow conditions can capture the change in average flow conditions over a 28-day period. For example, if the 14-day running average for June 28, 2002 (June 15–28) is 4,743 ft^3/s and the 14-day running average for June 15, 2002 (June 2–15) is 4,900 ft^3/s, then the 14-day difference (time derivative) for June 28, 2002 is –157 ft^3/s. The daily streamflow at Clyo, Ga., the 14-day average streamflow, and the 14-day difference in 14-day average flows are shown in figure 20. The time derivative signal shows the 14-day trend of the change in 14-day average streamflow conditions. There is a significant difference in the time derivative signal for the extended drought after the high flows of the El Niño in 1998. Prior to the drought, 14-day differences in 14-day average flows fluctuate by more than 10,000 ft^3/s. During the drought, fluctuations were less than 5,000 ft^3/s.

Correlation Analysis

The relations between the many variables and their various components are ascertained through correlation analyses to provide deeper understanding of system dynamics. For example, salinity intrusion is dependent on streamflow and tides, and correlation analysis provides a measure of relative contribution of each variable. Sensitivity analysis quantifies the relations between a dependent variable of interest and causal variables. Computing sensitivities requires defining the relation between variables through modeling.

Using statistical and(or) ANN software, the computer systematically correlates factors that most influence parameters of interest (for example, specific conductance) to candidate combinations of controlled and uncontrolled variables (for example, streamflow and tidal conditions). Correlation methods based on statistics and ANNs are applied in combination. Promising results identified by the analysis are validated by comparing them to known patterns of behavior.

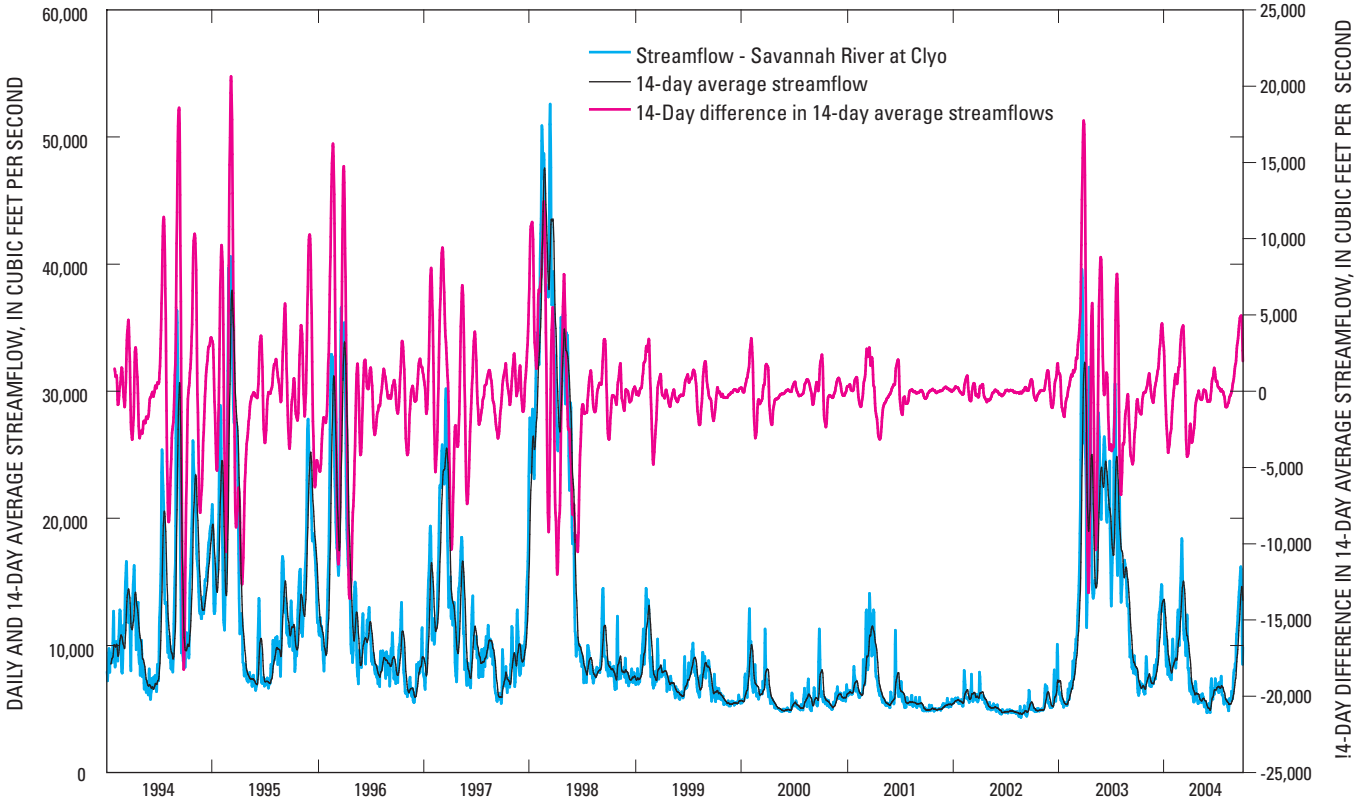

Figure 20. Daily flows, 14-day average flows, and 14-day differences in 14-day average flows for the Savannah River at Clyo, Ga., for the period 1994–2004. Note the scale for the 14-day differences in 14-day average flows is on the right.

State-Space Reconstruction

Chaos theory provides a conceptual framework called "state-space reconstruction" (SSR) for representing dynamic relations. Data collected at a point in time can be organized as a vector of measurements; for example, element one of the vector might be the water level, element two the streamflow, and so on. Engineers say that a process evolves from one state to another, in time, and that a vector of measurements, also referred to as a "state vector," represents the process state at the moment the measurements were taken. A sequence of state vectors represents a "state history." Mathematicians say that the state vector is a point in a "state space" having a number of dimensions equal to the number of elements in the vector. For example, eight vector elements equates to eight dimensions. Empirical modeling is the fitting of a multidimensional surface to the points arrayed in state space.

Chaos theory proposes that a process can be optimally represented (reconstructed) by a collection of state vectors, Y(t), using an optimal number of measurements equal to "local dimension" d_L that are spaced in time by integer multiples of an optimal time delay, τ_d (Abarbanel, 1996)[1]. For a multivariate process of k independent variables:

$$Y(t) = \{[x_1(t), x_1(t-\tau_{d1}),\ldots, x_1(t-(d_{L1}-1)\tau_{d1})], \ldots, [x_k(t), x_k(t-\tau_{dk}),\ldots, x_k(t-(d_{Lk}-1)\tau_{dk})]\} \quad (1)$$

where each $x(t,\tau_{di})$ represents a different dimension in state space, and therefore, a different element in a state vector. Values of d_{Li} and τ_{di} are estimated analytically or experimentally from the data. The mathematical formulations for models are derived from those for state vectors. To predict a dependent variable of interest y(t) from prior measurements (forecasting) of k independent variables (Roehl and others, 2000):

$$y(t) = F\{[x_1(t-\tau_{p1}), x_1(t-\tau_{p1}-\tau_{d1}), \ldots, x_1(t-\tau_{p1}-(d_{M1}-1)\tau_{d1})], \ldots,[x_k(t-\tau_{pk}), x_k(t-\tau_{pk}-\tau_{dk}), \ldots, x_k(t-\tau_{pk}-(d_{Mk}-1)\tau_{dk})]\} \quad (2)$$

where F is an empirical function such as an ANN, each $x(t,\tau_{pi},\tau_{di})$ is a different input to F, and τ_{pi} is yet another time delay. For each variable, τ_{pi} is specified according to one of the following constraints: time delay at which an input variable becomes uncorrelated to all other inputs, but can still provide useful information about y(t); time delay of the most recent available measurement of x_i; or time delay at which an input variable is most highly correlated to y(t). Here, the state space local dimension d_L of Equation 1 is replaced with a model

[1] In Chaos theory, d_L and t_d are called "dynamical invariants," and are analogous to the amplitude, frequency, and phase angle of periodic time series.

input variable dimension d_M, which is determined experimentally. It is noted that $d_M \leq d_L$, and tends to decrease with increasing k.

Input-Output Mapping and Problem Representation

The development of ANN models to predict the water level and pore-water salinity of the tidal marsh was undertaken in two phases. The first phase was to train the ANN models to simulate the water level and specific conductance at the USGS and the GPA riverine sites. Inputs to the ANN models of the USGS river network include time series, or signals, of streamflow, tidal water level, and tidal range. Because of the limited data set, the GPA river network sites were modeled using differences in water level and specific conductance with the USGS river network stations. Outputs from these models are water level and salinity at the river network stations. Simulated specific-conductance values are post-processed to salinity values using the equation documented by Miller and others (1988). The second phase was to train the ANN models to simulate water level and pore-water specific conductance at the USGS and the GPA marsh sites. Inputs for these models include the water-level and specific-conductance signals from the USGS and GPA river networks near the marsh gaging sites. Outputs from these models are water level and salinity at the marsh network stations.

One of the ultimate applications of the ANN models will be to simulate the change in water level and specific conductance in the marsh likely to result from a potential harbor deepening. As discussed previously, a 3D model, EFDC, has been applied and will be used to simulate water-level and salinity changes in the river resulting from geometric changes expected from proposed physical changes to the harbor. Using the USGS river network time series as input for the marsh, the ANN models can accommodate the integration of output from other models of the river. Rather than use the ANN river predictions as input to the ANN marsh models, EFDC predictions were used. The final application of the ANN models can be run under two different modes. Mode 1 uses the streamflow and tidal condition inputs and evaluates the effects of changing hydrologic conditions on water level and specific conductance of the river and marsh sites. Mode 2 uses EFDC predictions of changes from a base-case scenario at the USGS river network as inputs to evaluate the effects of changes in the channel geometry on water level and specific conductance of the marsh sites.

Decorrelation of Variables

Often, explanatory variables share information about the behavior of a response variable. It is difficult, if not impossible, to understand the individual effects of these variables (sometimes known as confounded or correlated variables), on a response variable. Empirical models have no notion of process physics, nor the nature of interrelations between input variables. To be able to clearly analyze the effects of confounded variables, the unique informational content of each variable must be determined by "de-correlating" the confounded variables. For the Savannah River application, the boundary input data, streamflow from Clyo, Ga., and water levels from Fort Pulaski, are both distant from the river and marsh gaging network near the SNWF. The Pearson correlation coefficient, R, between Clyo streamflows and the Savannah Harbor water level is -0.03, indicating very little correlation between the two time series.

The only variables in the application that needed to be decorrelated were data from the GPA specific-conductance stations (GPA10S, GPA11, GPA11R, and GPA12) used as inputs for the USGS marsh salinity models. Decorrelation is accomplished by generating an empirical correlation function and computing its residual error by subtracting the function's predicted values from the actual measurement. The residual error is the "unshared" information between the two signals. Single Input Single Ouput (SISO) ANN models were built to decorrelate data from GPA11, GPA11R, and GPA12 from GPA10S. The residual error signal was then used in the USGS marsh salinity models as the decorrelated inputs for those stations.

Artificial Neural Network Models

Models generally fall into one of two categories, deterministic (or mechanistic) or empirical. Deterministic models are created from first-principles equations, whereas empirical modeling adapts generalized mathematical functions to fit a line or surface through data from two or more variables. The most common empirical approach is OLS, which relates variables using straight lines, planes, or hyper-planes, whether the actual relations are linear or not. Calibrating either type of model attempts to optimally synthesize a line or surface through the observed data. Calibrating models is made difficult when data have substantial measurement error or are incomplete, and the variables for which data are available may only be able to provide a partial explanation of the causes of variability. The principal advantages that empirical models have over deterministic models are that they can be developed much faster and are often more accurate when the modeled systems are well characterized by data. Empirical models, however, are prone to problems when poorly applied. Overfitting and multicollinearity caused by correlated input variables can lead to invalid mappings between input and output variables (Roehl and others, 2003).

An ANN model is a flexible mathematical structure capable of describing complex nonlinear relations between input and output data sets. The architecture of ANN models is loosely based on the biological nervous system (Hinton, 1992). Although there are numerous types of ANNs, the most commonly used type is the multilayer perceptron (MLP) (Rosenblatt, 1958). As shown in figure 21, MLP ANN's are constructed from layers of interconnected processing elements called neurons, each executing a simple "transfer function."

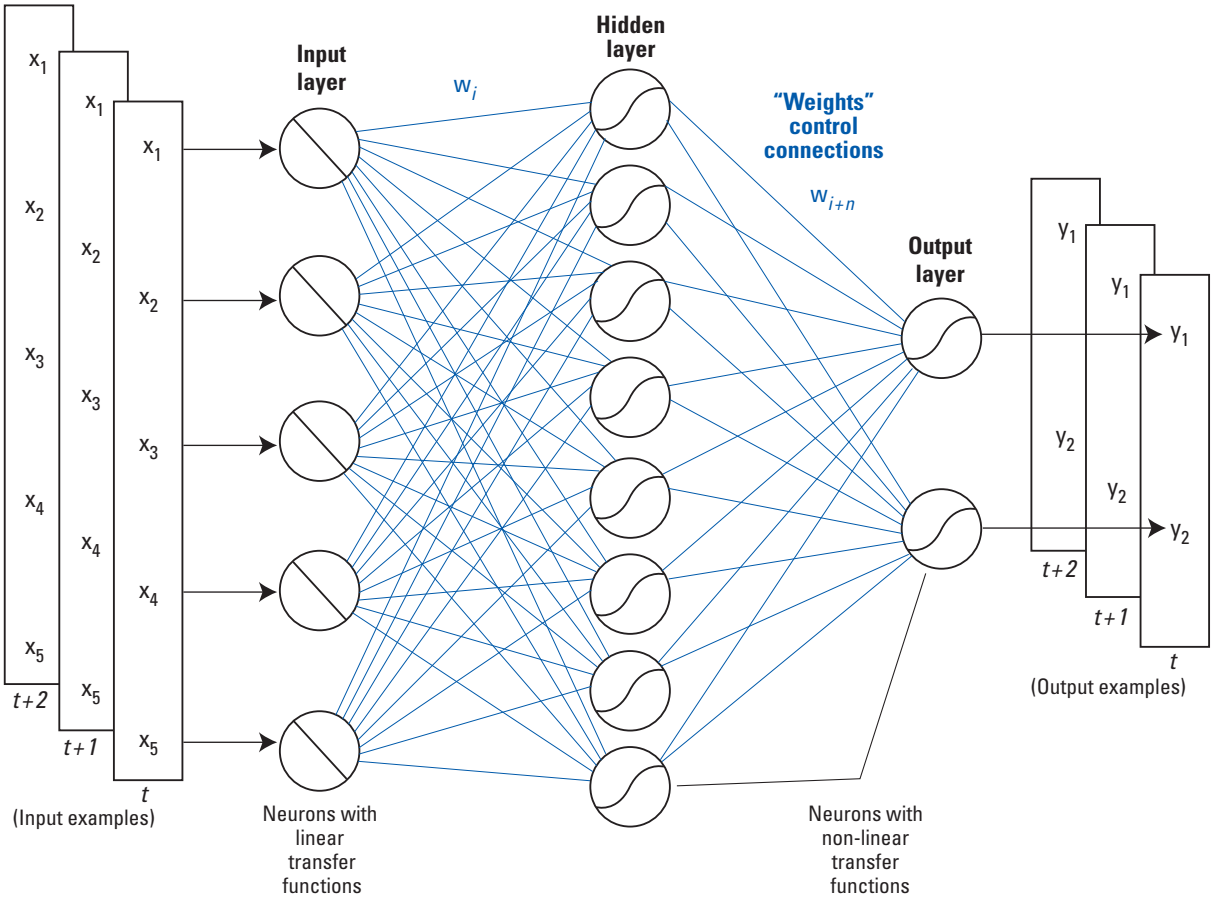

Figure 21. Multilayer perceptron artificial neural network architecture.

All input layer neurons are connected to every hidden layer neuron, and every hidden layer neuron is connected to every output neuron. There can be multiple hidden layers, but a single layer is sufficient for most problems.

Typically, linear transfer functions are used to simply scale input values to fall within the range that corresponds to the most linear part of the s-shaped sigmoid transfer functions used in the hidden and output layers. Each connection has a "weight," w_i, associated with it that scales the output received by a neuron from a neuron in an antecedent layer. The output of a neuron is a simple combination of the values it receives through its input connections and their weights, and the neuron's transfer function.

An ANN is "trained" by iteratively adjusting its weights to minimize the error by which it maps inputs to outputs for a data set comprising "input/output vector pairs." Simulation accuracy during and after training can be measured by a number of metrics, including coefficient of determination (R^2) and root mean square error (RMSE). An algorithm that is commonly used to train MLP ANNs is the back error propagation (BEP) training algorithm (Rumelhart and others, 1986). Jensen (1994) describes the details of the MLP ANN, the type of ANN used in this study. MLP ANNs can synthesize functions to fit high-dimension, nonlinear multivariate data. Devine and others (2003) and Conrads and Roehl (2005) describe their use of MLP ANN in multiple applications to model and control combined man-made and natural systems including disinfection byproduct formation, industrial air emissions monitoring, and surface-water systems affected by point and nonpoint source contaminants.

Experimentation with a number of ANN architectural and training parameters is a normal part of the modeling process. For correlation analysis or predictive modeling applications, a number of candidate ANNs are trained and evaluated for both their statistical accuracy and their representation of process physics. Interactions between combinations of variables also are considered. Finally, a satisfactory model can be exported for end-user deployment. In general, a high-quality predictive model can be obtained when:

- the data are well distributed throughout the state space (historical range of conditions) of interest,
- the input variables selected by the modeler share "mutual information" about the output variables, and
- the form "prescribed" or "synthesized" for the model used to "map" (correlate) input variables to output variables is a good one. Techniques such as OLS and physics-based finite-difference models prescribe the functional form of the model's fit of the calibration data. Machine learning techniques like ANN's synthesize a best fit to the data.

Subdividing a complex modeling problem into subproblems and then addressing each is a means to achieving the best possible results. A collection of submodels whose calculations are coordinated by a computer program constitutes a "super-model." For the Savannah study, individual ANN models (submodels) were developed for the river and marsh water level and salinity at each continuous station. These submodels were then incorporated into a "super-model" application that integrates the model controls, model database, and model outputs. The "super-model" for the project is the Model-to-Marsh (M2M) DSS described later in this report. The ANN models and plots described herein were developed using the iQuest™ data-mining software[2] (Version 2.03C DM Rev31). The ANN models were deployed in the DSS using the Visual Basic runtime library of the iQuest R/T™ software.

Statistical Measures of Prediction Accuracy

The R^2, the mean error (ME), root mean square error (RMSE), and percent model error (PME) have been computed for the training and testing data sets for each model and are listed in Appendix I. Model accuracy usually is reported in terms of R^2 and commonly is interpreted as the "goodness of the fit" of a model. A second interpretation is one of answering the question, "How much information does one variable or a group of variables have about the behavior of another variable?" In the first context, an $R^2 = 0.6$ might be disappointing, whereas in the latter, it is merely an accounting of how much information is shared by the variables being used. The developers believe that the river and marsh water-level and salinity models are unusually accurate relative to one-dimensional, two-dimensional, and three-dimensional finite-difference models developed for comparably complex estuaries and tidal marsh systems.

The ME and RMSE statistics provide a measure of the prediction accuracy of the ANN models. The ME is a measure of the bias of model predictions—whether the model over or under predicts the measured data. The ME is presented as the adjustment to the simulated values to equal the measured values. Therefore, a negative ME indicates an over simulation by the model and a positive ME indicates an under prediction by the ANN model. Mean errors near zero may be misleading because negative and positive discrepancies in the simulations can cancel each other. RMSE addresses the limitations of ME by computing the magnitude, rather than the direction (sign) of the discrepancies. The units of the ME and RMSE statistic are the same as the simulated variable of the model.

The minimum and maximum values of the measured output are listed in Appendix I. The accuracy of the models, as given by RMSE, should be evaluated with respect to the range of the output variable. A model may have a low RMSE, but if the range of the output variable is small, the model may only be accurate for a small range of conditions and the model error may be a relatively large percentage of the model response. Likewise, a model may have a large RMSE, but if the range of the output variable is large, the model error may be a relatively small percentage of the total model response. The PME was computed by dividing the RMSE by the range of the measured data. The models of the USGS river and marsh networks have the greatest range of the output variables.

Generally, the USGS river water-level and specific-conductance models have R^2 values in the 0.95 to 0.99 and 0.57 to 0.90 ranges, respectively, and PME values of 1.5 to 4.1 percent and 1.0 to 6.3 percent, respectively. (The statistics for the river models are based on the test data sets of the hourly models.) The USGS marsh water-level and specific-conductance models' range of R^2 values are 0.72 to 0.87 for water levels, 0.74 to 0.93 for specific conductance, and 3.4 to 5.4 percent and 4.0 to 10.6 percent, respectively, for PME. (Statistics for the marsh water level are based on the test data set of the hourly models, and statistics for the marsh specific-conductance predictions are based on all measured data.)

Development of Artificial Neural Network Models

The following sections describe how the water-level and salinity models were developed for the river and marsh sites. All the stations from the USGS and the GPA river and marsh networks were modeled. The river stations used to model the marshes were generally limited to the USGS river stations because their long period of record covers the largest range of hydrologic conditions. The model developments for each type of station—river water level, river salinity, marsh water level, and marsh pore-water salinity—follow a similar approach. One example is given for each type of model and is followed by a general description of the performance of all the stations of that particular type. Figures are shown for each type of model. A graph of measured and simulated data for a short period (1 to 2 months) is shown for the example station to show model performance. The graph of the example station is followed by graphs showing the performance of the daily river water-level and specific-conductance models for the period of record to show how well the models simulate the long-term trends of the system. The graphs of measured and simulated daily data are followed by graphs showing the performance of the hourly models for a short period (2 to 3 months). For the marsh models, the graph of the measured and simulated values for the example station is followed by graphs showing the performance of the hourly models. Model summaries for the example models (the input and output variables, size of training and testing data sets, and their respective R^2s) are given in table 3, and model summaries of all the models can be found in Appendix II. Summary statistics for all the models can be found in Appendix I.

[2] The iQuest™ software is exclusively distributed by Advanced Data Mining, LLC, 3620 Pelham Road, PMB 351, Greenville, SC 29615-5044 Phone: 864–201–8679, email: info@advdatamining.com: *http://www.advdatamining.com*.

The river models were developed in two stages. The first stage simulated the low-pass filtered daily water-level or specific-conductance signals to capture the long-term dynamics of the system. The second stage simulated the higher-frequency hourly water level or specific conductance, using the simulated water level and specific conductance as a carrier signal. Each river water-level model uses three general types of input signals, or time series: streamflow signal(s), water-level signal(s), and tidal range signal(s). The signals may be of the measured series values, filtered values, and/or a time derivative of the signals. The specific-conductance (salinity) models use an additional streamflow input: a time derivative of a moving window average, such as the 14-day difference in the 14-day average streamflows (fig. 19). The available data set for developing the models was randomly bifurcated into training and testing data sets. For the large data sets, such as the USGS riverine network stations dating back to 1994, a zone averaging, or box, filter of the data, was used to separate the data into training and testing data sets. Using the zone average filter, all the data are used in the test data set and a small selected sample of the data is used for the training data set. The filter separates the data set into user-specified number of zones or boxes and determines the input vectors with the highest information content and reserves these vectors for the training data set. The percentage of training and testing data depended on the length of the data set and the range of hydrologic conditions in the data set. Typically, the zone averaging filter uses a small percentage of the data (less than 10 percent) for the training data set. Model development summaries and variable descriptions can be found in Appendixes II and III.

Riverine Water-Level Model at Little Back River near Limehouse

The daily water-level model (wl8979a-2005-1) for Little Back River near Limehouse (station 02198979) uses streamflow, water-level, and tidal range inputs (table 3). The streamflow inputs are daily average streamflow (Q8500A) and the 1-day derivative of streamflow (DQ8500A). The water-level data inputs are daily water level from Fort Pulaski (FWL8980A) and the 1-day time derivative of daily water level lagged 1 day (DWLAD1). Gaps in the time series for Savannah River at Fort Pulaski (station 02198980) were filled by correlating to upstream water levels such as Front River at Broad Street (station 02198920). The tidal range inputs are daily tidal range (XWL8980A) and a 1-day time derivative of daily tidal range lagged 1 day (DXWLAD1). For testing and training the daily model, there were 78,980 data values available. Ten percent of the data was used for training and 90 percent was used for testing. The coefficient of determination, R^2, for the training and testing were 0.95 and 0.96, respectively (table 3, Appendices I and II). The daily model used two hidden-layer neurons.

The hourly water-level model (wl8979h-2005-1) uses the simulated daily water level from the daily model and Fort Pulaski water-level inputs. The simulated daily water-level input (PWL8979A) captures the long-term movement of the water level that is characterized by the streamflow and tidal range data in the daily model. The six water-level inputs; LG1NWL, LG1D3NWL, LG4D3NWL, LG7D3NWL, LG10D3NWL, LG13D3NWL, are the 1-hour lagged water level (LG1NWL), and 3-hour time derivatives of the water level lagged 1, 4, 7, 10, and 13 hours, respectively. The lagged water-level inputs capture the periodic semidiurnal tidal signal. For testing and training the hourly model, there were 79,216 data values available (approximately 11 years of hourly data from 1994 to 2005). The data set was bifurcated into training and testing data sets. Ten percent of the data was used for training and 90 percent was used for testing. The R^2 for the training and testing data were 0.98 and 0.98, respectively (table 3, Appendices I and II). The hourly model used two hidden-layer neurons.

The measured and simulated hourly water levels are shown in figure 22 for the first quarter of 2002. The model simulates the measured data well, but does not capture the full range of the tide and slightly under simulates the maximum and minimum water levels. The PME for the period of record is less than 3 percent (Appendix I)).

The daily water levels represent the chaotic portion of the water-level signal and the long-term trend of the system. The models are able to simulate this portion of the signal quite well (R^2 from 0.88 to 0.96) but miss the extreme high and low water levels (figs. 23 and 24). The simulations for the Front River at Houlihan Bridge (station 02198920, fig. 23*B*), under simulates the daily water levels more in the first half of the record than the second half. This may be the result of either a systematic change in the data collection or a change in the water-level behavior at the station. The under simulation for the first half of the time series explained the lower R^2 for the daily water-level model as compared to the other sites. The hourly water levels represent the periodic portion of the water-level signal and, generally, the models are able to simulate this portion of the signal quite well (R^2 from 0.98 to 0.995, figure 24).

Riverine Specific-Conductance Model at Little Back River at USFW Dock

The daily salinity model (sc89791a-2005-2) for Little Back River at USFW Dock uses six streamflow, three water-level, and three tidal range inputs. The streamflow inputs are daily average streamflow (Q8500A), the 1-day derivative of streamflow (D8500A), daily streamflow lagged 2 days (LAQ2), the 2-day change in streamflow (DAQ2), the 16-day change in streamflow (DAQ16), and the 30-day change in streamflow (DAQ30). The water-level data inputs are filtered daily water level from Fort Pulaski (FWL8980A), the 1-day time derivative of filtered daily water level (DWLA), and the 1-day time derivative of filtered daily water level lagged 2 days (LG2DWL). The tidal range daily inputs are daily tidal range (XWL8980A), the 1-day time derivative of daily tidal range (DXWLA), and the 1-day time derivative of daily tidal range lagged 2 days (LG2DXWLA). For testing and training

Table 3. Model name and model summary for four types of models used in the study.

[WL, water level; SC, specific conductance; XWL, tidal range; MWA, moving window average]

Model name	Model type	Input variables	Variable description	Training/testing data points	Hidden layer neurons
wl8979a-2005-1	Daily	Q8500A	daily average flow	7,987/70,993	2
		DQ8500A	1-day change in daily average flow		
		FWL8980A	filled, filtered daily WL		
		XWL8980A	daily tidal range		
		DXWLAD1	1-day change in tidal range, lagged 1 day		
		DWLAD1	1-day change in WL, lagged 1 day		
wl8979h-2005-1	Hourly	LG1NWL	1-hour lag in the in WL	8,029/71,187	2
		LG1D3NWL	1-hour lag in the 3-hour change in WL		
		LG4D3NWL	4-hour lag in the 3-hour change in WL		
		LG7D3NWL	7-hour lag in the 3-hour change in WL		
		LG10D3NWL	10-hour lag in the 3-hour change in WL		
		LG13D3NWL	13-hour lag in the 3-hour change in WL		
		PWL8979A	Predicted daily WL at 02198979		
sc89791a-2005-1	Daily	Q8500A	daily average flow	9,660/75,782	3
		DQ8500A	1-day change in daily average flow		
		LAQ2	2-day lag of the daily flow		
		DAQ2	2-day change in daily flow		
		DAQ16	16-day change in daily flow		
		DAQ30	30-day change in daily flow		
		FWL8980A	filled, filtered daily WL		
		XWL8980A	daily tidal range		
		DWLA	1-day change in WL		
		DXWLA	1-day change in tidal range		
		LG2DWLA	1-day change in WL, lagged 2 days		
		LG2DXWLA	1-day change in XWL, lagged 2 days		
		LG2DXWLA	1-day change in tidal range, lagged 2 days		
sc89791h-2005-1	Hourly	FWL8980A	filled, filtered daily WL	9,736/76,366	3
		XWL8980A	daily tidal range		
		NXWL	hourly WL		
		LG1NWL	1-hour lag in the in hourly WL		
		LG1D3NWL	1-hour lag in the 3-hour change in WL		
		LG4D3NWL	4-hour lag in the 3-hour change in WL		
		LG7D3NWL	7-hour lag in the 3-hour change in WL		
		LG10D3NWL	10-hour lag in the 3-hour change in WL		
		LG13D3NWL	13-hour lag in the 3-hour change in WL		
		PSC89791A	Predicted daily SC at 021989791		

Table 3. Model name and model summary for four types of models used in the study.—Continued

[WL, water level; SC, specific conductance; XWL, tidal range; MWA, moving window average]

Model name	Model type	Input variables	Variable description	Training/testing data points	Hidden layer neurons
pb2mwl-2005	Hourly	FWL8840	WL at station 02198840	3,284/18,228	2
		DFWL8840	difference with WL at 02198840		
		LG3DFWL8840	difference with WL at 02198840 lagged 3 days		
		LG6DFWL8840	difference with WL at 02198840 lagged 6 days		
		FWLDIF8977	WL at station 02198977		
		FWLDIF8979	WL at station 02198979		
		FWLDIF8920	WL at station 02198920		
pb2msc-2005-2	Hourly	SCDIF8840A	difference with SC between 02198840 and 021989791	2,142/18,770	1
		SCDIF8920A	difference with SC with difference with SC between 021988920 and 021989791		
		FSC89791A4WK	4-week MWAs of SC at 021989791		
		LG672FSC89791A4WKD4WK	difference between 4-week and lagged 4-week MWAs of SC at 021989791		
		FSC89791A2WKD4WK	difference between 2- and 4-week and lagged MWAs of SC at 021989791		
		FSC89791A1WKD2WK	difference between 1- and 2-week and lagged MWAs of SC at 021989791		
		FSC89791A48D1WK	difference between 2-day and 1-week and lagged MWAs of SC at 021989791		
		FSC89791DA48	difference between hourly and 2-day MWA of SC at 021989791		
		DFSC89791DA48	3-hour time derivative of SC at 021989791		
		LG3DFSC89791DA48	time derivative lagged 3 hours of SC at 021989791		
prb2msc	Hourly	RSC10S_12RS_A1WK	residual error of predicted weekly average SCGPA12RS (for decorrelation)	4,176/16,736	1
		RSC10S_11RB_A1WK	residual error of predicted weekly average SCGPA11RB (for decorrelation)		
		RSC10S_11B_A1WK	residual error of predicted weekly average SCGPA11B (for decorrelation)		
		PSCGPA10S_FLR_A1WK	1-week MWA of predicted hourly SC at GPA10S		

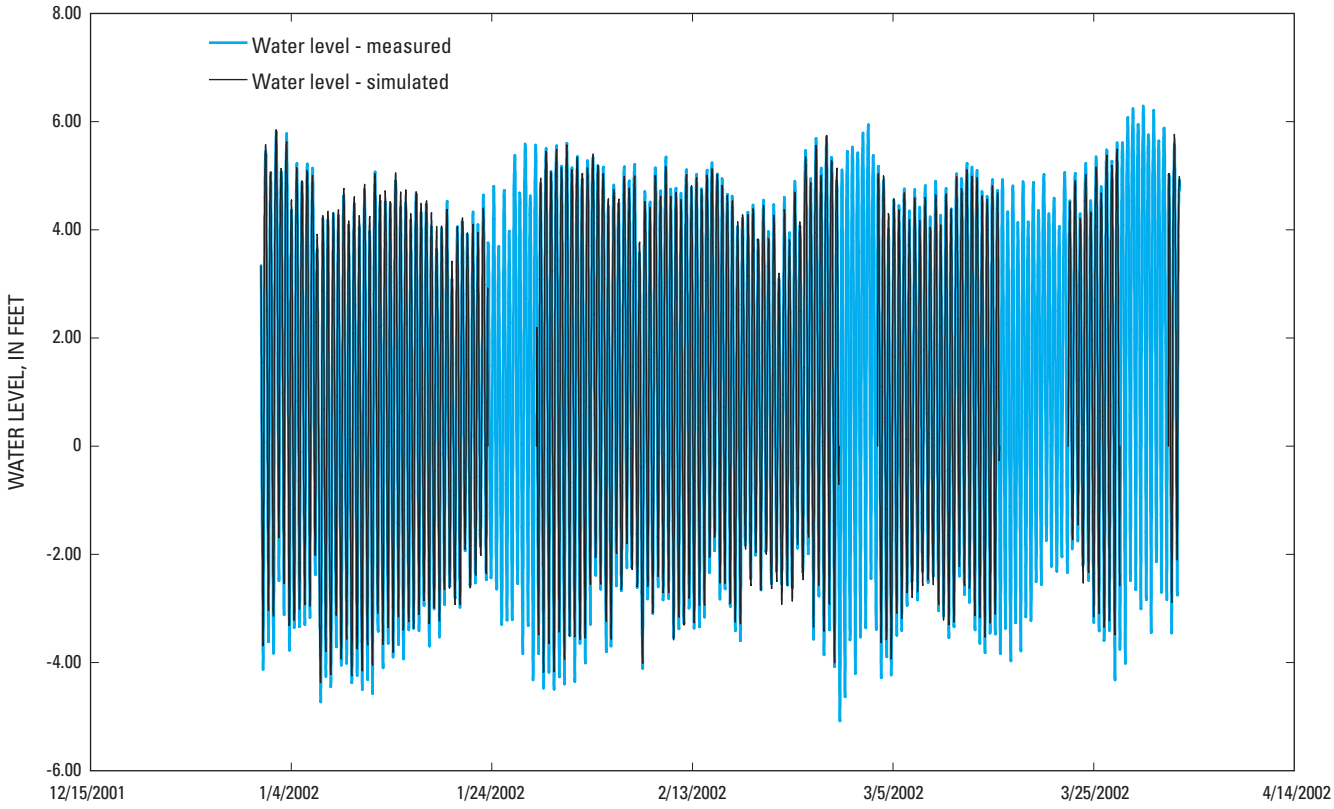

Figure 22. Measured and simulated hourly water levels at Little Back River near Limestone (station 02198979) for the period January 1 to March 31, 2002. Breaks in the prediction time series are caused by incomplete time series for one or more of the model inputs.

the daily model, there were 85,442 data values available. Eleven percent of the data was used for training, and 89 percent was used for testing. The R^2 for the training and testing were 0.89 and 0.87, respectively. The daily model used three hidden-layer neurons.

The hourly salinity model (sc89791h) uses simulated daily specific-conductance values from the daily model, two tidal range inputs, and six water-level inputs. The simulated daily specific-conductance input (PSC8979A) captures the long-term movement of the specific conductance that is characterized by the streamflow and tidal range data in the daily model. The two tidal range inputs are the daily tidal range (XWL8980A) and hourly tidal range (NXWL). The six water-level inputs—LG1NWL, LG1D3NWL, LG4D3NWL, LG7D3NWL, LG10D3NWL, LG13D3NWL—are 1-hour lagged water level, and 3-hour time derivatives of the water level lagged 1, 4, 7, 10, and 13 hours, respectively. The lagged water-level inputs capture the periodic semidiurnal tidal cycle signal. For testing and training the hourly model, there were 86,102 data values. Eleven percent of the data was used for training, and 89 percent was used for testing. The R^2 for the training and testing were 0.89 and 0.83, respectively. The hourly model used three hidden-layer neurons. A summary of the input variables, size of the training and testing data sets, number of hidden-layer neurons, and coefficient of determination for the hourly model can be found in table 3 and Appendix I.

The measured and simulated hourly salinities are shown in figure 25 for the summer of 2002. This period was the end of the 5-year drought that began in 1998 and had the highest salinity intrusions of the drought. The model simulates the measured data and captures the salinity intrusions occurring on a 14- and 28-day cycle. The model also is able to simulate the full range of the large salinity intrusion on about August 10, 2002.

The measured and simulated daily and hourly specific conductances for 1994 to 2005 for the four USGS river water-level gages are shown in figures 26 and 27. As with the water-level models, the daily specific conductance represents the chaotic portion of the signal, and the models are able to simulate this portion of the signal well (R^2 from 0.85 to 0.87, fig. 26) but do not capture the variability as well as the daily water-level models. The quality of hourly models, in terms of the coefficient of determination, vary from a R^2 of 0.57 at Savannah River at I-95 (station 02198840, fig. 27) to 0.87 at Front River at Houlihan Bridge (station 02198920, fig. 27). Although the specific-conductance model for I-95 explains only 57 percent of the variability, the results are quite satisfactory, in terms of timing and magnitude of response, for a station on the leading edge of the saltwater-freshwater interface where the salinity response is less than 0.5 psu.

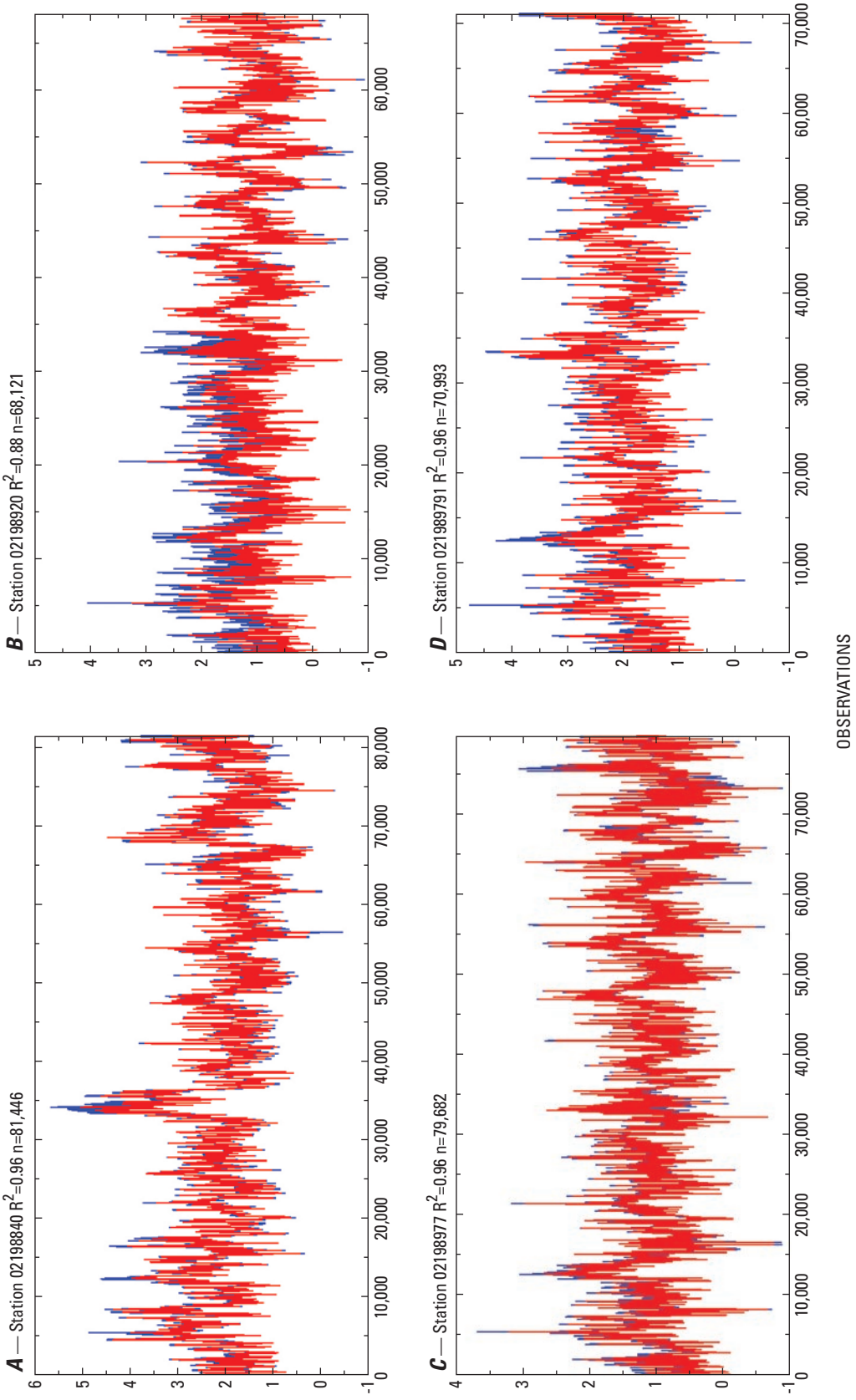

Figure 23. Measured (blue trace) and simulated (red trace) daily water levels for four USGS river gages for the period 1994 to 2004. Data to train the ANN models were bifurcated into training and testing sets. Graphs show data from the testing data set along with the coefficient of determination (R^2) and number (n) of data points.

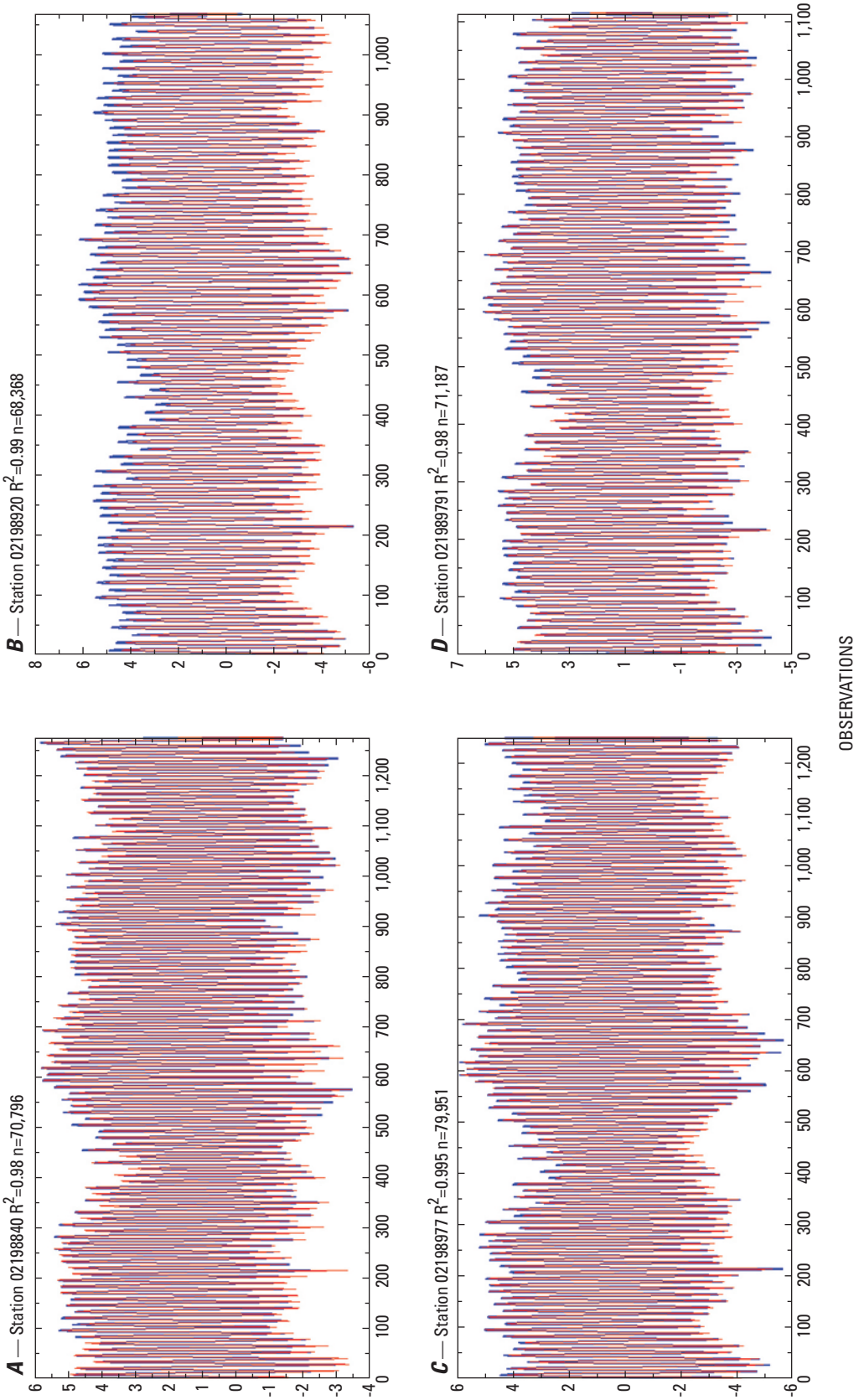

Figure 24. Measured (blue trace) and simulated (red trace) hourly water levels for four USGS river gages. Models were trained and tested on data from the period 1994 to 2004. Data to train the ANN models were bifurcated into training and testing sets. For clarity, only 1,100 observations (approximately 50 days) are shown from the testing data set along with the coefficient of determination (R^2) and number (n) of data points for the testing data set.

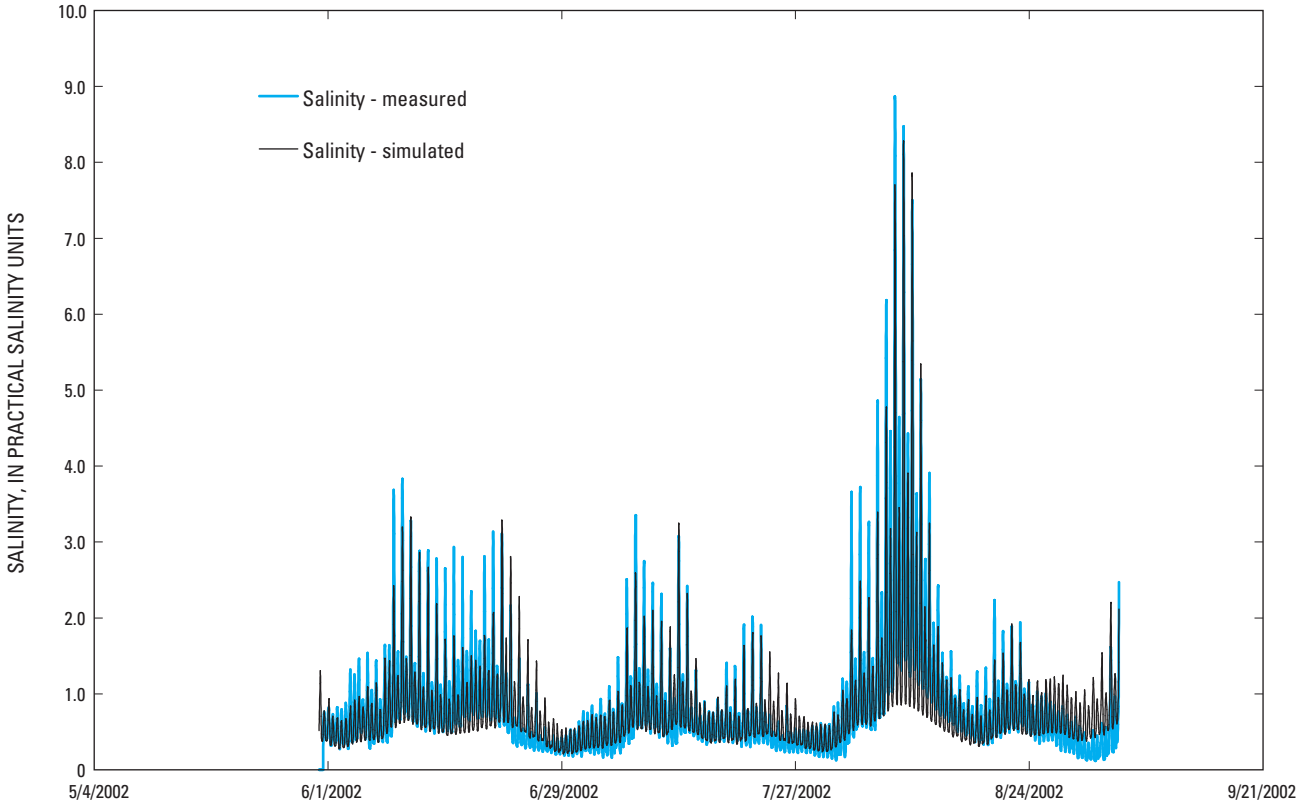

Figure 25. Measured and simulated hourly salinity at Little Back River at U.S. Fish and Wildlife Service Dock (station 02198979) for the period June 1 to August 31, 2002.

Marsh Water-Level Model at Little Back River at Site B2

The hourly water-level model (pb2mwl-2005) for Little Back River at Site B2 uses seven water-level inputs and differences in water levels from the four USGS riverine gages in the vicinity of SNWF. The water-level inputs include the water level at I-95 (station 02198840), 1-day change in water level, 1-day change in water level lagged 3 days, and 1-day change in water level lagged 6 days (variables FWL8840, DFWL8840, LG3DFWL8840, and LG6DFWL8840, respectively). Differences in water level at Site B2 and the USGS riverine gages are also used for inputs. These inputs include the difference in water level with stations 02198977, 02198979, and 02198920 (variables FWLDIF8977, FWLDIF8979, and FWLDIF8920, respectively). For testing and training the daily model, there were 21,512 data values available (approximately 2.5 years of hourly data from 1999 to 2005). Fifteen percent of the data was used for training and 85 percent was used for testing. The R^2 for the training and testing were 0.80 and 0.77, respectively. The daily model used two hidden-layer neurons.

The measured and simulated hourly water levels are shown in figure 28 for the first quarter of 2002. The model simulates the measured data well but does not capture the full range of the tide and slightly under simulates the maximum and minimum water levels.

The measured and simulated hourly water levels for the seven USGS marsh stations are shown in figures 29 and 30. The quality of marsh water-level models, in terms of the coefficient of determination, varies from a R^2 of 0.72 to 0.87. Generally, the models for the stations closer to the harbor (Sites B3, B4, and F1) explain more of the water-level variability (R^2 vary from 0.84 to 0.87) than the models for the stations farther from the harbor (R^2 vary from 0.72 to 0.79).

Marsh Specific-Conductance Model at Site B2

A potential mitigation scenario to ameliorate an increase in salinity in the vicinity of the SNWR would be to divert additional streamflow to the Middle and Little Back Rivers. One concern with using only the long-term USGS riverine gages to simulate the pore-water salinity in the marsh is that there would not be any data on the Middle Back River that may be important for evaluating mitigation alternatives. Data in this area are available from the GPA river networks. Although the data from these stations are limited to conditions from either the summer of 1997 or 1999, data from GPA10, GPA11, GPA11R, and GPA12 were used as inputs to

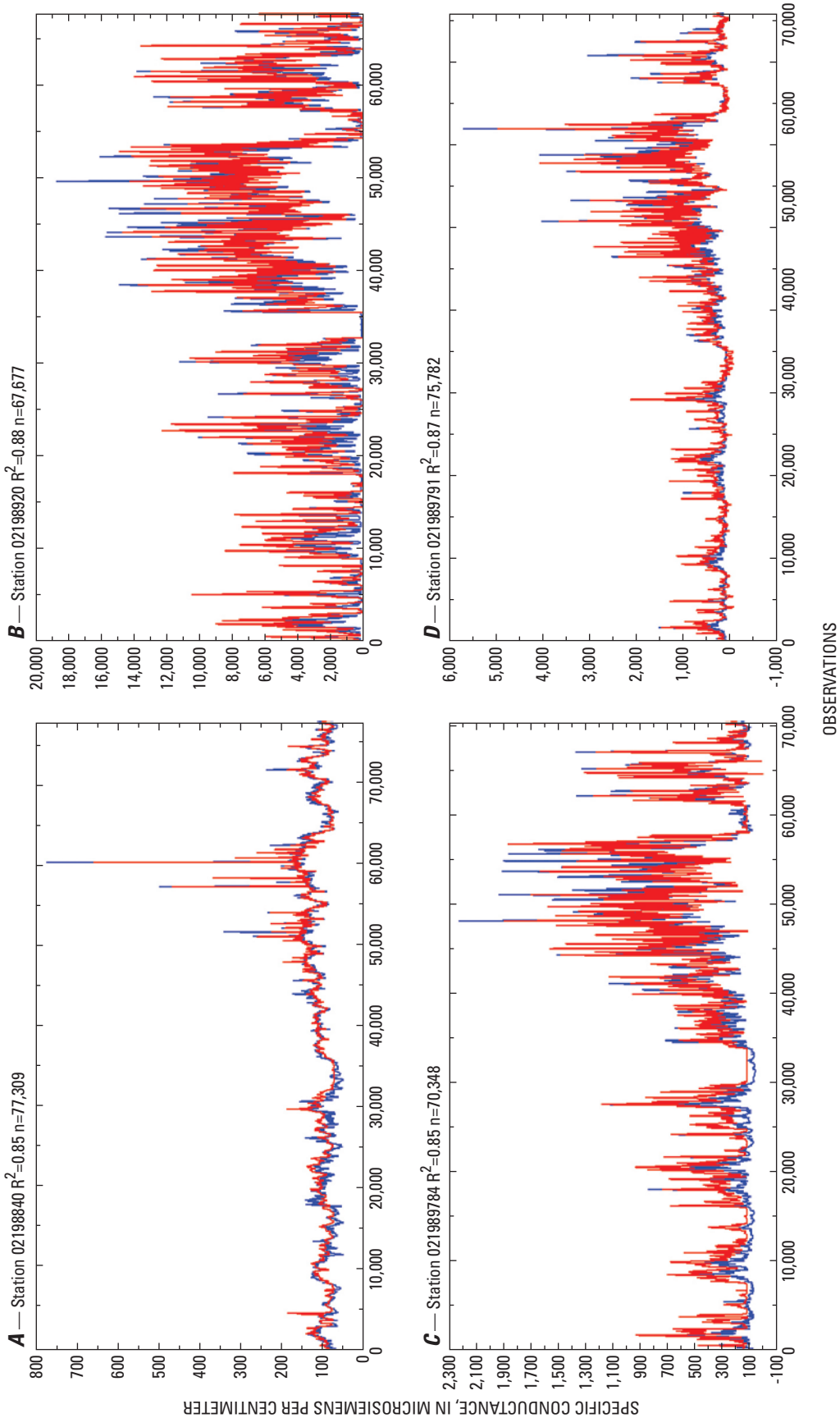

Figure 26. Measured and simulated daily specific conductance for four USGS river gages for the period 1994 to 2004. Data to train the ANN models were bifurcated into training and testing sets. Graphs show data from the testing data set along with the coefficient of determination (R^2) and number (n) of data points.

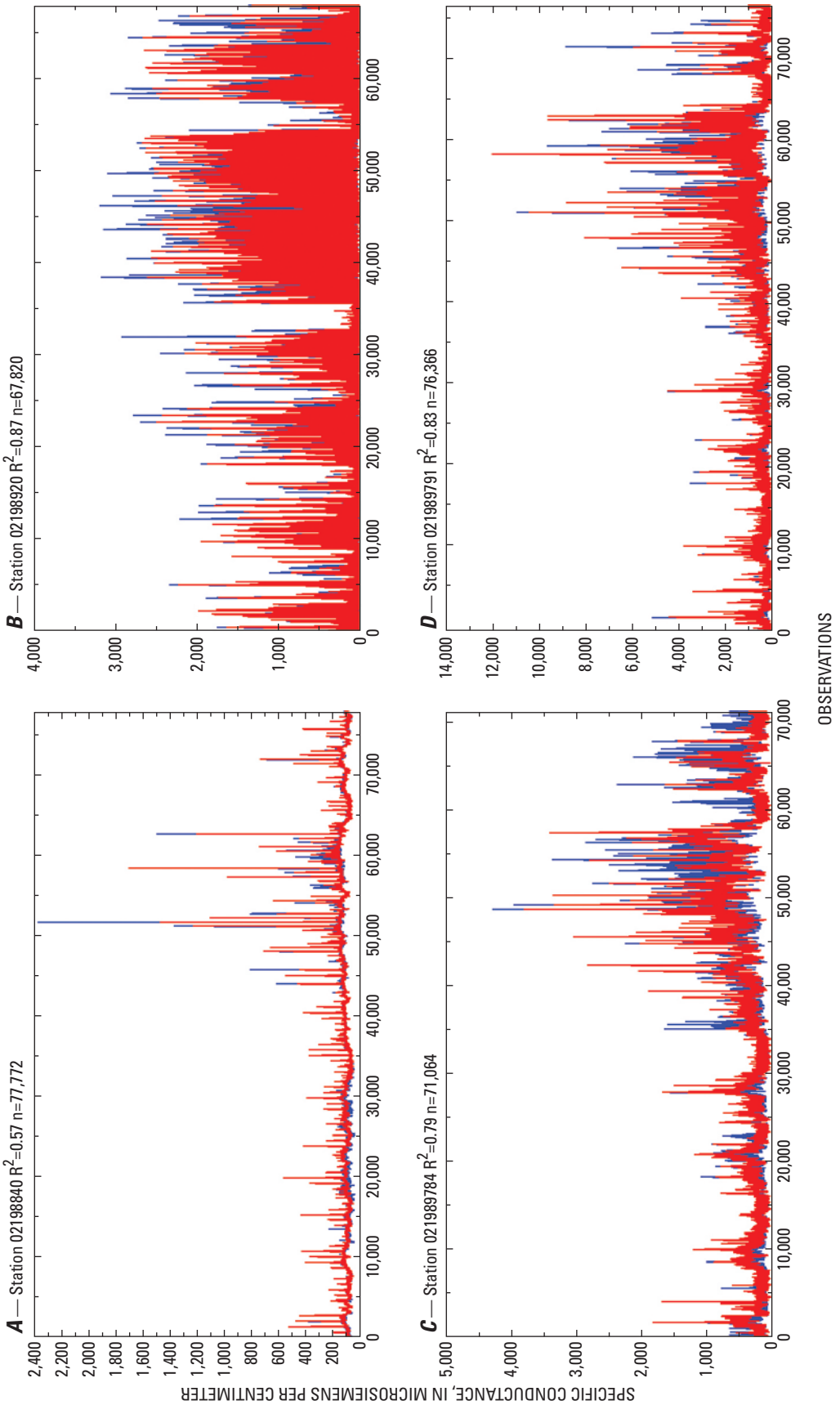

Figure 27. Measured (blue trace) and simulated (red trace) hourly specific conductance for four USGS river gages for the period 1994 to 2004. Data to train the ANN models were bifurcated into training and testing sets. Graphs show data from the testing data set along with the coefficient of determination (R^2) and number (n) of data points.

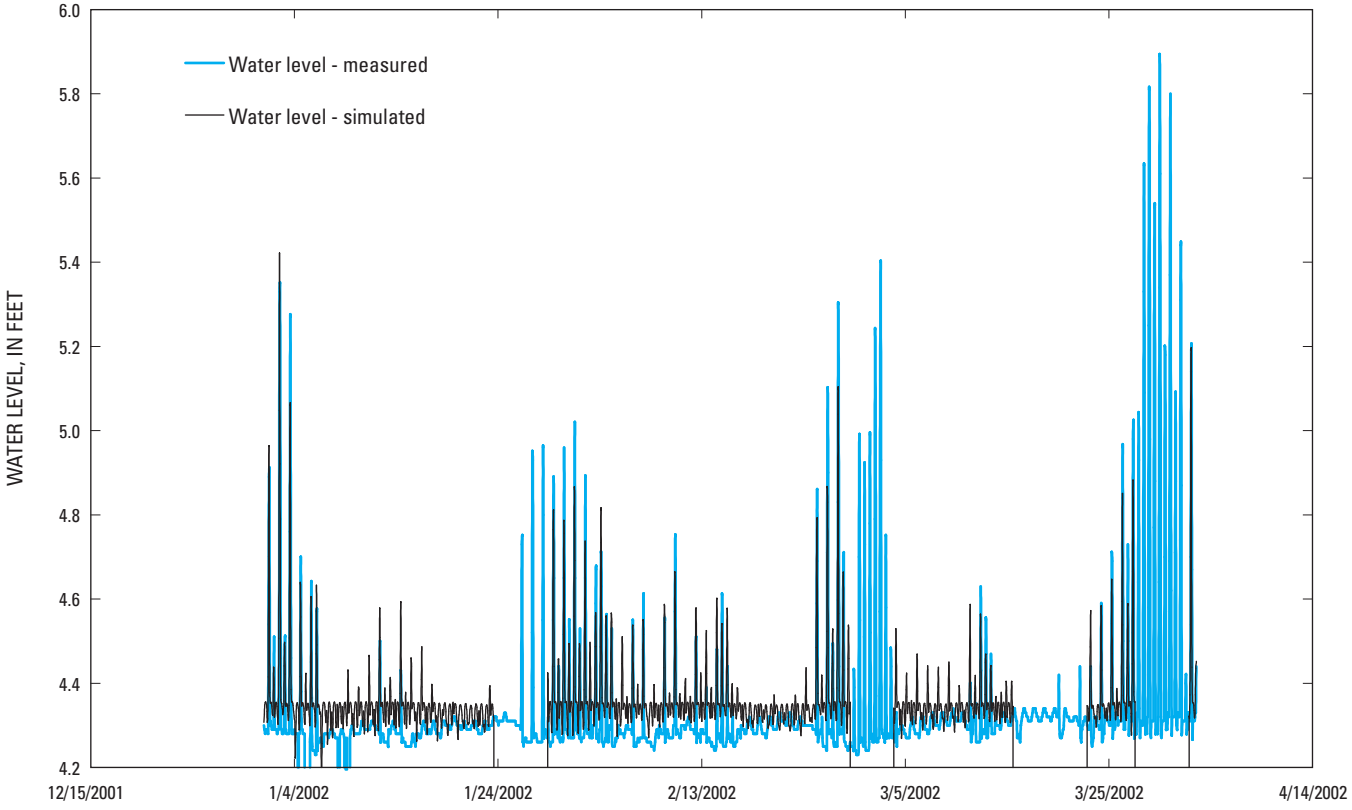

Figure 28. Measured and simulated hourly water levels at Site B2 on the Little Back River for the period January 1 to March 31, 2002. Breaks in the prediction time series are caused by incomplete time series for one or more of the model inputs.

the marsh salinity models to address spatial distribution of the river salinity inputs for the marsh salinity models.

There are two technical issues with using the short-term GPA data that need to be addressed. The first technical issue is that the GPA data are not concurrent with the USGS marsh data (summers of 1997 and 1999 compared to 2000–2005). The models for the four GPA stations were used to simulate the time series of specific conductance for the period 2000–2005. To generate the data for this period, the GPA models were used to make salinity predictions for a range of streamflow conditions much larger than measured during the summers of 1997 and 1999 (fig. 18*A*). The second issue is that the GPA data are highly correlated. To ensure that the data from the GPA site inputs unique information for the marsh predictions, the data for stations GPA11, GPA11R, and GPA12 were systematically decorrelated from GPA10.

The marsh pore-water salinities were modeled in two stages. The first stage used the USGS river data to simulate the marsh salinity. The second stage used the GPA river data to simulate the residual error (difference between the simulated and measured marsh salinity) from the first stage model. The final marsh salinity predictions are the sum of the predictions from the two models.

The first stage pore-water salinity model (pb2msc-2005-2) for Little Back River at Site B2 uses 10 specific-conductance inputs and differences in specific conductance from two USGS riverine gages in the vicinity of SNWF. Two inputs are the difference in specific conductance at the Little Back River at USFW Dock (021989791) and the Savannah River at I-95 (station 02198840) and Front River at Houlihan Bridge (station 02198920), variables SCDIF8840A and SCDIF8920A, respectively. There are four moving window average inputs of 48 hours, 1-, 2-, and 4-weeks (variables FSC89791A48, FSC89791D1WK, FSC89791D2WK, FSC89791D4WK) and four time derivative inputs (variables LG672FSC89791A4WKD4WK, FSC89791DA48, DFSC89791DA48, and LG3DFSC89791DA48). For testing and training the daily model, there were 20,912 data values available (approximately 5 years of hourly data from 1999 to 2005). Ten percent of the data was used for training, and 90 percent was used for testing. The R^2 for the training and testing were 0.83. The model used one hidden layer neuron.

The second stage model (prb2msc) simulates the residual error from the first stage marsh pore-water salinity model. Four inputs used to simulate the residual error included weekly averages of the decorrelated specific-conductance variable from each GPA site and a 1-week moving window average of specific conductance at GPA10 (variables RSC10S_11B_A1WK, RSC10S_11BR_A1WK, RSC10S_12RS_A1WK, and PSCGPA10S_FLR_A1WK, respectively). A summary of the

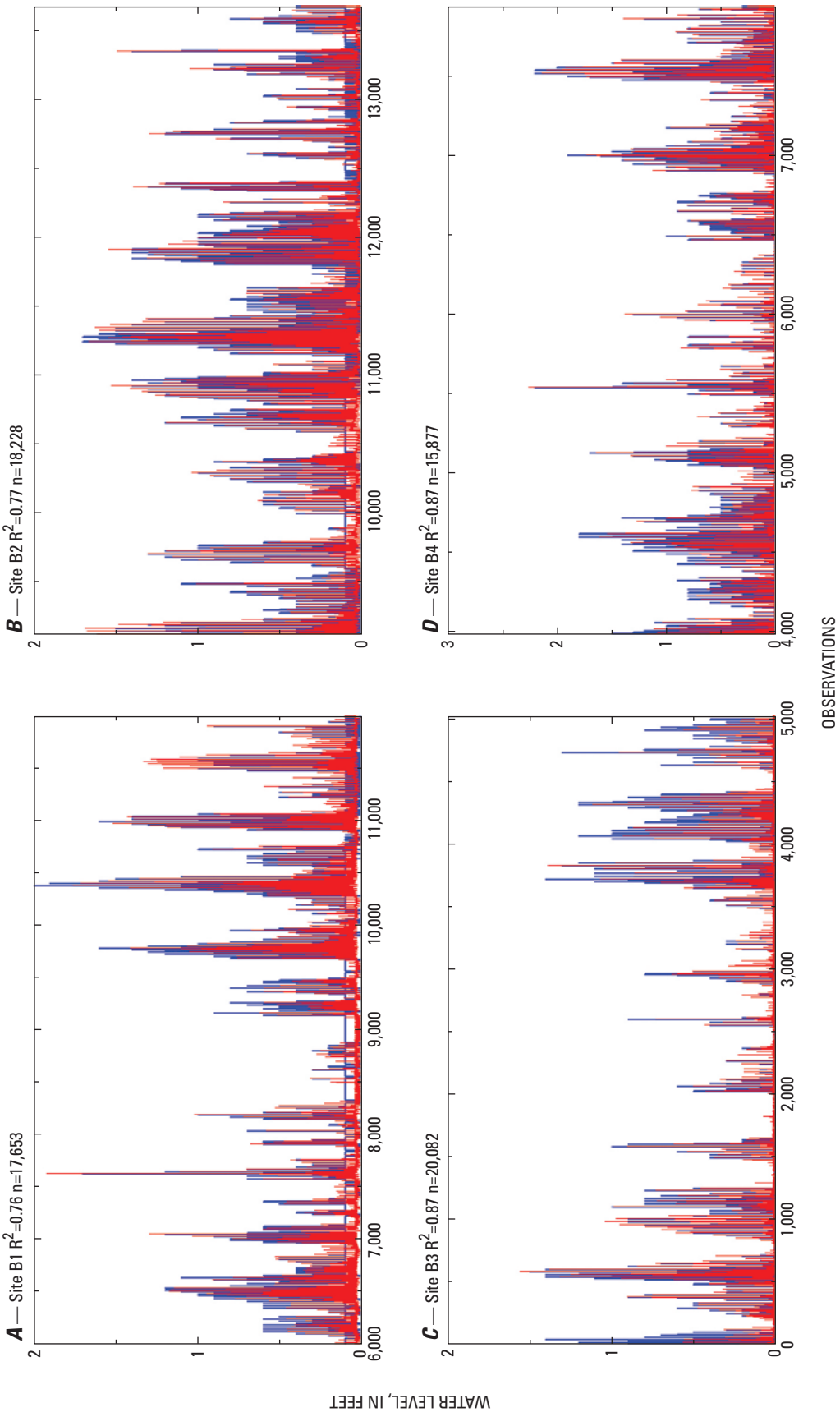

Figure 29. Measured (blue trace) and simulated (red trace) hourly water levels for four USGS marsh gages along the Little Back and Back Rivers for the period June 2000 to May 2005. Data to train the ANN models were bifurcated into training and testing sets. For clarity, only 4,500 to 5,000 observations (approximately 180 days) are shown from the testing data set along with the coefficient of determination (R^2) and number (n) of data points for the testing data set.

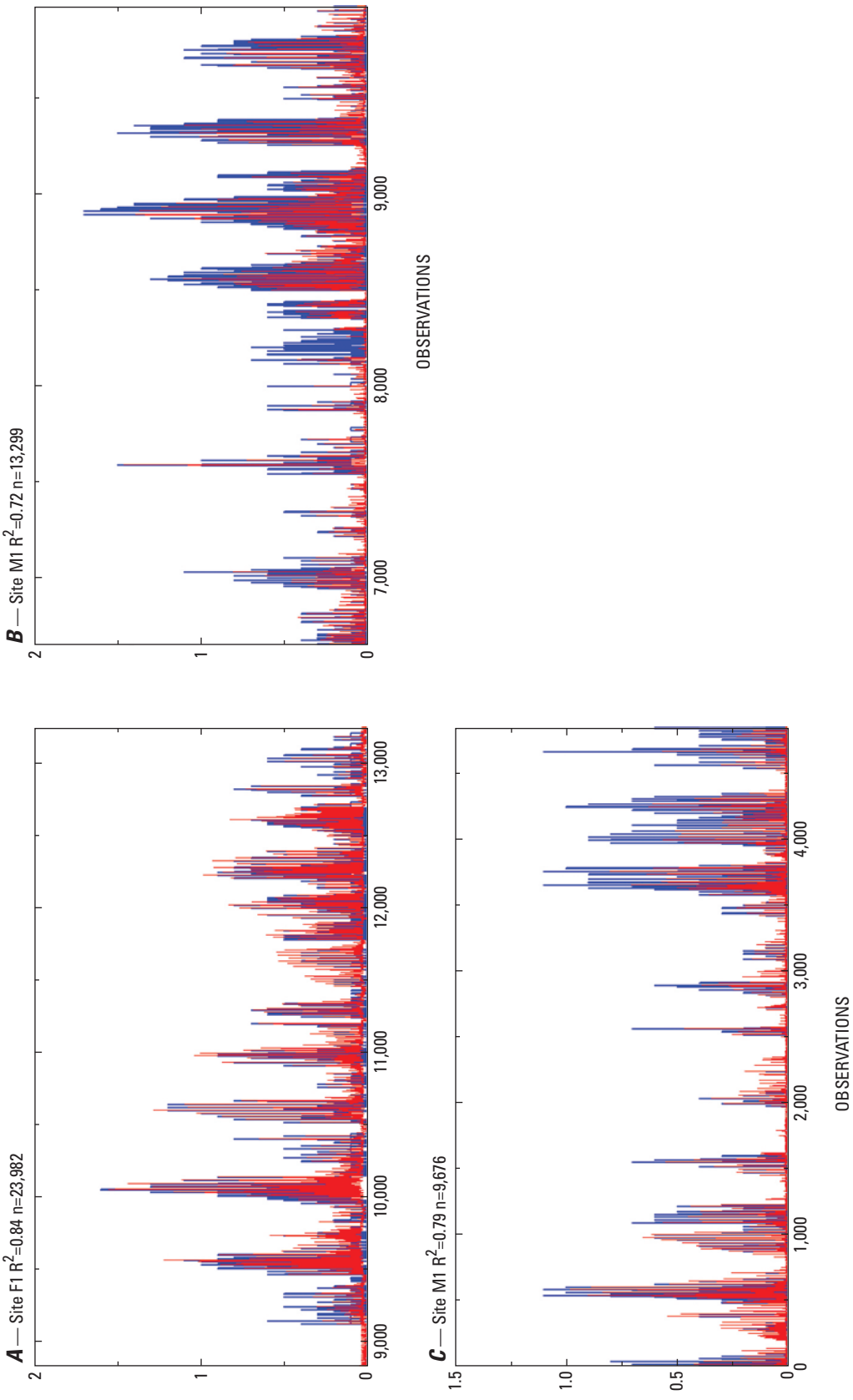

Figure 30. Measured (blue trace) and simulated (red trace) hourly water levels for the three USGS gages along the Middle Back and Front Rivers for the period June 2000 to May 2005. Data to train the ANN models were bifurcated into training and testing sets. For clarity, only 4,500 to 5,000 observations (approximately 180 days) are shown from the testing data set along with the coefficient of determination (R^2) and number (n) of data points for the testing data set.

input variables, size of the training and testing data sets, number of hidden-layer neurons, and coefficient of determination for the daily model can be found in table 3 and Appendix I.

The measured and simulated hourly pore-water salinities are shown in figure 31 for summer 2002. This period was the end of the 5-year drought that began in 1998 and had the highest salinity intrusions of the drought. The model simulates the salinity intrusions occurring on a 14- and 28-day cycle and generally under simulates the salinity concentrations.

The measured and simulated hourly salinity for the seven USGS marsh stations are shown in figures 32 and 33. The quality of marsh water-level models, in term of the coefficient of determination, varies from a R^2 of 0.74 to 0.93. Generally, the models follow the trend of the measured data, as reflected in the high R^2, but miss the variability over short time periods.

Analysis of Estuary Dynamics Using Three-Dimensional Response Surfaces

The river and marsh ANN models can be used to examine the effect of water level and tidal range in the harbor, Savannah River streamflow at Clyo on water levels, and specific conductance in the primary and secondary river channels and the marshes. Three-dimensional response surfaces can be generated to display two explanatory variables (water level, tidal range, or streamflow) with a response variable (specific-conductance or water level). The data for the surface are computed by the ANN model across the full range of the displayed input variables, while the "unshown" inputs (all the models have more than two inputs) are set to a constant value, such as a historical mid-range or mean value. Response surfaces are a valuable tool for understanding the dynamics of an estuary and for comparing how variable interactions differ throughout the system.

The conceptual model of salinity intrusion occurring during de-stratified conditions during neap tides (fig. 13) can be seen in the plot of the time series at GPA04 for summer 1999 (fig. 14). Salinity intrusion dynamics can also be seen in the response surfaces showing the interaction of daily streamflow, water level, and specific conductance for neap and spring tidal conditions (fig. 34). For example, the salinity intrusion on the Front River at Houlihan Bridge site (station 02198920) is shown in figure 34. The response surfaces show increasing streamflow along the x-axis (horizontal, out of the page), increasing water level along the y-axis (horizontal, into

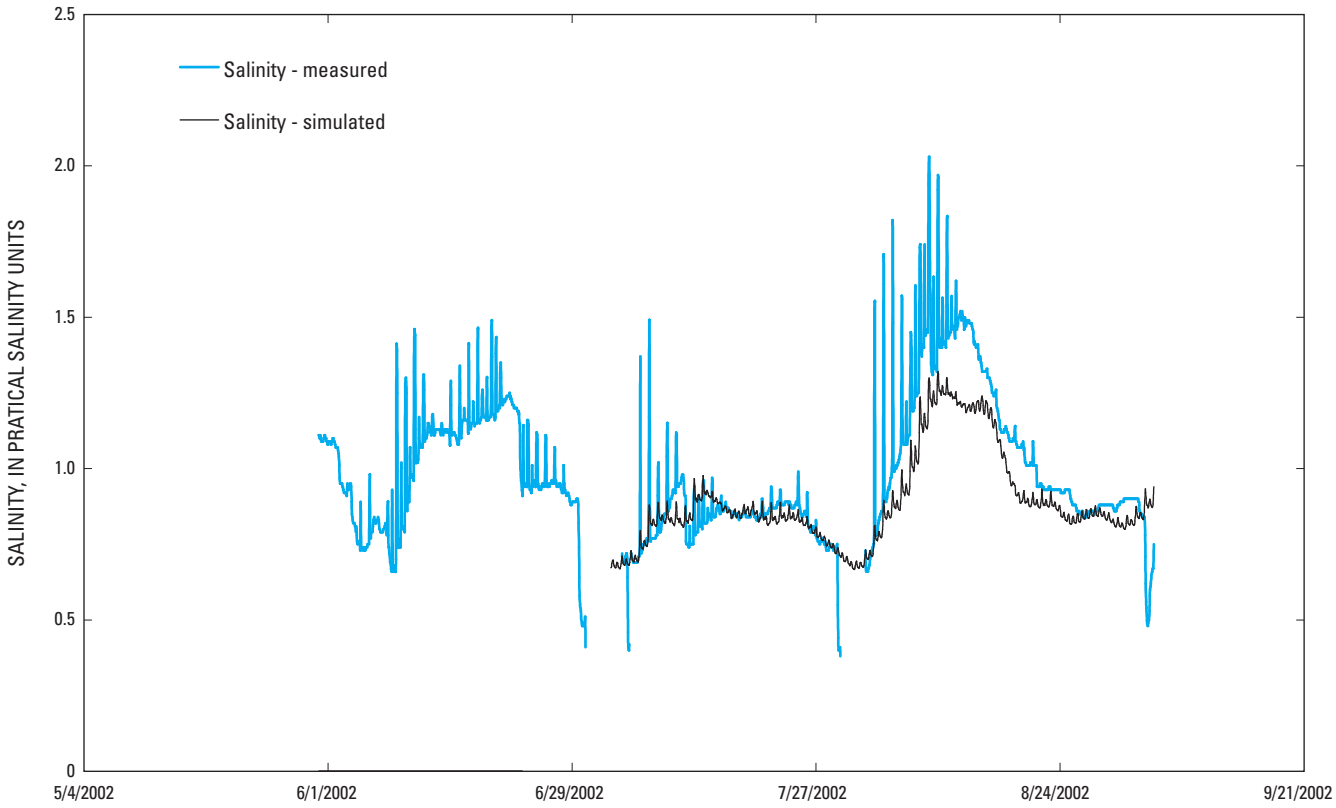

Figure 31. Measured and simulated hourly salinities at Little Back River at Site B2 for the period June 1 to August 31, 2002. Breaks in the prediction time series are caused by incomplete time series for one or more of the model inputs.

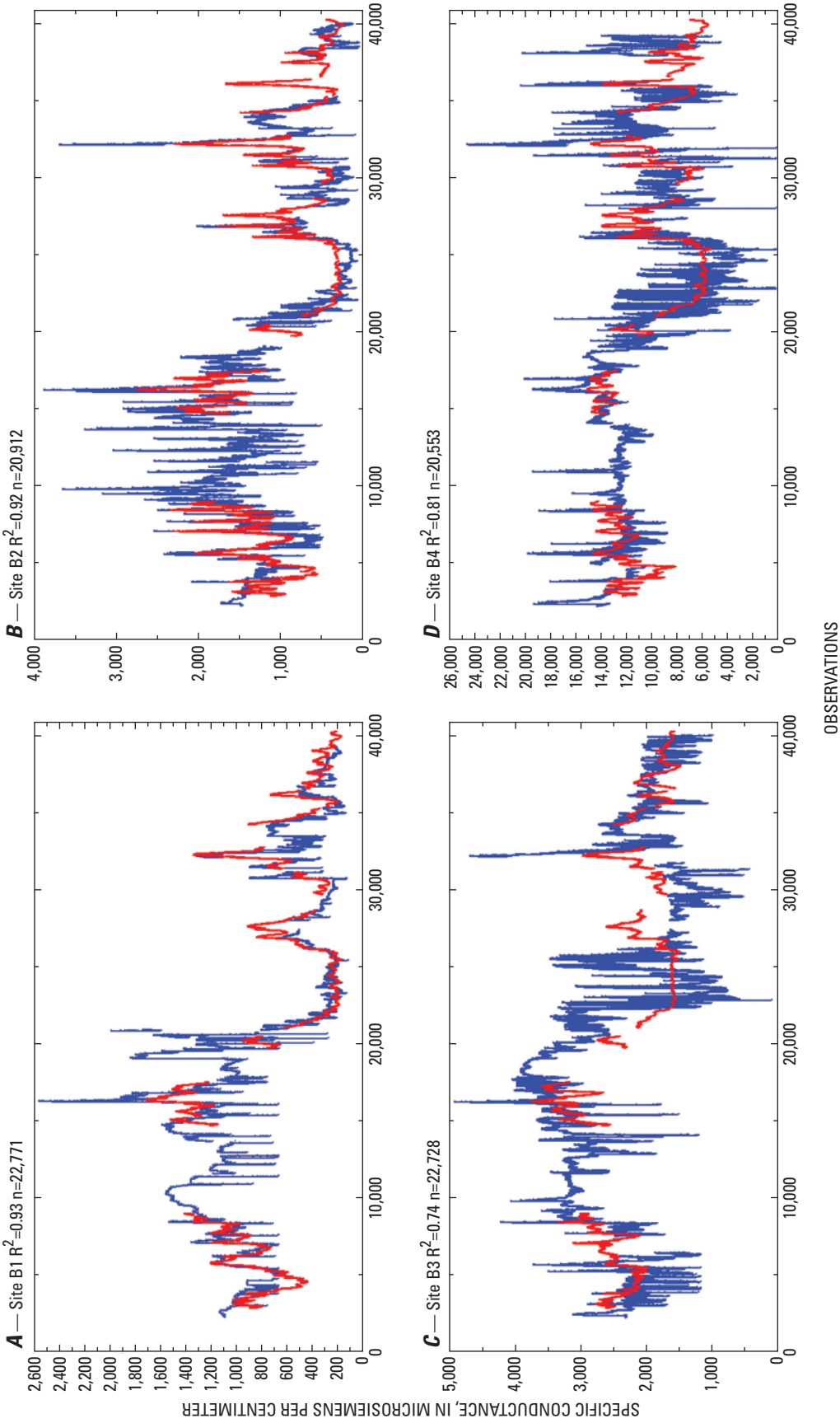

Figure 32. Measured (blue trace) and simulated (red trace) hourly specific conductance for four USGS gages along the Little Back and Back Rivers for the period June 2000 to May 2005. Data to train the ANN models were bifurcated into training and testing sets. Graphs show the complete data set along with the coefficient of determination (R^2) and number (n) of data points. Breaks in the simulated values are caused by one or more missing input values.

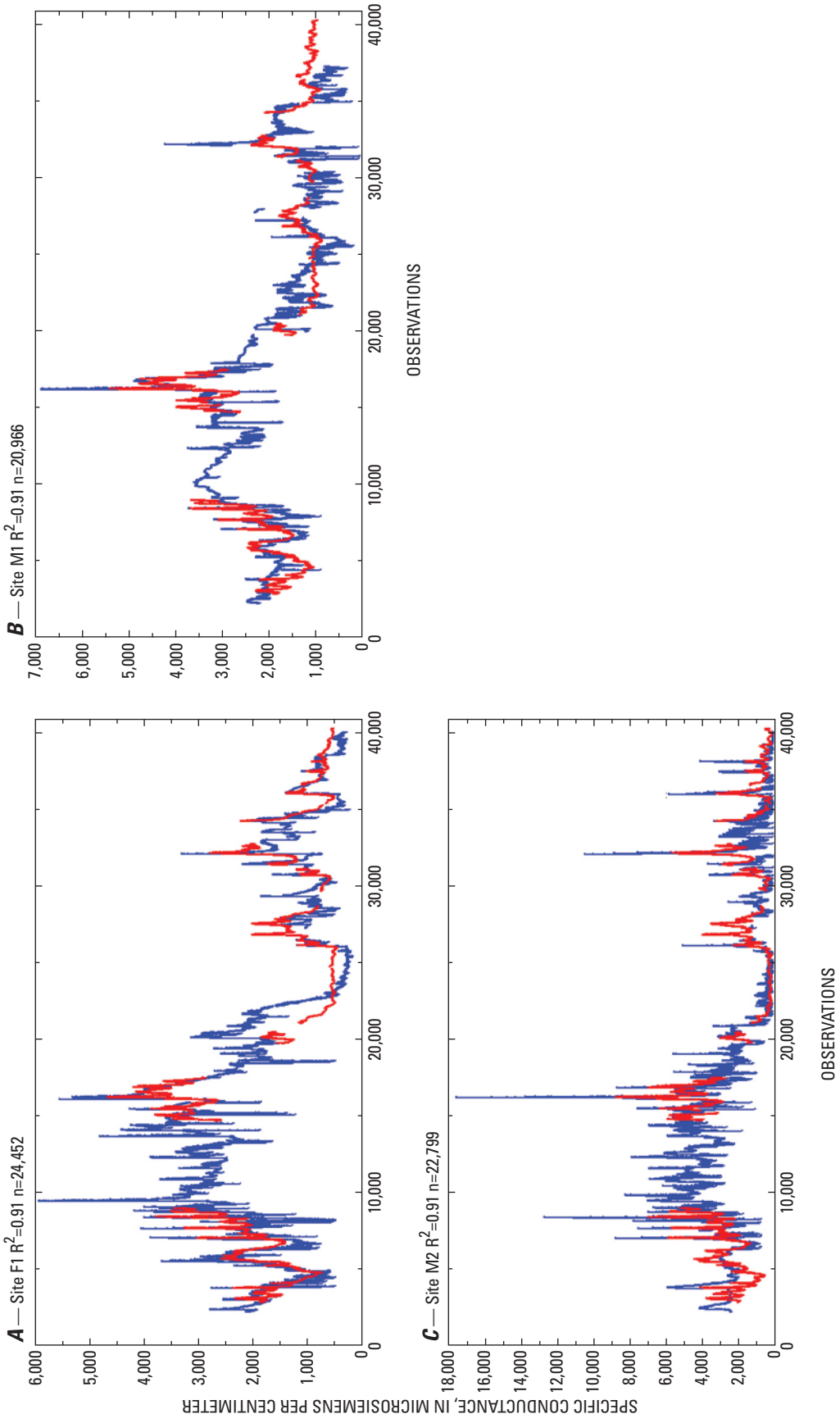

Figure 33. Measured (blue trace) and simulated (red trace) hourly specific conductance for four USGS gages along the Front and Middle Back Rivers for the period June 2000 to May 2005. Data to train the ANN models were bifurcated into training and testing sets. Graphs show data from the testing data set along with the coefficient of determination (R^2) and number (n) of data points. Breaks in the simulated values are caused by one or more missing input values.

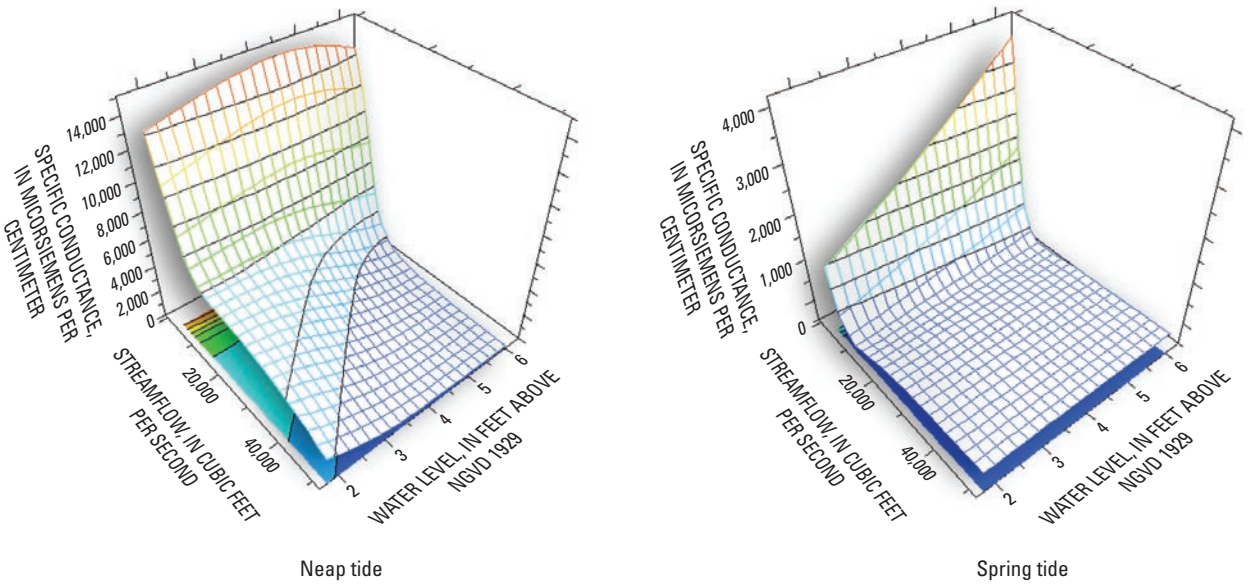

Figure 34. The interaction of water level (FWL8980A) and streamflow (Q8500A) on specific conductance for Front River at Houlihan Bridge (station 02198920) for neap and spring tide conditions. The response surface on the left shows specific conductance response at the gage under neap tide conditions (all other input values set to the mean historical condition for both response surfaces). The response surface on the right shows the gage response under spring tide conditions. Note differences in the z-axis (vertical) scale. During neap tides, salinity intrusion at Front Street is greatest during low-flow conditions through the full range of Harbor water-level conditions. During spring tides, salinity intrusion is greatest during low-flow conditions and increasing water-level conditions in the Harbor.

the page), and increasing specific-conductance (salinity) along the z-axis (vertical) for neap and spring tides (left and right response surfaces, respectively). All other variables were set to their historical means. In figure 34, the neap tide surface on the left shows that salinity intrusion occurs during low-flow conditions for the entire range of water levels in the harbor. Note the change across the response surface when flows are below 10,000 ft^3/s. The spring tide surface on the right in figure 34 shows that salinity intrusion during spring tides occurs only during low flow and increasing harbor water-level conditions. Note the slope of the edge of the response surface at low flows as water levels increase and specific conductance increases from 1,000 to 4,000 µS/cm.

The response surfaces at the I-95 Bridge (station 02198840) show different salinity intrusion dynamics (fig. 35), with the greatest salinity intrusions occurring on spring tides. The response surface at left shows that during neap tides, increases in salinity occur during low-flow conditions and all water-level conditions in the harbor. The response surface at right shows that during spring tides, similar specific-conductance levels occur during low-flow conditions and for most water levels. During very high harbor water-level conditions, salinity intrusion can be more than twice as high as during neap tides. The increased salinity intrusion is possibly due to decreased stratification and fully mixed conditions during neap and spring tides in the upper reaches of the river, which would limit intrusion to periods with increased volumes of saltwater (high water-level conditions), high mixing energy (spring tides), and limited upstream flow resistance to intruding saltwater (low-flow conditions). It should be remembered that the response surfaces show daily values. Maximum hourly specific-conductance intrusions during the drought ranged from 100 to 8,000 µS/cm.

The increased daily specific-conductance, or salinity, values during spring tides at I-95 (station 02198840) can also be seen by plotting streamflows, tidal ranges, and specific conductance with the other inputs set to their historical means. Figure 36 shows that during low flow and historical mean harbor water levels, daily specific conductance can increase as much as 100 µS/cm from neap to spring tides.

Figure 37 shows specific-conductance response surfaces for two sites on the Little Back River. The response surface at left for Little Back River at the USFW Dock (Station 021989791) shows that at mean harbor water levels, salinity intrusion is greatest during low flows and spring tides. Downstream at Little Back River near the Lucknow Canal (Station 021989784), higher specific conductance under similar water-level conditions occurs during low flows and neap tides. Although neither response surfaces show dramatic changes in specific-conductance response under different tidal

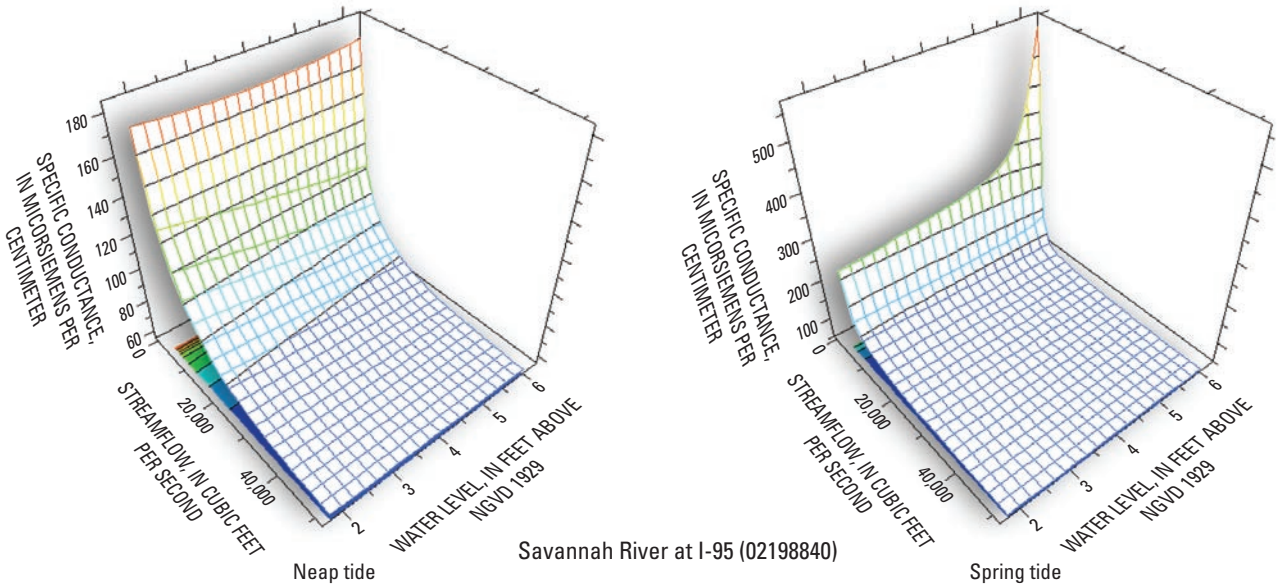

Figure 35. The interaction of water level (FWL8980A) and streamflow (Q8500A) on specific conductance at Savannah River at I-95 (station 02198840) for neap and spring tide conditions. The response surface on the left shows specific conductance response at the gage under neap tide conditions (all other input values set to the mean historical condition for both response surfaces). The response surface on the right shows the specific conductance response under spring tide conditions. Note differences in the z-axis (vertical) scale. During neap tides, salinity intrusion at I-95 is greatest during low-flow conditions through the full range of water-level conditions. During spring tides, salinity intrusion can be over twice as high as neap tide during low-flow and high water-level conditions.

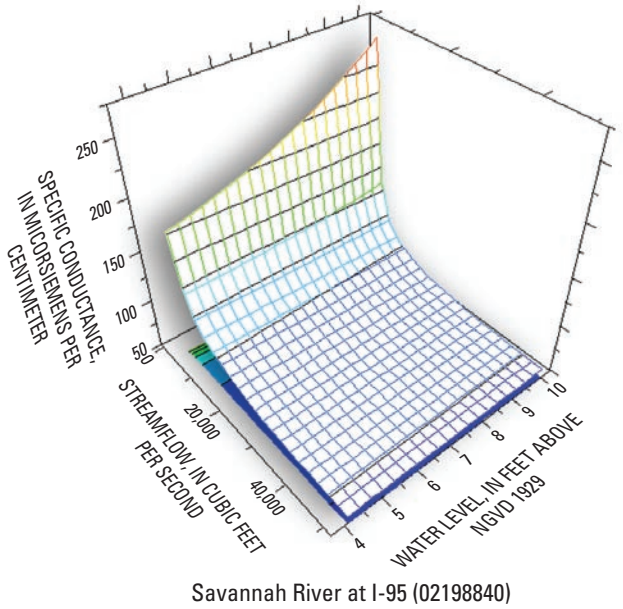

Figure 36. The interaction of tidal range (XWL8980A) and streamflow (Q8500A) on specific conductance at Savannah River at I-95 (station 02198840). The response surface shows the specific conductance response at the gage under mean water-level conditions (all other input values set to the mean historical condition for both surfaces). During mean water-level conditions, specific conductance intrusion at I-95 is greatest during low-flow and spring-tide conditions.

range conditions, they do indicate a gradual change in salinity intrusion behavior from the I-95 Bridge to the station near Lucknow Canal.

Response surfaces can also be used to analyze the influence of Savannah River streamflow and harbor water levels on the local water level in the vicinity of the SNWR. As noted above, streamflow at Clyo, Ga., (station 02198500) and harbor water levels (station 02198980) are virtually uncorrelated (R=-0.03). The effect of streamflow and water level on local water levels depends on their proximity to the harbor. Water levels in the upper reaches exhibit more riverine influence than the downstream stations. The riverine influence diminishes farther downstream, and the influence of the tide is more prominent. Figures 38 and 39 show response surfaces for four water-level gages. The upstream station, Savannah River at I-95 (fig. 38, left response surface), shows a significant contribution of streamflow to the local water level. The downstream station, the Front River at Broad Street (fig. 39, right response surface), shows that streamflow has a negligible influence on its water level. The other two stations, Front River at the Houlihan Bridge (station 02198920, fig. 38, right response surface) and Little Back River at Limehouse (station 02198979, fig. 39, left response surface), show large contributions of harbor water level and small contributions of streamflow to the local water levels.

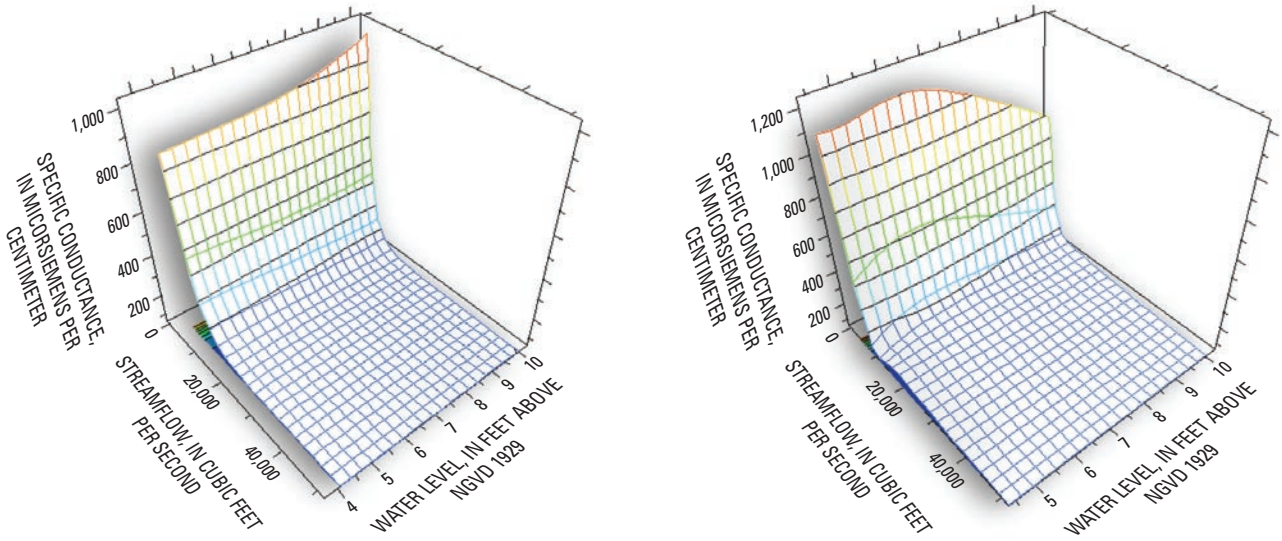

Figure 37. The interaction of tidal range (XWL8980A) and streamflow (Q8500A) on specific conductance at Little Back River at U.S. Fish and Wildlife Service Dock (station 021989791, left response surface) and for Little Back River at Lucknow Canal (station 021989784, right response surface). The response surface on the left shows higher salinity intrusion at the upstream station occurs during spring tides. The response surface on the right shows that high salinity intrusions occur during neap tides.

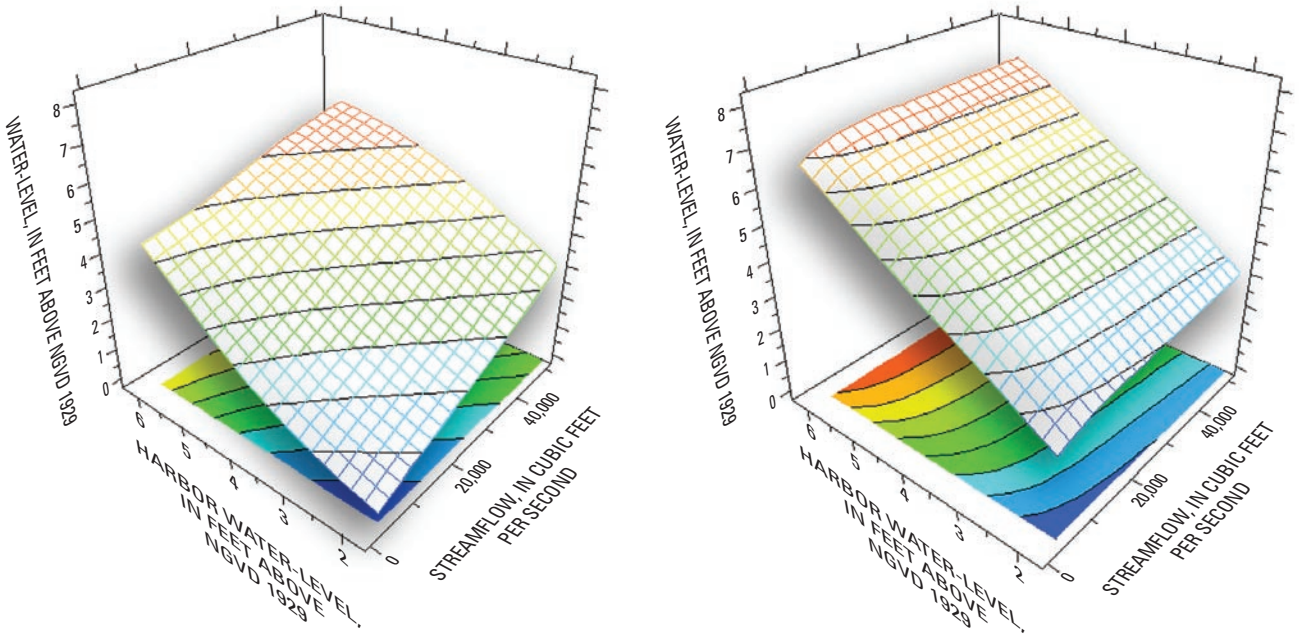

Figure 38. The interaction of harbor water level (FWL8980A) and streamflow (Q8500A) on local water levels at Savannah River at I-95 (station 02198840, left response surface) and for Front River at Houlihan Bridge (station 02198920, right response surface). The response surface of water levels on the left shows higher contribution of streamflow than the downstream station on the right.

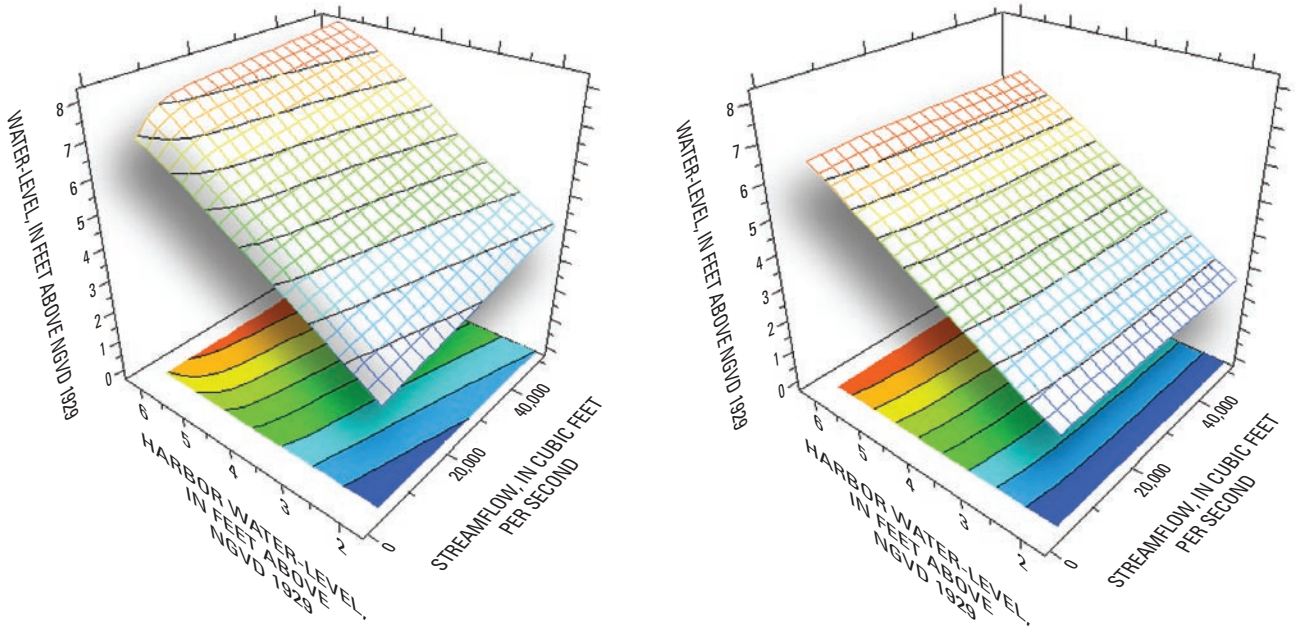

Little Black River at Limehouse (02198979) Front River at Broad Street (02198977)

Figure 39. The interaction of harbor water level (FWL8980A) and streamflow (Q8500A) on local water levels at Little Back River at Limehouse (station 02198979, left response surface) and at Front River at Broad Street (station 02198977, right response surface). Both response surfaces show larger contributions of harbor water levels than streamflow on local water-level conditions. The response surface on the right shows negligible influence of streamflow on local water levels.

Development of a Model-to-Marsh Decision Support System

Dutta and others (1997) define DSSs as, "systems helping decision-makers to solve various semistructured and unstructured problems involving multiple attributes, objectives, and goals …. Historically, the majority of DSSs have been either computer implementations of mathematical models or extensions of database systems and traditional management information systems." Environmental resource managers commonly use complex mathematical (mechanistic) models based on first principles physical equations to evaluate options for using the resource without damage. While there appears to be no strict criteria that distinguish a DSS from other types of programs, Dutta and others (1997) suggest that artificial intelligence (AI) is a characteristic of more advanced DSSs, "With the help of AI techniques DSSs have incorporated the heuristic models of decision-makers and provided increasingly richer support for decision-making. AI systems have also benefited from DSS research as they have scaled down their goal from replacing to supporting decision makers."

The authors have previously developed a DSS to support the permitting of three water-reclamation facilities that discharge into South Carolina's Beaufort River estuary (Conrads and others, 2002b; Conrads and others, 2003; Conrads and Roehl, 2005). The Beaufort DSS incorporated a water-quality model comprising several dozen ANN "submodels" that simulated both point and nonpoint source effects on water quality throughout the system. ANN execution speeds were also found to be much faster than mechanistic models, greatly reducing the turn-around time for users performing waste load allocation scenarios. The Beaufort DSS was a spreadsheet application that connected the ANN super-model to a database storing time series of the area's rainfall and riverine water level, specific conductance, water temperature, and dissolved oxygen from seven different USGS gaging stations. The DSS could run 3-year simulations under different point and nonpoint loading scenarios while providing users with streaming tabular output and graphics to provide situational awareness. Its graphical user interface (GUI) requires no typing. These features make the DSS easily distributed and immediately usable by all stakeholders. The development, performance, and features of the Savannah DSS are described below.

The development of a DSS for the Savannah River Estuary and surrounding wetlands, called the Model-to-Marsh DSS (M2M), required a number of steps (described previously), including (1) merging all the data into a single comprehensive database, (2) developing water-level and salinity ANN submodels, and (3) developing of a spreadsheet application that integrates the new database, output from an existing 3D hydrodynamic model, and ANN submodels into a single package that is easy to use and readily disseminated.

Architecture

Figure 40 shows the basic architectural elements of the DSS. The DSS reads and writes files for the various run-time options that can be selected by the user through the system's GUI. A historical database contains 11 years of hydrodynamic data that are read into the simulator along with the ANN submodels at the start of a simulation. Using GUI controls, the user can evaluate alternative flow scenarios, or load specially formatted output files from the 3D hydrodynamic model that adjust historical riverine water level and specific conductance to evaluate alternative channel geometries and "replumbing" scenarios. The outputs generated by the simulator are written to files for post processing a spreadsheet application used by the DSS's "2D Color-Gradient Visualization Program". The DSS also provides streaming graphics during simulations, visually representing historical and simulated behaviors side-by-side. These features are described in more detail below.

Historical Database

The measured data required extensive clean up for a variety of problems, including erroneous and missing values and phase shifts. The locations of the gaging stations are shown in figures 1 and 5. The resulting database comprises 11 years of half-hourly data (≈160,000 time stamps) for 110 variables. A summary of the historical databases stored in the DSS is described below.

- Clyo streamflow (Q_{clyo}) and harbor water levels—11 years of half-hourly water-level measurements in Savannah Harbor at Fort Pulaski, Ga., and river flows measured inland at Clyo, Ga., by the USGS.
- USGS riverine water level and specific conductance—11 years of half-hourly measurements collected from four stations in the Savannah River Estuary by the USGS.
- GPA riverine water level and specific conductance—half-hourly measurements collected on behalf of the GPA from 14 stations over 3 months each in 1997 and 1999. Some stations recorded both surface and bottom specific-conductance measurements.
- USGS marsh water level and specific conductance—71 months (June 1999 to May 2005) of half-hourly measurements from seven stations.
- GPA marsh water level and specific conductance—40 months (June 1999 to October 2002) of half-hourly specific conductance and water-level measurements from 10 stations.

Linkage to the Three-Dimensional Hydrodynamic Model

The ANN super-model comprises 127 submodels that are configured as follows. Simulation models of water level and specific conductance at four USGS stations in the main channel of the river were developed using Savannah River streamflow data and Savannah Harbor water-level data for inputs, incorporating multiple time delays, moving window averages, and time derivatives to capture the system's dynamic behavior. The simulations were then used as inputs to model the much shorter time series of water level and specific conductance at the many remaining riverine and marsh stations. This provided one set of ANN models that link the river's main channel behavior to tidal forcing and fresh water flowing down the river, and a second set that links main channel behaviors to backwater riverine and marsh behaviors.

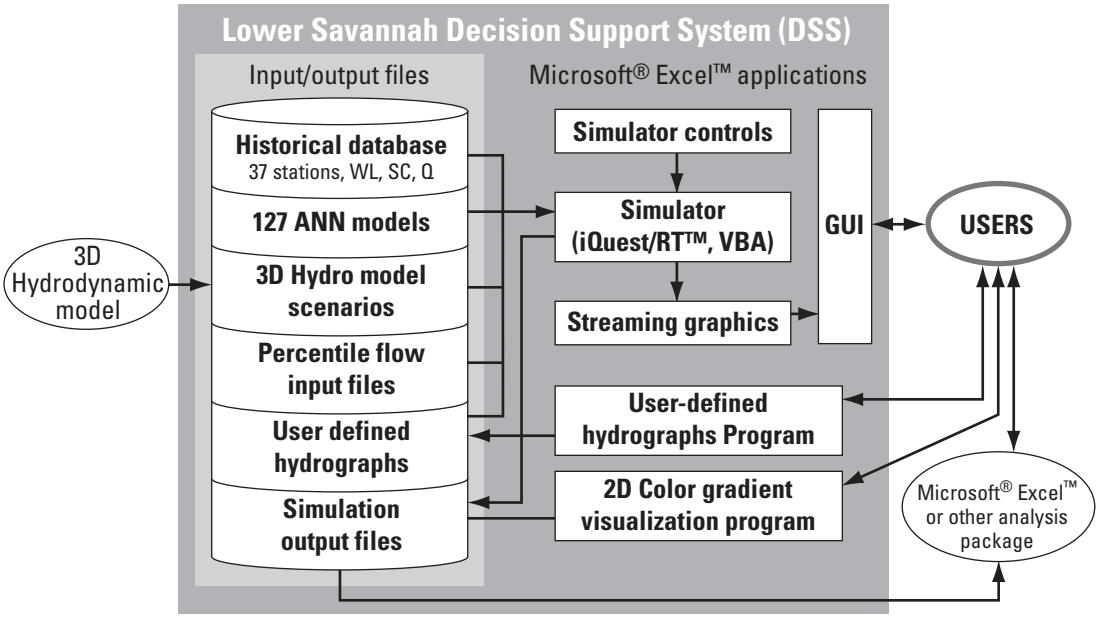

Figure 40. Architecture of the lower Savannah River Estuary Decision Support System (DSS).

Linking the 3D hydrodynamic model to the simulator is accomplished by reading in a file of simulated differences in water-level and specific-conductance values for the river, which reflect hypothetical channel geometry and replumbing scenarios run in the hydrodynamic model, to drive the riverine and marsh ANN models.

Much of the continuous data was collected during a record-setting 5-year drought, raising concerns that the relatively short time series from the riverine and marsh stations was not representative of "typical" hydrodynamic conditions. River flows had been at record lows, leading to unprecedented salinity intrusion, even without a deepened harbor (fig. 12). This concern was mitigated by the fact that the main channel ANNs were able to "learn" the full range of behaviors exhibited over 11 years, starting long before the onset of the drought. Therefore, ANNs could both "hindcast" the riverine and marsh behaviors to nondrought conditions, and be retrained on post-drought conditions as new data become available.

Model Simulation Control, User-Defined Hydrographs Program, Streaming Graphics, and Two-Dimensional Color-Gradient Visualization Program

The Simulator in the M2M DSS integrates the historical database with the 127 ANN models. The Date/Time Controls on the User Controls panel (fig. 41) are used to adjust start and end dates and time-step size for a simulation. The Simulator allows the user to run "What-if?" simulations by varying the streamflow from its historical values. The user has five Simulation Input Variable Options:

- Percent of historical Clyo streamflows,
- User-set Clyo streamflow to constant value,
- Percentile hydrograph of daily Clyo streamflow,
- User-defined daily hydrograph for Clyo streamflow, and
- 3D-model inputs at the USGS river stations and selected GPA river stations.

Explanations of how to use each of the options in the M2M can be found in the User's Manual in Appendix IV.

Streaming graphics display output while a simulation is running for any four simulated variables selected by the user (fig. 42). Each graph displays the historical time series, the simulated output using the measured streamflow (to show model accuracy), and the simulated output using streamflow set by the user using the GUI controls or an input file.

To spatially visualize the marsh salinity response, the DSS is distributed with the "2D Color-Gradient Visualization Program" (fig. 43) that interpolates and extrapolates simulator output to fill and color a grid of the study area. The program provides a qualitative view of the large-scale, longitudinal gradients of the marsh parallel to the river, rather than a quantitative view of small-scale lateral gradients in the marsh perpendicular to the river. For the application, the seven USGS marsh gages were used because of the large range of measured hydrologic conditions, especially nondrought conditions, compared with the GPA marsh sites.

Although the marsh data time series provides a temporally detailed description of changing salinity conditions, the seven sites provide only information on large-scale, longitudinal gradients in the system rather than small-scale, lateral variations in the marsh. Ecological interest in marsh salinity response typically is on seasonal and annual time scales rather than the smaller time scales of riverine responses of hours and days. For the color-gradient visualization program, users can select moving window averages of 1–12 months from the M2M simulator results.

Spatial visualization is based on a 100 meter (m) (107.6 square feet) grid of the study area. The 29,000-cell grid covers the tidal marshes from I-95 to the Highway 17 bridges on the Back and Front Rivers (fig. 2). Interpolation is performed using a simple ratio of linear distances between nearest USGS marsh gages and distance from a cell to the nearest stations. To enlarge the areal extent of measured marsh data (see

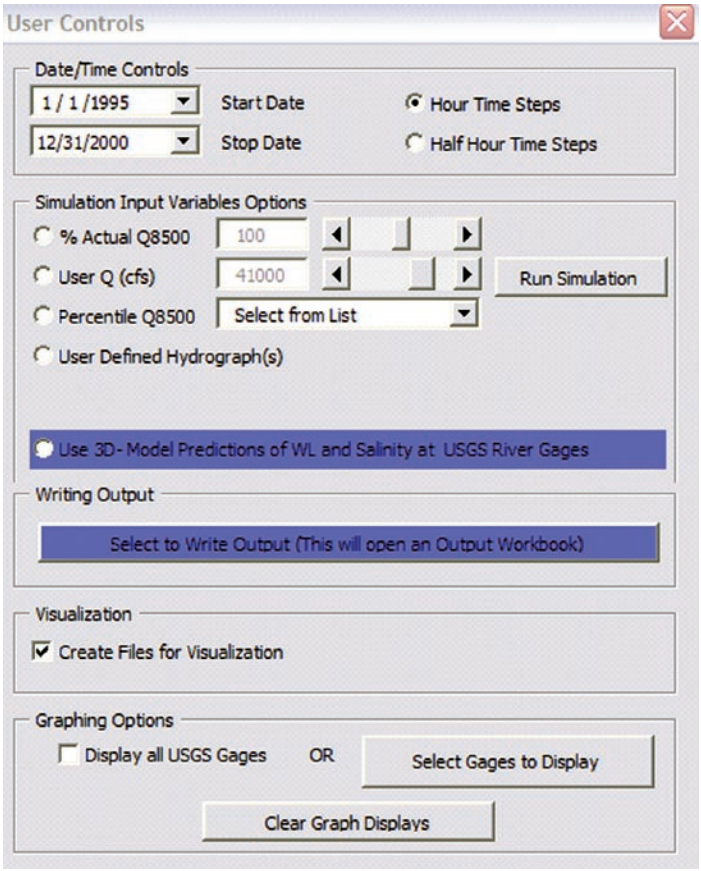

Figure 41. Simulator controls used to set parameters and run a simulation.

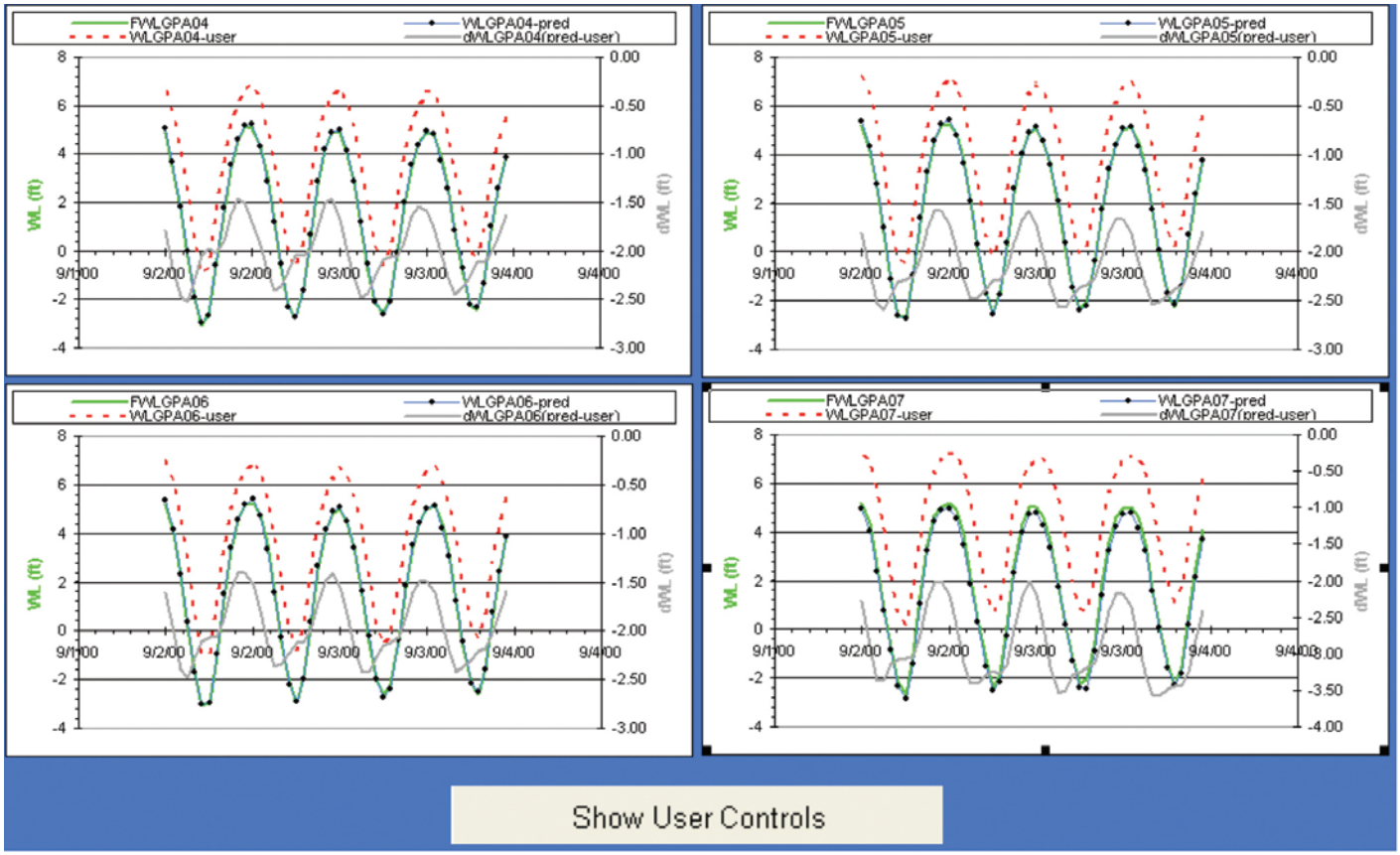

Figure 42. Streaming graphics displayed during simulation.

USGS marsh network, fig. 5*C*), riverine gages on the Savannah River at I-95 (Station 02198840, fig. 5*A*) and Back River upstream from the Tide Gate (GPA05, fig. 5*B*) were added to interpolate and extrapolate cells above Sites M1 and M2 and below Site B4.

The program allows the user to configure the color scale and export all salinity values and grid parameters, i.e., cell size, and corner coordinates, as an ASCII file for input into a mapping package such as ArcView™. In addition to the 100-m grid, a 10-m (107.6 square feet) grid (2,900,000 cells) was developed to minimize numerical computation errors when overlaying the grid data and irregular polygons in GIS applications.

Application of the Model-to-Marsh Decision Support System

The development of the ANN models and the DSS application for the Savannah River Estuary had two objectives. The first was to provide the ecologists responsible for developing marsh succession models of the tidal marshes with a predictive tool that could simulate riverine water-level and salinity responses to changes in hydrologic conditions, and to simulate marsh water-level and pore-water salinity responses to changing river conditions. The models allow ecologists to evaluate the system under different hydrologic conditions to better understand the relation between riverine and marsh water-level and salinity dynamics. The second objective was to integrate predictions from the 3D EFDC model with the predictive marsh succession models. Ultimately, the M2M is a tool to assist in understanding the complex Savannah River Estuary system, and to evaluate alternative scenarios for the potential harbor deepening. The following sections describe the application of the M2M to various hydrologic scenarios.

User-Defined Hydrology

As discussed previously, salinity dynamics result from three large-scale forcing factors: (1) harbor tidal range; (2) water levels at Fort Pulaski; and (3) Savannah streamflows. Tidal range and water-level variability depend on orbital mechanics and meteorological conditions, and are not regulated. The streamflow depends on meteorological conditions, the hydrologic cycle, and a combination of regulated streamflow upstream from Augusta and unregulated streamflow downstream from Augusta. The M2M allows the user to set the input streamflow conditions to evaluate river and marsh dynamics, and alternative regulated streamflow conditions.

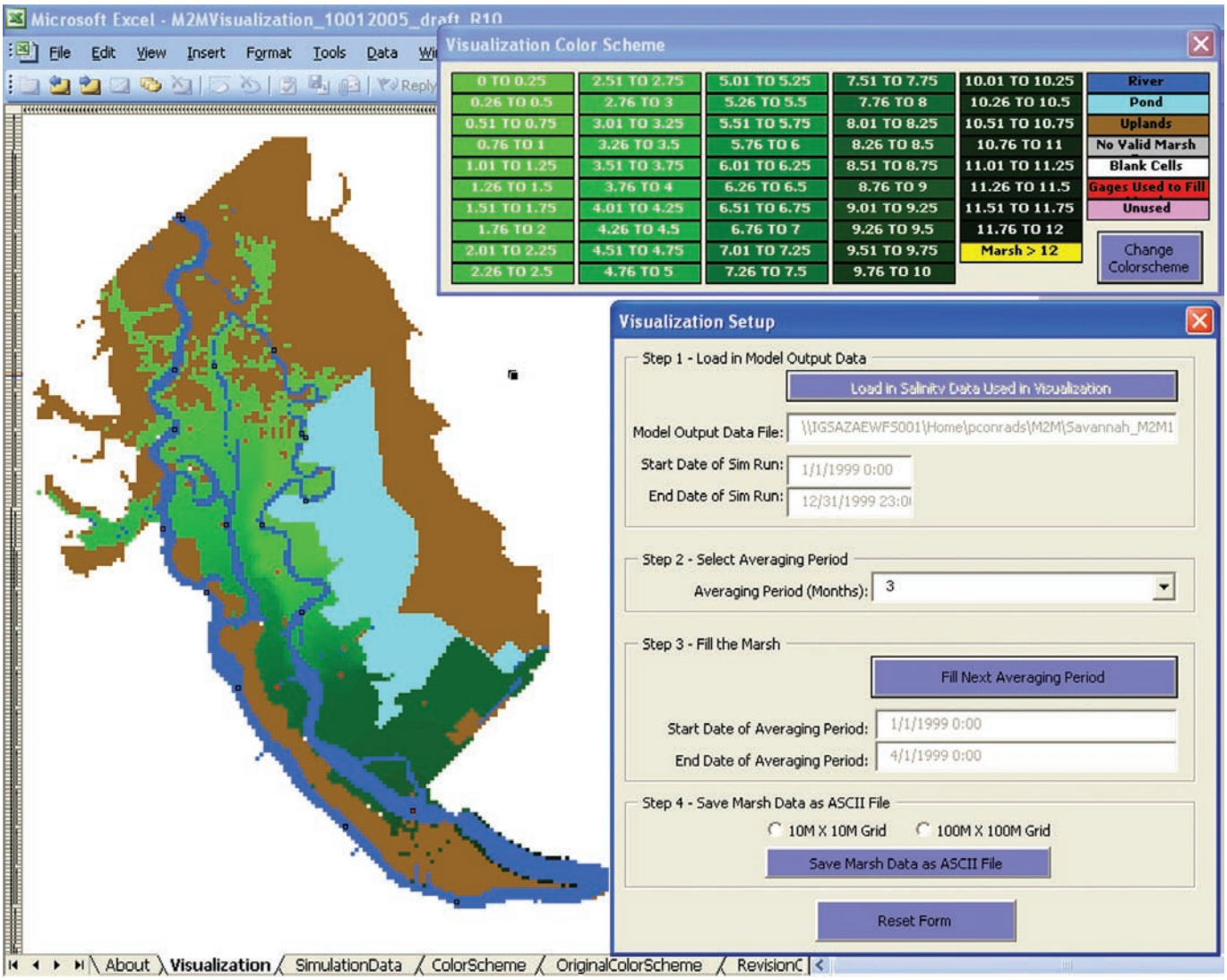

Figure 43. Screen capture of the Two-Dimensional Color-Gradient Visualization Program. Left image shows spatial distribution of marsh salinity based on data from the seven USGS marsh stations. Panel in the upper right of the screen shows the user-specified color scheme. Panel in the lower right shows the user's controls of the visualization program.

Percentile and Constant Streamflow

It is instructive to analyze riverine and estuarine systems under extreme conditions. Often the critical dynamics of a system manifest themselves during these periods rather than during average hydrologic conditions. The 5-year drought (1998–2002) in South Carolina and Georgia provides an opportunity to analyze salinity dynamics and hydrologic conditions during the worst extended drought on record. To evaluate the state of the hydrology of the Savannah River for a particular year, an actual daily streamflow hydrograph can be compared to a percentile flow hydrograph. During the last year of the drought, 2002, the daily streamflow recorded at Clyo, Ga., was at or below the 5th percentile flow for the entire historical record. Figure 44 shows the actual daily 2002 streamflow at Clyo, Ga., with selected percentile flow hydrographs. During the first 5 months of the year, the streamflow was establishing new record lows. During the summer, flows generally were between the 5th percentile and the historical minimum flows. It was not until early fall that streamflows increased consistently above the 5th percentile. During the summer, large salinity intrusions were recorded throughout the USGS river and marsh gaging networks.

To evaluate the effect of low-flow conditions on the salinity response in the system, the M2M was set up to simulate a constant streamflow of 6,000 ft^3/s during 2002. The salinity response to the constant flows on the Little Back River at the USFW Dock (station 021989791) is shown in figure 45 along with the measured and constant streamflows, and harbor tidal range. Constant flow does not manifest the high streamflow

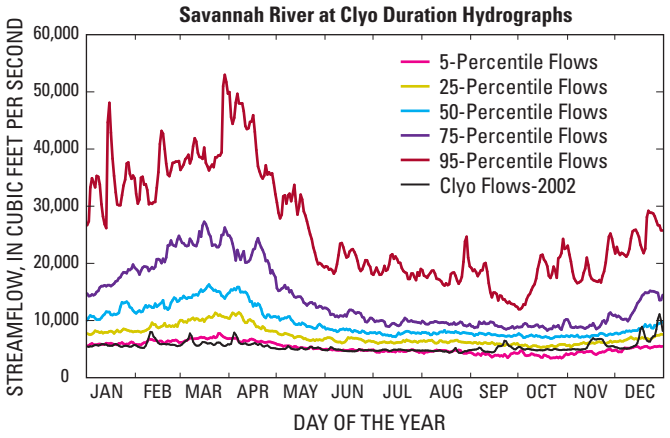

Figure 44. Duration hydrographs for Savannah River near Clyo, Ga., and daily hydrograph for the calendar year 2002 streamflows. Percentile flows are based on streamflow data from 1929 to 2003.

pulses, which exceeded 8,000 ft^3/s, in February through April and December. During the summer low-flow period, the constant 6,000 ft^3/s flow was substantially greater than the measured 2002 conditions.

The constant streamflow did not significantly affect the salinity intrusions during the first 4 months (January to April) of 2002 when the average measured streamflow was approximately 6,000 ft^3/s. During this period, the greatest intrusions occur on 14- and 28-day cycles that are co-incident with the spring tides. The three higher-flow pulses during this period did not occur during the spring tides. During the low-flow period after May, the constant flow is above the actual flow and did substantially affect salinity levels. For the actual flow conditions, the salinity intrusions (blue line) were approximately 3.0 psu, with the greatest intrusion of 8.0 psu occurring in early August. The salinity response to the constant 6,000 ft^3/s (red line) shows that the difference in the flows decreases the early salinity intrusions to approximately 1.5 to 2.0 psu, and the high intrusion in August fell to approximately 4.0 psu.

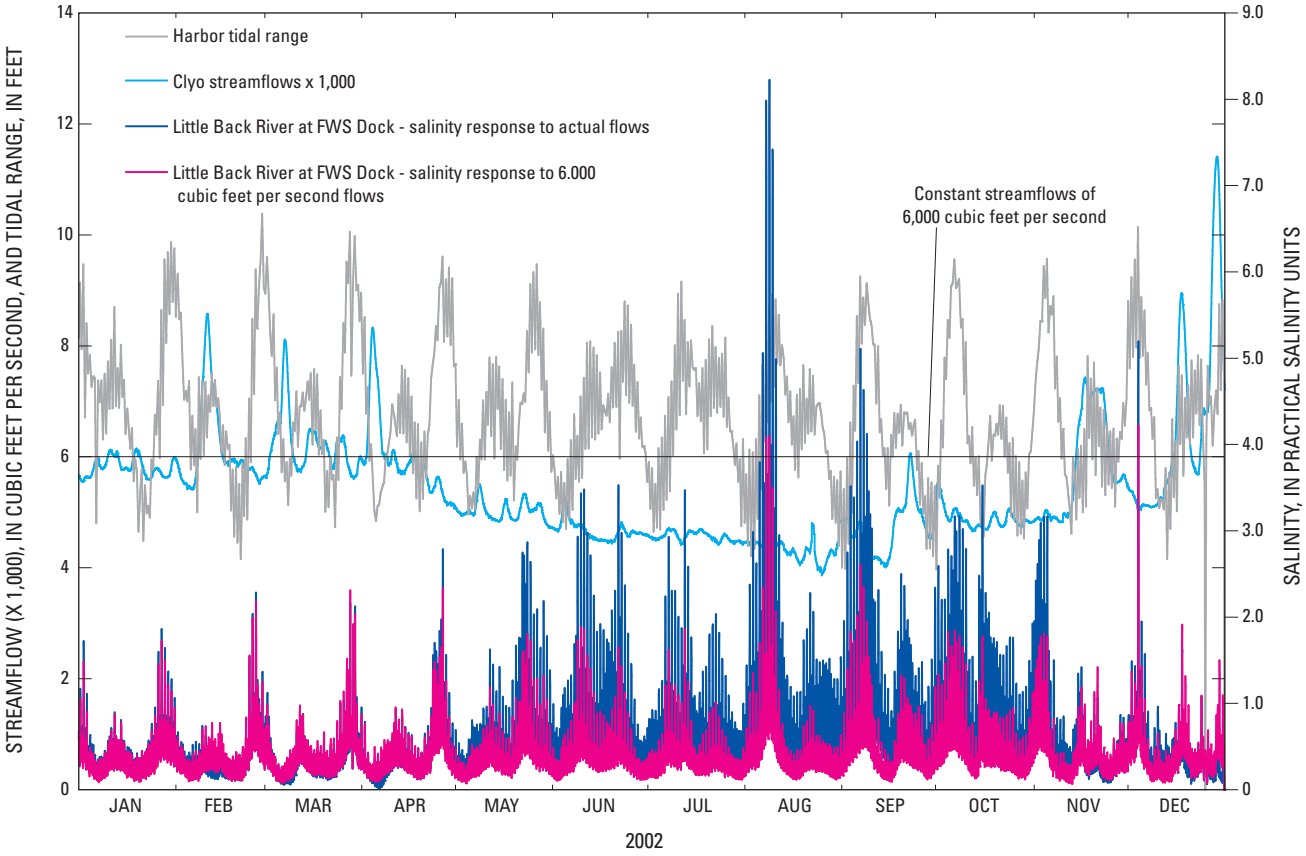

Figure 45. Salinity response at Little Back River at U.S. Fish and Wildlife Service Dock (station 021989791) for calendar year 2002 streamflows and constant 6,000 ft^3/s streamflows. Tidal range for Savannah River at Fort Pulaski (station 02198980) also are shown.

The reduction in the salinity intrusion by constant streamflow also had a substantial effect on the pore-water salinity in the tidal marshes. Figure 46 shows the pore-water salinity response to the actual and constant 6,000 ft^3/s streamflows. Some of the input data for the marsh ANN models were missing during the first 3 months of the year, and predictions are not shown. For Site B1, the salinity response to the measured streamflow is between 0.5 and 1.0 psu, with the large intrusion in August being approximately 1.2 psu. The constant streamflow decreased the pore-water salinity by approximately 50 percent to 0.5 psu or less. The response to the increased streamflow virtually changed Site B1 from an oligohaline marsh to a tidal freshwater marsh (fig. 15). Downstream at Site B2, there is a similar substantial decrease in the salinity for the measured and constant 6,000 ft^3/s streamflows. Note the similarities in the responses in the marsh pore-water salinity at Site B1 for measured flow conditions and Site B2 for the constant flow conditions. The slight increase in the streamflow of the constant input changed the marsh response at Site B2 to one that is equivalent to the marsh upstream during measured conditions.

Percent of Historical Streamflow

Another user-specified streamflow option is percent of historical streamflow. This allows the DSS user to modify the measured streamflow from 50 to 200 percent of the historical value. The salinity response on the Little Back River at USFW Dock (station 021989781) for a 25-percent increase in streamflow during 2002 is shown in figure 47. There is an overall decrease in salinity with high streamflow. In the constant flow simulation above, during the first 4 months the three flow pulses were decreased substantially but there was little response in salinity owing to the timing of the 28-day spring tide cycle (fig. 45). With the 25-percent increase in streamflow (fig. 47), there is a consistent reduction in the salinity, with the largest percentage reduction occurring during spring tides. During the low flows in August, the 25-percent increase in streamflows was not as great a difference over the actual streamflow as the constant 6,000 ft^3/s simulation; therefore the large salinity intrusion values were reduced to 5 psu, rather than the 4 psu with the 6,000 ft^3/s constant flow.

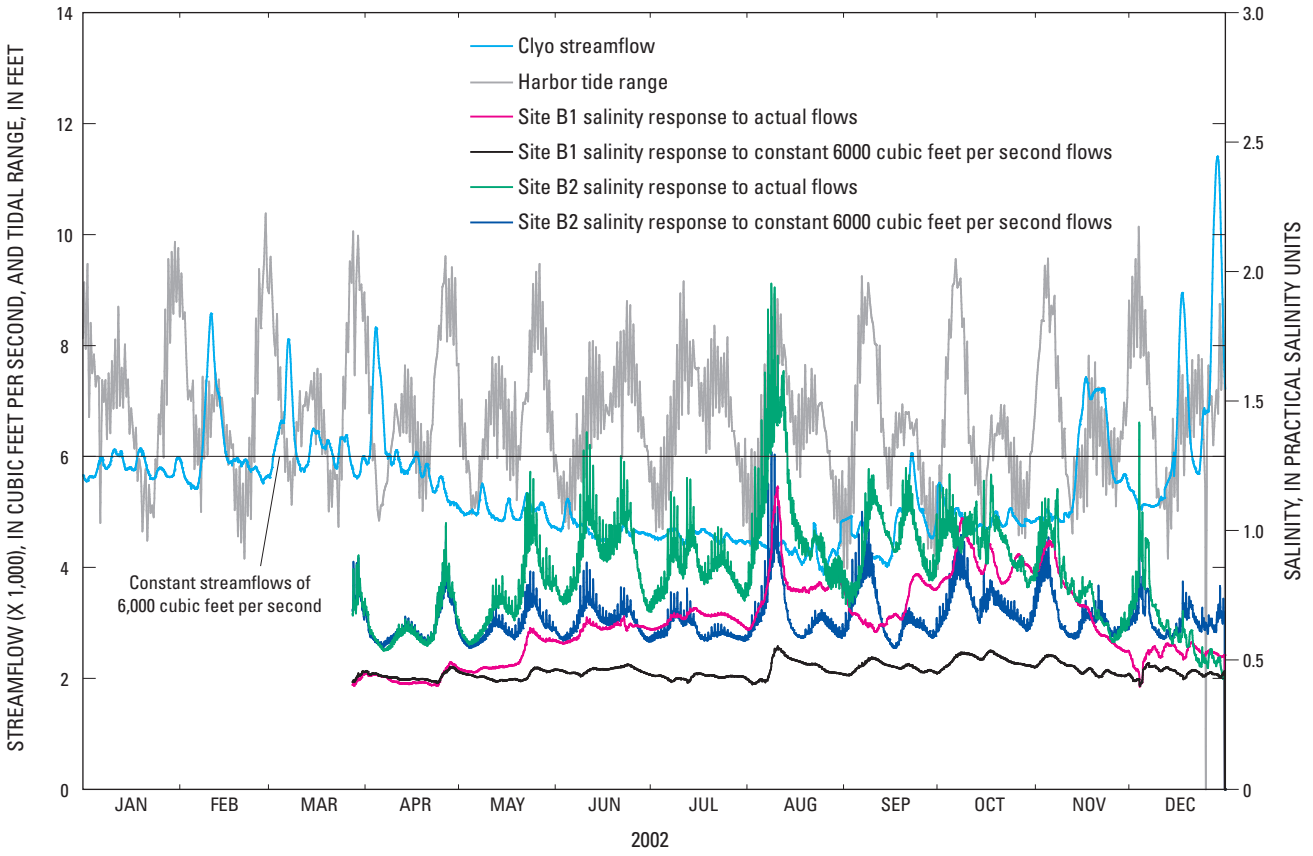

Figure 46. Hourly salinity response for two tidal marsh sites (B1 and B2) off the Little Back River for calendar year 2002 streamflows and constant 6,000 ft^3/s streamflows. Tidal range for Savannah River at Fort Pulaski (station 02198980) also are shown.

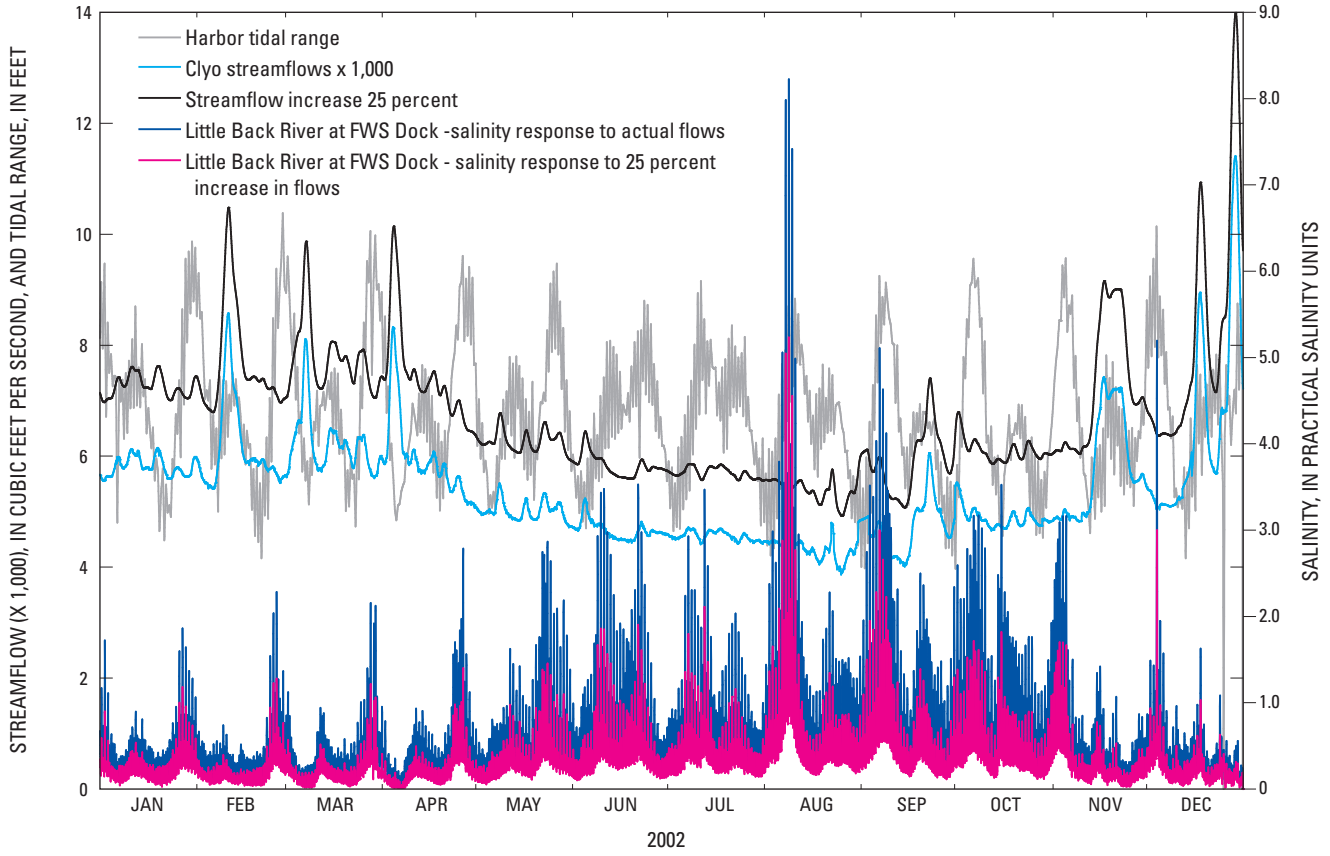

Figure 47. Hourly salinity response at Little Back River at U.S. Fish and Wildlife Service Dock (station 021989791) for calendar year 2002 streamflows and a 25-percent increase in streamflows. Tidal range for Savannah River at Fort Pulaski (station 02198980) also are shown.

The marsh response to the 25-percent higher streamflow during 2002 is shown in figure 48 for marsh sites B1, B2, and B3. The three sites have similar and different responses to higher streamflow. Generally, the three sites respond more to the higher streamflow beginning in June, with Site B3 showing the greatest response. For the 14-day period around the large salinity intrusion in August 2002, Site B2 had the greatest percentage change (approximately 300 percent) of the three sites. For 2002, Site B3 showed the largest overall response (to 0.8 psu). The different responses at the marsh sites show that percentage change in flow does not yield a consistent, proportional change in salinity.

The marsh responses to a 25-percent increase in streamflow can also be displayed as frequency distributions to reveal the changes in the occurrence of salinity in the pore-water. The cumulative percent distribution of salinity occurrences for the three marsh sites at a 25-percent increase in streamflow is shown in figure 49. For all three sites, the increase in streamflow shifts the frequency distribution to the left as pore-water salinity concentrations decrease. The differences in the slopes and the shapes of the frequency response curves show that the marshes are responding differently to marsh and river salinity dynamics. The 25-percent increase shifted the salinity frequency at Site B2 to conditions that are similar to the actual flow conditions at Site B1 upstream.

Percentile Hydrograph of Daily Streamflow

Percentile hydrographs can be used as inputs to the M2M to estimate riverine and marsh water-level and salinity responses for these graduated streamflow conditions. The user selects the time period to simulate and the percentile hydrograph to use as input. The M2M DSS will simulate the water-level and salinity responses using the measured harbor water level and tidal range data from the selected time period. The percentile flow hydrograph option allows, “normalized” water-level and salinity conditions to be determined. For example, for a period when the system is experiencing extreme low-flow conditions, a percentile flow hydrograph (for example the 25th to 75th percentile) will allow “normal” salinities and water levels to be estimated. Figure 50 shows the salinity response at the USFW Dock on the Little Back River (station 021989791) during 2002. The response for the 25th percentile flow hydrograph can be considered the “normal” response to

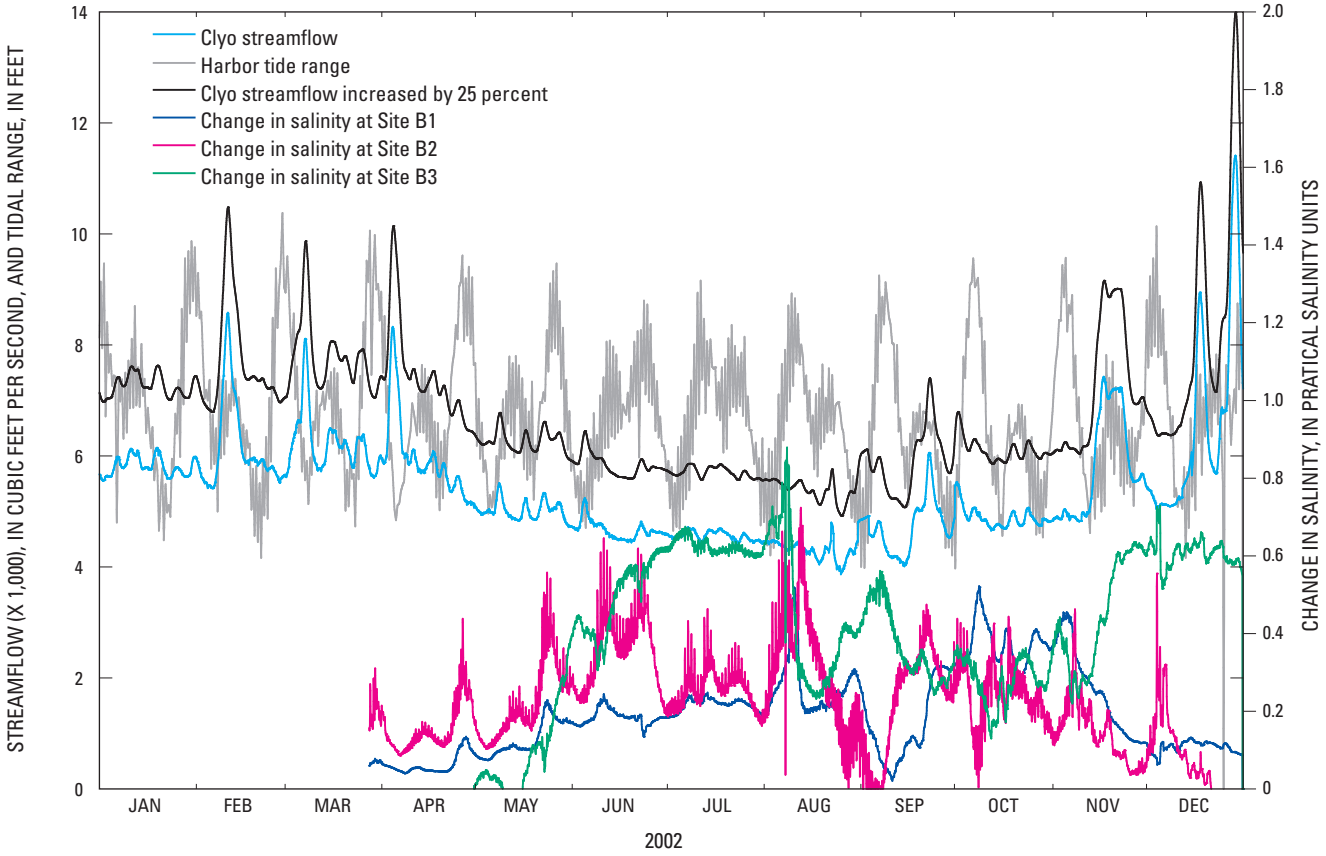

Figure 48. Hourly salinity response for three tidal marsh sites (B1, B2, and B3) along the Little Back River for a 25-percent increase in calendar year 2002 streamflows. Salinity response is the difference between salinity response for actual streamflows and a 25-percent increase in streamflows. Tidal range for Savannah River at Fort Pulaski (station 02198980) also are shown.

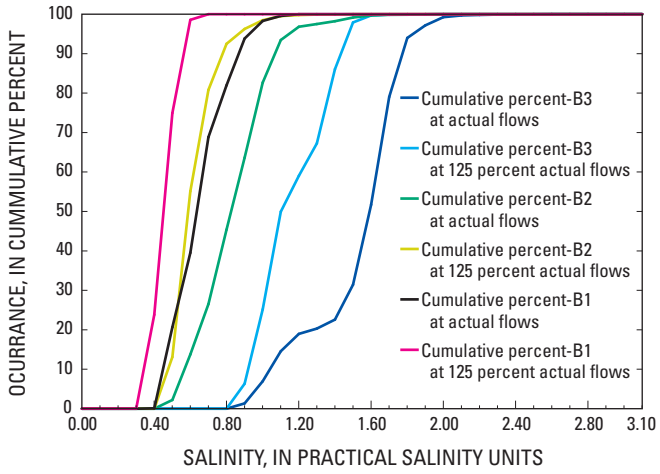

Figure 49. Frequency-distribution curves of salinity occurrence for three tidal marsh sites (B1, B2, and B3) along the Little Back River for 2002 streamflow conditions and a 25-percent increase in streamflow conditions.

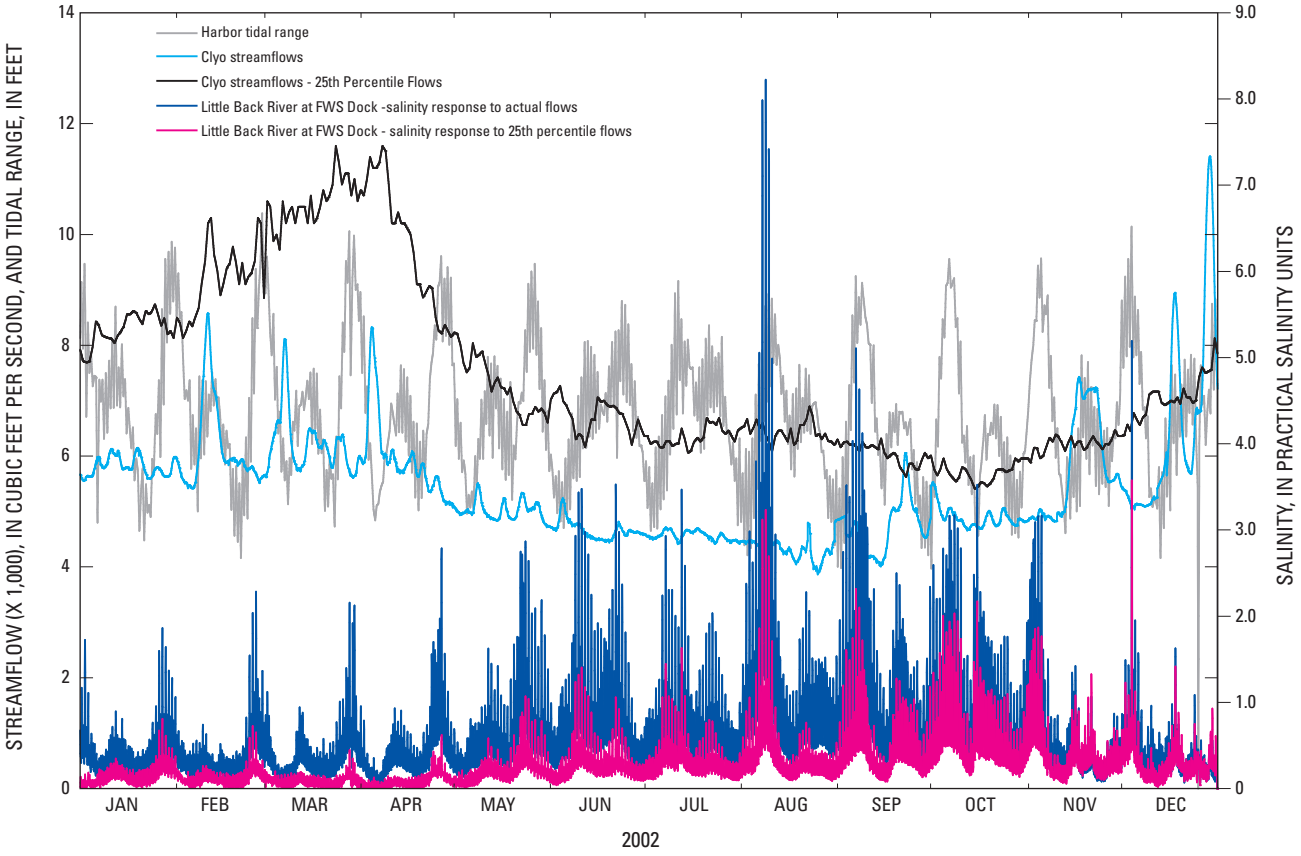

Figure 50. Hourly salinity response at U.S. Fish and Wildlife Service Dock (station 021989791) for calendar year 2002 streamflows and the 25th percentile duration hydrograph. Percentile flows based on streamflows from 1929 to 2003. Tidal range for Savannah River at Fort Pulaski (station 02198980) also are shown.

statistically derived streamflow conditions. The effect of the drought in 2002 is the difference between the salinity response to the actual flows and the 25th percentile hydrograph. During the seasonally high flows in the spring, the salinity intrusion in April is reduced from about 2.0 psu to less than 0.5 psu. During the extreme low flows during the summer, salinity intrusions of 3.0 psu are reduced to 1.0 to 1.5 psu, and 8.0 psu is reduced to 3.0 psu. With the return of slightly higher flows in the fall and winter, the reductions of the intrusions are lower.

The pore-water salinity response at three marsh sites for three different percentile flow conditions were simulated for the 2002 calendar year (fig. 51). When the streamflow is reduced to the 15th percentile, the pore-water salinities increase and the frequency distributions are shifted to the right. The frequency distribution for 15th percentile at Site B1 is similar to the 25th frequency distribution for Site B2. Further reduction in the streamflows to the 5th percentile shifts the frequency distributions even farther to the right. Sites B1 and B2 are shifted from freshwater tidal marsh to oligohaline marsh conditions.

User-Defined Streamflow Hydrograph

The fourth option for user-defined streamflow input M2M is a user-defined hydrograph. With this option, a half-hourly flow hydrograph is created outside of the M2M DSS. A simulation period is selected and the M2M uses the user-defined hydrograph and tidal conditions for the simulation period as inputs. Two scenarios were simulated using this option. In the first scenario, a hydrograph for the 2002 calendar year was created with the minimum flow set to 5,000 ft^3/s. The actual and user-defined hydrographs for 2002 and the salinity response at USFW Dock on the Little Back River (station 021989791) are shown in figure 52. During 2002, flows did not drop below 5,000 ft^3/s until May. From May to September, the minimum 5,000 ft^3/s streamflow usually is greater than the actual flow. The minimum streamflows decreased the salinity level but not as much as the constant 6,000 ft^3/s shown in figure 45. The large salinity intrusion in August was decreased by less than 1.5 psu. The apparent difference in actual and user-defined streamflow salinity responses in early

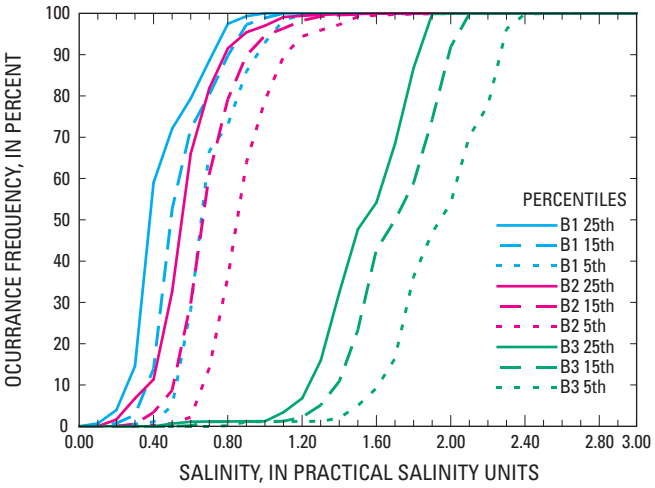

Figure 51. Frequency-distribution curves of salinity occurrence for three tidal marsh sites (B1, B2, and B3) along the Little Back River for 5th, 15th, and 25th percentile duration hydrographs.

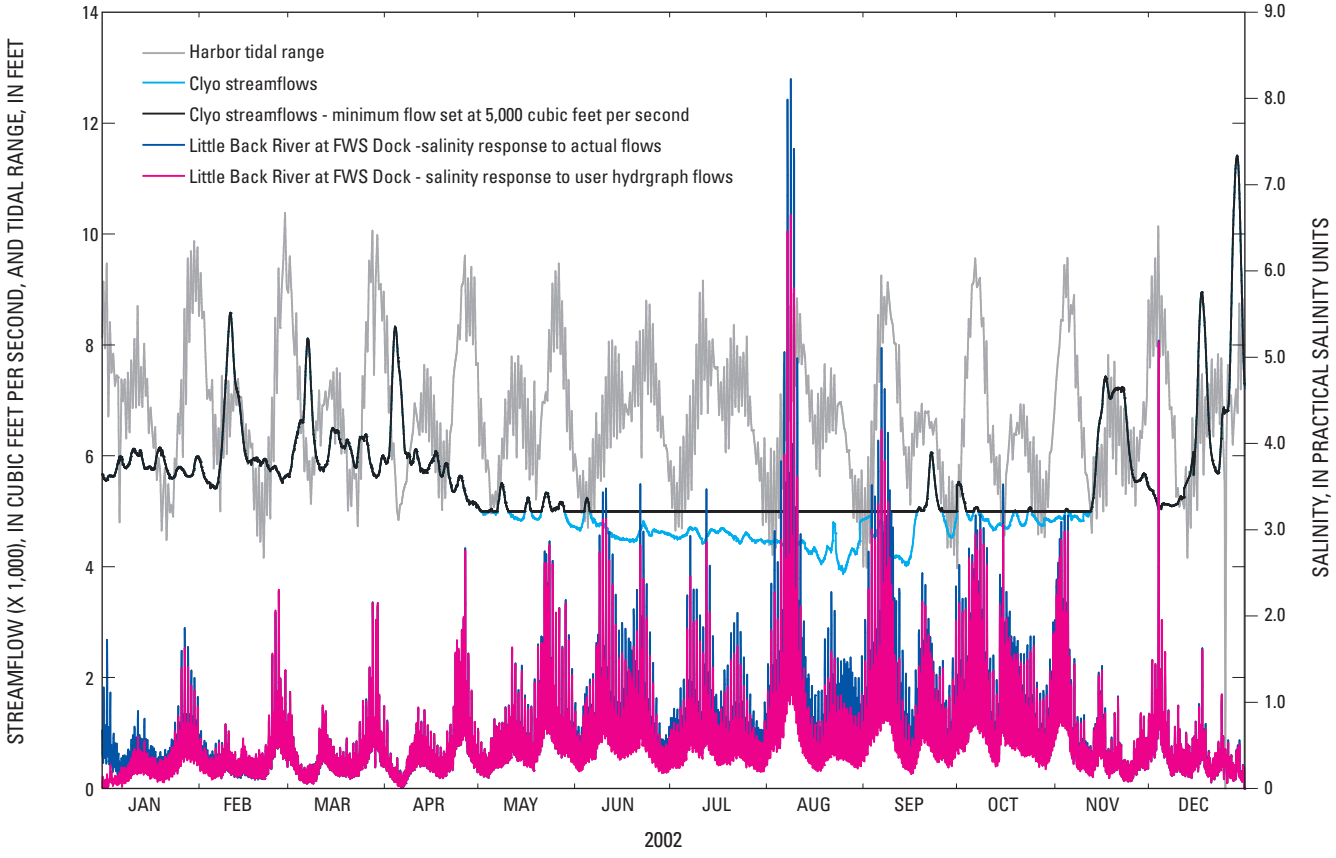

Figure 52. Hourly salinity response at U.S. Fish and Wildlife Service Dock (station 021989791) for calendar year 2002 streamflows and minimum flows set at 5,000 ft^3/s. Tidal range for Savannah River at Fort Pulaski (station 02198980) also are shown.

January are an artifact of missing 2001 values in the user-defined hydrograph for computing model inputs such as long-term time derivatives and moving window averages.

In the second user-defined hydrograph scenario (fig. 53), a hydrograph was created that shifted the higher streamflow pulses that occurred during the first 4 months of 2002 to coincide with the spring tides to evaluate whether the salinity intrusion would be substantially reduced. In addition to shifting the three pulses early in the year, a pulse of approximately 8,500 ft^3/s was inserted to coincide with the August spring tide and the coincident large salinity intrusion. The results of the simulation are shown in figure 54. The shifting of the pulses did decrease the salinity intrusions at the end of January, February, and March. The intrusion in January had the largest reduction and may be due to the larger magnitude and duration of this streamflow pulse compared to the subsequent two pulses. The timed flow pulse inserted to reduce the August salinity intrusion reduced the magnitude of the salinity intrusion by more than 4 psu.

Inputs to Model-to-Marsh from Three-Dimensional Model Output

The fifth option for user-defined inputs to the M2M DSS is output from the 3D hydrodynamic EFDC model of the Savannah River Estuary. Using this option, the differences between a historical baseline simulation and alternative harbor geometry are used for input to the M2M simulator. Inputs for the USGS marsh models include the differences from the EFDC simulations generated at the USGS river stations and at the decorrelated GPA river stations (GPA11, GPA11R, and GPA12).

One scenario was run using the historical streamflow and tidal conditions of the 1999 calendar year and a hypothetical deepening of the harbor. Two simulations were generated with the EFDC model. The first was the actual historical conditions from 1999. The second simulation was using the same boundary input conditions but a different channel geometry file representing a 4-ft deepening of the harbor. The difference between the two EFDC simulations are post-processed for the specified USGS and GPA river stations for input to the M2M simulator.

The two-dimensional color-gradient visualization program was used to display the results from the scenario. Four visualization files are generated by the M2M simulator as input to the marsh visualization program: actual conditions, simulated actual conditions, user-defined conditions, and the difference between simulated actual conditions and user-defined conditions. The user-defined conditions represent the simulated salinity values resulting from the EFDC deepening scenario. The difference between the simulated actual conditions and user-defined conditions show the effects of the scenario. Figure 55 shows the baseline simulation on the left and the user-defined condition on the right. The darker shades of green on the right panel (fig. 55*B*) indicate the increased marsh salinity concentrations resulting from a deepening of the harbor for a 2-month period in 1999.

The same deepening scenario is displayed in figure 56 as the difference between the historical condition and the deepened condition. The marsh salinity concentrations show the effect of a deepening. Figures 55 and 56 do not use the same color gradient. As expected, the effect is more evident closer to the harbor and diminishes farther upstream.

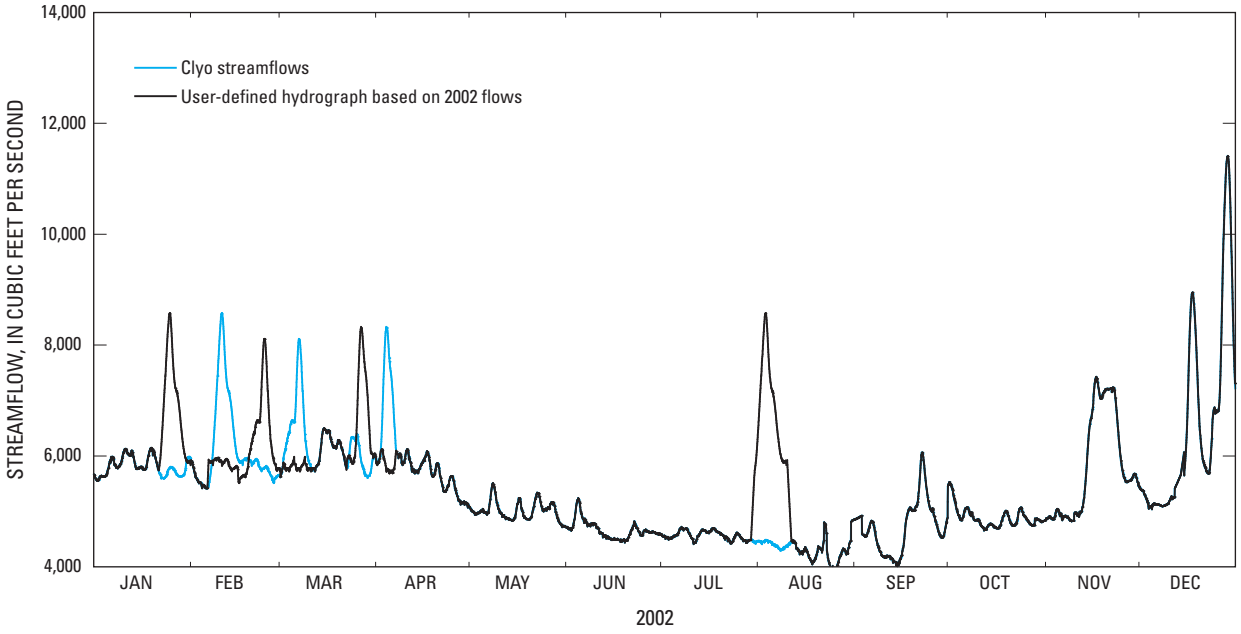

Figure 53. The 2002 streamflow hydrograph and a user-defined hydrograph for input into the Model-to-Marsh application. Hydrograph generated to time streamflow pulses to occur during spring tides and reduce salinity intrusion.

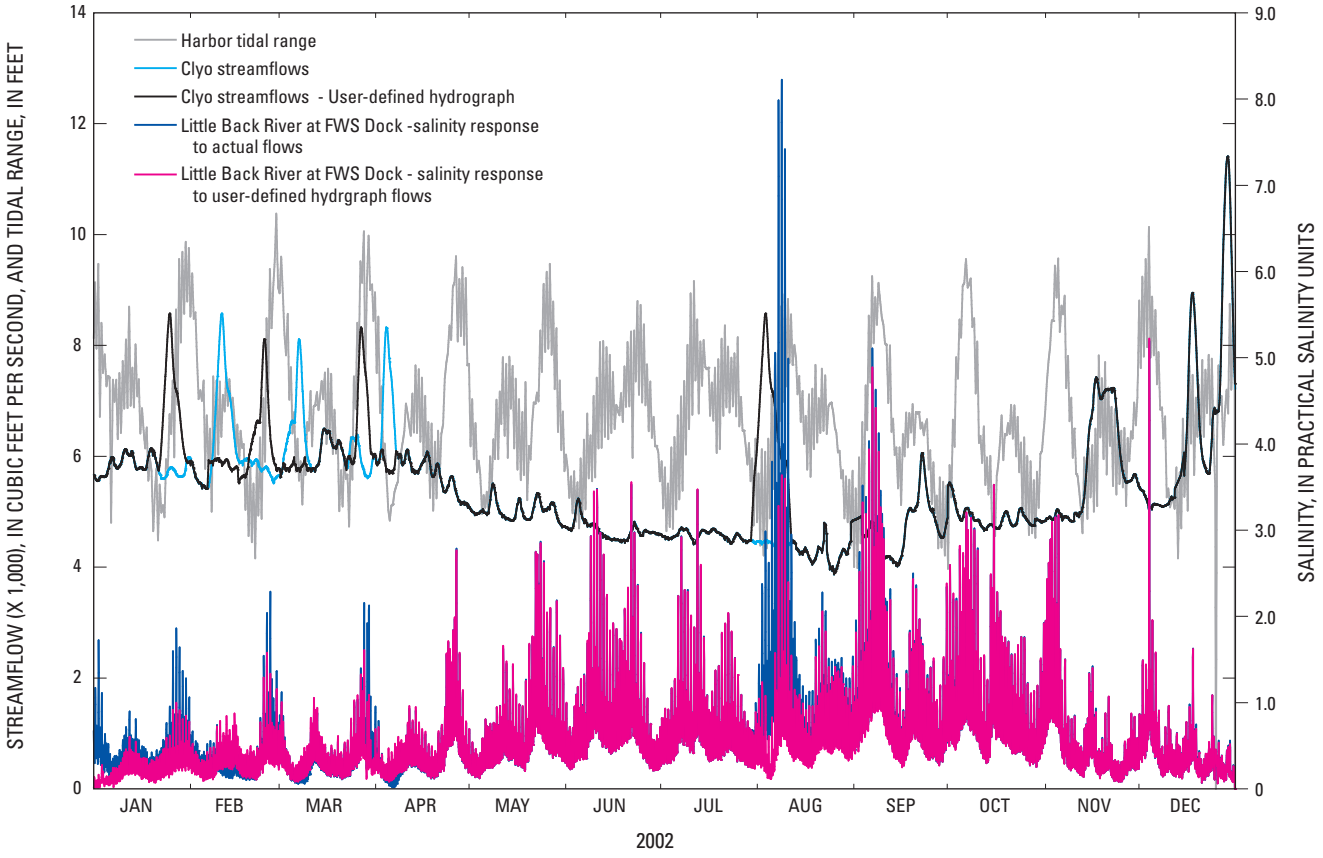

Figure 54. Hourly salinity response at U.S. Fish and Wildlife Service Dock (station 021989791) for calendar year 2002 streamflows and user-defined hydrograph with streamflow pulses inserted to occur during spring tides to reduce salinity intrusion. Tidal range for Savannah River at Fort Pulaski (station 02198980) also are shown.

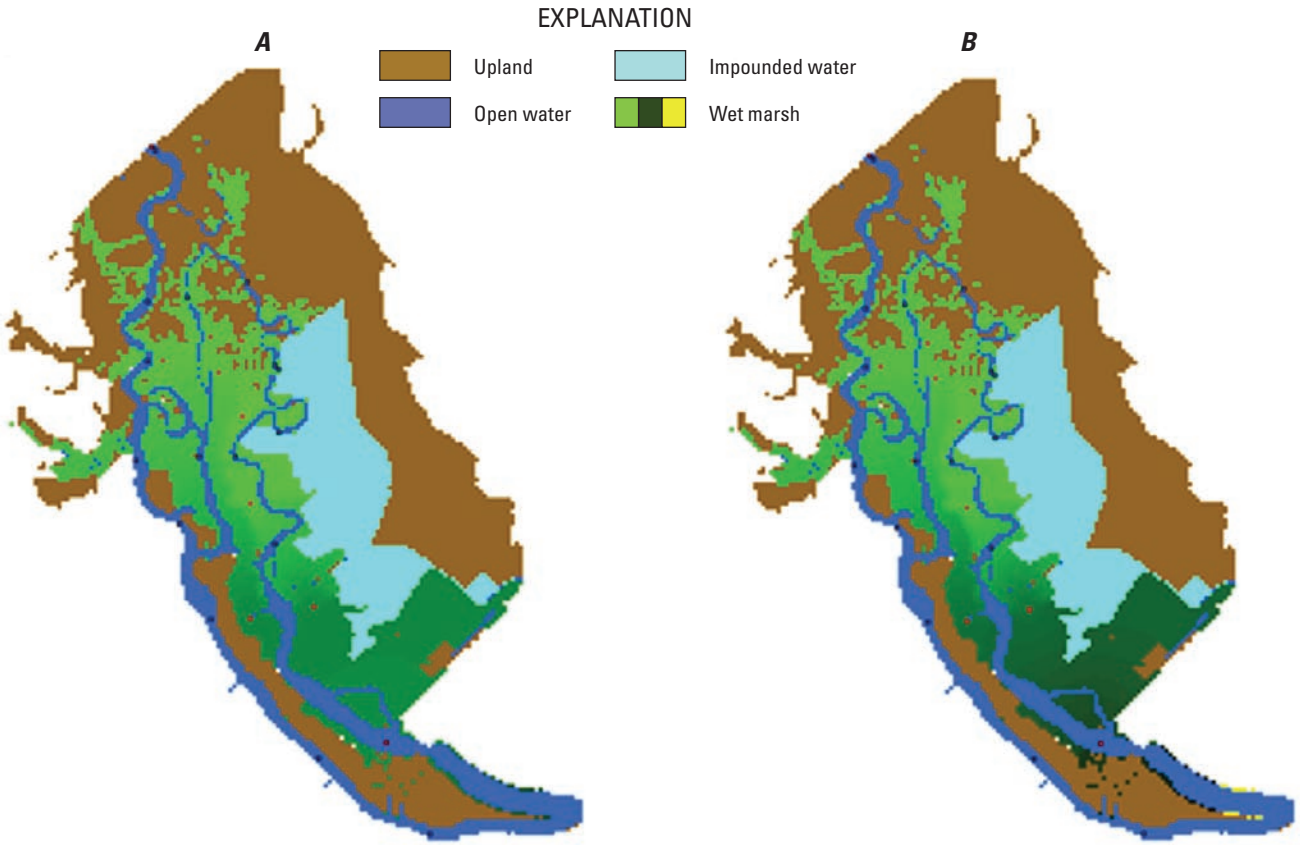

Figure 55. Two-dimensional color-gradient visualization of marsh salinity predictions for actual conditions (*A*, left panel) and a deepened condition (*B*, right panel) for the period July 1 to August 31, 1999. Both panels use the same green color gradient (values from 0.0–12 psu) to represent average marsh pore-water salinity concentrations. The panel on the right shows slightly higher (darker green) marsh pore-water salinity concentrations due to the deepening of the harbor.

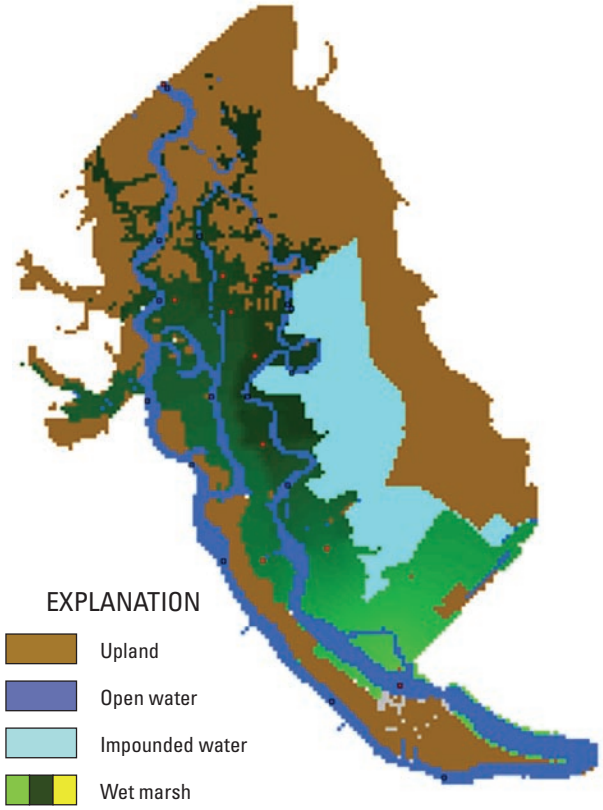

Figure 56. Two-dimensional color-gradient visualization of differences in average marsh salinity prediction for actual conditions and a deepened condition for the period July 1 to August 31, 1999. The panel uses a green color gradient (values from –3.0 to 0 psu). Lighter green color shades indicate greater differences between the two simulations.

Summary

To evaluate potential effects of a proposed deepening of the Savannah Harbor, the Georgia Ports Authority (GPA) has undertaken hydrodynamic and ecological studies of the river and marshes in the vicinity of the SNWR. The freshwater tidal marshes support a diversity of plants and wildlife and were formerly one of the largest freshwater tidal marshes along the East Coast. The potential deepening of the harbor will alter the salinity dynamics of the system and could adversely affect the freshwater tidal marshes. Two models have been developed to evaluate effects and simulate possible mitigation scenarios to minimize potential deepening effects. The GPA and the U.S. Army Corps of Engineers funded the development of hydrodynamic and ecological models to evaluate the potential effects of a proposed deepening of Savannah Harbor. A three-dimensional (3D) hydrodynamic and water-quality model was developed that simulates water levels and salinity throughout the riverine network for anticipated changes in shipping channel geometry. The other models are marsh succession models that predict the changes in marsh plant communities as a result of changes in marsh pore-water salinity. To link the predictive capacity of the two modeling efforts, artificial neural network (ANN) models were developed using data-mining techniques to simulate riverine and marsh water-level and salinity dynamics.

The river and marsh ANN models, historical database, model simulation controls, streaming graphics, and model output were integrated into a decision support system (DSS) named the Model-to-Marsh (M2M). The M2M can be run under two different modes. One mode allows the user to manipulate the streamflow inputs to the system. Four options are available: constant streamflows, percent of historical streamflows, percentile streamflow hydrographs, and user-defined hydrograph. The other mode allows users to input the simulated change in riverine conditions from the 3D hydrodynamic model. Output from the M2M includes tabular time series of measured data, predictions of the measured data, predictions of the user-specified conditions, and differences in simulated and user-specified values. A two-dimensional (2D) plan view visualization routine was also developed that displays marsh salinity conditions. The visualization routine uses marsh predictions at seven locations and interpolates and extrapolates values across the marsh on either a 10- or 100-meter grid. The 2D grid is formatted to be compatible with geographic information system (GIS) applications. The M2M is a spreadsheet application that facilitates the dissemination and utility of the DSS.

The empirical ANN models were developed using data-mining techniques. Data mining is a powerful tool for converting large databases into knowledge to solve problems that are otherwise imponderable because of the large numbers of explanatory variables or poorly understood process physics. Since the last harbor modification in 1994, there are four databases of time series of river and marsh water level and specific conductance (field measurement for salinity). The USGS has maintained a network of continuous streamflow, water-level, and specific-conductance river gages since the 1980s and a network of continuous tidal marsh water-level and salinity gages since 1999. To support the 3D hydrodynamic model development, the GPA collected continuous water-level and water-quality data during the summers of 1997 and 1999. The GPA also collected continuous tidal marsh water-level and specific-conductance data from 1999 to 2002.

Development of models with good predictive ability through the full range of historical conditions is dependent on the availability of measured data covering the full range of conditions in the system. Depending on the period of time when these data collection networks were active, each data set covered different ranges of Savannah River streamflow conditions. For the river networks, the USGS stations recorded water level and specific conductance for the full range of historical streamflow conditions from 4,320 to 52,600 ft^3/s. The GPA network measured conditions for a flow range of 5,440 to 11,600 ft^3/s, which represents median flow conditions (the 25th and 75th percentiles for the period of record). For the tidal marsh networks, the USGS gaging network measured hydrologic conditions of 4,320 to 39,600 ft^3/s, which represents a low- to high-flow condition (from minimum flow to greater than 95th percentile flows for the period of record). The GPA network measured conditions from 4,320 to 14,100 ft^3/s, which like the GPA river network, represents median flow conditions.

For the application of the ANN models to the Savannah River, data-mining methods are applied to maximize the information content in raw data. Signal processing techniques included signal decomposition, digital filtering, time derivatives, time delays, running averages, and differences between stations. Signal inputs to the ANN model used "state space reconstruction" (SSR) for representing dynamic relations of the system. The development of ANN models to simulate the water level and pore-water salinity of the tidal marsh was undertaken in two phases. The first phase was to train ANN models to simulate the water level and specific conductance at the USGS and the GPA riverine sites. Inputs to the ANN models of the USGS river network include time series, or signals, of streamflow, tidal water level, and tidal range. The second phase was to train ANN models to simulate water level and pore-water specific conductance at the USGS and the GPA marsh sites. Inputs for these models include the water-level and specific-conductance signals from the USGS river network at the marsh gaging sites.

For a complex system like the Savannah River Estuary and tidal marshes, the statistical accuracy of the models and predictive capability are satisfactory. The salinity models are able to simulate the 14- and 28-day salinity intrusion cycles in the rivers and capture the salinity dynamics responses in the marshes. The models of the USGS river and marsh networks have the greatest range of the output variables. Generally, the river water-level models have coefficient of determination (R^2) values ranging from 0.88 to 0.99 and the specific-conductance

models have R^2 values ranging from 0.57 to 0.87. The marsh water-level models have R^2 values ranging from 0.72 to 0.87 and the specific-conductance models have R^2 values ranging from 0.53 to 0.85.

The M2M application was used to simulate four user-specified flow options in the applications. The first scenario simulated the 2002 conditions using a constant streamflow of 6,000 ft^3/s. During the low-flow conditions in the summer when the actual flows were less than 6,000 ft^3/s, there was a reduction in the salinity intrusion into the Little Back River. The constant 6,000 ft^3/s reduced the amount of streamflow for three higher streamflow pulses that occurred in the spring of 2002. The reductions in the streamflow did not cause an increase in the salinity intrusion for these three events related to the timing with the 28-day spring tidal cycle. For the Little Back River, salinity intrusion is greatest during spring tides, and the three higher streamflow pulses did not occur during the optimal tidal phase. The constant streamflow also had a significant effect on the pore-water salinity response in the tidal marshes. The response to the increased streamflow during the low-flow conditions of the summer essentially changed Site B1 from an oligohaline marsh to a tidal freshwater marsh.

A second option for user-specified inflows for the M2M application is percent of historical streamflows. A 25-percent increase in streamflow for 2002 was simulated, and there was an overall decrease in the salinity with the increase in flow. With the 25-percent increase in streamflows, salinity intrusion is reduced during these periods due to the increase in streamflow with the largest percentage reductions occurring during spring tides.

Percentile hydrographs can be used as a third option as inputs to the M2M to estimate riverine and marsh water-level and salinity response for these streamflow conditions. Using the percentile flow hydrograph option, “normalized” water-level and salinity conditions can be determined for a particular time period. Three percentile streamflow conditions, the 5th, 15th, and 25th percentile hydrographs, were simulated with the M2M application for the 2002 calendar year. The marsh response for these conditions showed Sites B1 and B2 shifting from freshwater tidal marsh conditions to oligohaline marsh conditions as flow conditions were reduced from the 25th to the 5th percentile.

The fourth option for streamflow inputs to the M2M application is a user-defined hydrograph. For this scenario, a hydrograph was created that shifted the higher streamflow pulses that occurred during the first 4 months of 2002 to coincide with the spring tides to evaluate whether the salinity intrusion would be significantly reduced. The shifting of the three pulses to coincide with the spring tides did decrease the salinity intrusions at the end of January, February, and March 2002.

The final option for inputs to the M2M application is output from the 3D EFDC model. For this scenario, the EFDC model was used to simulate the effects of a hypothetical 4-ft deepening of the harbor based on the historical hydrologic and tidal conditions for calendar year 1999. The differences at selected USGS and GPA river gages were post-processed and used as input to the M2M. The 2-month average marsh salinities for the period July through August 1999 showed the highest effects in the marshes closest to the harbor and proximal to the Front River with diminishing increases farther upstream.

References

Abarbanel, H.D.I., 1996, Analysis of observed chaotic data: Springer-Verlag New York, Inc., NewYork, p. 4–12, 39.

Ambrose, R.B., Wool, T.A., and Martin, J.L., 1993, The water quality analysis simulation program, WASP5, part A—model documentation: U.S. Environmental Protection Agency, Athens, Ga., 210 p.

Applied Science Associates and Applied Technology and Management, 1998, Hydrodynamic and water quality modeling of the Lower Savannah River estuary, engineering report prepared for the Georgia Ports Authority, Savannah, Ga.: Applied Technology and Management, Inc., Atlanta, Ga., variously paged.

Applied Technology and Management, 1998, Hydrodynamics and water quality modeling of the Lower Savannah River estuary, engineering report prepared for Georgia Ports Authority, Savannah, Ga.: Applied Technology and Management, Inc., Charleston, S.C., May 1998, variously paged.

Applied Technology and Management, 2000, Hydrodynamic and water quality monitoring of the Lower Savannah River estuary, August 2 through October 9, 1999: Applied Technology and Management, Inc., April 2000, variously paged.

Applied Technology and Management, 2003, Savannah Harbor deepening project tidal marsh studies data report, volume 1. Report submitted to Georgia Ports Authority, March 2003, variously paged.

Barber, H.E., and Gann, A.R., 1989, A history of the Savannah District U.S. Army Corps of Engineers, 1829–1989: Savannah District, U.S. Army Corps of Engineers, Savannah, Ga., 554 p.

Bossart, J., Kitchens, W.M., and Dusek, M.L., 2001, Assessing salinity induced changes to tidal freshwater and oligohaline marsh habitats in the lower Savannah River: Watershed 2002 Specialty Conference, Fort Lauderdale, 2002.

Conrads, P.A., and Roehl, E.A., 1999, Comparing physics-based and neural network models for predicting salinity, water temperature, and dissolved oxygen concentration in a complex tidally affected river basin: South Carolina Environmental Conference, Myrtle Beach, March 1999.

Conrads, P.A., and Roehl, E.A., 2005, Integration of data mining techniques with mechanistic models to determine the impacts of non-point source loading on dissolved oxygen in tidal waters: South Carolina Environmental Conference, Myrtle Beach, March 2005.

Conrads, P.A., Roehl, E.A., and Cook, J.B., 2002a, Estimation of tidal marsh loading effects in a complex estuary: American Water Resources Association Annual Conference, New Orleans, May 2002.

Conrads, P.A., Roehl, E.A., and Martello, W.P., 2002b, Estimating point-source impacts on the Beaufort River using neural network models: American Water Resources Association Annual Conference, New Orleans, May 2002.

Conrads, P.A., Roehl, E.A., and Martello, W.P., 2003, Development of an empirical model of a complex, tidally affected river using artificial neural networks: Water Environment Federation TMDL 2003 Specialty Conference, Chicago, Illinois, November 2003.

Cowardin, L.M., Carter, V.M., Golet, F.C., and LaRoe, E.T., 1979, Classification of wetlands and deepwater habitats of the United States: U.S. Fish and Wildlife Service, FWS/OBS-79/31.

Devine, T.W., Roehl, E.A., and Busby, J.B., 2003, Virtual sensors—cost effective monitoring: Air and Waste Management Association Annual Conference, June 2003.

Dusek, M.L., 2003, Multi-scale spatial and temporal change in the tidal marshes of the Lower Savannah River Delta: Thesis presented to the graduate school of the University of Florida.

Dutta, Soumitra, Wierenga, Berend, Dalebout, Arco, 1997, Case-based reasoning systems: from automation to decision-aiding and stimulation: Knowledge and Data Engineering, IEEE Transactions on, v. 9, no. 6, p. 911–922.

Dyer, K.R., 1997, Estuaries—A physical introduction, 2nd ed.: John Wiley and Sons, Ltd, West Sussex, England, p. 4.

Georgia Environmental Protection Division, 1988, Savannah River classification study: Environmental Protection Division, Georgia Department of Natural Resources, Atlanta, Ga., January 1988 (revised).

Georgia Ports Authority, 1998, Environmental impact statement—Savannah Harbor expansion feasibility study: Prepared by Lockwood Greene and Applied Technology and Management, 1998, variously paged.

Gough, Laura, and Grace, J.B., 1998, Effects of flooding, salinity, and herbivory on coastal plant communities, Louisiana, United States: Oecologia, v. 117, no. 4, p. 527–535.

Granger, M.L., 1968, History of the Savannah District, 1829–1968: Savannah District, U.S. Army Corps of Engineers, Savannah District, 114 p.

Hamrick, J.M., 1992, A three-dimensional environmental fluid dynamics computer code: theoretical and computational aspects: The College of William and Mary, Virginia Institute of Marine Science, Special Report 317, 63 p.

Harleman, D.R.F., 1977, User's manual for the M.I.T. transient water quality network model—including nitrogen-cycle dynamics for rivers and estuaries: U.S. Environmental Protection Agency, EPA-600/3-77-010, Corvallis, Oreg., January 1977, 229 p.

Hinton, G.E., 1992, How neural networks learn from experience: Scientific American, September 1992, p. 145–151.

Howard, R.J., and Mendelsson, I.A., 1999, Salinity as a constraint on growth of oligohaline marsh macrophytes—Salt pulses and recovery potential: American Journal of Botany 86, p. 795–806.

Huvel, C.J., Multer, R.H., Senter, P.K., and Boyd, M.S., 1979, Savannah Harbor investigation and model study—volume IV reanalysis of freshwater control plan numerical model study, technical report 2-550: U.S. Army Corps of Engineers, Waterways Experiment Stations, September 1979.

Hydroscience, Inc., 1970, Water quality analysis of the Savannah River Estuary: Westwood, New Jersey, June 1970, 115 p. plus Addendum.

Jensen, B.A., 1994, Expert Systems—Neural networks, instrument engineers' handbook (3d ed.): Chilton, Radnor, Pa., p. 48–54.

Lamar, W.L., 1942, Industrial quality of the public water supplies in Georgia, 1940: U.S. Geological Survey, Water-Supply Paper 912, 83 p.

Latham, P.J., 1990, Plant distributions and competitive interactions along a gradient of tidal freshwater and brackish marshes: Dissertation presented to the graduate school of the University of Florida.

Latham, P.J., and Kitchens, W.M., 1995, Changes in vegetation and interstitial salinities following tide gate removal on the lower Savannah River, 1986–1994: Florida Cooperative Fish and Wildlife Research Unit, Gainesville, Fla., 16 p.

Lawler, Matusky, and Skelly Engineers, 1983, Development and application of a transport-dispersion water quality model for the Savannah River estuary—volume 1 application report: Pearl River, N.Y., 158 p.

Lawler, Matusky, and Skelly Engineers, 1986, Evaluation of the Savannah River estuary model, Letter Report: Pearl River, N.Y., March 4, 1986, 10 p. plus attachments.

Loftin, C.S., McCloskey, J.R., Kitchens, W.M., and Dusek, M.L., 2003, Changes in vegetation distributions in the Lower Savannah River tidal marsh following removal of a tidal flap gate, *in* W.M. Kitchens and others, 2003, Tidal wetland studies and tidal wetland resource utilization studies, Final Report: U.S. Geological Survey Florida Cooperative Fish and Wildlife Research Unit, 42 p.

Miller, R.L., Bradford, W.L., and Peters, N.E., 1988, Specific conductance: theoretical considerations and application to analytical quality control: U.S. Geological Survey Water-Supply Paper 2311, 16 p.

Muin, M., and Spauling, M.L., 1997, Three-dimensional boundary fitted circulation model: Journal of Hydraulic Engineering, January 1997, American Society of Civil Engineering, p. 2–12.

Odum, W.E., Smith, T.J., III, Hoover, J.K., and McIvor, C.C., 1984, The ecology of tidal freshwater marshes of the United States east coast—A community profile: U.S. Fish and Wildlife Service, FWS/OBS-83/17, Washington, D.C., 177 p.

Olinger, L.W., 1970, Procedure for evaluating the pollution assimilative capacity of the Savannah estuary: Federal Water Pollution Control Administration, Athens, Ga., April 1970, 30 p.

Pearlstine, L.G., Kitchens, W.M., Latham, P.J., and Bartleson, R.D., 1993, Tide gate influences on a tidal marsh: American Water Resources Association, Water Resources Bulletin, v. 29, no. 6, December 1993, p. 1009–1019.

Pearlstine, L.G., Latham, P.J., Kitchens, W.M., and Bartleson, R.D., 1990, Development and application of a habitat succession model for the wetland complex of the SNWR: volume II, final report, Submitted to the U.S. Fish and Wildlife Service, Savannah Coast Refuges, by the Florida Cooperative Fish and Wildlife Research Unit, Gainesville, Fla.

Pennington, C.H., and Bond, C.L., 1981, Savannah River estuary study—volume 1: water quality data report, miscellaneous paper EL-81, U.S. Army Corps of Engineers Waterways Experiment Studies, Vicksburg, Miss., April 1981, 85 p.

Press, W.H., Teukolsky, S.A., Vetterling, W.T., and Flannery, B.P., 1993, Numerical recipes in C: The art of scientific computing, Cambridge University Press, 1007 p.

Rhodes, R.F., 1949, The hydraulics of a tidal river as illustrated by the Savannah Harbor, Georgia: U.S. Army Corps of Engineers, Savannah District, Savannah, Ga., January 1949.

Risley, J.C., Roehl, E.A., and Conrads, P.A., 2002, Estimating water temperatures in small streams in western Oregon using neural network models: U.S. Geological Survey Water-Resources Investigations Report 02-4218, 59 p.

Roehl, E.A., and Conrads, P.A., 1999, Near real-time control for matching wastewater discharges to the assimilative capacity of a complex, tidally affected river basin: 1999 South Carolina Environmental Conference, Myrtle Beach, March 15–16, 1999.

Roehl, E.A., Conrads, P.A., and Cook, J.B., 2003, Discussion of using complex permittivity and artificial neural networks for contaminant prediction: Journal of Environmental Engineering, Nov. 2003, p. 1069–1071.

Roehl, E.A., Conrads, P.A., Roehl, T.A.S., 2000, Real-time control of the salt front in a complex tidally affected river basin: Smart Engineering System Design: Volume 10, Proceedings of the Artificial Neural Networks In Engineering Conference: ASME Press, New York, p. 947–954.

Rosenblatt, Frank, 1958, The perceptron: a probabilistic model for information storage and organization in the brain: Psychological Review, 65, 1958, p. 386–408.

Rumelhart, D.E., Hinton, G.E., and Williams, R.J., 1986, Learning internal representations by error Propagation, Parallel Distributed Processing—Explorations in the Microstructure of Cognition, Volume 1, Cambridge, Mass.: The MIT Press, p. 318–362.

Sanders, C.L., Kubik, H.E., Hoke, J.T., and Kirby, W.H., 1990, Flood frequency of the Savannah River at Augusta, Georgia: U.S. Geological Survey Water-Resources Investigations Report 90-4024, 87 p.

Shingler, J.H.C., 1981, Savannah River Estuary Study—volume II hydrodynamic data report, Miscellaneous Paper EL-81, U.S. Army Corps of Engineers Waterways Experiment Studies, Vicksburg, Miss., August 1981, 226 p.

Spaulding, M.L., 1984, A vertically averaged circulation model using boundary-fitted coordinates: Journal of Physical Oceanography, v. 14, no. 5, p. 973–982.

Streeter, H.W., and Phelps, E.B., 1925, A study of the pollution and natural purification of the Ohio River, Illinois—factors concerned in the phenomena of oxidation and reaeration: U.S. Public Health Service Bulletin 146, Washington, D.C.

Swanson, J.C., 1986, A three-dimensional numerical model system of coastal circulation and water quality, PhD dissertation, University of Rhode Island, Kingston, R.I.

Tetra Tech, 2005, Development of the EFDC hydrodynamic model for the Savannah Harbor. Prepared for the U.S. Army Corps of Engineers—Savannah District: Tetra Tech, Inc., Atlanta, Ga.

Tiner, R.W., 1977, An inventory of South Carolina's coastal marshes: Office of Conservation and Management, South Carolina Wildlife and Marine Resources Department, Charleston, S.C., Technical Report Number 23, 33 p.

U.S. Army Corps of Engineers, 1991, Tidal hydraulics—engineering manual: U.S. Army Corps of Engineers Technical Report No. EM 1110-2-1607, Washington, D.C.

U.S. Army Corps of Engineers Waterways Experiment Station, 1961a, Savannah Harbor investigations and model study: volume III—results of model investigation, section 1—model verification and results of general studies, Technical Report No. 2-580, Vicksburg, Miss.

U.S. Army Corps of Engineers Waterways Experiment Station, 1961b, Savannah Harbor investigations and model study: volume III—results of model investigation, section 2—test of improvement plans, Technical Report No. 2-580, Vicksburg, Miss.

U.S. Army Corps of Engineers Waterways Experiment Station, 1963, Savannah Harbor investigations and model study: volume III—results of model investigation, section 3—results of supplemental tests, Technical Report No. 2-580, Vicksburg, Miss.

U.S. Environmental Protection Agency, 2004, Draft total maximum daily load (TMDL) for dissolved oxygen in Savannah Harbor, Savannah River Basin, Chatham and Effingham Counties, Georgia: U.S. Environmental Protection Agency, Region 4, Atlanta, Ga., 20 p.

Weiss, S.M., and Indurkhya, Nitin, 1998, Predictive data mining—a practical guide: Morgan Kaufmann Publishers, Inc., San Francisco, p. 1.

Wool, T.A., Ambrose, R.B., Martin, J.L., and Comer, E.A., 2001, Water quality analysis simulation program (WASP) version 6.0 draft, user's manual: U.S. Environmental Protection Agency, Region 4, Atlanta, Ga., 259 p.

Appendices I–IV

Appendix I. Summary statistics for the water-level and specific-conductance models used in the study.

[WL, water level; SC, specific conductance; Min, minimum; Max, maximum; n, number of data points; R^2, coefficient of determination; SSE, sum of squared error; ME, mean error; RMSE, root mean square error; PME, percent model error]

Model name	Gage number	Output variable	Range of output variable		Training		SSE	ME	RMSE	PME	Range of output variable		Testing					
			Min	Max	n	R^2					Min	Max	n	R^2	SSE	ME	RMSE	PME
USGS river network water-level models																		
wl8840a-2005-1	2198840	WL-daily	–0.31	4.46	11051	0.969	165.57	0.000	0.12	2.6%	–0.48	5.66	81446	0.964	1911	0.022	0.15	2.5%
wl8840h-2005-1	2198840	WL-hourly	–3.98	6.87	2303	0.987	199.33	–0.000	0.29	2.7%	–4.32	7.09	70796	0.983	7935	0.025	0.33	2.9%
wl8920a-2005-1	2198920	WL-daily	–0.94	3.07	10482	0.977	84.06	–0.000	0.09	2.2%	–0.95	4.05	68121	0.883	2803	0.183	0.20	4.1%
wl8920h-2005-1	2198920	WL-hourly	–7.08	6.73	10538	0.995	467.38	0.000	0.21	1.5%	–6.46	7.34	68368	0.991	5492	0.186	0.28	2.1%
wl8977a-2005-1	2198977	WL-daily	–0.91	3.07	10612	0.960	137.193	0.000	0.11	2.9%	–0.91	3.68	79682	0.965	857	0.028	0.10	2.3%
wl8977h-2005-1	2198977	WL-hourly	–7.20	6.85	10717	0.994	528.459	–0.000	0.22	1.6%	–6.65	7.13	79951	0.995	3422	0.029	0.21	1.5%
wl8979a-2005-1	2198979	WL-daily	–0.30	3.86	7987	0.952	141.946	–0.000	0.13	3.2%	–0.32	4.75	70993	0.961	1153	0.043	0.13	2.5%
wl8979h-2005-1	2198979	WL-hourly	–4.70	6.86	8029	0.984	980.854	–0.000	0.35	3.0%	–4.86	7.15	71187	0.981	10071	0.034	0.38	3.1%
USGS river network specific-conductance models																		
sc8840a-2005-1	2198840	SC-daily	60	773	10056	0.887	1763591.2	0.047	13	1.9%	45.95	773.40	77309	0.851	12414716	–3.254	13	1.7%
sc8840h-2005-1	2198840	SC-hourly	59	8370	10197	0.879	21846887	0.056	46	0.6%	30.00	2374.60	77772	0.567	42270460	–3.236	23	1.0%
sc8920a-2005-1	2198920	SC-daily	68	18667	9836	0.897	1.41E+10	0.864	1198	6.4%	50.48	18725.80	67677	0.883	8.80E+10	–367.667	1141	6.1%
sc8920h-2005-1	2198920	SC-hourly	6	31169	9900	0.900	3.84E+10	–0.732	1971	6.3%	30.00	31934.70	67820	0.867	2.32E+11	–308.104	1850	5.8%
sc89784a-2005-1	21989784	SC-daily	79	2198	8534	0.880	1.62E+8	0.160	138	6.5%	50.45	2229.85	70348	0.853	1.02E+9	–60.755	121	5.5%
sc89784h-2005-1	21989784	SC-hourly	72	5821	8600	0.825	2.92E+8	0.006	184	3.2%	40.00	4286.00	71064	0.793	1.62E+9	–56.100	151	3.6%
sc89791a-2005-1	21989791	SC-daily	78	5693	9660	0.887	5.97E+8	0.870	249	4.4%	51.64	5689.54	75782	0.870	2.89E+9	–65.833	195	3.5%
sc89791h-2005-1	21989791	SC-hourly	75	15200	9736	0.888	1.10E+9	0.336	336	2.2%	50.00	10972.59	76366	0.826	5.42E+9	–63.386	266	2.4%
USGS marsh network water-level models																		
pb1mwl-2005	B1	WL-hourly	–0.10	1.50	3143	0.770	12.88	0.000	0.06	4.0%	–0.10	1.60	17653	0.762	67.48	–0.001	0.06	3.6%
pb2mwl-2005	B2	WL-hourly	0.00	1.80	3284	0.797	37.00	0.000	0.11	5.9%	0.00	2.20	18228	0.768	229.15	–0.002	0.11	5.1%
pb3mwl-2005	B3	WL-hourly	0.00	1.80	3558	0.858	19.22	–0.000	0.07	4.1%	0.00	2.10	20082	0.866	105.25	–0.000	0.07	3.4%
pb4mwl-2005	B4	WL-hourly	0.00	2.00	2879	0.887	19.31	–0.002	0.08	4.1%	0.00	2.30	15877	0.872	127.81	0.000	0.09	3.9%
pf1mwl-2005	F1	WL-hourly	0.00	1.50	4243	0.839	19.61	0.000	0.07	4.5%	0.00	2.00	23982	0.836	113.20	–0.001	0.07	3.4%
pm1mwl-2005	M1	WL-hourly	0.00	1.40	2424	0.694	22.38	0.000	0.10	6.9%	0.00	1.70	13299	0.722	111.83	0.001	0.09	5.4%
pm2mwl-2005	M2	WL-hourly	0.00	1.40	1751	0.808	12.22	0.000	0.08	6.0%	0.00	1.80	9676	0.778	73.91	–0.002	0.09	4.9%
USGS marsh network specific-conductance models																		
pb1msc-2005-2	B1	SC-hourly	117	2433	2333	0.857	6.56E+7	–0.050	168	7.2%	53.60	2561.60	20555	0.849	5.98E+8	0.207	171	6.8%
pb2msc-2005-2	B2	SC-hourly	52	3055	2142	0.826	1.41E+8	–0.684	257	8.5%	50.50	3881.00	18770	0.832	1.22E+9	0.823	255	6.7%
pb3msc-2005-2	B3	SC-hourly	619	4478	2326	0.549	6.17E+8	0.657	515	13.4%	98.50	4921.80	20519	0.532	5.48E+9	–4.510	517	10.7%
pb4msc-2005-2	B4	SC-hourly	131	21845	2093	0.654	9.59E+9	–2.247	2142	9.9%	50.00	24624.80	18577	0.641	9.06E+10	14.870	2209	9.0%

Appendix I. Summary statistics for the water-level and specific-conductance models used in the study.—Continued

[WL, water level; SC, specific conductance; Min, minimum; Max, maximum; n, number of data points; R^2, coefficient of determination; SSE, sum of squared error; ME, mean error; RMSE, root mean square error; PME, percent model error]

Model name	Gage number	Output variable	Range of output variable		Training		SSE	ME	RMSE	PME	Range of output variable		Testing					
			Min	Max	n	R^2					Min	Max	n	R^2	SSE	ME	RMSE	PME
USGS marsh network specific-conductance models—Continued																		
pf1msc-2005-2	F1	SC-hourly	165	5236	2496	0.816	4.77E+8	0.439	437	8.6%	161.90	5565.50	22073	0.820	4.14E+9	–14.661	433	8.0%
pm1msc-2005-2	M1	SC-hourly	56	6853	2147	0.809	3.83E+8	0.252	423	6.2%	50.30	6886.89	18927	0.808	3.27E+9	–2.905	416	6.1%
pm2msc-2005-2	M2	SC-hourly	67	12721	2323	0.841	1.03E+9	-0.078	666	5.3%	52.40	17588.40	20593	0.830	1.02E+10	10.500	704	4.0%
Decorrelation models																		
dc_gpa_a1wk_10s_11b	GPA11	SC-decorrelated-hourly	101	9825	7644	0.800	7.37E+9	–1.863	982	10.1%	100.51	9836.66	30459	0.804	2.85E+10	–23.431	967	9.9%
dc_gpa_a1wk_10s_11rb	GPA11r	SC-decorrelated-hourly	101	9825	7750	0.957	1.62E+9	–1.837	457	4.7%	100.51	9836.66	30921	0.958	6.25E+9	–1.805	450	4.6%
dc_gpa_a1wk_10s_12rs	GPA12	SC-decorrelated-hourly	101	9825	7750	0.881	4.48E+9	–0.273	760	7.8%	100.51	9836.66	30921	0.880	1.79E+10	0.863	761	7.8%
Residual models																		
prb1msc	B1	SC-residual-hourly	–543	780	4547	0.080	1.16E+8	0.005	160	12.1%	–610.27	797.10	18224	0.087	4.90E+8	1.615	164	11.7%
prb2msc	B2	SC-residual-hourly	–895	1291	4176	0.067	2.49E+8	–0.158	244	11.2%	–931.97	1652.73	16736	0.059	1.03E+9	0.915	248	9.6%
prb3msc	B3	SC-residual-hourly	–1422	1889	4519	0.020	1.18E+9	0.089	510	15.4%	–1505.04	1920.47	18209	0.018	4.80E+9	–6.018	513	15.0%
prb4msc	B4	SC-residual-hourly	–7437	9515	4097	0.020	1.96E+10	0.213	2185	12.9%	–10521.66	11200.50	16456	0.020	7.83E+10	–41.183	2182	10.0%
prf1msc	F1	SC-residual-hourly	–2214	2046	4873	0.055	9.10E+8	2.199	432	10.1%	–2213.96	2046.15	19579	0.050	3.47E+9	9.212	421	9.9%
prm1msc	M1	SC-residual-hourly	–1411	2029	4163	0.073	6.80E+8	0.169	404	11.8%	–1434.29	1575.44	16803	0.065	2.71E+9	1.600	402	13.3%
prm2msc	M2	SC-residual-hourly	–2721	5548	4539	0.034	2.16E+9	0.138	691	8.4%	–3576.68	8438.79	18260	0.016	8.87E+9	3.267	697	5.8%
USGS marsh network final specific-conductance predictions[1]																		
pb1msc+prb1msc	B1	SC-hourly	54	2562	22771	0.930	605979116.053	146	163	6.5%								
pb2msc+prb2msc	B2	SC-hourly	51	3881	20912	0.920	1279931410.674	189	247	6.5%								
pb3msc+prb3msc	B3	SC-hourly	99	4922	22728	0.740	5976021278.970	204	513	10.6%								
pb4msc+prb4msc	B4	SC-hourly	50	24625	20553	0.810	97902484501.427	863	2183	8.9%								
pf1msc+prf1msc	F1	SC-hourly	162	5945	24452	0.910	4381284781.595	314	423	7.3%								
pm1msc+prm1msc	M1	SC-hourly	50	6887	20966	0.906	3391670091.831	350	402	5.9%								
pm2msc+prm2msc	M2	SC-hourly	50	17588	22799	0.913	11031369048.355	497	696	4.0%								

Appendix I. Summary statistics for the water-level and specific-conductance models used in the study.—Continued

[WL, water level; SC, specific conductance; Min, minimum; Max, maximum; n, number of data points; R^2, coefficient of determination; SSE, sum of squared error; ME, mean error; RMSE, root mean square error; PME, percent model error]

Model name	Gage number	Output variable	Range of output variable		Training		SSE	ME	RMSE	PME	Range of output variable		Testing					
			Min	Max	n	R^2					Min	Max	n	R^2	SSE	ME	RMSE	PME
GPA river network water-level models																		
wlgpa04d-2005	GPA04	WL-hourly	–1.22	1.27	4215	0.640	134.44	–0.024	0.18	7.2%	–0.79	1.35	1079	0.626	35.47	–0.023	0.18	8.5%
wlgpa05d-2005	GPA05	WL-hourly	–1.12	3.71	4344	0.638	148.27	0.070	0.18	3.8%	–1.00	0.72	1133	0.676	36.01	0.067	0.18	10.4%
wlgpa06d-2005	GPA06	WL-hourly	–0.64	0.88	4305	0.176	166.61	–0.037	0.20	12.9%	–0.65	0.92	1124	0.152	45.26	–0.045	0.20	12.8%
wlgpa07d-2005	GPA07	WL-hourly	–1.81	1.10	1606	0.641	85.52	–0.031	0.23	7.9%	–1.34	1.06	416	0.638	23.15	–0.035	0.24	9.9%
wlgpa08d-2005	GPA08	WL-hourly	–0.77	0.97	4614	0.238	153.87	0.029	0.18	10.5%	–0.78	0.74	1175	0.216	36.88	0.021	0.18	11.7%
wlgpa09d-2005	GPA09	WL-hourly	–1.39	1.59	4642	0.338	877.16	0.019	0.43	14.6%	–1.36	1.43	1192	0.310	230.22	0.027	0.44	15.8%
wlgpa10d-2005	GPA10	WL-hourly	–2.18	1.79	2187	0.230	138.00	–0.125	0.25	6.3%	–1.07	3.34	587	0.233	42.88	–0.112	0.27	6.1%
wlgpa11d-2005	GPA11	WL-hourly	–1.27	1.94	1578	0.534	180.26	–0.037	0.34	10.5%	–1.49	1.97	434	0.570	46.47	–0.021	0.33	9.5%
wlgpa11rd-2005	GPA11R	WL-hourly	–1.53	0.86	1617	0.863	57.56	–0.012	0.19	7.9%	–1.57	0.79	399	0.855	15.06	–0.015	0.19	8.3%
wlgpa12d-2005	GPA12	WL-hourly	–3.08	1.92	2846	0.272	1733.72	–0.045	0.78	15.6%	–2.93	1.61	749	0.242	461.76	–0.033	0.79	17.3%
wlgpa13d-2005	GPA13	WL-hourly	–3.52	1.91	2123	0.917	301.34	–0.008	0.38	6.9%	–3.48	1.75	561	0.926	72.48	–0.022	0.36	6.9%
wlgpa14d-2005	GPA14	WL-hourly	–0.95	1.63	1630	0.914	54.32	–0.016	0.18	7.1%	–0.86	1.56	424	0.909	14.23	–0.022	0.18	7.6%
wlgpa21d-2005	GPA21	WL-hourly	–0.71	0.84	2227	0.030	117.57	0.006	0.23	14.8%	–0.68	0.76	551	0.004	29.40	0.004	0.23	16.1%
wlgpa22d-2005	GPA22	WL-hourly	–1.04	1.36	1502	0.884	57.72	0.012	0.20	8.2%	–1.01	1.40	384	0.867	15.60	0.011	0.20	8.4%
wlgpa23d-2005	GPA23	WL-hourly	–0.77	1.43	2754	0.816	98.93	0.013	0.19	8.6%	–0.90	1.31	696	0.798	27.75	0.006	0.20	9.0%
wlgpa24md-2005	GPA24M	WL-hourly	–0.89	1.24	2755	0.760	126.14	0.089	0.21	10.0%	–0.86	1.28	697	0.741	35.18	0.088	0.22	10.5%
wlgpa25md-2005	GPA25M	WL-hourly	–0.97	1.44	2750	0.653	158.93	0.001	0.24	10.0%	–1.10	1.14	697	0.645	39.98	0.002	0.24	10.7%
wlgpa26d-2005	GPA26	WL-hourly	–1.19	1.29	2210	0.788	85.62	–0.008	0.20	7.9%	–0.92	1.19	553	0.786	23.05	0.003	0.20	9.7%
GPA river network specific-conductance models																		
scgpa04bd-2005	GPA04B	SC-hourly[2]	–39814	–8970	4284	0.522	4.04E+10	1124	3072	10.0%	–37572	–10000	1090	0.491	1.12E+10	1264	3202.85	11.6%
scgpa04sd-2005	GPA04S	SC-hourly[2]	–27602	2556	4511	0.650	2.93E+10	901	2549	8.5%	–26373	–775	1145	0.666	7.30E+9	796	2527	9.9%
scgpa05bd-2005	GPA05B	SC-hourly[2]	–21759	1084	3901	0.714	1.87E+10	–2161	2190	9.6%	–21367	–178	1021	0.702	5.13E+9	–2082	2244	10.6%
scgpa06bd-2005	GPA06B	SC-hourly[2]	–37739	–502	4155	0.676	5.80E+10	2127	3737	10.0%	–37574	–621	1090	0.678	1.46E+10	1960	3663	9.9%
scgpa06sd-2005	GPA06S	SC-hourly[2]	–20801	11578	4131	0.641	1.68E+10	497	2017	6.2%	–19027	9616	1044	0.630	4.20E+9	428	2008	7.0%
scgpa07bd-2005	GPA07B	SC-hourly[2]	–15830	147	2042	0.806	3.14E+9	175	1241	7.8%	–15880	41	555	0.808	9.45E+8	140	1307	8.2%
scgpa07sd-2005	GPA07S	SC-hourly[2]	–16314	100	2376	0.857	2.65E+9	–388	1057	6.4%	–15529	97	598	0.861	7.79E+8	–471	1143	7.3%
scgpa08bd-2005	GPA08B	SC-hourly[2]	–30232	5712	4792	0.402	5.98E+10	672	3533	9.8%	–30249	592	1216	0.428	1.35E+10	799	3335	10.8%
scgpa08sd-2005	GPA08S	SC-hourly[2]	–6751	19219	4112	0.419	8.33E+9	–320	1424	5.5%	–4379	15676	1030	0.409	1.72E+9	–331	1294	6.4%
scgpa09bd-2005	GPA09B	SC-hourly[2]	–23857	9668	4611	0.260	1.31E+10	400	1686	5.0%	–21042	3490	1178	0.295	3.07E+9	369	1616	6.6%
scgpa09sd-2005	GPA09S	SC-hourly[2]	–10331	13666	1640	0.546	1.93E+9	–49	1085	4.5%	–9256	10335	410	0.568	3.86E+8	–71	973	5.0%

Appendix I. Summary statistics for the water-level and specific-conductance models used in the study.—Continued

[WL, water level; SC, specific conductance; Min, minimum; Max, maximum; n, number of data points; R^2, coefficient of determination; SSE, sum of squared error; ME, mean error; RMSE, root mean square error; PME, percent model error]

Model name	Gage number	Output variable	Range of output variable		Training		SSE	ME	RMSE	PME	Range of output variable		Testing					
			Min	Max	n	R^2					Min	Max	n	R^2	SSE	ME	RMSE	PME
GPA river network specific-conductance models—Continued																		
scgpa10bd-2005	GPA10B	SC-hourly[2]	–5530	19498	2335	0.919	1.75E+9	–84	866	3.5%	–4965	13853	625	0.908	4.30E+8	–113	831	4.4%
scgpa10sd-2005	GPA10S	SC-hourly[2]	–3999	16271	1609	0.899	1.15E+9	–366	846	4.2%	–4321	13949	410	0.887	3.20E+8	–410	886	4.8%
scgpa11bd-2005	GPA11B	SC-hourly[2]	–6645	1386	1777	0.534	2.53E+8	–66	378	4.7%	–6422	1237	470	0.430	7.57E+7	–77	402	5.3%
scgpa11rbd-2005	GPA11RB	SC-hourly[2]	–13115	16987	1288	0.662	3.98E+9	–633	1759	5.8%	–12878	15785	326	0.743	7.36E+8	–733	1507	5.3%
scgpa12bd-2005	GPA12B	SC-hourly[2]	–569	21688	3003	0.986	6.51E+8	–66	466	2.1%	–298	20393	787	0.985	1.65E+8	–76	458	2.2%
scgpa12rsd-2005	GPA12RS	SC-hourly[2]	–4958	20297	1455	0.847	2.63E+9	–384	1345	5.3%	–4131	18648	367	0.861	6.21E+8	–532	1304	5.7%
scgpa13bd-2005	GPA13B	SC-hourly[2]	–1769	2620	2120	0.408	8.06E+7	84	195	4.4%	–1411	2212	561	0.502	2.06E+7	83	192	5.3%
scgpa14bd-2005	GPA14B	SC-hourly[2]	–53	36	4502	0.662	2.55E+5	5	8	8.4%	–45	31	1169	0.657	6.84E+4	5	8	10.2%
scgpa15sd-2005	GPA15S	SC-hourly[2]	–5267	769	5540	0.555	3.90E+8	–2	265	4.4%	–5180	560	1359	0.518	1.00E+8	4	271	4.7%
scgpa21bd-2005	GPA21B	SC-hourly[2]	–39980	–9982	1759	0.577	2.03E+10	56	3399	11.3%	–39856	–10000	427	0.503	5.19E+9	–149	3495	11.7%
scgpa21sd-2005	GPA21S	SC-hourly[2]	–20970	8773	2396	0.606	1.03E+10	–927	2074	7.0%	–21397	5496	597	0.594	2.57E+9	–1063	2078	7.7%
scgpa22bd-2005	GPA22B	SC-hourly[2]	–28249	–660	1328	0.329	1.45E+10	–99	3307	12.0%	–25199	–1255	334	0.269	3.81E+9	–415	3388	14.1%
scgpa22sd-2005	GPA22S	SC-hourly[2]	–11036	18858	1602	0.627	4.29E+9	212	1637	5.5%	–12626	14317	393	0.627	1.09E+9	217	1670	6.2%
GPA marsh network water-level models																		
ps1canalwl-2005	Site 1	WL-hourly	–0.80	6.01	815	0.983	59.48	–0.000	0.27	4.0%	–0.8	6.27	7911	0.983	680.61	–0.007	0.29	4.1%
ps1marshwl-2005	Site 1	WL-hourly	4.88	5.57	1726	0.648	2.17	0.000	0.04	5.1%	4.86	5.66	7208	0.610	13.02	–0.001	0.04	5.3%
[3]ps1marshwlat-2005	Site 1	WL-hourly	4.73	5.89	1371	0.672	8.09	–0.000	0.08	6.7%								
ps2canalwl-2005	Site 2	WL-hourly	0.56	5.70	613	0.922	96.17	–0.001	0.40	7.7%	0.56	5.76	2398	0.936	390.11	0.004	0.40	7.8%
ps2marshwl-2005	Site 3	WL-hourly	3.55	4.65	796	0.741	3.67	0.000	0.07	6.2%	3.47	4.78	2306	0.740	13.30	–0.002	0.08	5.8%
ps3canalwl-2005	Site 3	WL-hourly	–0.50	6.29	877	0.976	78.46	–0.000	0.30	4.4%	–0.5	6.56	12699	0.961	2004.13	–0.013	0.40	5.6%
ps3marshwl-2005	Site 4	WL-hourly	3.89	5.32	2077	0.891	3.87	0.000	0.04	3.0%	3.85	5.32	12595	0.806	43.74	–0.002	0.06	4.0%
ps4canalwl-2005	Site 4	WL-hourly	–2.78	5.94	809	0.986	68.59	0.001	0.29	3.3%	–2.79	6.12	7784	0.985	818.92	–0.012	0.32	3.6%
ps4marshwl-2005	Site 5	WL-hourly	4.06	5.16	1764	0.902	1.76	–0.000	0.03	2.9%	4.06	5.25	7762	0.858	12.98	–0.001	0.04	3.4%
ps5canalwl-2005	Site 5	WL-hourly	–0.35	6.36	4805	0.989	226.77	0.000	0.22	3.2%	–0.22	8.59	5784	0.619	10029.90	1.632	1.32	14.9%
ps5marshwl-2005	Site 6	WL-hourly	4.62	5.60	1965	0.911	1.61	–0.000	0.03	2.9%	4.61	5.61	10219	0.891	10.16	–0.003	0.03	3.2%
ps6canalwl-2005	Site 6	WL-hourly	0.18	6.13	791	0.990	22.32	–0.000	0.17	2.8%	0.18	6.78	7408	0.983	441.83	–0.003	0.24	3.7%
ps6marshwl-2005	Site 6	WL-hourly	4.83	5.47	1647	0.804	1.31	0.000	0.03	4.4%	4.83	5.6	6637	0.763	7.89	–0.002	0.03	4.5%
[3]ps6marshwlat-2005	Site 6	WL-hourly	4.67	5.84	1720	0.960	1.65	–0.000	0.03	2.6%								
ps7canalwl-2005	Site 7	WL-hourly	–0.93	5.69	572	0.924	177.69	0.000	0.56	8.4%	–0.93	6	2739	0.933	881.28	–0.024	0.57	8.2%
[3]ps7marshwl-2005	Site 7	WL-hourly	4.19	5.28	2822	0.701	13.81	–0.000	0.07	6.4%								

Appendix I. Summary statistics for the water-level and specific-conductance models used in the study.—Continued

[WL, water level; SC, specific conductance; Min, minimum; Max, maximum; n, number of data points; R^2, coefficient of determination; SSE, sum of squared error; ME, mean error; RMSE, root mean square error; PME, percent model error]

Model name	Gage number	Output variable	Range of output variable		Training		SSE	ME	RMSE	PME	Range of output variable		Testing					
			Min	Max	n	R^2					Min	Max	n	R^2	SSE	ME	RMSE	PME
GPA marsh network water-level models—Continued																		
[3]ps8canalwl-2005	Site 8	WL-hourly	0.18	5.74	430	0.996	6.54	0.000	0.12	2.2%								
ps9canalwl-2005	Site 9	WL-hourly	1.00	5.68	805	0.991	14.87	0.000	0.14	2.9%	0.99	6.18	7829	0.988	213.29	–0.001	0.17	3.2%
ps9marshwl-2005	Site 9	WL-hourly	3.89	5.13	1801	0.827	8.63	0.000	0.07	5.6%	3.89	5.27	7882	0.762	55.80	0.000	0.08	6.1%
ps10canalwl-2005	Site 10	WL-hourly	–0.26	6.29	694	0.982	45.82	0.000	0.26	3.9%	–0.26	6.68	5982	0.980	513.02	–0.010	0.29	4.2%
ps10marshwl-2005	Site 10	WL-hourly	3.99	5.09	1530	0.906	1.73	0.000	0.03	3.1%	3.98	5.19	5985	0.904	9.32	–0.005	0.04	3.3%
GPA marsh network specific-conductance models																		
ps1canalsc-2005	Site 1	SC-hourly	0	22990	750	0.926	1.51E+9	1.3	1420.82	6.2%	0	23690	7559	0.885	1.34E+10	–179	1331.61	5.6%
ps1marshsc-2005	Site 1	SC-hourly	0	16740	1441	0.726	1.29E+9	0.3	946.81	5.7%	0	16740	3990	0.722	2.11E+9	–45.0	727.38	4.3%
ps2canalsc-2005	Site 2	SC-hourly	694	25157	1301	0.913	3.27E+9	9.0	1586.61	6.5%	0	25869	6355	0.897	1.54E+10	–110	1556.94	6.0%
ps2marshsc-2005	Site 2	SC-hourly	5	21870	902	0.882	4.00E+9	2.4	2107.13	9.6%	0	21870	2733	0.876	8.97E+9	45.7	1812.32	8.3%
ps3canalsc-2005	Site 3	SC-hourly	0	19750	2118	0.812	3.88E+9	0.0	1354.12	6.9%	0	23010	11954	0.813	1.28E+10	–75.0	1034.87	4.5%
ps3marshsc-2005	Site 3	SC-hourly	0	13320	2062	0.845	1.84E+9	1.7	945.09	7.1%	0	13320	11025	0.826	5.25E+9	–34.5	690.13	5.2%
ps4canalsc-2005	Site 4	SC-hourly	0	13535	1798	0.865	9.28E+8	4.3	718.82	5.3%	0	14330	7463	0.839	2.85E+9	0.8	618.05	4.3%
ps4marshsc-2005	Site 4	SC-hourly	0	9590	1658	0.897	3.11E+8	0.0	433.36	4.5%	0	9890	5535	0.861	7.44E+8	–14.5	366.70	3.7%
ps5canalsc-2005	Site 5	SC-hourly	0	11600	1500	0.814	8.42E+8	2.8	749.72	6.5%	0	45780	4312	0.000	3.22E+11	19536	8643.49	18.9%
ps5marshsc-2005	Site 5	SC-hourly	0	21300	4108	0.630	1.78E+10	–2.4	2082.09	9.8%	0	21300	12677	0.548	3.99E+10	6.6	1774.24	8.3%
ps6canalsc-2005	Site 6	SC-hourly	0	20830	1617	0.834	3.17E+9	–1.1	1401.02	6.7%	0	22290	6115	0.825	7.58E+9	3.1	1113.54	5.0%
ps6marshsc-2005	Site 6	SC-hourly	0	19170	1673	0.859	1.50E+9	1.0	947.45	4.9%	0	20940	5953	0.814	3.62E+9	–40.7	779.94	3.7%
ps7canalsc-2005	Site 7	SC-hourly	0	24710	3665	0.873	1.18E+10	3.1	1794.83	7.3%	0	22260	3049	0.000	1.70E+11	1214	7469.44	33.6%
prs7marshpwc	Site 7	SC-hourly	88	6089	1539	0.150	3.26E+9	1.0	1456.37	24.3%	0	8180.38	6136	0.141	1.28E+10	–14.1	1444.55	17.7%
ps7marshpwsc-2005-2	Site 7	SC-hourly	0	20180	4270	0.650	1.11E+10	–1.0	1612.68	8.0%	0	22180	4260	0.679	1.07E+10	21.0	1585.22	7.1%
ps8canalsc-2005	Site 8	SC-hourly	0	5797	1458	0.871	7.40E+7	0.3	225.48	3.9%	0	5797	4752	0.831	2.73E+8	24.1	239.74	4.1%
ps9canalsc-2005	Site 9	SC-hourly	0	16240	1806	0.847	1.10E+9	–10.6	780.87	4.8%	0	16240	6905	0.826	2.58E+9	–11.1	611.35	3.8%
prs9marshpwc	Site 9	SC-hourly	88	3729	1519	0.098	2.20E+8	-0.0	380.82	10.5%	0	3781.08	6052	0.097	8.34E+8	–1.5	371.28	9.8%
ps9marshpwsc-2005-2	Site 9	SC-hourly	0	6002	4221	0.518	7.95E+8	–0.1	434.09	7.2%	0	6002	4205	0.556	7.27E+8	–20.5	415.90	6.9%
prs10marshpwc	Site 10	SC-hourly	88	2184	1460	0.100	8.41E+9	0.4	2401.70	114.6%	0	2188.51	5797	0.101	3.17E+10	77.0	2338.85	106.9%
ps10marshpwsc-2005-2	Site 10	SC-hourly	0	17400	3195	0.851	2.42E+9	1.1	870.58	5.0%	0	17370	4917	0.324	3.70E+10	–1834	2743.72	15.8%

[1] Sum of results from marsh and residual models. Statistics for period of record for each USGS marsh site.

[2] Models predicted differences from one of the USGS river gages. Observed minimum conductance is difference with USGS river gage and may be negative.

[3] Due to data quality concerns, data set was not bifurcated into training and testing datasets.

Appendix II. Model summary of artificial neural network models used in the Model-to-Marsh application.

[R^2, coefficient of determination]

Model	Input variables	Output variable	Number of hidden neurons	Training matrix size	Testing matrix size	R^2 training	R^2 testing
USGS river network water-level models							
wl8840a-2005-1	Q8500A DQ8500A FWL8980A XWL8980A DXWLAD1 DWLAD1	WL8840A	3	11051	81446	0.969	0.964
wl8840h-2005-1	LG1NWL LG1D3NWL LG4D3NWL LG7D3NWL LG10D3NWL LG13D3NWL PWL8840A	WL8840	3	2303	70796	0.987	0.983
wl8920a-2005-1	Q8500A DQ8500A FWL8980A XWL8980A DXWLAD1 DWLAD1	WL8920A	3	10482	68121	0.977	0.883
wl8920h-2005-1	LG1NWL LG1D3NWL LG4D3NWL LG7D3NWL LG10D3NWL LG13D3NWL PWL8920A	WL8920	2	10538	68368	0.995	0.991
wl8977a-2005-1	Q8500A DQ8500A FWL8980A XWL8980A DXWLAD1 DWLAD1	WL8977A	2	10612	79682	0.960	0.965
wl8977h-2005-1	LG1NWL LG1D3NWL LG4D3NWL LG7D3NWL LG10D3NWL LG13D3NWL PWL8977A	WL8977	2	10717	79951	0.994	0.995

Appendix II. Model summary of artificial neural network models used in the Model-to-Marsh application.—Continued

[R^2, coefficient of determination]

Model	Input variables	Output variable	Number of hidden neurons	Training matrix size	Testing matrix size	R^2 training	R^2 testing
USGS river network water-level models—Continued							
wl8979a-2005-1	Q8500A DQ8500A FWL8980A XWL8980A DXWLAD1 DWLAD1	WL8979A	2	7987	70993	0.952	0.961
wl8979h-2005-1	LG1NWL LG1D3NWL LG4D3NWL LG7D3NWL LG10D3NWL LG13D3NWL PWL8979A	WL8979	2	8029	71187	0.984	0.981
USGS river network specific-conductance models							
sc8840a-2005-1	Q8500A DQ8500A LAQ2 DAQ2 DAQ16 DAQ30 FWL8980A XWL8980A DWLA DXWLA	SC8840A	3	10056	77309	0.887	0.851
sc8840h-2005-1	LG1NWL LG1D3NWL LG4D3NWL LG7D3NWL PSC8840A NXWL	SC8840	2	10197	77772	0.879	0.567
sc8920a-2005-1	Q8500A DQ8500A LAQ2 DAQ2 DAQ16 DAQ30 FWL8980A XWL8980A DWLA DXWLA LG2DWLA LG2DXWLA	SC8920A	2	9836	67677	0.897	0.883

Appendix II. Model summary of artificial neural network models used in the Model-to-Marsh application.—Continued

[R^2, coefficient of determination]

Model	Input variables	Output variable	Number of hidden neurons	Training matrix size	Testing matrix size	R^2 training	R^2 testing
USGS river network specific-conductance models—Continued							
sc8920h-2005-1	FWL8980A XWL8980A NXWL LG1NWL LG1D3NWL LG4D3NWL LG7D3NWL LG10D3NWL LG13D3NWL PSC8920A	SC8920	2	9900	67820	0.900	0.867
sc89784a-2005-1	Q8500A DQ8500A LAQ2 DAQ2 DAQ16 DAQ30 FWL8980A XWL8980A DWLA DXWLA LG2DWLA LG2DXWLA	SC89784A	3	8534	70348	0.880	0.853
sc89784h-2005-1	PSC89784A FWL8980A XWL8980A NXWL LG1NWL LG1D3NWL LG4D3NWL LG7D3NWL LG10D3NWL LG13D3NWL	SC89784	3	8600	71064	0.825	0.793
sc89791a-2005-1	Q8500A DQ8500A LAQ2 DAQ2 DAQ16 DAQ30 FWL8980A XWL8980A	SC89791A	3	9660	75782	0.887	0.870

Appendix II. Model summary of artificial neural network models used in the Model-to-Marsh application.—Continued

[R^2, coefficient of determination]

Model	Input variables	Output variable	Number of hidden neurons	Training matrix size	Testing matrix size	R^2 training	R^2 testing
USGS river network specific-conductance models—Continued							
sc89791a-2005-1 (cont.)	DWLA						
	DXWLA						
	LG2DWLA						
	LG2DXWLA						
sc89791h-2005-1	FWL8980A	SC89791	3	9736	76366	0.888	0.826
	XWL8980A						
	NXWL						
	LG1NWL						
	LG1D3NWL						
	LG4D3NWL						
	LG7D3NWL						
	LG10D3NWL						
	LG13D3NWL						
	PSC89791A						
USGS marsh network water-level models							
pb1mwl-2005	FWL8840	B1MWL	2	3143	17653	0.770	0.762
	DFWL8840						
	LG3DFWL8840						
	LG6DFWL8840						
	FWLDIF8977						
	FWLDIF8979						
	FWLDIF8920						
pb2mwl-2005	FWL8840	FB2MWL	2	3284	18228	0.797	0.768
	DFWL8840						
	LG3DFWL8840						
	LG6DFWL8840						
	FWLDIF8977						
	FWLDIF8979						
	FWLDIF8920						
pb3mwl-2005	FWL8840	FB3MWL	2	3558	20082	0.858	0.866
	DFWL8840						
	LG3DFWL8840						
	LG6DFWL8840						
	FWLDIF8977						
	FWLDIF8979						
	FWLDIF8920						
pb4mwl-2005	FWL8840	FB4MWL-0P1	2	2879	15877	0.887	0.883
	DFWL8840						
	LG3DFWL8840						
	LG6DFWL8840						

Appendix II. Model summary of artificial neural network models used in the Model-to-Marsh application.—Continued

[R^2, coefficient of determination]

Model	Input variables	Output variable	Number of hidden neurons	Training matrix size	Testing matrix size	R^2 training	R^2 testing
USGS marsh network water-level models—Continued							
pb4mwl-2005 (cont.)	FWLDIF8977						
	FWLDIF8979						
	FWLDIF8920						
pf1mwl-2005	FWL8840	FF1MWL	2	4243	23982	0.839	0.836
	DFWL8840						
	LG3DFWL8840						
	LG6DFWL8840						
	FWLDIF8977						
	FWLDIF8979						
	FWLDIF8920						
pm1mwl-2005	FWL8840	FM1MWL	2	2424	13299	0.694	0.722
	DFWL8840						
	LG3DFWL8840						
	LG6DFWL8840						
	FWLDIF8977						
	FWLDIF8979						
	FWLDIF8920						
pm2mwl-2005	FWL8840	M2MWL	2	1751	9676	0.808	0.778
	DFWL8840						
	LG3DFWL8840						
	LG6DFWL8840						
	FWLDIF8977						
	FWLDIF8979						
	FWLDIF8920						
USGS marsh network specific-conductance models							
pb1msc-2005-2	SCDIF8840A	B1MSC	1	2333	20555	0.857	0.849
	SCDIF8920A						
	FSC89791A4WK						
	LG672FSC89791A4WKD4WK						
	FSC89791A2WKD4WK						
	FSC89791A1WKD2WK						
	FSC89791A48D1WK						
	FSC89791DA48						
	DFSC89791DA48						
	LG3DFSC89791DA48						
pb2msc-2005-2	SCDIF8840A	B2MSC	1	2142	18770	0.827	0.832
	SCDIF8920A						
	FSC89791A4WK						
	LG672FSC89791A4WKD4WK						
	FSC89791A2WKD4WK						

Appendix II. Model summary of artificial neural network models used in the Model-to-Marsh application.—Continued

[R^2, coefficient of determination]

Model	Input variables	Output variable	Number of hidden neurons	Training matrix size	Testing matrix size	R^2 training	R^2 testing
USGS marsh network specific-conductance models—Continued							
pb2msc-2005-2 (cont.)	FSC89791A1WKD2WK FSC89791A48D1WK FSC89791DA48 DFSC89791DA48 LG3DFSC89791DA48						
pb3msc-2005-2	SCDIF8840A SCDIF8920A FSC89791A4WK LG672FSC89791A4WKD4WK FSC89791A2WKD4WK FSC89791A1WKD2WK FSC89791A48D1WK FSC89791DA48 DFSC89791DA48 LG3DFSC89791DA48	B3MSC	1	2326	20519	0.549	0.532
pb4msc-2005-2	SCDIF8840A SCDIF8920A FSC89791A4WK LG672FSC89791A4WKD4WK FSC89791A2WKD4WK FSC89791A1WKD2WK FSC89791A48D1WK FSC89791DA48 DFSC89791DA48 LG3DFSC89791DA48	B4MSC	1	2093	18577	0.654	0.641
pf1msc-2005-2	SCDIF8840A SCDIF8920A FSC89791A4WK LG672FSC89791A4WKD4WK FSC89791A2WKD4WK FSC89791A1WKD2WK FSC89791A48D1WK FSC89791DA48 DFSC89791DA48 LG3DFSC89791DA48	F1MSC	1	2496	22073	0.816	0.820
pm1msc-2005-2	SCDIF8840A SCDIF8920A FSC89791A4WK LG672FSC89791A4WKD4WK FSC89791A2WKD4WK	M1MSC	1	2147	18927	0.809	0.808

Appendix II. Model summary of artificial neural network models used in the Model-to-Marsh application.—Continued

[R^2, coefficient of determination]

Model	Input variables	Output variable	Number of hidden neurons	Training matrix size	Testing matrix size	R^2 training	R^2 testing
USGS marsh network specific-conductance models—Continued							
pm1msc-2005-2 (cont.)	FSC89791A1WKD2WK FSC89791A48D1WK FSC89791DA48 DFSC89791DA48 LG3DFSC89791DA48						
pm2msc-2005-2	SCDIF8840A SCDIF8920A FSC89791A4WK LG672FSC89791A4WKD4WK FSC89791A2WKD4WK FSC89791A1WKD2WK FSC89791A48D1WK FSC89791DA48 DFSC89791DA48 LG3DFSC89791DA48	M2MSC	1	2323	20593	0.841	0.830
GPA river specific-conductance decorrelation models							
dc_gpa_a1wk_10s_11b	PSCGPA11B_FLR_A1WK	PSCGPA10S_FLR_A1WK	1	7644	30459	0.800	0.804
dc_gpa_a1wk_10s_11rb	PSCGPA11RB_FLR_A1WK	PSCGPA10S_FLR_A1WK	1	7750	30921	0.957	0.958
dc_gpa_a1wk_10s_12rs	PSCGPA12RS_FLR_A1WK	PSCGPA10S_FLR_A1WK	1	7750	30921	0.881	0.880
Residual USGS marsh models							
prb1msc	RSC10S_12RS_A1WK RSC10S_11RB_A1WK RSC10S_11B_A1WK PSCGPA10S_FLR_A1WK	RB1MSC	1	4547	18224	0.080	0.087
prb2msc	RSC10S_12RS_A1WK RSC10S_11RB_A1WK RSC10S_11B_A1WK PSCGPA10S_FLR_A1WK	RB2MSC	1	4176	16736	0.067	0.059
prb3msc	RSC10S_12RS_A1WK RSC10S_11RB_A1WK RSC10S_11B_A1WK PSCGPA10S_FLR_A1WK	RB3MSC	1	4519	18209	0.020	0.018
prb4msc	RSC10S_12RS_A1WK RSC10S_11RB_A1WK RSC10S_11B_A1WK PSCGPA10S_FLR_A1WK	RB4MSC	1	4097	16456	0.020	0.020
prf1msc	RSC10S_12RS_A1WK RSC10S_11RB_A1WK RSC10S_11B_A1WK PSCGPA10S_FLR_A1WK	RF1MSC	1	4873	19579	0.042	0.050

Appendix II. Model summary of artificial neural network models used in the Model-to-Marsh application.—Continued

[R^2, coefficient of determination]

Model	Input variables	Output variable	Number of hidden neurons	Training matrix size	Testing matrix size	R^2 training	R^2 testing
		Residual USGS marsh models—Continued					
prm1msc	RSC10S_12RS_A1WK RSC10S_11RB_A1WK RSC10S_11B_A1WK PSCGPA10S_FLR_A1WK	RM1MSC	1	4163	16803	0.073	0.065
prm2msc	RSC10S_12RS_A1WK RSC10S_11RB_A1WK RSC10S_11B_A1WK PSCGPA10S_FLR_A1WK	RM2MSC	1	4539	18260	0.034	0.016
		GPA river network water-level models					
wlgpa04d-2005	WL8977 D3WL8977 D3WL8977(006) D3WL8977(012) D3WL8977(018) D3WL8977(024)	DWL8977GPA04	2	4215	1079	0.640	0.626
wlgpa05d-2005	WL8977 D3WL8977 D3WL8977(006) D3WL8977(012) D3WL8977(018) D3WL8977(024)	DWL8977GPA05	2	4344	1133	0.638	0.676
wlgpa06d-2005	WL8977 D3WL8977 D3WL8977(006) D3WL8977(012) D3WL8977(018) D3WL8977(024)	DWL8977GPA06	2	4305	1124	0.176	0.152
wlgpa07d-2005	WL8920 D3WL8920 D3WL8920(006) D3WL8920(012) D3WL8920(018) D3WL8920(024)	DWL8920GPA07	2	1606	416	0.641	0.639
wlgpa08d-2005	WL8920 D3WL8920 D3WL8920(006) D3WL8920(012) D3WL8920(018) D3WL8920(024)	DWL8920GPA08	2	4614	1175	0.238	0.216

Appendix II. Model summary of artificial neural network models used in the Model-to-Marsh application.—Continued

[R^2, coefficient of determination]

Model	Input variables	Output variable	Number of hidden neurons	Training matrix size	Testing matrix size	R^2 training	R^2 testing
GPA river network water-level models—Continued							
wlgpa09d-2005	WL8920 D3WL8920 D3WL8920(006) D3WL8920(012) D3WL8920(018) D3WL8920(024)	DWL8920GPA09	3	4642	1192	0.338	0.310
wlgpa10d-2005	WL8920 D3WL8920 D3WL8920(006) D3WL8920(012) D3WL8920(018) D3WL8920(024)	DWL8920GPA10	2	2187	587	0.230	0.233
wlgpa11d-2005	WL8979 D3WL8979 D3WL8979(006) D3WL8979(012) D3WL8979(018) D3WL8979(024)	DWL8979GPA11	2	1578	434	0.534	0.570
wlgpa11rd-2005	WL8920 D3WL8920 D3WL8920(006) D3WL8920(012) D3WL8920(018) D3WL8920(024)	DWL8920GPA11R	2	1617	399	0.863	0.855
wlgpa12d-2005	WL8920 D3WL8920 D3WL8920(006) D3WL8920(012) D3WL8920(018) D3WL8920(024)	DWL8920GPA12	2	2846	749	0.272	0.242
wlgpa13d-2005	WL8979 D3WL8979 D3WL8979(006) D3WL8979(012) D3WL8979(018) D3WL8979(024)	DWL8979GPA13	2	2123	561	0.917	0.926
wlgpa14d-2005	WL8840 D3WL8840 D3WL8840(006) D3WL8840(012) D3WL8840(018) D3WL8840(024)	DWL8840GPA14	2	1630	424	0.914	0.909

Appendix II. Model summary of artificial neural network models used in the Model-to-Marsh application.—Continued

[R^2, coefficient of determination]

Model	Input variables	Output variable	Number of hidden neurons	Training matrix size	Testing matrix size	R^2 training	R^2 testing
GPA river network water-level models—Continued							
wlgpa21d-2005	WL8977 D3WL8977 D3WL8977(006) D3WL8977(012) D3WL8977(018) D3WL8977(024)	DWL8977GPA21	2	2227	551	0.030	0.004
wlgpa22d-2005	WL8920 D3WL8920 D3WL8920(006) D3WL8920(012) D3WL8920(018) D3WL8920(024)	DWL8920GPA22	2	1502	384	0.884	0.867
wlgpa23d-2005	WL8977 D3WL8977 D3WL8977(006) D3WL8977(012) D3WL8977(018) D3WL8977(024)	DWL8977GPA23	2	2754	696	0.816	0.798
wlgpa24md-2005	WL8977 D3WL8977 D3WL8977(006) D3WL8977(012) D3WL8977(018) D3WL8977(024)	DWL8977GPA24M	2	2755	697	0.760	0.741
wlgpa25md-2005	WL8977 D3WL8977 D3WL8977(006) D3WL8977(012) D3WL8977(018) D3WL8977(024)	DWL8977GPA25M	2	2750	697	0.653	0.645
wlgpa26d-2005	WL8977 D3WL8977 D3WL8977(006) D3WL8977(012) D3WL8977(018) D3WL8977(024)	DWL8977GPA26	2	2210	553	0.788	0.786
GPA river network specific-conductance models							
scgpa04bd-2005	SC8920 D3SC8920 D3SC8920(006)	DSC8920GPA04B	3	4284	1090	0.522	0.491

Appendix II. Model summary of artificial neural network models used in the Model-to-Marsh application.—Continued

[R^2, coefficient of determination]

Model	Input variables	Output variable	Number of hidden neurons	Training matrix size	Testing matrix size	R^2 training	R^2 testing
GPA river network specific-conductance models—Continued							
scgpa04bd-2005 (cont.)	D3SC8920(012) D3SC8920(018) D3SC8920(024) WL8977 D3WL8977 D3WL8977(006) D3WL8977(012) D3WL8977(018) D3WL8977(024)						
scgpa04sd-2005	SC8920 D3SC8920 D3SC8920(006) D3SC8920(012) D3SC8920(018) D3SC8920(024) WL8977 D3WL8977 D3WL8977(006) D3WL8977(012) D3WL8977(018) D3WL8977(024)	DSC8920GPA04S	2	4511	1145	0.650	0.666
scgpa05bd-2005	SC8920 D3SC8920 D3SC8920(006) D3SC8920(012) D3SC8920(018) D3SC8920(024) WL8977 D3WL8977 D3WL8977(006) D3WL8977(012) D3WL8977(018) D3WL8977(024)	DSC8920GPA05B	3	3901	1021	0.714	0.702
scgpa06bd-2005	SC8920 D3SC8920 D3SC8920(006) D3SC8920(012) D3SC8920(018) D3SC8920(024) WL8977	DSC8920GPA06B	3	4155	1090	0.676	0.678

Appendix II. Model summary of artificial neural network models used in the Model-to-Marsh application.—Continued

[R^2, coefficient of determination]

Model	Input variables	Output variable	Number of hidden neurons	Training matrix size	Testing matrix size	R^2 training	R^2 testing
GPA river network specific-conductance models—Continued							
scgpa06bd-2005 (cont.)	D3WL8977						
	D3WL8977(006)						
	D3WL8977(012)						
	D3WL8977(018)						
	D3WL8977(024)						
scgpa06sd-2005	SC8920	DSC8920GPA06S	2	4131	1044	0.641	0.630
	D3SC8920						
	D3SC8920(006)						
	D3SC8920(012)						
	D3SC8920(018)						
	D3SC8920(024)						
	WL8977						
	D3WL8977						
	D3WL8977(006)						
	D3WL8977(012)						
	D3WL8977(018)						
	D3WL8977(024)						
scgpa07bd-2005	SC89791	DSC89791GPA07B	2	2042	555	0.806	0.808
	D3SC89791						
	D3SC89791(006)						
	D3SC89791(012)						
	D3SC89791(018)						
	D3SC89791(024)						
	WL8979						
	D3WL8979						
	D3WL8979(006)						
	D3WL8979(012)						
	D3WL8979(018)						
	D3WL8979(024)						
scgpa07sd-2005	SC89791	DSC89791GPA07S	2	2376	598	0.857	0.861
	D3SC89791						
	D3SC89791(006)						
	D3SC89791(012)						
	D3SC89791(018)						
	D3SC89791(024)						
	WL8979						
	D3WL8979						
	D3WL8979(006)						
	D3WL8979(012)						
	D3WL8979(018)						
	D3WL8979(024)						

Appendix II. Model summary of artificial neural network models used in the Model-to-Marsh application.—Continued

[R^2, coefficient of determination]

Model	Input variables	Output variable	Number of hidden neurons	Training matrix size	Testing matrix size	R^2 training	R^2 testing
GPA river network specific-conductance models—Continued							
scgpa08bd-2005	DSC89791GPA07S SC8920 D3SC8920 D3SC8920(006) D3SC8920(012) D3SC8920(018) D3SC8920(024) WL8920 D3WL8920 D3WL8920(006) D3WL8920(012) D3WL8920(018) D3WL8920(024)	DSC8920GPA08B	2	4792	1216	0.402	0.428
scgpa08sd-2005	SC8920 D3SC8920 D3SC8920(006) D3SC8920(012) D3SC8920(018) D3SC8920(024) WL8920 D3WL8920 D3WL8920(006) D3WL8920(012) D3WL8920(018) D3WL8920(024)	DSC8920GPA08S	2	4112	1030	0.419	0.409
scgpa09bd-2005	SC8920 D3SC8920 D3SC8920(006) D3SC8920(012) D3SC8920(018) D3SC8920(024) WL8920 D3WL8920 D3WL8920(006) D3WL8920(012) D3WL8920(018) D3WL8920(024)	DSC8920GPA09B	2	4611	1178	0.260	0.295
scgpa09sd-2005	SC8920 D3SC8920 D3SC8920(006)	DSC8920GPA09S	2	1640	410	0.546	0.568

Appendix II. Model summary of artificial neural network models used in the Model-to-Marsh application.—Continued

[R^2, coefficient of determination]

Model	Input variables	Output variable	Number of hidden neurons	Training matrix size	Testing matrix size	R^2 training	R^2 testing
GPA river network specific-conductance models—Continued							
scgpa09sd-2005 (cont.)	D3SC8920(012) D3SC8920(018) D3SC8920(024) WL8920 D3WL8920 D3WL8920(006) D3WL8920(012) D3WL8920(018) D3WL8920(024)						
scgpa10bd-2005	SC8920 D3SC8920 D3SC8920(006) D3SC8920(012) D3SC8920(018) D3SC8920(024) WL8920 D3WL8920 D3WL8920(006) D3WL8920(012) D3WL8920(018) D3WL8920(024)	DSC8920GPA10B	2	2335	625	0.919	0.908
scgpa10sd-2005	SC8920 D3SC8920 D3SC8920(006) D3SC8920(012) D3SC8920(018) D3SC8920(024) WL8920 D3WL8920 D3WL8920(006) D3WL8920(012) D3WL8920(018) D3WL8920(024)	DSC8920GPA10S	2	1609	410	0.899	0.887
scgpa11bd-2005	SC89791 D3SC89791 D3SC89791(006) D3SC89791(012) D3SC89791(018) D3SC89791(024) WL8979	DSC89791GPA11B	2	1777	470	0.534	0.430

Appendix II. Model summary of artificial neural network models used in the Model-to-Marsh application.—Continued

[R^2, coefficient of determination]

Model	Input variables	Output variable	Number of hidden neurons	Training matrix size	Testing matrix size	R^2 training	R^2 testing
GPA river network specific-conductance models—Continued							
scgpa11bd-2005 (cont.)	D3WL8979						
	D3WL8979(006)						
	D3WL8979(012)						
	D3WL8979(018)						
	D3WL8979(024)						
scgpa11rbd-2005	SC8920	DSC8920GPA11RB	2	1288	326	0.662	0.743
	D3SC8920						
	D3SC8920(006)						
	D3SC8920(012)						
	D3SC8920(018)						
	D3SC8920(024)						
	WL8920						
	D3WL8920						
	D3WL8920(006)						
	D3WL8920(012)						
	D3WL8920(018)						
	D3WL8920(024)						
scgpa12bd-2005	SC8920	DSC8920GPA12B	2	3003	787	0.986	0.985
	D3SC8920						
	D3SC8920(006)						
	D3SC8920(012)						
	D3SC8920(018)						
	D3SC8920(024)						
	WL8920						
	D3WL8920						
	D3WL8920(006)						
	D3WL8920(012)						
	D3WL8920(018)						
	D3WL8920(024)						
scgpa12rsd-2005	SC8920	DSC8920GPA12RS	2	1455	367	0.847	0.861
	D3SC8920						
	D3SC8920(006)						
	D3SC8920(012)						
	D3SC8920(018)						
	D3SC8920(024)						
	WL8920						
	D3WL8920						
	D3WL8920(006)						
	D3WL8920(012)						
	D3WL8920(018)						
	D3WL8920(024)						

Appendix II. Model summary of artificial neural network models used in the Model-to-Marsh application.—Continued

[R^2, coefficient of determination]

Model	Input variables	Output variable	Number of hidden neurons	Training matrix size	Testing matrix size	R^2 training	R^2 testing
GPA river network specific-conductance models—Continued							
scgpa13bd-2005	SC89791 D3SC89791 D3SC89791(006) D3SC89791(012) D3SC89791(018) D3SC89791(024) WL8979 D3WL8979 D3WL8979(006) D3WL8979(012) D3WL8979(018) D3WL8979(024)	DSC89791GPA13B	2	2120	561	0.408	0.502
scgpa14bd-2005	SC8840 D3SC8840 D3SC8840(006) D3SC8840(012) D3SC8840(018) D3SC8840(024) WL8840 D3WL8840 D3WL8840(006) D3WL8840(012) D3WL8840(018) D3WL8840(024)	DSC8840GPA14B	2	4502	1169	0.662	0.657
scgpa15sd-2005	SC89791 D3SC89791 D3SC89791(006) D3SC89791(012) D3SC89791(018) D3SC89791(024) WL8979 D3WL8979 D3WL8979(006) D3WL8979(012) D3WL8979(018) D3WL8979(024)	DSC89791GPA15S	2	5540	1359	0.555	0.518
scgpa21bd-2005	SC8920 D3SC8920 D3SC8920(006) D3SC8920(012)	DSC8920GPA21B	2	1759	427	0.577	0.503

Appendix II. Model summary of artificial neural network models used in the Model-to-Marsh application.—Continued

[R^2, coefficient of determination]

Model	Input variables	Output variable	Number of hidden neurons	Training matrix size	Testing matrix size	R^2 training	R^2 testing
GPA river network specific-conductance models—Continued							
scgpa21bd-2005 (cont.)	D3SC8920(018) D3SC8920(024) WL8977 D3WL8977 D3WL8977(006) D3WL8977(012) D3WL8977(018) D3WL8977(024)						
scgpa21sd-2005	SC8920 D3SC8920 D3SC8920(006) D3SC8920(012) D3SC8920(018) D3SC8920(024) WL8977 D3WL8977 D3WL8977(006) D3WL8977(012) D3WL8977(018) D3WL8977(024)	DSC8920GPA21S	3	2396	597	0.606	0.594
scgpa22bd-2005	SC8920 D3SC8920 D3SC8920(006) D3SC8920(012) D3SC8920(018) D3SC8920(024) WL8920 D3WL8920 D3WL8920(006) D3WL8920(012) D3WL8920(018) D3WL8920(024)	DSC8920GPA22B	2	1328	334	0.329	0.269
scgpa22sd-2005	SC8920 D3SC8920 D3SC8920(006) D3SC8920(012) D3SC8920(018) D3SC8920(024) WL8920 D3WL8920	DSC8920GPA22S	2	1602	393	0.627	0.627

Appendix II. Model summary of artificial neural network models used in the Model-to-Marsh application.—Continued

[R^2, coefficient of determination]

Model	Input variables	Output variable	Number of hidden neurons	Training matrix size	Testing matrix size	R^2 training	R^2 testing
GPA river network specific-conductance models—Continued							
scgpa22sd-2005 (cont.)	D3WL8920(006)						
	D3WL8920(012)						
	D3WL8920(018)						
	D3WL8920(024)						
GPA marsh network water-level models							
ps1canalwl-2005	FWL8840	S1CANALWL	2	815	7911	0.983	0.983
	DFWL8840						
	LG3DFWL8840						
	LG6DFWL8840						
	FWLDIF8977						
	FWLDIF8979						
	FWLDIF8920						
ps1marshwl-2005	FWL8840	S1MARSHWL	3	1726	7208	0.648	0.610
	DFWL8840						
	LG3DFWL8840						
	LG6DFWL8840						
	FWLDIF8977						
	FWLDIF8979						
	FWLDIF8920						
1ps1marshwlat-2005	FWL8840	S1MARSHWLAT	2	1371		0.672	
	DFWL8840						
	LG3DFWL8840						
	LG6DFWL8840						
	FWLDIF8977						
	FWLDIF8979						
	FWLDIF8920						
ps2canalwl-2005	FWL8840	S2CANALWL	2	613	2398	0.922	0.936
	DFWL8840						
	LG3DFWL8840						
	LG6DFWL8840						
	FWLDIF8977						
	FWLDIF8979						
	FWLDIF8920						
ps2marshwl-2005	FWL8840	S2MARSHWL	2	796	2306	0.741	0.740
	DFWL8840						
	LG3DFWL8840						
	LG6DFWL8840						
	FWLDIF8977						
	FWLDIF8979						
	FWLDIF8920						

Appendix II. Model summary of artificial neural network models used in the Model-to-Marsh application.—Continued

[R^2, coefficient of determination]

Model	Input variables	Output variable	Number of hidden neurons	Training matrix size	Testing matrix size	R^2 training	R^2 testing
GPA marsh network water-level models—Continued							
ps3canalwl-2005	FWL8840 DFWL8840 LG3DFWL8840 LG6DFWL8840 FWLDIF8977 FWLDIF8979 FWLDIF8920	S3CANALWL	2	877	12699	0.976	0.961
ps3marshwl-2005	FWL8840 DFWL8840 LG3DFWL8840 LG6DFWL8840 FWLDIF8977 FWLDIF8979 FWLDIF8920	S3MARSHW	2	2077	12595	0.891	0.806
ps4canalwl-2005	FWL8840 DFWL8840 LG3DFWL8840 LG6DFWL8840 FWLDIF8977 FWLDIF8979 FWLDIF8920	S4CANALWL	2	809	7784	0.986	0.985
ps4marshwl-2005	FWL8840 DFWL8840 LG3DFWL8840 LG6DFWL8840 FWLDIF8977 FWLDIF8979 FWLDIF8920	S4MARSHWL	3	1764	7762	0.902	0.858
ps5canalwl-2005	FWL8840 DFWL8840 LG3DFWL8840 LG6DFWL8840 FWLDIF8977 FWLDIF8979 FWLDIF8920	S5CANALWL	1	4805	5784	0.989	0.619
ps5marshwl-2005	FWL8840 DFWL8840 LG3DFWL8840 LG6DFWL8840 FWLDIF8977 FWLDIF8979 FWLDIF8920	S5MARSHWL	3	1965	10219	0.911	0.891

Appendix II. Model summary of artificial neural network models used in the Model-to-Marsh application.—Continued

[R^2, coefficient of determination]

Model	Input variables	Output variable	Number of hidden neurons	Training matrix size	Testing matrix size	R^2 training	R^2 testing
GPA marsh network water-level models—Continued							
ps6canalwl-2005	FWL8840 DFWL8840 LG3DFWL8840 LG6DFWL8840 FWLDIF8977 FWLDIF8979 FWLDIF8920	S6CANALWL	3	791	7408	0.990	0.983
ps6marshwl-2005	FWL8840 DFWL8840 LG3DFWL8840 LG6DFWL8840 FWLDIF8977 FWLDIF8979 FWLDIF8920	S6MARSHWL	3	1647	6637	0.804	0.763
1ps6marshwlat-2005	FWL8840 DFWL8840 LG3DFWL8840 LG6DFWL8840 FWLDIF8977 FWLDIF8979 FWLDIF8920	S6MARSHWLAT	2	1720		0.960	
ps7canalwl-2005	FWL8840 DFWL8840 LG3DFWL8840 LG6DFWL8840 FWLDIF8977 FWLDIF8979 FWLDIF8920	S7CANALWL	3	572	2739	0.924	0.933
1ps7marshwl-2005	FWL8840 DFWL8840 LG3DFWL8840 LG6DFWL8840 FWLDIF8977 FWLDIF8979 FWLDIF8920	S7MARSHWL	2	2822		0.701	
1ps8canalwl-2005	FWL8840 DFWL8840 LG3DFWL8840 LG6DFWL8840 FWLDIF8977 FWLDIF8979 FWLDIF8920	S8CANALWL	1	430		0.996	

Appendix II. Model summary of artificial neural network models used in the Model-to-Marsh application.—Continued

[R^2, coefficient of determination]

Model	Input variables	Output variable	Number of hidden neurons	Training matrix size	Testing matrix size	R^2 training	R^2 testing
GPA marsh network water-level models—Continued							
ps9canalwl-2005	FWL8840 DFWL8840 LG3DFWL8840 LG6DFWL8840 FWLDIF8977 FWLDIF8979 FWLDIF8920	S9CANALWL	2	805	7829	0.991	0.988
ps9marshwl-2005	FWL8840 DFWL8840 LG3DFWL8840 LG6DFWL8840 FWLDIF8977 FWLDIF8979 FWLDIF8920	S9MARSHWL	3	1801	7882	0.827	0.762
ps10canalwl-2005	FWL8840 DFWL8840 LG3DFWL8840 LG6DFWL8840 FWLDIF8977 FWLDIF8979 FWLDIF8920	S10CANALWL	2	694	5982	0.982	0.980
ps10marshwl-2005	FWL8840 DFWL8840 LG3DFWL8840 LG6DFWL8840 FWLDIF8977 FWLDIF8979 FWLDIF8920	S10MARSHWL	3	1530	5985	0.906	0.904
GPA marsh network specific-conductance models							
ps1canalsc-2005	FWL8840 DFWL8840 LG3DFWL8840 LG6DFWL8840 FSC89791 DFSC89791 LG3DFSC89791 LG6DFSC89791 FSCDIF8840 FSCDIF8920	S1CANALSC	3	750	7559	0.926	0.885

Appendix II. Model summary of artificial neural network models used in the Model-to-Marsh application.—Continued

[R^2, coefficient of determination]

Model	Input variables	Output variable	Number of hidden neurons	Training matrix size	Testing matrix size	R^2 training	R^2 testing
GPA marsh network specific-conductance models—Continued							
ps1marshsc-2005	FWL8840 DFWL8840 LG3DFWL8840 LG6DFWL8840 FSC89791 DFSC89791 LG3DFSC89791 LG6DFSC89791 FSCDIF8840 FSCDIF8920	S1MARSHSC	2	1441	3990	0.726	0.722
ps2canalsc-2005	FWL8840 DFWL8840 LG3DFWL8840 LG6DFWL8840 FSC89791 DFSC89791 LG3DFSC89791 LG6DFSC89791 FSCDIF8840 FSCDIF8920	S2CANALSC	3	1301	6355	0.913	0.897
ps2marshsc-2005	FWL8840 DFWL8840 LG3DFWL8840 LG6DFWL8840 FSC89791 DFSC89791 LG3DFSC89791 LG6DFSC89791 FSCDIF8840 FSCDIF8920	S2MARSHSC	3	902	2733	0.882	0.876
ps3canalsc-2005	FWL8840 DFWL8840 LG3DFWL8840 LG6DFWL8840 FSC89791 DFSC89791 LG3DFSC89791 LG6DFSC89791 FSCDIF8840 FSCDIF8920	S3CANALSC	3	2118	11954	0.812	0.813

Appendix II. Model summary of artificial neural network models used in the Model-to-Marsh application.—Continued

[R^2, coefficient of determination]

Model	Input variables	Output variable	Number of hidden neurons	Training matrix size	Testing matrix size	R^2 training	R^2 testing
GPA marsh network specific-conductance models—Continued							
ps3marshsc-2005	S3CANALSC FWL8840 DFWL8840 LG3DFWL8840 LG6DFWL8840 FSC89791 DFSC89791 LG3DFSC89791 LG6DFSC89791 FSCDIF8840 FSCDIF8920	S3MARSHSC	3	2062	11025	0.845	0.826
ps4canalsc-2005	FWL8840 DFWL8840 LG3DFWL8840 LG6DFWL8840 FSC89791 DFSC89791 LG3DFSC89791 LG6DFSC89791 FSCDIF8840 FSCDIF8920	S4CANALSC	3	1798	7463	0.865	0.839
ps4marshsc-2005	FWL8840 DFWL8840 LG3DFWL8840 LG6DFWL8840 FSC89791 DFSC89791 LG3DFSC89791 LG6DFSC89791 FSCDIF8840 FSCDIF8920	S4MARSHSC	2	1658	5535	0.897	0.861
ps5canalsc-2005	FWL8840 DFWL8840 LG3DFWL8840 LG6DFWL8840 FSC89791 DFSC89791 LG3DFSC89791 LG6DFSC89791 FSCDIF8840 FSCDIF8920	S5CANALSC	2	1500	4312	0.814	0.000

Appendix II. Model summary of artificial neural network models used in the Model-to-Marsh application.—Continued

[R^2, coefficient of determination]

Model	Input variables	Output variable	Number of hidden neurons	Training matrix size	Testing matrix size	R^2 training	R^2 testing
GPA marsh network specific-conductance models—Continued							
ps5marshsc-2005	FWL8840 DFWL8840 LG3DFWL8840 LG6DFWL8840 FSC89791 DFSC89791 LG3DFSC89791 LG6DFSC89791 FSCDIF8840 FSCDIF8920	S5MARSHSC	3	4108	12677	0.630	0.548
ps6canalsc-2005	FWL8840 DFWL8840 LG3DFWL8840 LG6DFWL8840 FSC89791 DFSC89791 LG3DFSC89791 LG6DFSC89791 FSCDIF8840 FSCDIF8920	S6CANALSC	3	1617	6115	0.834	0.825
ps6marshsc-2005	FWL8840 DFWL8840 LG3DFWL8840 LG6DFWL8840 FSC89791 DFSC89791 LG3DFSC89791 LG6DFSC89791 FSCDIF8840 FSCDIF8920	S6MARSHSC	3	1673	5953	0.859	0.814
ps7canalsc-2005	FWL8840 DFWL8840 LG3DFWL8840 LG6DFWL8840 FSC89791 DFSC89791 LG3DFSC89791 LG6DFSC89791 FSCDIF8840 FSCDIF8920	S7CANALSC	3	3665	3049	0.873	0.000

Appendix II. Model summary of artificial neural network models used in the Model-to-Marsh application.—Continued

[R^2, coefficient of determination]

Model	Input variables	Output variable	Number of hidden neurons	Training matrix size	Testing matrix size	R^2 training	R^2 testing
GPA marsh network specific-conductance models—Continued							
prs7marshpwc	RSC10S_12RS_A1WK RSC10S_11RB_A1WK RSC10S_11B_A1WK PSCGPA10S_FLR_A1WK	RS7MARSHPWC	1	1539	6136	0.150	0.141
ps7marshpwsc-2005-2	FSC89791A4WK FSC89791A24DA4WK AQ8500A168L72	S7MARSHPWSC	1	4270	4260	0.650	0.679
ps7marshsc-2005	FWL8840 DFWL8840 LG3DFWL8840 LG6DFWL8840 FSC89791 DFSC89791 LG3DFSC89791 LG6DFSC89791 FSCDIF8840 FSCDIF8920	S7MARSHSC	2	3386	3118	0.685	0.000
ps8canalsc-2005	FWL8840 DFWL8840 LG3DFWL8840 LG6DFWL8840 FSC89791 DFSC89791 LG3DFSC89791 LG6DFSC89791 FSCDIF8840 FSCDIF8920	S8CANALSC	2	1458	4752	0.871	0.831
ps9canalsc-2005	FWL8840 DFWL8840 LG3DFWL8840 LG6DFWL8840 FSC89791 DFSC89791 LG3DFSC89791 LG6DFSC89791 FSCDIF8840 FSCDIF8920	S9CANALSC	3	1806	6905	0.847	0.826
prs9marshpwc	RSC10S_12RS_A1WK RSC10S_11RB_A1WK RSC10S_11B_A1WK PSCGPA10S_FLR_A1WK	RS9MARSHPWC	1	1519	6052	0.098	0.097

Appendix II. Model summary of artificial neural network models used in the Model-to-Marsh application.—Continued

[R^2, coefficient of determination]

Model	Input variables	Output variable	Number of hidden neurons	Training matrix size	Testing matrix size	R^2 training	R^2 testing
GPA marsh network specific-conductance models—Continued							
ps9marshpwsc-2005-2	FSC89791A4WK FSC89791A24DA4WK AQ8500A168L72	S9MARSHPWSC	1	4221	4205	0.518	0.556
prs10marshpwc	RSC10S_12RS_A1WK RSC10S_11RB_A1WK RSC10S_11B_A1WK PSCGPA10S_FLR_A1WK	RS10MARSHPWC	1	1460	5797	0.100	0.101
ps10marshswsc-2005	FWL8840 DFWL8840 LG3DFWL8840 LG6DFWL8840 FSC89791 DFSC89791 LG3DFSC89791 LG6DFSC89791 FSCDIF8840 FSCDIF8920	S10MARSHSWSC	3	1810	6718	0.896	0.855

[1] Due to data quality concerns, data set was not bifurcated into training and testing datasets.

Appendix III. Variables used in artifical neural network models.

[SC, specific conductance; USGS, U.S. Geological Survey; WL, water level; GPA, Georgia Ports Authority; XWL, tidal range; MWA, moving window average]

Variable	Description
AQ8500A168L72	168-hour average flow at station 02198500—lagged 72 hours
B1MSC	Hourly SC at USGS marsh site B1
B1MWL	SC at station B1—hourly
B2MSC	Hourly SC at USGS marsh site B2
B3MSC	Hourly SC at USGS marsh site B3
B4MSC	Hourly SC at USGS marsh site B4
D3SC8840	3-hour difference in SC at station 02198840
D3SC8840(006)	3-hour difference in SC at station 02198840—lagged 6 hours
D3SC8840(012)	3-hour difference in SC at station 02198840—lagged 12 hours
D3SC8840(018)	3-hour difference in SC at station 02198840—lagged 18 hours
D3SC8840(024)	3-hour difference in SC at station 02198840—lagged 24 hours
D3SC8920	3-hour difference in SC at station 02198920
D3SC8920(006)	3-hour difference in SC at station 02198920—lagged 6 hours
D3SC8920(012)	3-hour difference in SC at station 02198920—lagged 12 hours
D3SC8920(018)	3-hour difference in SC at station 02198920—lagged 18 hours
D3SC8920(024)	3-hour difference in SC at station 02198920—lagged 24 hours
D3SC89791	3-hour difference in SC at station 021989791
D3SC89791(006)	3-hour difference in SC at station 021989791—lagged 6 hours
D3SC89791(012)	3-hour difference in SC at station 021989791—lagged 12 hours
D3SC89791(018)	3-hour difference in SC at station 021989791—lagged 18 hours
D3SC89791(024)	3-hour difference in SC at station 021989791—lagged 24 hours
D3WL8840	3-hour difference in WL at station 02198840
D3WL8840(006)	3-hour difference in WL at station 02198840—lagged 6 hours
D3WL8840(012)	3-hour difference in WL at station 02198840—lagged 12 hours
D3WL8840(018)	3-hour difference in WL at station 02198840—lagged 18 hours
D3WL8840(024)	3-hour difference in WL at station 02198840—lagged 24 hours
D3WL8920	3-hour difference in WL at station 02198920
D3WL8920(006)	3-hour difference in WL at station 02198920—lagged 6 hours
D3WL8920(012)	3-hour difference in WL at station 02198920—lagged 12 hours
D3WL8920(018)	3-hour difference in WL at station 02198920—lagged 18 hours
D3WL8920(024)	3-hour difference in WL at station 02198920—lagged 24 hours
D3WL8977	3-hour difference in WL at station 02198977
D3WL8977(006)	3-hour difference in WL at station 02198977—lagged 6 hours
D3WL8977(012)	3-hour difference in WL at station 02198977—lagged 12 hours
D3WL8977(018)	3-hour difference in WL at station 02198977—lagged 18 hours

Appendix III. Variables used in artifical neural network models.—Continued

[SC, specific conductance; USGS, U.S. Geological Survey; WL, water level; GPA, Georgia Ports Authority; XWL, tidal range; MWA, moving window average]

Variable	Description
D3WL8977(024)	3-hour difference in WL at station 0219897—lagged 24 hours
D3WL8979	3-hour difference in WL at station 02198979
D3WL8979(006)	3-hour difference in WL at station 02198979—lagged 6 hours
D3WL8979(012)	3-hour difference in WL at station 02198979—lagged 12 hours
D3WL8979(018)	3-hour difference in WL at station 02198979—lagged 18 hours
D3WL8979(024)	3-hour difference in WL at station 02198979—lagged 24 hours
DAQ16	16-day change in daily flow at station 02198500
DAQ2	2-day change in daily flow at station 02198500
DAQ30	30-day change in daily flow at station 02198500
DFSC89791	1-day difference in filtered SC at station 021989791
DFSC89791DA48	1-day difference in filtered 48-hour differences of SC at station 021989791
DFWL8840	1-day difference in filtered WL at station 02198840
DQ8500A	1-day difference in daily average flow at station 02198500
DSC8840GPA14B	Difference in SC between 02198840 and GPA14b
DSC8920GPA04B	Difference in SC between 02198920 and GPA04s
DSC8920GPA04S	Difference in SC between 02198920 and GPA04b
DSC8920GPA05B	Difference in SC between 02198920 and GPA05b
DSC8920GPA06B	Difference in SC between 02198920 and GPA06b
DSC8920GPA06S	Difference in SC between 02198920 and GPA06s
DSC8920GPA08B	Difference in SC between 02198920 and GPA08b
DSC8920GPA08S	Difference in SC between 02198920 and GPA08s
DSC8920GPA09B	Difference in SC between 02198920 and GPA09b
DSC8920GPA09S	Difference in SC between 02198920 and GPA09s
DSC8920GPA10B	Difference in SC between 02198920 and GPA10b
DSC8920GPA10S	Difference in SC between 02198920 and GPA10s
DSC8920GPA11RB	Difference in SC between 02198920 and GPA11b
DSC8920GPA12B	Difference in SC between 02198920 and GPA12b
DSC8920GPA12RS	Difference in SC between 02198920 and GPA12rs
DSC8920GPA21B	Difference in SC between 02198920 and GPA21b
DSC8920GPA21S	Difference in SC between 02198920 and GPA21s
DSC8920GPA22B	Difference in SC between 02198920 and GPA22b
DSC8920GPA22S	Difference in SC between 02198920 and GPA22s
DSC89791GPA07B	Difference in SC between 021989791 and GPA07b
DSC89791GPA07S	Difference in SC between 021989791 and GPA07s
DSC89791GPA11B	Difference in SC between 021989791 and GPA11b

Appendix III. Variables used in artifical neural network models.—Continued

[SC, specific conductance; USGS, U.S. Geological Survey; WL, water level; GPA, Georgia Ports Authority; XWL, tidal range; MWA, moving window average]

Variable	Description
DSC89791GPA13B	Difference in SC between 021989791 and GPA15s
DSC89791GPA15S	Difference in SC between 021989791 and GPA13b
DWL8840GPA14	Difference in WL between 02198840 and GPA14
DWL8920GPA07	Difference in WL between 02198920 and GPA07
DWL8920GPA08	Difference in WL between 02198920 and GPA08
DWL8920GPA09	Difference in WL between 02198920 and GPA09
DWL8920GPA10	Difference in WL between 02198920 and GPA10
DWL8920GPA11R	Difference in WL between 02198920 and GPA11r
DWL8920GPA12	Difference in WL between 02198920 and GPA12
DWL8920GPA22	Difference in WL between 02198920 and GPA22
DWL8977GPA04	Difference in WL between 02198977 and GPA04
DWL8977GPA05	Difference in WL between 02198977 and GPA05
DWL8977GPA06	Difference in WL between 02198977 and GPA06
DWL8977GPA21	Difference in WL between 02198977 and GPA21
DWL8977GPA23	Difference in WL between 02198977 and GPA23
DWL8977GPA24M	Difference in WL between 02198977 and GPA24m
DWL8977GPA25M	Difference in WL between 02198977 and GPA25m
DWL8977GPA26	Difference in WL between 02198977 and GPA26
DWL8979GPA11	Difference in WL between 02198979 and GPA11
DWL8979GPA13	Difference in WL between 02198979 and GPA13
DWLA	1-day change in WL
DWLAD1	1-day change in WL, lagged 1 day
DXWLA	1-day change in tidal range (XWL)
DXWLAD1	1-day change in tide range, lagged 1 day
F1MSC	Hourly SC at USGS marsh site F1M
FB2MWL	Filtered WL at station F2—hourly
FB3MWL	Filtered WL at station B3—hourly
FB4MWL-0P1	Filtered WL at station B4—hourly
FF1MWL	Filtered WL at station F1—hourly
FM1MWL	Filtered WL at station M1—hourly
FSC89791	Filtered SC at station 021989791
FSC89791A1WKD2WK	Difference between 1- and 2-week lagged MWAs of FSC89791
FSC89791A24DA4WK	Difference between 24-day and 2-week lagged MWAs of FSC89791
FSC89791A48D1WK	Difference between 2-day and 1-week and lagged MWAs of FSC89791
FSC89791A4WK	4-week MWA of FSC89791

Appendix III. Variables used in artifical neural network models.—Continued

[SC, specific conductance; USGS, U.S. Geological Survey; WL, water level; GPA, Georgia Ports Authority; XWL, tidal range; MWA, moving window average]

Variable	Description
FSC89791DA48	Difference between hourly and 2-day MWA of FSC89791
FSCDIF8840	Difference with SC at station 02198840 and station 021989791
FSCDIF8920	Difference with SC station 02198840 and station 02198920
FWL8840	Filled WL at station 02198840
FWL8980A	Filled, filtered daily WL
FWLDIF8920	Filled WL difference between station 02198840 and station 02198920
FWLDIF8977	Filled WL difference between station 02198840 and station 02198977
FWLDIF8979	Filled WL difference between station 02198840 and station 02198979
LAQ2	2-day lag of the daily flow at station 02198500
LG10D3NWL	10-hour lag in the 3 hour change in WL at station 02198980
LG13D3NWL	13-hour lag in the 3 hour change in WL at station 02198980
LG1D3NWL	1-hour lag in the 3 hour change in WL at station 02198980
LG1NWL	1-hour lag in the in hourly WL at station 02198980
LG2DWLA	1-day change in WL, lagged 2 day at station 02198980
LG2DXWLA	1-day change in tidal range, lagged 2 days at station 02198980
LG3DFSC89791	1-day change in SC at station 021989791 lagged 3 hours
LG3DFSC89791DA48	48-hour average of 1-day change in SC at station 021989791 lagged 3 hours
LG3DFWL8840	Difference with WL at station 02198840 lagged 3 days
LG4D3NWL	4-hour lag in the 3 hour change in WL
LG672FSC89791A4WKD4WK	Difference between 4-week and lagged 4-week MWAs of SC at station 021989791
LG6DFSC89791	SC difference at 021989791 lagged 6 hours
LG6DFWL8840	WL difference at 02198840 lagged 6 days
LG7D3NWL	7-hour lag in the 3 hour change in WL at station 02198980
M1MSC	Hourly SC at marsh site M1
M2MSC	Hourly SC at marsh site M2
M2MWL	Hourly WL at marsh site M2
NXWL	Tidal range at station 02198980
PSC8840A	Predicted daily SC at station 02198840
PSC8920A	Predicted daily SC at station 02198920
PSC89784A	Predicted daily SC at station 021989784
PSC89791A	Predicted daily SC at station 021989791
PSCGPA10S_FLR_A1WK	1-week MWA of floored predicted hourly SC at GPA10S
PSCGPA11B_FLR_A1WK	1-week MWA of floored predicted hourly SC at GPA11B
PSCGPA11RB_FLR_A1WK	1-week MWA of floored predicted hourly SC at GPA11RB
PSCGPA12RS_FLR_A1WK	1-week MWA of floored predicted hourly SC at GPA12RS

Appendix III. Variables used in artifical neural network models.—Continued

[SC, specific conductance; USGS, U.S. Geological Survey; WL, water level; GPA, Georgia Ports Authority; XWL, tidal range; MWA, moving window average]

Variable	Description
PWL8840A	Predicted daily WL at station 02198840
PWL8920A	Predicted daily WL at station 02198920
PWL8977A	Predicted daily WL at station 02198977
PWL8979A	Predicted daily WL at station 02198979
Q8500A	Daily average flow at station 02198500
RB1MSC	Residual error of predicted hourly SC at USGS marsh site B1
RB2MSC	Residual error of predicted hourly SC at USGS marsh site B2
RB3MSC	Residual error of predicted hourly SC at USGS marsh site B3
RB4MSC	Residual error of predicted hourly SC at USGS marsh site B4
RF1MSC	Residual error of predicted hourly SC at USGS marsh site F1
RM1MSC	Residual error of predicted hourly SC at USGS marsh site M1
RM2MSC	Residual error of predicted hourly SC at USGS marsh site M2
RS10MARSHPWC	Residual error of predicted hourly SC at USGS marsh site S10
RS7MARSHPWC	Residual error of predicted hourly SC at USGS marsh site S7
RS9MARSHPWC	Residual error of predicted hourly SC at USGS marsh site S9
RSC10S_11B_A1WK	Residual error of predicted weekly average floored SCGPA11B (for decorrelation)
RSC10S_11B_A1WK	Residual error of predicted weekly average floored SCGPA11B (for decorrelation)
RSC10S_11RB_A1WK	Residual error of predicted weekly average floored SCGPA11RB (for decorrelation)
RSC10S_11RB_A1WK	Residual error of predicted weekly average floored SCGPA11RB (for decorrelation)
RSC10S_12RS_A1WK	Residual error of predicted weekly average floored SCGPA12RS (for decorrelation)
S10CANALWL	Hourly WL at GPA marsh site S10 canal porewater
S10MARSHSWSC	Hourly SC at GPA marsh site S10 surface water
S10MARSHWL	Hourly WL at GPA marsh site S10
S1CANALSC	Hourly SC at GPA marsh site S1 canal
S1CANALWL	Hourly WL at GPA marsh site S1 canal
S1MARSHSC	Hourly SC at GPA marsh site S1
S1MARSHWL	Hourly WL at GPA marsh site S1
S1MARSHWLAT	Hourly WL at GPA marsh site S1 aquatape
S2CANALSC	Hourly SC at GPA marsh site S2 canal
S2CANALWL	Hourly WL at GPA marsh site S2 canal
S2MARSHSC	Hourly SC at GPA marsh site S2 canal
S2MARSHWL	Hourly WL at GPA marsh site S2
S3CANALSC	Hourly SC at GPA marsh site S3
S3CANALWL	Hourly WL at GPA marsh site S3 canal
S3MARSHSC	Hourly SC at GPA marsh site S3

Appendix III. Variables used in artifical neural network models.—Continued

[SC, specific conductance; USGS, U.S. Geological Survey; WL, water level; GPA, Georgia Ports Authority; XWL, tidal range; MWA, moving window average]

Variable	Description
S3MARSHWL	HourlyWL at GPA marsh 3
S4CANALSC	Hourly SC at GPA marsh site S4 canal
S4CANALWL	Hourly WL at GPA marsh site S4 canal
S4MARSHSC	Hourly SC at GPA marsh site S4
S4MARSHWL	Hourly WL at GPA marsh site S4
S5CANALSC	Hourly SC at GPA marsh site S5 canal
S5CANALWL	Hourly WL at GPA marsh site S5 canal
S5MARSHSC	Hourly SC at GPA marsh site S5
S5MARSHWL	Hourly WL at GPA marsh site S5 canal
S6CANALSC	Hourly SC at GPA marsh site S6 canal
S6CANALWL	Hourly WL at GPA marsh site S6 canal
S6MARSHSC	Hourly SC at GPA marsh site S6 canal
S6MARSHWL	Hourly WL at GPA marsh site S6 canal
S6MARSHWLAT	Hourly WL at GPA marsh site S6 aquatape
S7CANALSC	Hourly SC at GPA marsh site S7 canal
S7CANALWL	Hourly WL at GPA marsh site S7 canal
S7MARSHPWSC	Hourly SC at GPA marsh site S7 porewater
S7MARSHSC	Hourly SC at GPA marsh site S7
S7MARSHWL	Hourly WL at GPA marsh site S7
S8CANALSC	Hourly SC at GPA marsh site S8 canal
S8CANALWL	Hourly WL at GPA marsh site S8 canal
S9CANALSC	Hourly SC at GPA marsh site S9 canal
S9CANALWL	Hourly WL at GPA marsh site S9 canal
S9MARSHPWSC	Hourly SC at GPA marsh site S9 porewater
S9MARSHWL	Hourly WL at GPA marsh site S9
SC8840	SC at station 02198840—hourly data
SC8840A	SC at 02198840—daily data
SC8920	SC at station 02198920—hourly data
SC8920A	SC at station 02198920—daily data
SC89784	SC at station 021989784—hourly data
SC89784A	SC at station 021989784—daily data
SC89791	SC at station 021989791—hourly data
SC89791A	SC at station 021989791—daily data
SCDIF8840A	Difference between daily (filtered) SC at gages 89791 and 8840
WL8840	WL at station 02198840—hourly data

Appendix III. Variables used in artifical neural network models.—Continued

[SC, specific conductance; USGS, U.S. Geological Survey; WL, water level; GPA, Georgia Ports Authority; XWL, tidal range; MWA, moving window average]

Variable	Description
WL8840A	WL at station 02198840—daily data
WL8920	WL at station 02198920—hourly data
WL8920A	WL at station 02198920—daily data
WL8977	WL at station 02198977—hourly data
WL8977A	WL at station 02198977—daily data
WL8979	WL at station 02198979—daily data
WL8979A	WL at station 02198979—hourly data
XWL8980A	Daily tidal range

Appendix IV. User's Manual for Model-to-Marsh Decision Support System

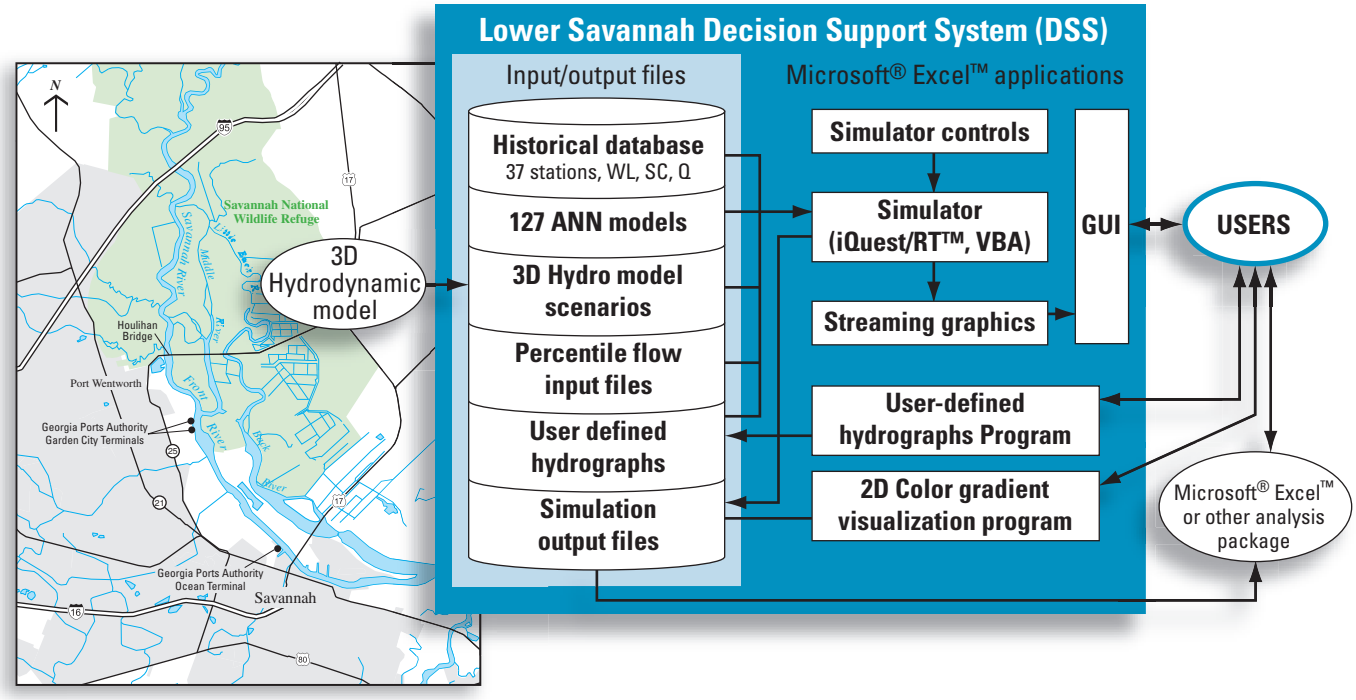

Contents

Contents—continued

Figures

1. Introduction

This document describes how to install and operate the Model-to-Marsh (M2M) application hereafter called the M2M DSS. This M2M DSS predicts how the flow rate (Q) down the Savannah River, as measured at a USGS gage at Clyo, Ga. (station 02198500), and tidal forces, as measured by the water level (WL) at a gage in Savannah Harbor at Fort Pulaski, Ga. (station 02198890), impact the water levels and specific conductivities (SC) at a number of gages on the Savannah, Back, and Little Back Rivers (fig. 1). In turn, the predictions made at these locations will be used to predict the water level and specific conductance of the tidal marshes. The model is an Excel™/VBA (Visual Basic for Applications)[1] program that integrates a large data set, artificial neural network (ANN) models, streaming graphics, and a graphical user-interface. The data set is composed of half-hour samples of Q, WL, and SC covering the period from March 1994 to May 2005. Data through May 2005 were used to develop the ANNs, and are included as separate files, one file for each year of data. This allows the user to run long-term simulations to evaluate permutations of the actual historical record.

2. Installation and System Requirements

Copy the folder titled SavannahM2M to your computer's hard drive. You may place this folder anywhere on your system. The only requirement is that all the files stay in the same directory.

Copy the following files to your computer's System32 directory:

admquestrt.dll
mscomct2.ocx

For example: on a Microsoft XP or Windows 2000 system, the path would be C:\Windows\System32\.

If present, you should delete the file NE32.dll from the System32 directory (you would have this if you loaded an earlier version of the Savannah Phase II application).

Register the above files by typing the following at the Run Prompt (usually accessed from the start menu). This assumes the path is c:\windows\system32.

Regsvr32 c:\windows\system32\admquestrt.dll
Regsvr32 c:\windows\system32\mscomct2.ocx

The program was developed and tested using Microsoft Excel™ 2002. This version or any later version should be used to run the program.

3. Removal

When the M2M DSS is no longer needed, delete the folder containing the applications and its contents.

[1] Any use of trade, product, or firm names is for descriptive purposes only and does not imply endorsement by the U.S. Government.

4. Operation

Three Excel™ programs make up the application. In each program the latest release date is included in the file name in the format mmddyyyy (month/day/year). The three programs are:

SavannahM2M_mmddyyyy.xls
This is the main program from which all simulations are run. This program is hereafter referred to as the model.

CreateUserHydrograph_mmddyyyy.xls
This program is used to create user-defined hydrographs which can be used to run simulations. This is described in greater detail in section 6.

M2MVisualization_mmddyyyy.xls
This program is used to interpolate salinity levels throughout the marsh and visualize the results. This is described in greater detail in section 7.

The remainder of this section will describe how to use the M2M DSS.

The M2M DSS is opened like a standard Excel™ workbook. Simply open the .xls file. Depending on the security settings you have set up for Excel™, you may have to Enable Macros.

The model workbook consists of the following worksheets: *About, Controls, AllUSGSGraphs, SelectedGraphs, RiverOutputTemplate, MarshOutputTemplate,* and *RevisionControl.*

A description of each worksheet and its use/function follows.

4.1. *About* Worksheet

When the workbook opens, the *About* worksheet (fig. A1) is automatically displayed for 5 seconds. This sheet contains the version number of the M2M DSS and contact information for the program's developers. After displaying for 5 seconds, the user is automatically taken to the *Controls* worksheet. The user may return to the *About* worksheet at any time for contact/version information.

4.2. *Controls* Worksheet

The *Controls* worksheet (fig. A2) contains a map of the Savannah River Basin and a *User Controls* user form, which is used to control each simulation run. This form can be moved, closed, and reopened as needed. If closed (by selecting the X in the upper right corner of the form), it is reopened by selecting the "Show User Controls" command button which appears when the form is closed. Figure A2 shows the worksheet divided into six sections which are described next.

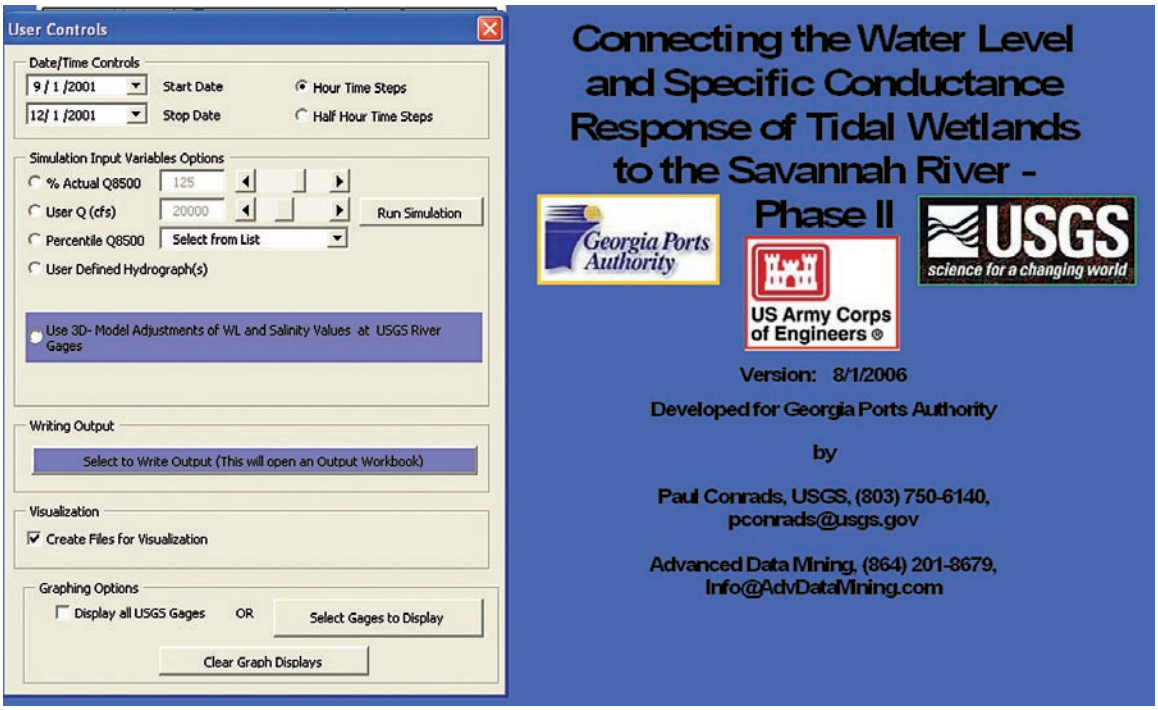

Figure A1. *About* worksheet.

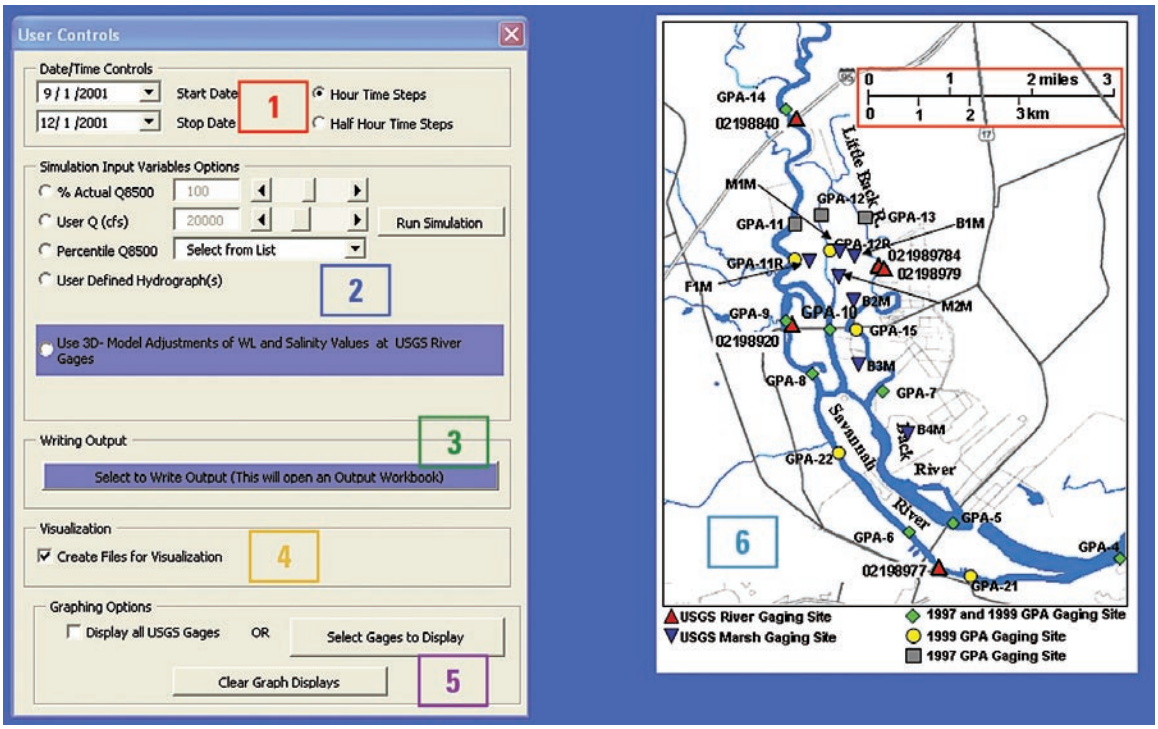

Figure A2. *Controls* worksheet.

4.2.1. Date/Time Controls

This section is used to set the start date, end date, and step size of a simulation run. The start and end dates are set using the calendar combo boxes. Dates selected must be between 3/1/1994 and 5/1/2005. The step size is selected by choosing either the "Hour" or "Half-Hour Time Step" option button. Suggested maximum simulation run if saving output is 2 years.

4.2.2. Simulation Input Variable Options

This section is used to select the model inputs used in modeling the WL and salinity at the various river and marsh gages. The user can opt to set the flow at Clyo(Q) in one of four ways, or the user can input adjustments made by the EFDC hydrodynamic model of WL and salinity at the USGS river gages to predict the effects in the marsh. The five options are described below.

- Percent of Actual Q8500: This sets the user Q as a percentage of the actual historical Q. The percentage is varied using the scroll bar. The setting will display in the text box to the left of the scroll bar. Allowable range is 1–200 percent.
- User Q: This sets the user Q to a fixed value. The value is varied using the scroll bar to select a value. The setting displays in the text box to the left of the scroll bar. Allowable range is 100 to 53,000 cfs.
- Percentile File: Select one of the percentile files (5–95%) from the drop-down box. These files consist of a percentile of the daily mean value from 1929 to 2002.
- User-Defined Hydrograph: This allows the user to select hydrograph file(s) created using the CreateUserhydrographmmddyyyy.xls application from a browser window. The user will be prompted to select the UserHydrograph files(s). Up to 2 years (2 yearly files) may be selected. To select multiple files (the files must cover successive years), simply hold down the <Ctl> key when picking files. Each UserHydrograph file spans 1 year. Instructions for creating the files are provided in detail in this manual in section 6. The user must make sure that the simulation dates selected are not outside the dates spanned by the UserHydrograph file(s).
- 3D-Model Adjustments of WL and Salinity Values at USGS River Gages: The user will be prompted to select the data file(s) containing the adjustments from a browser window. The format requirements for the data file(s) are provided in section 4.2.5. The program will use these values to make predictions in the marsh.

This section also contains the "Run Simulation" command button. When all simulation controls are set, selecting this button will begin the simulation run. There will be some delay while the data files needed for the simulations are loaded.

4.2.3. Writing Output

Select the "Select to Write Output" button to have the outputs written to a workbook. You will be prompted for the name of the workbook that will be created to hold the output. Once the simulation run is complete, the file will be saved and closed. The output file consists of 2 worksheets—one containing river data and the other marsh data (figs. A4, A5). Data written to the output file include flow at Clyo (Q), WL in the Savannah Harbor (WL8980), and for each modeled gaging location:

- historical data,
- predicted value based on actual data or predicted USGS riverine (pred),
- the change predicted due to the user settings (pred-user), and
- the new prediction.

Gages measuring water level are preceded by "WL," and those measuring salinity are preceded by "Sal." Appendix A lists the measured and modeled data in the output file.

4.2.4. Visualization

Checking the box labeled "Create Files for Visualization" will save four files to the VisualizationFiles directory. The files will contain the data for the gages needed by the M2MVisualization program (described in this manual in section 7).

The files saved are:

- SavVisActual_m_dd_yyyy_h_mm.cvs (where m=month, dd=day, yyyy=year, h=hour, mm=minutes) will contain the actual data for the gages;
- SavVisPred_m_dd_yyyy_h_mm.cvs will contain the predicted values based on actual Q;
- SavVisUser_m_dd_yyyy_h_mm.cvs will contain the predicted values based on user settings; and
- SavVisDelta_m_dd_yyyy_h_mm.cvs will contain the changes due to user settings.

4.2.5. Graphing Options

This section controls what the user views while the simulation is running. The user can opt to view all USGS river and Back River gage values or the user may select any of four gages to display (recommended). Selecting the "Select Gages to Display" button will pop up a window showing all the graphing options (fig. A3). Select any four and then click "Done." For each gage selected, the graph will display actual values, predicted values (of historical conditions), predicted values of user-defined conditions, and differences between actual and user-defined conditions. Clearing the graphing displays will clear all data from the graphs.

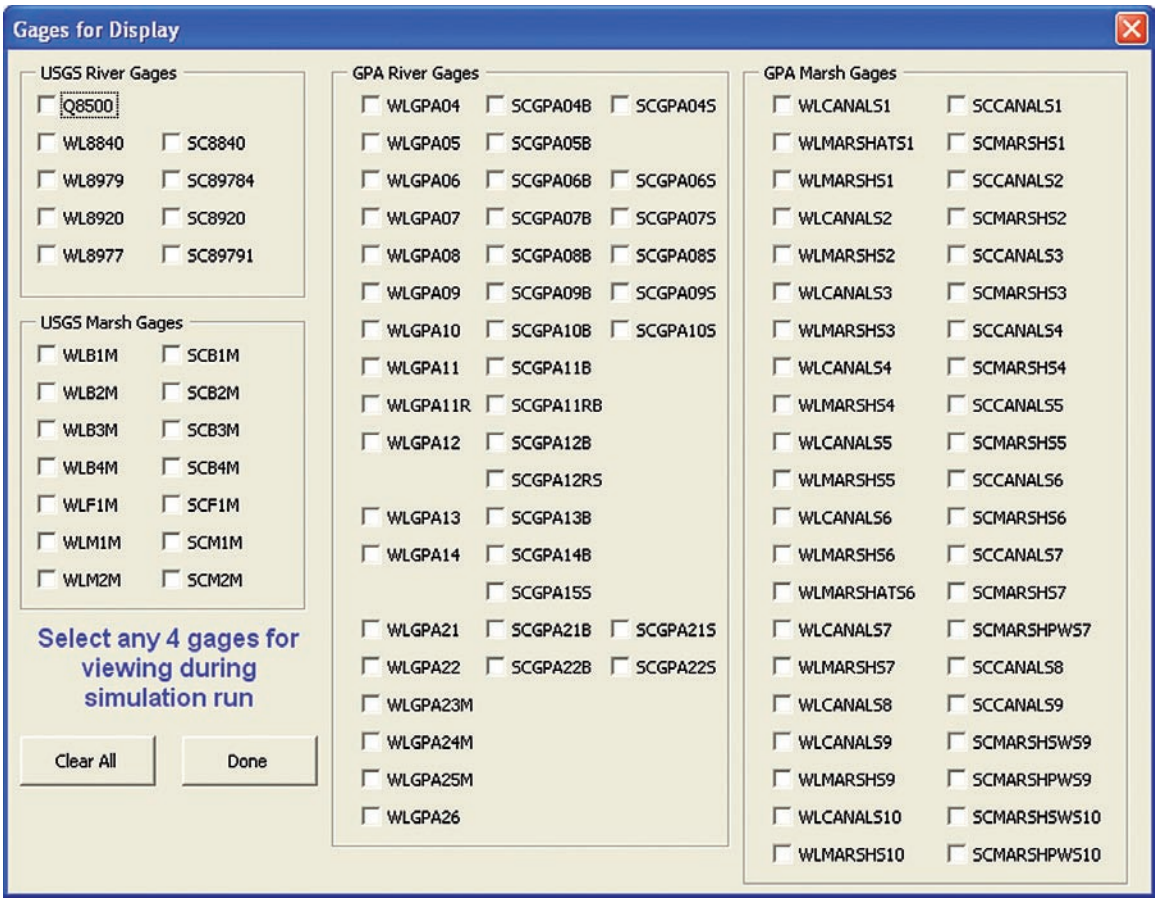

Figure A3. Graph selection form.

4.2.6. Savannah Map

This map displays the locations of most of the gages modeled in the application.

4.3. *AllUSGSGraphs* Worksheet

The *AllUSGSGraphs* worksheet (fig. A6) displays the WL and salinity for the USGS river gages as well as the flow at Clyo (section 1 of fig. A6). This worksheet automatically displays during a simulation run if the user has chosen the option to "Display All USGS Gages" on the *Controls* worksheet. Once the simulation run is complete, the user can return to the *Controls* worksheet by clicking on the "Show User Controls" command button (section 2 of fig. A6).

4.4. *SelectedGraphs* Worksheet

The *SelectedGraphs* worksheet (fig. A7*)* displays the WL and salinity for any four gages selected on the Graph Selection Form (fig. A3). This worksheet automatically displays during a simulation run if the user has chosen the "Select Gages to Display" option. Once the simulation run is complete, the user can return to the *Controls* worksheet by clicking on the "Show User Controls" command button.

4.5. *RiverOutputTemplate* and *MarshOutputTemplate* Worksheets

The two output template worksheets show the format of the output files created when "Select to Write Output" is selected (fig. A2).

4.6. *RevisionControl* Worksheet

The ***RevisionControl*** worksheet shows a brief description of changes made to the program with each revision.

	1	2	3	4	5	6	7	8	9	10	11	12	13	14	15
1	DATETIME	ROW	Q8500	Q8500A	Q8500-use	WL8980	XWL8980	Sal8840	Sal8840-pr	dSal8840([	Sal8840-u	WL8840	WL8840-pr	dWL8840([	WL8840-u
2	1/1/2002	1	5670	5713.71	7740	-0.28	8.127501	0.051247	0.062449	0.009117	0.04213	3.3	3.097175	-0.18067	3.460675
3	1/1/2002 1:00	3	5662	5706.1	7733.75	-2.11	8.240001	0.048619	0.057799	0.00951	0.039109	1.64	1.268404	-0.2396	1.879599
4	1/1/2002 2:00	5	5662	5698.62	7727.5	-3.63	8.352501	0.048619	0.053164	0.009473	0.039147	-0.06	-0.25676	-0.24833	0.188325
5	1/1/2002 3:00	7	5647	5691.29	7721.25	-4.4	8.465001	0.048182	0.053761	0.00934	0.038843	-1.6	-1.52403	-0.22498	-1.37502
6	1/1/2002 4:00	9	5647	5684.12	7715	-3.56	8.577501	0.048182	0.056107	0.009061	0.039121	-2.86	-2.88022	-0.18029	-2.67971
7	1/1/2002 5:00	11	5647	5677.12	7708.75	-1.77	8.690001	0.047746	0.05759	0.008887	0.038859	-3.69	-3.39974	-0.15333	-3.53667
8	1/1/2002 6:00	13	5640	5670.29	7702.5	0.37	8.802502	0.048182	0.057491	0.0089	0.039282	-2.08	-1.85648	-0.18015	-1.89985
9	1/1/2002 7:00	15	5632	5663.65	7696.25	2.6	8.915002	0.048182	0.056533	0.009018	0.039165	0.2	0.746222	-0.1836	0.383597
10	1/1/2002 8:00	17	5625	5657.19	7690	4.09	9.027502	0.049932	0.057085	0.008958	0.040974	2.41	3.050076	-0.13427	2.54427
11	1/1/2002 9:00	19	5617	5650.92	7683.75	4.74	9.14	0.056088	0.059284	0.008706	0.047382	4.09	4.501727	-0.08364	4.173638
12	1/1/2002 10:00	21	5609	5644.85	7677.5	4.65	9.04	0.063622	0.060857	0.008637	0.055084	4.84	5.158915	-0.06232	4.902317
13	1/1/2002 11:00	23	5602	5638.99	7671.25	3.51	8.94	0.071663	0.061461	0.009221	0.062442	5.15	5.330155	-0.07354	5.223538
14	1/1/2002 12:00	25	5602	5633.35	7665	2.01	8.839999	0.067188	0.079668	0.014295	0.052892	4.99	4.888905	-0.12189	5.111892
15	1/1/2002 13:00	27	5594	5627.93	7658.75	0.21	8.739999	0.054765	0.091489	0.018285	0.03648	4.07	3.89399	-0.19267	4.26267
16	1/1/2002 14:00	29	5587	5622.74	7652.5	-1.75	8.639998	0.048619	0.061447	0.012018	0.036601	2.55	2.506562	-0.25856	2.808564
17	1/1/2002 15:00	31	5587	5617.8	7646.25	-3.27	8.539998	0.049057	0.053247	0.009621	0.039435	0.85	0.840478	-0.27484	1.124841
18	1/1/2002 16:00	33	5579	5613.1	7640	-3.95	8.439998	0.049494	0.056432	0.009164	0.04033	-0.8	-0.49439	-0.25719	-0.54281
19	1/1/2002 17:00	35	5579	5608.67	7633.75	-3.09	8.339997	0.049494	0.059557	0.008824	0.04067	-2.23	-1.93862	-0.21882	-2.01118
20	1/1/2002 18:00	37	5571	5604.51	7627.5	-1.07	8.239997	0.049932	0.059798	0.008841	0.041091	-3.13	-2.75685	-0.18494	-2.94506
21	1/1/2002 19:00	39	5571	5600.62	7621.25	1.01	8.139997	0.049932	0.057196	0.009214	0.040718	-1.43	-1.02367	-0.20428	-1.22572
22	1/1/2002 20:00	41	5571	5597.02	7615	2.91	8.039996	0.049932	0.055658	0.00947	0.040463	0.97	1.287558	-0.1856	1.155596
23	1/1/2002 21:00	43	5564	5593.7	7608.75	3.99	7.94	0.054324	0.056458	0.009451	0.044873	3.05	3.326842	-0.12858	3.178576
24	1/1/2002 22:00	45	5564	5590.68	7602.5	3.85	8.057693	0.060512	0.060363	0.00905	0.051462	4.32	4.630055	-0.08066	4.400662
25	1/1/2002 23:00	47	5556	5587.98	7596.25	2.93	8.175385	0.067188	0.063844	0.008701	0.058487	4.76	4.851083	-0.07883	4.838835
26	1/2/2002	49	5556	5585.58	7590	1.54	8.293077	0.062288	0.064135	0.008977	0.05331	4.4	4.3282	-0.12197	4.521968
27	1/2/2002 1:00	51	5556	5583.52	7586.792	-0.09	8.410769	0.052125	0.063214	0.010252	0.041873	3.2	3.20384	-0.1937	3.393702
28	1/2/2002 2:00	53	5556	5581.78	7583.584	-1.77	8.528461	0.05037	0.056677	0.010526	0.039844	1.58	1.572192	-0.2444	1.824404
29	1/2/2002 3:00	55	5556	5580.38	7580.376	-3.28	8.646152	0.049932	0.053299	0.010529	0.039403	-0.04	0.033229	-0.25374	0.21374
30	1/2/2002 4:00	57	5548	5579.32	7577.168	-4.02	8.763844	0.049494	0.055628	0.010284	0.03921	-1.49	-1.26279	-0.23262	-1.25738
31	1/2/2002 5:00	59	5556	5578.6	7573.96	-3.04	8.881536	0.049057	0.05958	0.00985	0.039206	-2.73	-2.56155	-0.19236	-2.53764
32	1/2/2002 6:00	61	5556	5578.23	7570.752	-1.29	8.999228	0.048619	0.061012	0.009737	0.038882	-3.37	-2.93386	-0.168	-3.202
33	1/2/2002 7:00	63	5556	5578.18	7567.544	0.99	9.11692	0.049057	0.060315	0.009902	0.039154	-1.63	-1.33812	-0.18699	-1.44301
34	1/2/2002 8:00	65	5564	5578.45	7564.336	3.13	9.234612	0.049057	0.05781	0.010302	0.038755	0.71	1.360634	-0.17637	0.886372
35	1/2/2002 9:00	67	5564	5579.04	7561.128	4.71	9.352304	0.052564	0.058269	0.010278	0.042287	2.92	3.463959	-0.12308	3.043079
36	1/2/2002 10:00	69	5571	5579.92	7557.92	5.45	9.47	0.059182	0.06034	0.01001	0.049173	4.44	4.783849	-0.07476	4.514761
37	1/2/2002 11:00	71	5571	5581.08	7554.712	5.15	9.257692	0.067635	0.062272	0.009769	0.057865	5.14	5.404792	-0.05623	5.19623
38	1/2/2002 12:00	73	5571	5582.49	7551.504	4.14	9.045384	0.083383	0.064426	0.010864	0.072519	5.46	5.522354	-0.07231	5.53231
39	1/2/2002 13:00	75	5571	5584.12	7548.296	2.33	8.833076	0.100705	0.101306	0.021147	0.079558	5.4	5.29962	-0.11774	5.517737
40	1/2/2002 14:00	77	5564	5585.96	7545.088	0.62	8.620769	0.065849	0.120748	0.027224	0.038625	4.7	4.384307	-0.20123	4.90123

RiverOutputTemplate / MarshOutputTemplate / Sheet3 /

Figure A4. Output workbook—river output.

	1	2	3	4	5	6	7	8	9	10	11	12	13	14	15	16	17	18
1	DATETIME	ROW	S1CANAL	S1CANAL	dS1CANA	S1CANAL	S1MARSH	S1MARSH	dS1MARS	S1MARSH	S1MARSH	S1MARSH	dS1MARS	S1MARSH	S2CANAL	S2CANAL	dS2CANA	S2CANAL
11	1/1/2002 9:00	19	4.4	4.233431	-0.04097	4.440975	?	4.86155	-0.01203	4.873581	5.1	5.053614	-0.00387	5.103868	?	5.080973	0.105447	4.975526
12	1/1/2002 10:00	21	4.9	4.810073	-0.02321	4.923213	?	4.890724	-0.01833	4.909055	5.1	5.084976	-0.00909	5.109094	?	5.079346	0.024129	5.055217
13	1/1/2002 11:00	23	5.2	5.010074	-0.02428	5.224277	?	4.96892	-0.02066	4.989582	5.2	5.150597	-0.0167	5.216703	?	4.263006	-0.10815	4.371156
14	1/1/2002 12:00	25	4.7	4.817895	-0.05272	4.75272	?	4.974326	-0.00915	4.983475	5.1	5.120988	-0.01221	5.112212	?	2.795732	-0.20741	3.003144
15	1/1/2002 13:00	27	3.2	3.741564	-0.1238	3.323802	?	4.897757	-0.01043	4.908188	5.1	5.063102	-0.0094	5.109403	?	1.498792	0.028499	1.470293
16	1/1/2002 14:00	29	1.3	1.668833	-0.18064	1.480639	?	4.930774	-0.00715	4.937922	5.1	5.066496	-0.00661	5.106613	?	0.737862	0.002835	0.735027
17	1/1/2002 15:00	31	-0.6	-0.12386	-0.10917	-0.49083	?	4.953959	-0.004	4.957958	5.1	5.086568	0.000275	5.099725	?	0.585311	-0.00928	0.594589
18	1/1/2002 16:00	33	-0.8	-0.83929	-0.04574	-0.75426	?	4.96242	-0.00243	4.964848	5.1	5.089053	0.003103	5.096897	?	0.560467	0.000713	0.559754
19	1/1/2002 17:00	35	-0.8	-0.93102	-0.0166	-0.7834	?	4.959907	-0.00279	4.962695	5.1	5.084052	0.001818	5.098182	?	0.56253	-0.00152	0.564048
20	1/1/2002 18:00	37	-0.8	-0.83965	-0.0169	-0.7831	?	4.923231	-0.00668	4.929914	5.1	5.066787	-0.00226	5.102255	?	0.66039	-0.03139	0.691778
21	1/1/2002 19:00	39	-0.8	-0.53186	-0.07395	-0.72605	?	4.895179	-0.01303	4.908213	5.1	5.057617	-0.00653	5.106532	?	0.931233	0.059319	0.871914
22	1/1/2002 20:00	41	1.6	1.019562	-0.13864	1.758644	?	4.885307	-0.01456	4.899863	5.1	5.061142	-0.01113	5.111131	?	2.774626	-0.2212	2.99583
23	1/1/2002 21:00	43	3.5	3.153306	-0.08609	3.586092	?	4.89735	-0.01033	4.907682	5.1	5.065211	-0.00533	5.105328	?	4.553693	0.119133	4.43456
24	1/1/2002 22:00	45	4.5	4.309094	-0.04049	4.540486	?	4.904096	-0.01036	4.914458	5.1	5.06497	-0.00367	5.103673	?	4.629604	0.120087	4.509517
25	1/1/2002 23:00	47	4.6	4.592368	-0.03584	4.635837	?	4.893066	-0.01402	4.907089	5.1	5.073677	-0.00507	5.105069	?	4.078264	0.068793	4.00947
26	1/2/2002	49	4	4.230497	-0.0661	4.066103	?	4.81532	-0.01547	4.830786	5.1	5.066043	-0.00512	5.10512	?	2.602628	-0.1669	2.769526
27	1/2/2002 1:00	51	2.4	2.672258	-0.13757	2.537569	?	4.839892	-0.01671	4.856602	5.1	5.049404	-0.00383	5.103826	?	1.1507	-0.09708	1.24778
28	1/2/2002 2:00	53	0.5	0.686228	-0.14778	0.647775	?	4.895675	-0.01342	4.909093	5.1	5.051389	-0.00491	5.10491	?	0.602999	-0.05871	0.661713
29	1/2/2002 3:00	55	-0.8	-0.44104	-0.08607	-0.71393	?	4.926709	-0.00849	4.935194	5.1	5.054803	-0.00825	5.108254	?	0.486011	-0.10945	0.594466
30	1/2/2002 4:00	57	-0.8	-0.86472	-0.03161	-0.76839	?	4.946339	-0.00433	4.950669	5.1	5.069739	-0.00181	5.10181	?	0.496727	-0.03327	0.529998
31	1/2/2002 5:00	59	-0.8	-0.87335	-0.00709	-0.79291	?	4.947193	-0.00393	4.951127	5.1	5.073103	-0.00065	5.10065	?	0.522936	-0.01221	0.535147
32	1/2/2002 6:00	61	-0.8	-0.82511	-0.0135	-0.7865	?	4.902864	-0.00822	4.911087	5.1	5.051223	-0.00489	5.104887	?	0.612459	-0.04533	0.657793
33	1/2/2002 7:00	63	-0.8	-0.6193	-0.0619	-0.7381	?	4.877658	-0.01539	4.893052	5.1	5.049689	-0.00827	5.108265	?	0.984927	-0.00407	0.988996
34	1/2/2002 8:00	65	1.4	0.783406	-0.13106	1.531059	?	4.856405	-0.01633	4.872731	5.1	5.049603	-0.0081	5.108097	?	2.833343	0.139266	2.694077
35	1/2/2002 9:00	67	3.6	3.174683	-0.07985	3.679848	?	4.859972	-0.01199	4.871958	5.1	5.051253	-0.00504	5.105036	?	5.019635	0.134763	4.884871
36	1/2/2002 10:00	69	4.8	4.612719	-0.0332	4.833205	?	4.901357	-0.01318	4.914538	5.1	5.061014	-0.0051	5.1051	?	5.238348	0.071357	5.16699
37	1/2/2002 11:00	71	5.3	5.099253	-0.01846	5.318455	?	5.056316	-0.02741	5.083727	5.3	5.129875	-0.01514	5.315139	?	5.209116	-0.0022	5.211315
38	1/2/2002 12:00	73	5.5	5.260937	-0.0212	5.521205	?	5.367211	-0.0205	5.387707	5.4	5.273676	-0.02193	5.42193	?	4.286773	-0.18948	4.476256
39	1/2/2002 13:00	75	5.2	5.139106	-0.04147	5.241475	?	5.25933	0.004903	5.254426	5.2	5.196799	-0.01916	5.219164	?	2.974405	-0.39355	3.367952
40	1/2/2002 14:00	77	4	4.392848	-0.11587	4.115873	?	4.949241	-0.00604	4.955279	5.1	5.08522	-0.01034	5.110335	?	1.60978	0.088332	1.521448
41	1/2/2002 15:00	79	2.2	2.649571	-0.18924	2.389237	?	4.942667	-0.00531	4.947973	5.1	5.082737	-0.00436	5.104365	?	0.863025	0.053775	0.80925
42	1/2/2002 16:00	81	0.3	0.581739	-0.15703	0.457031	?	4.95913	-0.00301	4.962142	5.1	5.099497	0.00275	5.09725	?	0.652722	0.016288	0.636433
43	1/2/2002 17:00	83	-0.8	-0.55907	-0.06824	-0.73176	?	4.964196	-0.00243	4.966627	5.1	5.09756	0.003681	5.096319	?	0.597647	0.00533	0.592317
44	1/2/2002 18:00	85	-0.8	-0.81985	-0.03684	-0.76316	?	4.957023	-0.00356	4.960583	5.1	5.093638	0.00146	5.09854	?	0.650096	-0.00022	0.650319
45	1/2/2002 19:00	87	-0.8	-0.73886	-0.04698	-0.75302	?	4.917243	-0.00677	4.924013	5.1	5.070693	-0.00245	5.102451	?	0.764779	0.008533	0.756246
46	1/2/2002 20:00	89	0.2	-0.02463	-0.11451	0.314507	?	4.910738	-0.01043	4.921171	5.1	5.07709	-0.00614	5.106138	?	2.077451	0.170395	1.907056
47	1/2/2002 21:00	91	2.2	1.770218	-0.13056	2.330564	?	4.916291	-0.00915	4.927445	5.1	5.082408	-0.00587	5.105867	?	3.566931	0.220033	3.345898
48	1/2/2002 22:00	93	3.7	3.427089	-0.07546	3.775461	?	4.927451	-0.007	4.934453	5.1	5.078259	-0.00398	5.103985	?	4.237403	0.189918	4.047485
49	1/2/2002 23:00	95	4.4	4.33568	-0.04121	4.441215	?	4.944885	-0.01011	4.954992	5.1	5.077634	-0.00436	5.104363	?	4.659252	0.1106	4.548652

RiverOutputTemplate / MarshOutputTemplate / Sheet3 /

Figure A5. Output workbook—marsh output.

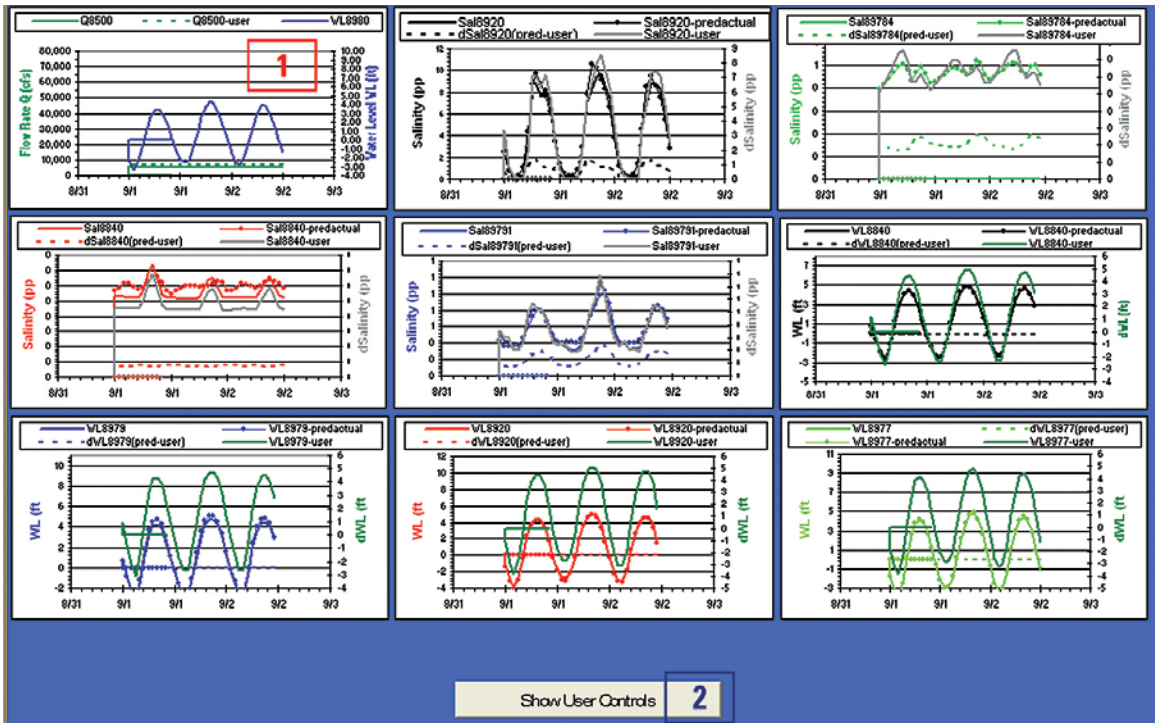

Figure A6. *AllUSGSGraphs* worksheet.

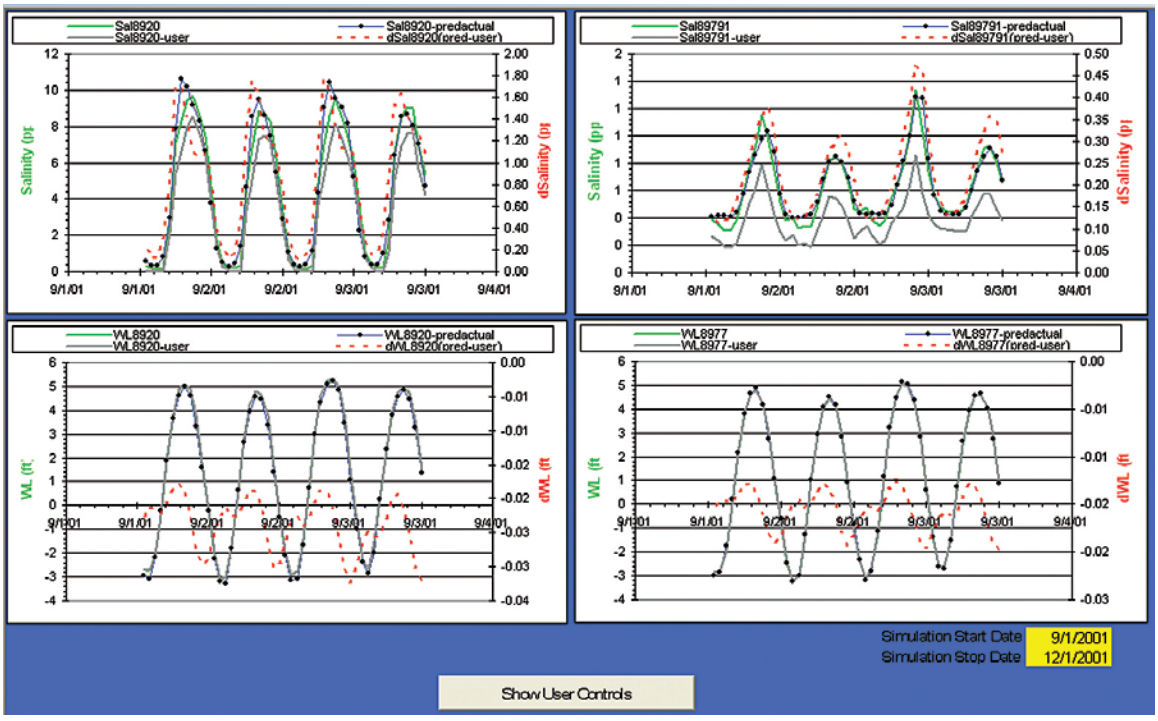

Figure A7. *SelectedGraphs* worksheet.

5. Running the Models Using 3D Hydrodynamic Model Predictions (EFDC) as Inputs

The 3D hydrodynamic model predictions datafile must have a specific format to be used by the M2M. The file format requirements can be found in the file 3DHydroModel_fileformat.csv located in the application directory and also are mentioned below:

- Comma-delimited file.
- First row is a header row.
- Subsequent rows contain the data values. In the year column, put the time stamp (in standard Excel™ number format, for example, 1/1/1900 0:00 = 1; 1/1/1994 0:00 = 34335; 1/1/1994 0:30 = 34335.02083). The first row of data is row 1. Data increments must be in half-hour steps; therefore, a non-leap year would contain 17,520 rows and a leap year 17,568 rows of data.
- A "?" indicates no data available.
- A sample file with instructions is located in \EFDCHydroModelSimData\EFDC_fileformat_r3.

6. Creating a UserHydrograph

A separate Excel™ program called Createuserhydrograph_mmddyyyy.xls is used to generate a UserHydrograph file. Each UserHydrograph created must include 1 year of half-hour values. This application is contained in the same folder as the model.

Three worksheets are in the workbook: *About, UserHydrographtemplate,* and *Userformsheet.*

6.1. *About* Worksheet

The *About* Worksheet (fig. A8) contains the contact and revision information for the application. It will display for 5 seconds and then the *UserHydrographtemplate* worksheet will display.

6.2. *UserHydrographtemplate* Worksheet

The *UserHydrographtemplate* worksheet (fig. A9 and hereafter referred to as the template) contains your choices for generating a hydrograph. This application can be used in two ways. The user can cut and paste in flow values and then save the values to the file, or the user can generate a hydrofile from scratch by setting setpoints for flow values. The program will then fill in the remaining values by interpolating between setpoints.

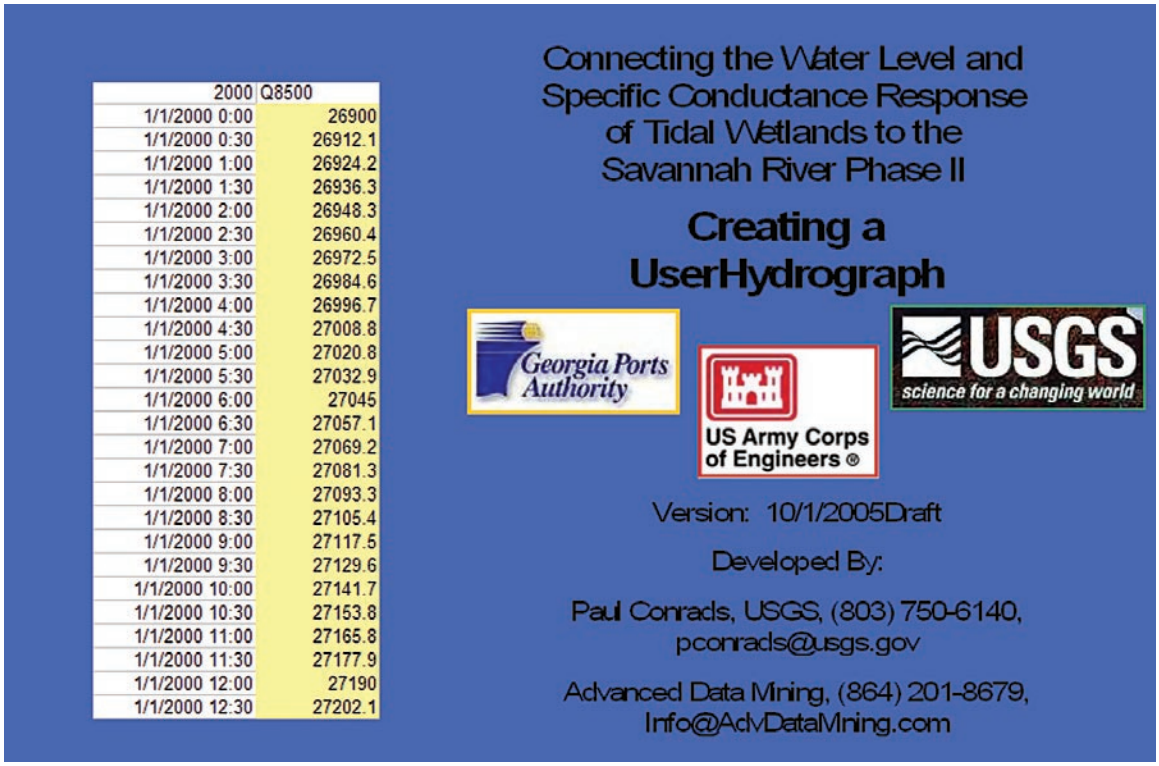

Figure A8. *About* worksheet.

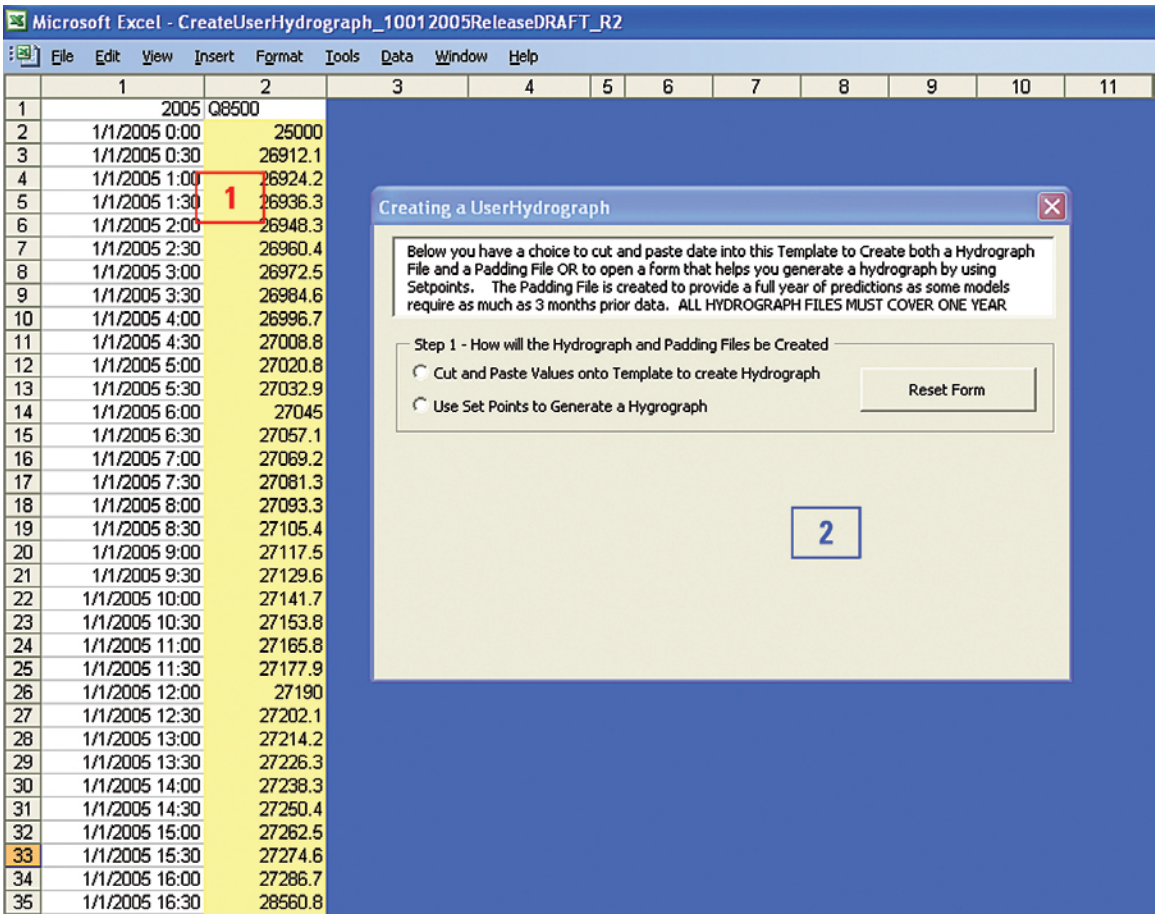

	1	2
1	2005	Q8500
2	1/1/2005 0:00	25000
3	1/1/2005 0:30	26912.1
4	1/1/2005 1:00	26924.2
5	1/1/2005 1:30	26936.3
6	1/1/2005 2:00	26948.3
7	1/1/2005 2:30	26960.4
8	1/1/2005 3:00	26972.5
9	1/1/2005 3:30	26984.6
10	1/1/2005 4:00	26996.7
11	1/1/2005 4:30	27008.8
12	1/1/2005 5:00	27020.8
13	1/1/2005 5:30	27032.9
14	1/1/2005 6:00	27045
15	1/1/2005 6:30	27057.1
16	1/1/2005 7:00	27069.2
17	1/1/2005 7:30	27081.3
18	1/1/2005 8:00	27093.3
19	1/1/2005 8:30	27105.4
20	1/1/2005 9:00	27117.5
21	1/1/2005 9:30	27129.6
22	1/1/2005 10:00	27141.7
23	1/1/2005 10:30	27153.8
24	1/1/2005 11:00	27165.8
25	1/1/2005 11:30	27177.9
26	1/1/2005 12:00	27190
27	1/1/2005 12:30	27202.1
28	1/1/2005 13:00	27214.2
29	1/1/2005 13:30	27226.3
30	1/1/2005 14:00	27238.3
31	1/1/2005 14:30	27250.4
32	1/1/2005 15:00	27262.5
33	1/1/2005 15:30	27274.6
34	1/1/2005 16:00	27286.7
35	1/1/2005 16:30	28560.8

Figure A9. *UserHydrographtemplate* worksheet.

Found on the *Template* worksheet is the *Creating a UserHydrograph* UserForm (hereafter called OptionForm) which steps the user through the process of creating a UserHydrograph (section 2 of fig. A9 shows the opened OptionForm).

6.2.1. Creating a UserHydrograph using the Cut and Paste Option

The cut and paste option allows the user to use flow values created outside of this program. The user pastes flow values into the specified location on the *Template* worksheet. Figure A10 shows the OptionForm with the cut and paste option selected. The steps to perform are:

- Select the option to cut and paste values onto the template.
- Select the year using the year combo box. Any year between 1994 and 2002 is allowed.

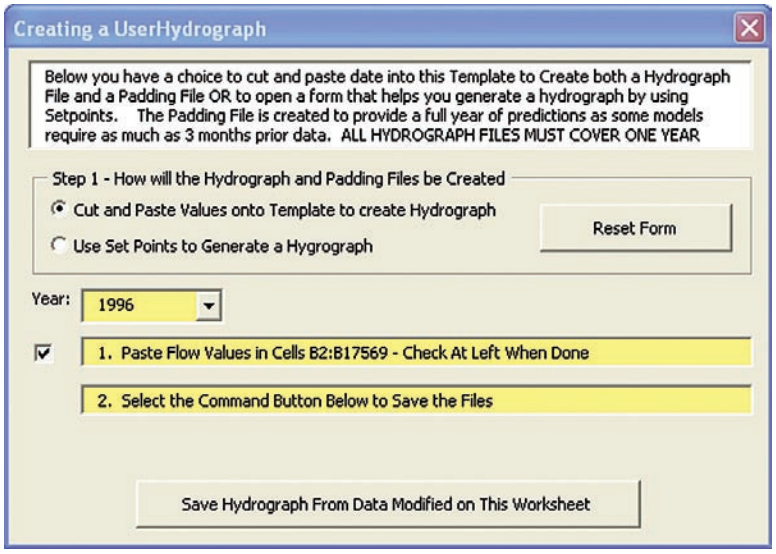

Figure A10. OptionForm with "Cut and Paste" option.

- Paste the flow values in the specified cells on the worksheet. The user must supply 1 full year of half-hour values. If the year selected is a leap year, the user must provide 366 days of values.
- Save the hydrograph values to file by selecting the "Save Hydrograph" command button.

6.2.2. Creating a UserHydrograph using the Set Points Option

The set points option allows the user to set values for specific dates. Once all set points are selected, the program will interpolate between set points to generate the remaining flow values. Figure A11 shows details of the OptionForm when the "use set points to generate a hydrograph" option is selected. The steps to perform are:

- Select the "Use Set Points" option.
- Select the "Generate Hydrograph Flows" command button. This will open the UserForm worksheet and the Create UserHydrograph Form (hereafter called SetPointForm).

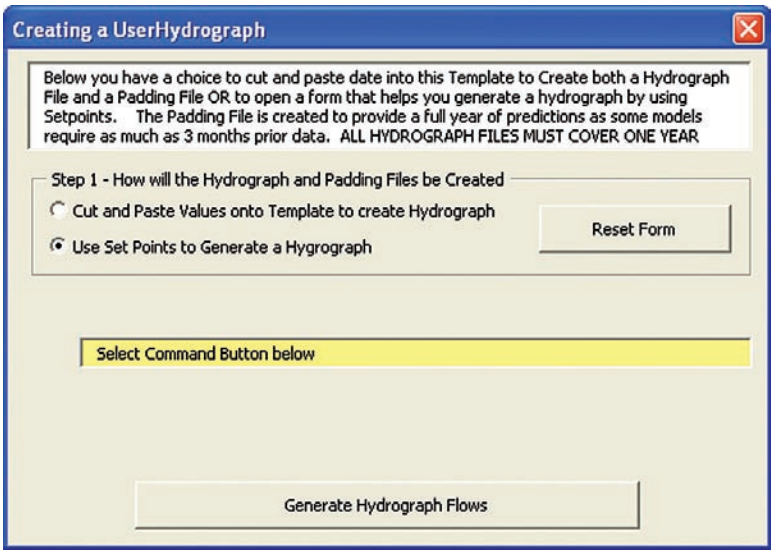

Figure A11. OptionForm with "Generate a Hydrograph" option selected.

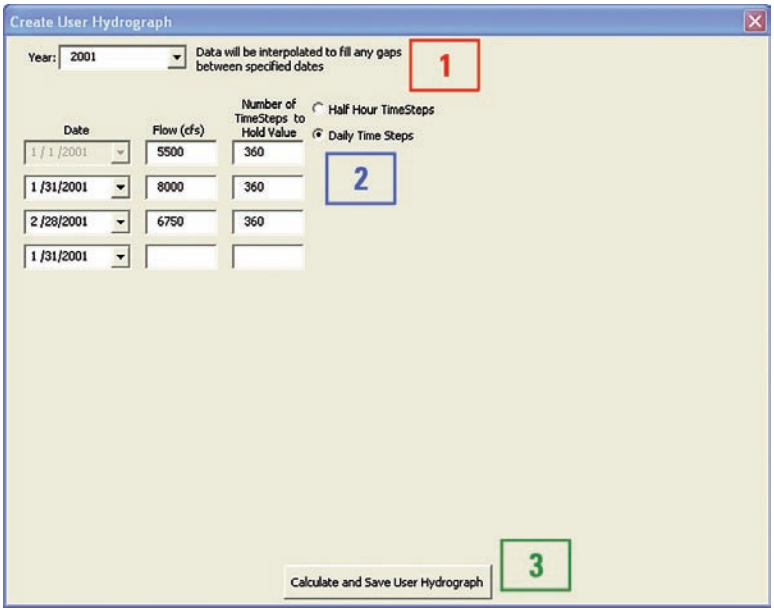

Figure A12. Create UserHydrograph form.

6.2.2.1. Create *UserHydrograph* Worksheet

The Create UserHydrograph form (fig. A12) allows the user to specify set points for the UserHydrograph. The program will then interpolate between the specified set points to create a UserHydrograph. The steps are as follows:

- Select any year between 1994 and 2005 (section 1 of fig. A12) for the UserHydrograph.
- Enter a flow for the first set point. The first set point is automatically set to January 1 of the specified year.
- Enter a hold time for the value. The user has two choices for units in setting a hold time. The user may select that the hold time be specified in half-hour time steps or daily time steps using the provided option buttons (section 2 of fig. A12). For example, if the user has specified a hold time of 1 and selected daily time steps, the flow value specified will stay constant for 1 day. If the user has selected half-hour time steps, the flow value specified will stay constant for 1 half hour.
- A user may specify up to 24 set points. After a set point has been entered, a new blank set point will become visible.
- After all set points have been entered, select the "Calculate and Save UserHydrograph" command button (section 3 of fig. A12). This will interpolate values between setpoints, holding any given value for the specified hold time. If the last set point is not at year's end, the program will hold the last set point value to year's end.
- The user will be prompted for the name of the UserHydrograph file. A workbook will open with the UserHydrograph data and the file saved. Figure A13 shows the user windows which pop up for choosing the file name and saving of the file.

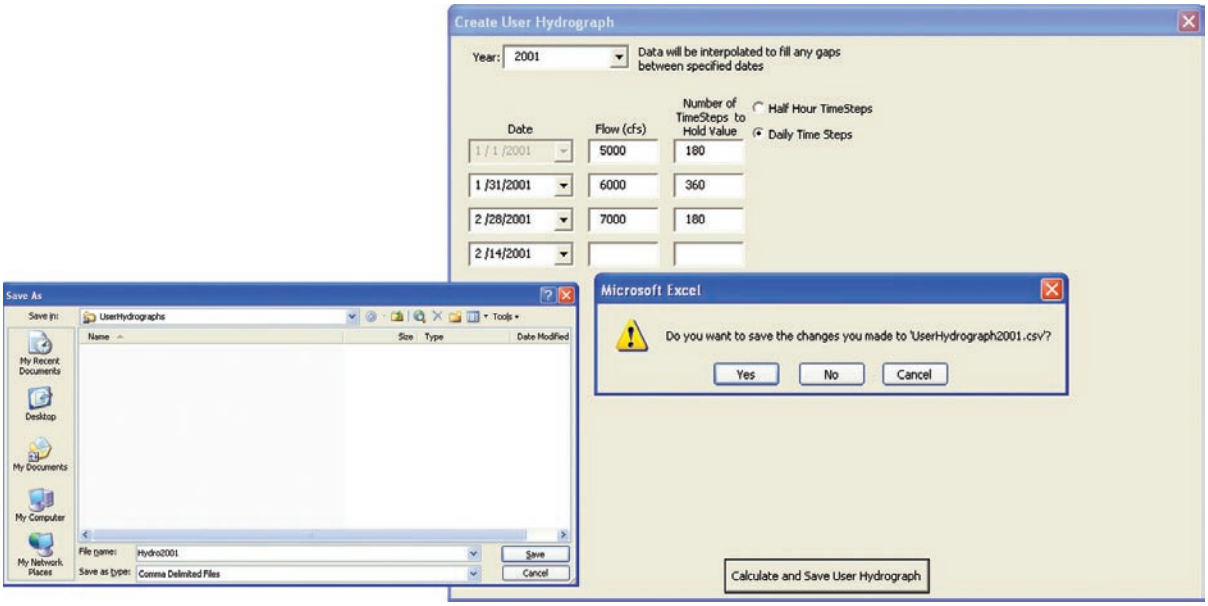

Figure A13. Saving the UserHydrograph.

6.3. *Revision Control* Worksheet

The *Revision Control* worksheet notes each revision and its changes.

7. Marsh Filling and Visualization

The application ***M2MVisualization_mmddyyy.xls*** (hereafter referred to as M2M) is used to fill salinity values for the entire marsh area using salinity values from various gages. The program uses output from the model program to fill the marsh values. To create these files, the user must select "Save Visualization Files" when running a simulation using the model. The files are saved in the VisualizationFiles folder.

The M2M application consists of seven worksheets which are described below.

7.1. *About* Worksheet

The ***About*** worksheet (fig. A14) contains contact and revision information.

7.2. *Visualization* Worksheet

The ***Visualization*** worksheet (fig. A15) contains the visualization of the marsh and all controls for handling the filling and colorization of the marsh. The controls for filling the marsh are contained on the *Visualization Setup* UserForm (section 2 of fig. A15). Controls for changing the color scheme of the visualization grid are contained in the *Visualization Color Scheme* UserForm (section 3 of fig. A15).

7.2.1. Visualization Grid

The visualization grid (section 1 of fig. A15) displays the Savannah River, Back River, marsh, and surrounding areas. The river, upland area, and pond are displayed in blue, brown, and light blue, respectively. These remain fixed. The marsh areas shown in figure A15 are displayed in various shades of green depending on the salinity. An example of this is shown in figure A16.

7.2.2. *Visualization Setup* UserForm

The *Visualization Setup* UserForm is used to control the filling of the marsh for visualization (fig. A17). The form is divided into four steps which are described below.

7.2.2.1. Step 1—Load in Model Output Data

Here the user selects the file containing the salinity data which will be used to fill the marsh. Selecting the "Load in Salinity Data Used in Visualization" command button will open a browser window from which the user can select the desired file. The only data which can be read into this program is the visualization data created by the model program during the simulation run. The next three text boxes are for display only (no user input allowed) and will display the name of the data file selected, the start date of the simulation run for the selected file, and the end date of the simulation run for the selected file.

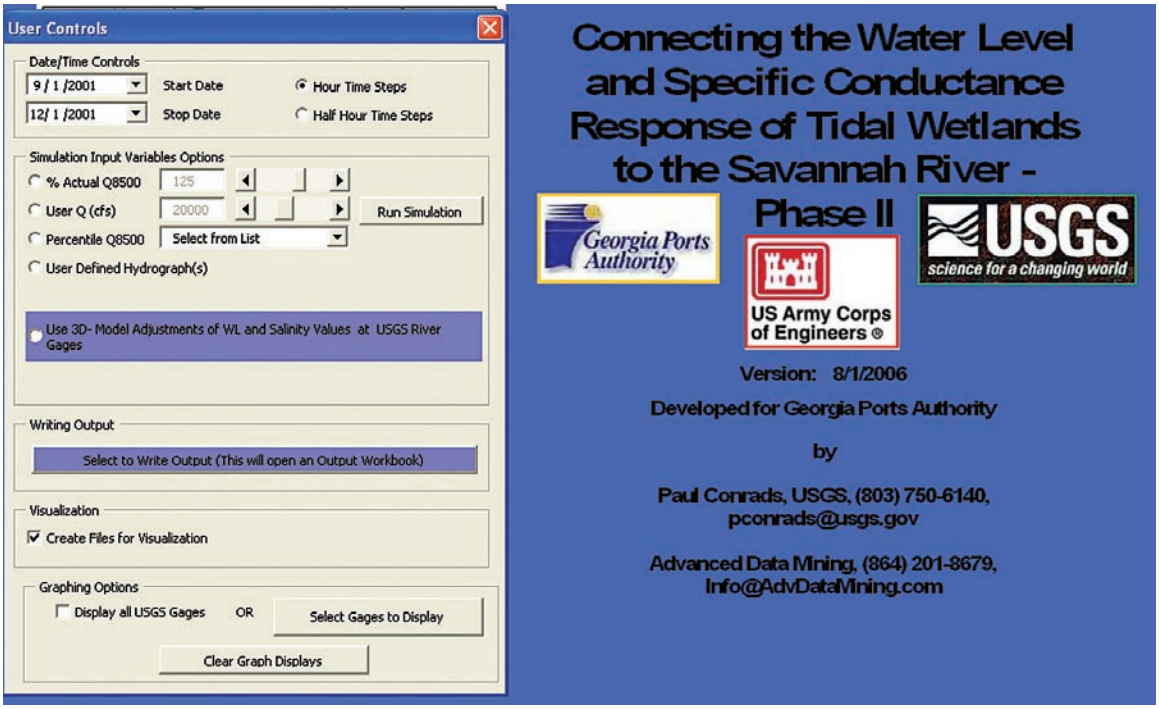

Figure A14. *About* worksheet for M2M visualization application.

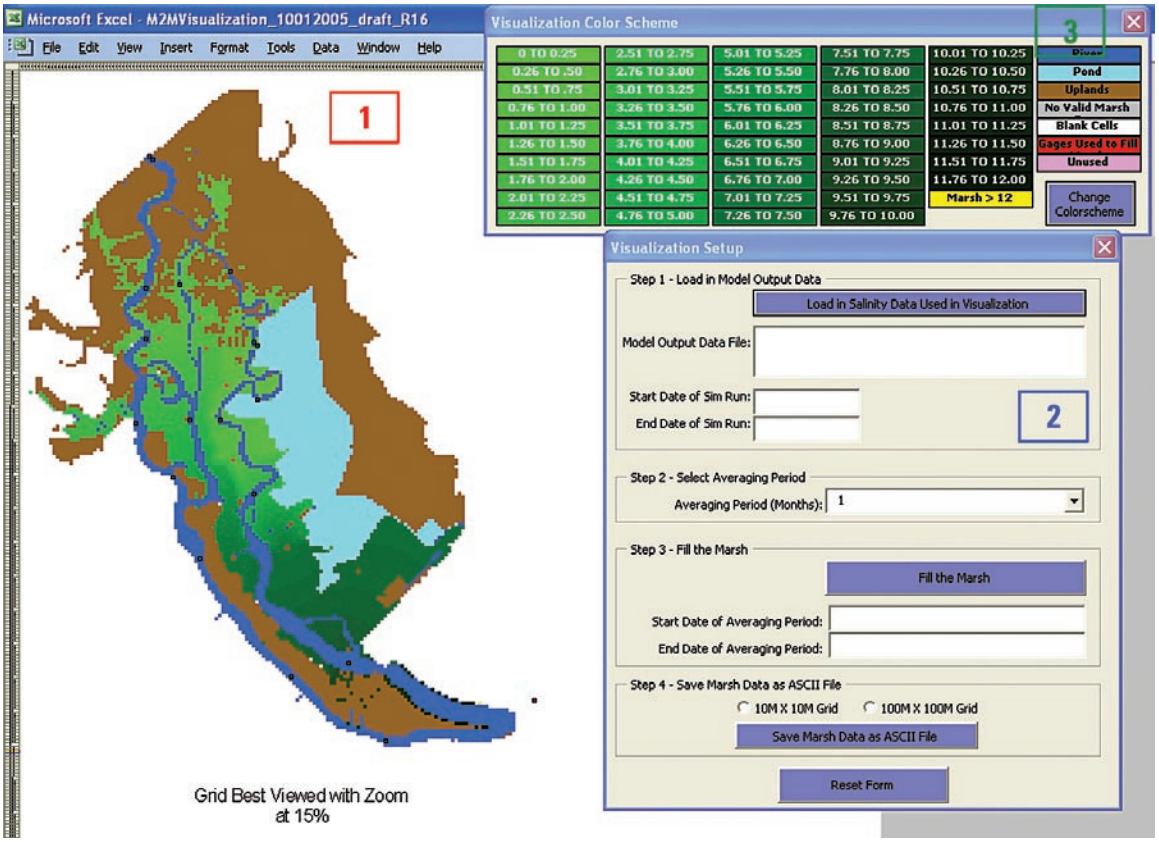

Figure A15. *Visualization* worksheet from M2M application.

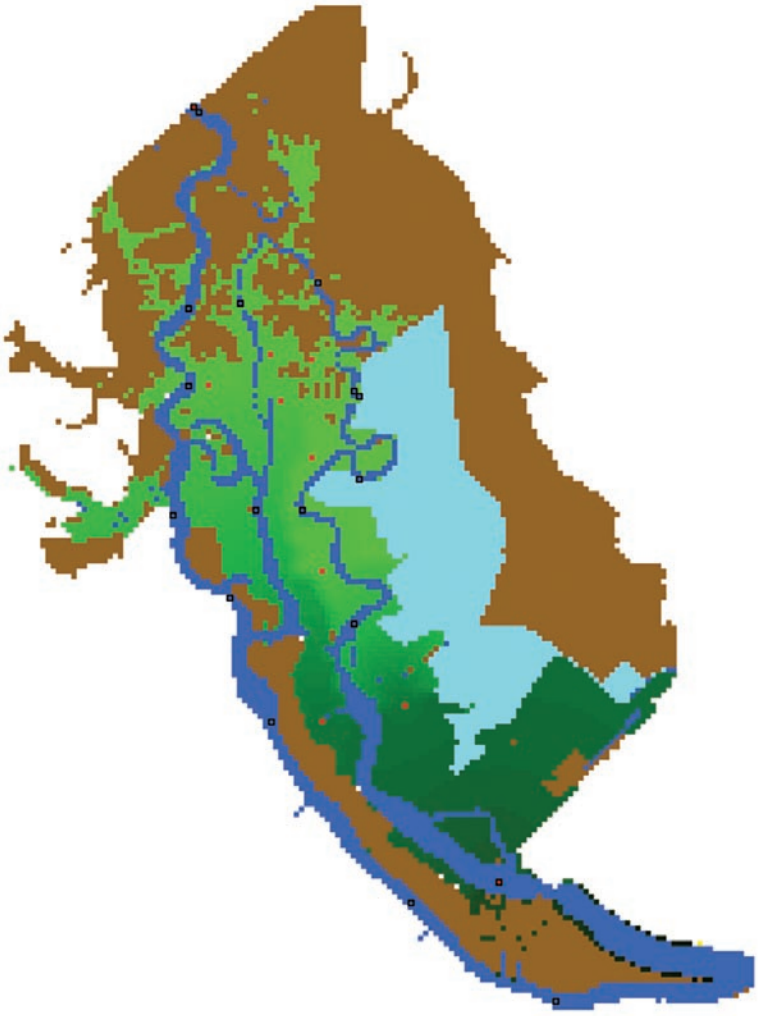

Figure A16. Color gradient of marsh area. Darker shades of green represent increasing salinity concentrations.

7.2.2.2. Step 2—Select Averaging Period

The visualization data contains half-hourly or hourly data created by the model program. This data can be averaged in increments of 1 month up to 1 year or over 2 years. The averaging period to be used for filling is selected using the combo box in step 2.

7.2.2.3. Step 3—Fill the Marsh

Selecting the "Fill the Marsh" command button will compute averages for the gage locations given the selected averaging period. These averages will be used to interpolate the marsh salinity values. The marsh will then be filled with the colorization based on the color scheme used. In the color scheme used in figure A16, the darker green values correlate to higher salinity values. The two text boxes below the "Fill the Marsh" command button are for display only and show the start and end dates of the averaging period.

7.2.2.4. Step 4—Save Marsh Data as ASCII File

To save the marsh data to file, first select either "10M X 10M Grid" or "100M X 100M Grid." Selecting the "Save Marsh Data as ASCII File" command button will then save the filled marsh data. The data can then serve as input for other applications. The format of the saved marsh data is a space-delimited file with six rows of header information defining the grid followed by the data. The header below is for a 10M X 10M grid:

```
ncols,1490
nrows,1950
xllcorner, 957290.6875
yllcorner, 757059.0625
cellsize, 32.80839895
NODATA_value,-9999
<data>
```

Also note that the following constant values are used: 888 = river; 777 = impounded water; 222 = upriver.

7.2.3. *Visualization Color Scheme* UserForm

The *Visualization Color Scheme* UserForm (hereafter called ColorForm) displays the current color scheme for the colorization of the marsh. The values superimposed on the colored cells indicate the use of the color (fig. A18). For example, salinity values of 0–0.25 are colored the lightest green. Any salinity value greater than 12 is colored yellow. The colored cells on the far right indicate the constant colors used in the grid. This color scheme can be changed by selecting the "Change Colorscheme" command button. Selecting this button will take the user to the *ColorScheme* worksheet.

7.3. *ColorScheme* Worksheet

The *ColorScheme* worksheet (fig. A19) is used to change the colors used in the visualization of the marsh pore-water salinity. Excel™ allows 56 colors. The user can assign any desired RGB values to a particular color index.

- Column 2 of the ColorScheme worksheet indicates the color index being assigned. The user cannot change these values.
- Columns 3, 4, and 5 have the red, green, and blue components of the color, respectively. The values used can range from 0 to 255. The user changes these values to change the color scheme.
- Column 6 shows the color setting based on the user RGB values selected.
- Cell 7:2 contains the user-set maximum salinity value. The user enters this value.

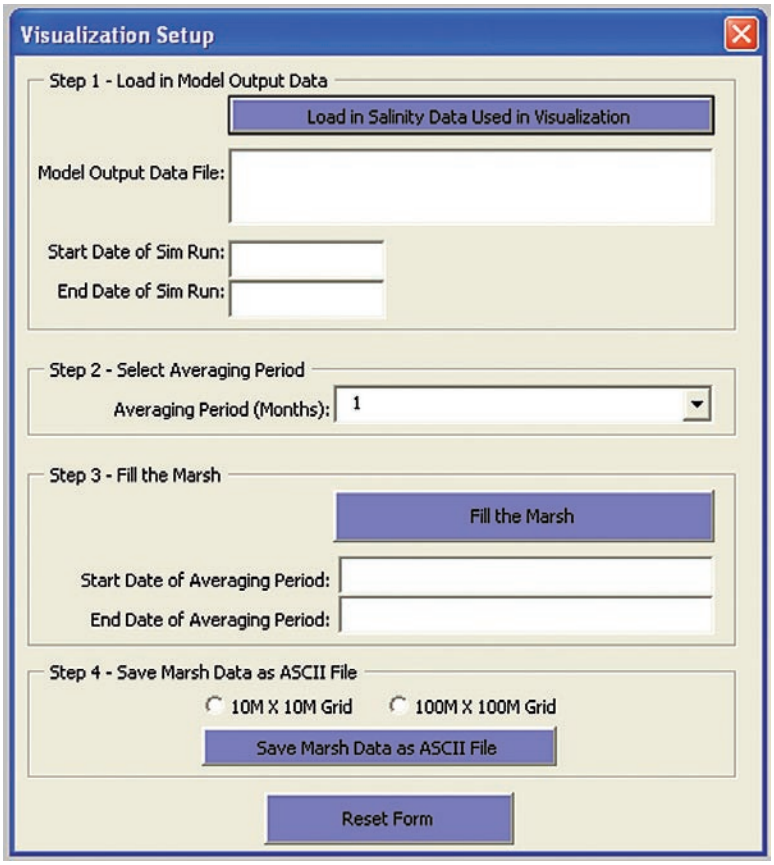

Figure A17. *Visualization Setup* UserForm.

Figure A18. Visualization color scheme UserForm.

7.3.1. Color Values for the Marsh Salinity Levels

In section 1 of figure A19, the user can alter the RGB values for the 49 color indexes used in coloring the marsh. Color index 1 is for the lowest salinity value, and color index 48 is for the maximum salinity value. Any salinity value greater than the maximum set will be colored using color index 49. To determine the salinity values used for color index 2 to color index 47, the total range is divided into 48 equal parcels.

7.3.2. Color Values for Constant Values

In section 2 of figure A19, the colors are selected for constant areas. These defined areas are:

- river, pond (imprisoned water), uplands, no valid marsh data, blank cells, gages used to fill marsh, and 1 unused.

7.3.3. Maximum Salinity Setting

In section 3 of figure A19—specifically cell 7:2 of the worksheet—the user sets the maximum salinity value which is used in creating the color gradients.

7.3.4. Reset the Color Scheme

Selecting the "Reset Color Scheme" command button will update the color index to match the new user settings. The new colors will display in column 6 of the worksheet.

7.4. *Simulation Data* Worksheet

The *Simulation Data* worksheet (fig. A20) contains the data read in from the visualization file.

7.5. Original Colorscheme Worksheet

This worksheet contains the original colorscheme and is read only. To restore the original scheme, the user can copy and paste the values from this worksheet onto the *ColorScheme* worksheet.

7.6. *Revision Control* Worksheet

The *Revision Control* worksheet notes each revision and its changes.

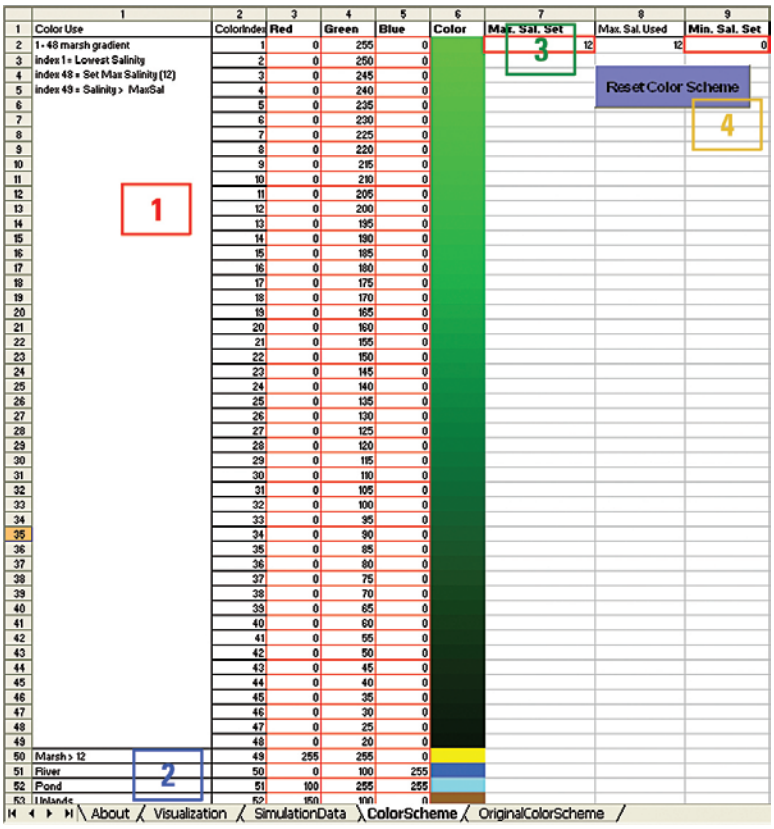

Figure A19. *ColorScheme* worksheet.

	1	2	3	4	5	6	7	8	9	10	11
1	DATETIME	ROW	Q8500	Q8500A	Q8500-user	WL8980	XWL8980	Sal8840	Sal8840-predactualactual	dSal8840(pred-user)	Sal8840-user
2	1/1/2002	1	5670	5713.709961	7740	-0.280000001	8.127500534	0.051247172	0.062448699	0.009117066	0.042130105
3	1/1/2002 1:00	3	5662	5706.1	7733.75	-2.109999895	8.240000725	0.048619405	0.057799461	0.009509987	0.039109416
4	1/1/2002 2:00	5	5662	5698.62	7727.5	-3.630000114	8.352500916	0.048619405	0.053164087	0.009472686	0.03914652
5	1/1/2002 3:00	7	5647	5691.29	7721.25	-4.400000095	8.465001106	0.048182335	0.053761111	0.009339521	0.038842812
6	1/1/2002 4:00	9	5647	5684.12	7715	-3.559999943	8.577501297	0.048182335	0.056106812	0.009061083	0.039121252
7	1/1/2002 5:00	11	5647	5677.12	7708.75	-1.769999981	8.690001488	0.047745524	0.057589566	0.008886621	0.038858905
8	1/1/2002 6:00	13	5640	5670.29	7702.5	0.370000005	8.802501678	0.048182335	0.057490681	0.008900477	0.039281856
9	1/1/2002 7:00	15	5632	5663.65	7696.25	2.599999905	8.915001869	0.048182335	0.056532614	0.009017611	0.039164726
10	1/1/2002 8:00	17	5625	5657.19	7690	4.090000153	9.02750206	0.049932155	0.057084997	0.008958422	0.040973734
11	1/1/2002 9:00	19	5617	5650.92	7683.75	4.739999771	9.140000343	0.056087506	0.059284067	0.008705749	0.047381755
12	1/1/2002 10:00	21	5609	5644.85	7677.5	4.650000095	9.039999962	0.063621584	0.060857221	0.008537164	0.055084415
13	1/1/2002 11:00	23	5602	5638.99	7671.25	3.50999999	8.93999958	0.071663164	0.061460733	0.009221225	0.062441938
14	1/1/2002 12:00	25	5602	5633.35	7665	2.00999999	8.839999199	0.067187854	0.079668316	0.014295464	0.052892391
15	1/1/2002 13:00	27	5594	5627.93	7658.75	0.209999993	8.739998817	0.054764591	0.091489297	0.01828481	0.036479782
16	1/1/2002 14:00	29	5587	5622.74	7652.5	-1.75	8.639998436	0.048619405	0.061446846	0.012018203	0.036601201

Figure A20. *Simulation data* worksheet.

Appendix A

The Output workbook will consist of two or more worksheets (*RiverOutput* worksheet and *MarshOutput* worksheet. The USGS and GPA river data are found on the *RiverOutput* worksheet and the USGS and GPA Marsh Data on the *MarshOutput* worksheet. If more data is collected than will fit on one worksheet (limit is 65,536 rows of data), additional worksheets will be created as needed.

The Output workbook will contain the following information for each gage modeled:

- actual (or historical) value,
- predicted actual value (predicted output using historical Clyo flow),
- predicted-user (predicted delta due to user set flows or EFDC adjustments), and
- user value (predicted user value calculated by offsetting the historical value [or predicted actual if historical not available] by the delta calculated by taking the difference of actual and user predictions).

RiverOutput worksheet

Color Explanation	
Actual (historical) data	
Predicted (predicted using actual flow conditions)	
Difference (predicted actual – predicted user)	
User (predicted using user flow conditions or EFDC deltas)	

Column heading	Heading description
DATETIME	Simulation Date and Time
ROW	Row Number in Historical Data File
Q8500	Actual flow at Clyo
Q8500A	Filtered Actual Flow at Clyo
Q8500-user	User Set Flow
WL8980	Water Level at Fort Pulaski
XWL8980	Tidal Range
Sal8840	Actual Salinity
Sal8840-predactualactual	Predicted Salinity Using Actual Flow
dSal8840(pred-user)	Difference Between Predicted and User Values
Sal8840-user	Predicted Salinity Using User Set Flow
WL8840	Actual Water Level
WL8840-predactualactual	Predicted Water Level Using Actual Flow
dWL8840(pred-user)	Predicted Water Level Using User Set Flow
WL8840-user	Difference Between Predicted and User Values
Sal8920	Actual Salinity
Sal8920-predactual	Predicted Salinity Using Actual Flow
dSal8920(pred-user)	Difference Between Predicted and User Values
Sal8920-user	Predicted Salinity Using User Set Flow
WL8920	Actual Water Level
WL8920-predactual	Predicted Water Level Using Actual Flow
dWL8920(pred-user)	Predicted Water Level Using User Set Flow
WL8920-user	Difference Between Predicted and User Values
Sal89784	Actual Salinity
Sal89784-predactual	Predicted Salinity Using Actual Flow

***RiverOutput* worksheet—Continued**

Color Explanation	
Actual (historical) data	
Predicted (predicted using actual flow conditions)	
Difference (predicted actual – predicted user)	
User (predicted using user flow conditions or EFDC deltas)	

Column heading	Heading description
dSal89784(pred-user)	Difference Between Predicted and User Values
Sal89784-user	Predicted Salinity Using User Set Flow
Sal89791	Actual Salinity
Sal89791-predactual	Predicted Salinity Using Actual Flow
dSal89791(pred-user)	Difference Between Predicted and User Values
Sal89791-user	Predicted Salinity Using User Set Flow
WL8979	Actual Water Level
WL8979-predactual	Predicted Water Level Using Actual Flow
dWL8979(pred-user)	Predicted Water Level Using User Set Flow
WL8979-user	Difference Between Predicted and User Values
WL8977	Actual Water Level
WL8977-predactual	Predicted Water Level Using Actual Flow
dWL8977(pred-user)	Predicted Water Level Using User Set Flow
WL8977-user	Difference Between Predicted and User Values
WLGPA04	Actual Water Level
WLGPA04-predactual	Predicted Water Level Using Actual Flow
dWLGPA04(pred-user)	Predicted Water Level Using User Set Flow
WLGPA04-user	Difference Between Predicted and User Values
WLGPA05	Actual Water Level
WLGPA05-predactual	Predicted Water Level Using Actual Flow
dWLGPA05(pred-user)	Predicted Water Level Using User Set Flow
WLGPA05-user	Difference Between Predicted and User Values
WLGPA06	Actual Water Level
WLGPA06-predactual	Predicted Water Level Using Actual Flow
dWLGPA06(pred-user)	Predicted Water Level Using User Set Flow
WLGPA06-user	Difference Between Predicted and User Values
WLGPA07	Actual Water Level
WLGPA07-predactual	Predicted Water Level Using Actual Flow
dWLGPA07(pred-user)	Predicted Water Level Using User Set Flow
WLGPA07-user	Difference Between Predicted and User Values
WLGPA08	Actual Water Level
WLGPA08-predactual	Predicted Water Level Using Actual Flow
dWLGPA08(pred-user)	Predicted Water Level Using User Set Flow
WLGPA08-user	Difference Between Predicted and User Values

***RiverOutput* worksheet—Continued**

Color Explanation	
Actual (historical) data	
Predicted (predicted using actual flow conditions)	
Difference (predicted actual – predicted user)	
User (predicted using user flow conditions or EFDC deltas)	

Column heading	Heading description
WLGPA09	Actual Water Level
WLGPA09-predactual	Predicted Water Level Using Actual Flow
dWLGPA09(pred-user)	Predicted Water Level Using User Set Flow
WLGPA09-user	Difference Between Predicted and User Values
WLGPA10	Actual Water Level
WLGPA10-predactual	Predicted Water Level Using Actual Flow
dWLGPA10(pred-user)	Predicted Water Level Using User Set Flow
WLGPA10-user	Difference Between Predicted and User Values
WLGPA11	Actual Water Level
WLGPA11-predactual	Predicted Water Level Using Actual Flow
dWLGPA11(pred-user)	Predicted Water Level Using User Set Flow
WLGPA11-user	Difference Between Predicted and User Values
WLGPA11R	Actual Water Level
WLGPA11R-predactual	Predicted Water Level Using Actual Flow
dWLGPA11R(pred-user)	Predicted Water Level Using User Set Flow
WLGPA11R-user	Difference Between Predicted and User Values
WLGPA12	Actual Water Level
WLGPA12-predactual	Predicted Water Level Using Actual Flow
dWLGPA12(pred-user)	Predicted Water Level Using User Set Flow
WLGPA12-user	Difference Between Predicted and User Values
WLGPA13	Actual Water Level
WLGPA13-predactual	Predicted Water Level Using Actual Flow
dWLGPA13(pred-user)	Predicted Water Level Using User Set Flow
WLGPA13-user	Difference Between Predicted and User Values
WLGPA14	Actual Water Level
WLGPA14-predactual	Predicted Water Level Using Actual Flow
dWLGPA14(pred-user)	Predicted Water Level Using User Set Flow
WLGPA14-user	Difference Between Predicted and User Values
WLGPA21	Actual Water Level
WLGPA21-predactual	Predicted Water Level Using Actual Flow
dWLGPA21(pred-user)	Predicted Water Level Using User Set Flow
WLGPA21-user	Difference Between Predicted and User Values
WLGPA22	Actual Water Level
WLGPA22-predactual	Predicted Water Level Using Actual Flow

***RiverOutput* worksheet—Continued**

Color Explanation	
Actual (historical) data	
Predicted (predicted using actual flow conditions)	
Difference (predicted actual – predicted user)	
User (predicted using user flow conditions or EFDC deltas)	

Column heading	Heading description
dWLGPA22(pred-user)	Predicted Water Level Using User Set Flow
WLGPA22-user	Difference Between Predicted and User Values
WLGPA23M	Actual Water Level
WLGPA23M-predactual	Predicted Water Level Using Actual Flow
dWLGPA23M(pred-user)	Predicted Water Level Using User Set Flow
WLGPA23M-user	Difference Between Predicted and User Values
WLGPA24M	Actual Water Level
WLGPA24M-predactual	Predicted Water Level Using Actual Flow
dWLGPA24M(pred-user)	Predicted Water Level Using User Set Flow
WLGPA24M-user	Difference Between Predicted and User Values
WLGPA25M	Actual Water Level
WLGPA25M-predactual	Predicted Water Level Using Actual Flow
dWLGPA25M(pred-user)	Predicted Water Level Using User Set Flow
WLGPA25M-user	Difference Between Predicted and User Values
WLGPA26	Actual Water Level
WLGPA26-predactual	Predicted Water Level Using Actual Flow
dWLGPA26(pred-user)	Predicted Water Level Using User Set Flow
WLGPA26-user	Difference Between Predicted and User Values
SalGPA04B	Actual Salinity
SalGPA04B-predactual	Predicted Salinity Using Actual Flow
dSalGPA04B(pred-user)	Difference Between Predicted and User Values
SalGPA04B-user	Predicted Salinity Using User Set Flow
SalGPA04S	Actual Salinity
SalGPA04S-predactual	Predicted Salinity Using Actual Flow
dSalGPA04S(pred-user)	Difference Between Predicted and User Values
SalGPA04S-user	Predicted Salinity Using User Set Flow
SalGPA05B	Actual Salinity
SalGPA05B-predactual	Predicted Salinity Using Actual Flow
dSalGPA05B(pred-user)	Difference Between Predicted and User Values
SalGPA05B-user	Predicted Salinity Using User Set Flow
SalGPA06B	Actual Salinity
SalGPA06B-predactual	Predicted Salinity Using Actual Flow
dSalGPA06B(pred-user)	Difference Between Predicted and User Values
SalGPA06B-user	Predicted Salinity Using User Set Flow

***RiverOutput* worksheet—Continued**

Color Explanation	
Actual (historical) data	
Predicted (predicted using actual flow conditions)	
Difference (predicted actual – predicted user)	
User (predicted using user flow conditions or EFDC deltas)	

Column heading	Heading description
SalGPA06S	Actual Salinity
SalGPA06S-predactual	Predicted Salinity Using Actual Flow
dSalGPA06S(pred-user)	Difference Between Predicted and User Values
SalGPA06S-user	Predicted Salinity Using User Set Flow
SalGPA07B	Actual Salinity
SalGPA07B-predactual	Predicted Salinity Using Actual Flow
dSalGPA07B(pred-user)	Difference Between Predicted and User Values
SalGPA07B-user	Predicted Salinity Using User Set Flow
SalGPA07S	Actual Salinity
SalGPA07S-predactual	Predicted Salinity Using Actual Flow
dSalGPA07S(pred-user)	Difference Between Predicted and User Values
SalGPA07S-user	Predicted Salinity Using User Set Flow
SalGPA08B	Actual Salinity
SalGPA08B-predactual	Predicted Salinity Using Actual Flow
dSalGPA08B(pred-user)	Difference Between Predicted and User Values
SalGPA08B-user	Predicted Salinity Using User Set Flow
SalGPA08S	Actual Salinity
SalGPA08S-predactual	Predicted Salinity Using Actual Flow
dSalGPA08S(pred-user)	Difference Between Predicted and User Values
SalGPA08S-user	Predicted Salinity Using User Set Flow
SalGPA09B	Actual Salinity
SalGPA09B-predactual	Predicted Salinity Using Actual Flow
dSalGPA09B(pred-user)	Difference Between Predicted and User Values
SalGPA09B-user	Predicted Salinity Using User Set Flow
SalGPA09S	Actual Salinity
SalGPA09S-predactual	Predicted Salinity Using Actual Flow
dSalGPA09S(pred-user)	Difference Between Predicted and User Values
SalGPA09S-user	Predicted Salinity Using User Set Flow
SalGPA10B	Actual Salinity
SalGPA10B-predactual	Predicted Salinity Using Actual Flow
dSalGPA10B(pred-user)	Difference Between Predicted and User Values
SalGPA10B-user	Predicted Salinity Using User Set Flow
SalGPA10S	Actual Salinity
SalGPA10S-predactual	Predicted Salinity Using Actual Flow

***RiverOutput* worksheet—Continued**

Color Explanation	
Actual (historical) data	
Predicted (predicted using actual flow conditions)	
Difference (predicted actual – predicted user)	
User (predicted using user flow conditions or EFDC deltas)	

Column heading	Heading description
dSalGPA10S(pred-user)	Difference Between Predicted and User Values
SalGPA10S-user	Predicted Salinity Using User Set Flow
SalGPA11B	Actual Salinity
SalGPA11B-predactual	Predicted Salinity Using Actual Flow
dSalGPA11B(pred-user)	Difference Between Predicted and User Values
SalGPA11B-user	Predicted Salinity Using User Set Flow
SalGPA11RB	Actual Salinity
SalGPA11RB-predactual	Predicted Salinity Using Actual Flow
dSalGPA11RB(pred-user)	Difference Between Predicted and User Values
SalGPA11RB-user	Predicted Salinity Using User Set Flow
SalGPA12B	Actual Salinity
SalGPA12B-predactual	Predicted Salinity Using Actual Flow
dSalGPA12B(pred-user)	Difference Between Predicted and User Values
SalGPA12B-user	Predicted Salinity Using User Set Flow
SalGPA12RS	Actual Salinity
SalGPA12RS-predactual	Predicted Salinity Using Actual Flow
dSalGPA12RS(pred-user)	Difference Between Predicted and User Values
SalGPA12RS-user	Predicted Salinity Using User Set Flow
SalGPA13B	Actual Salinity
SalGPA13B-predactual	Predicted Salinity Using Actual Flow
dSalGPA13B(pred-user)	Difference Between Predicted and User Values
SalGPA13B-user	Predicted Salinity Using User Set Flow
SalGPA14B	Actual Salinity
SalGPA14B-predactual	Predicted Salinity Using Actual Flow
dSalGPA14B(pred-user)	Difference Between Predicted and User Values
SalGPA14B-user	Predicted Salinity Using User Set Flow
SalGPA15S	Actual Salinity
SalGPA15S-predactual	Predicted Salinity Using Actual Flow
dSalGPA15S(pred-user)	Difference Between Predicted and User Values
SalGPA15S-user	Predicted Salinity Using User Set Flow
SalGPA21B	Actual Salinity
SalGPA21B-predactual	Predicted Salinity Using Actual Flow
dSalGPA21B(pred-user)	Difference Between Predicted and User Values
SalGPA21B-user	Predicted Salinity Using User Set Flow

***RiverOutput* worksheet—Continued**

Color Explanation	
Actual (historical) data	
Predicted (predicted using actual flow conditions)	
Difference (predicted actual – predicted user)	
User (predicted using user flow conditions or EFDC deltas)	

Column heading	Heading description
SalGPA21S	Actual Salinity
SalGPA21S-predactual	Predicted Salinity Using Actual Flow
dSalGPA21S(pred-user)	Difference Between Predicted and User Values
SalGPA21S-user	Predicted Salinity Using User Set Flow
SalGPA22B	Actual Salinity
SalGPA22B-predactual	Predicted Salinity Using Actual Flow
dSalGPA22B(pred-user)	Difference Between Predicted and User Values
SalGPA22B-user	Predicted Salinity Using User Set Flow
SalGPA22S	Actual Salinity
SalGPA22S-predactual	Predicted Salinity Using Actual Flow
dSalGPA22S(pred-user)	Difference Between Predicted and User Values
SalGPA22S-user	Predicted Salinity Using User Set Flow

***MarshOutput* worksheet**

Color Explanation	
Actual (historical) data	
Predicted (predicted using actual flow conditions)	
Difference (predicted actual – predicted user)	
User (predicted using user flow conditions or EFDC deltas)	

Column heading	Heading description
DATETIME	Simulation Date and Time
ROW	Row Number in Historical Data File
S1CANALWL	Actual Water Level
S1CANALWL-predactualactual	Predicted Water Level Using Actual Flow
dS1CANALWL(pred-user)	Predicted Water Level Using User Set Flow
S1CANALWL-user	Difference Between Predicted and User Values
S1MARSHWLAT	Actual Water Level
S1MARSHWLAT-predactual	Predicted Water Level Using Actual Flow
dS1MARSHWLAT(pred-user)	Predicted Water Level Using User Set Flow
S1MARSHWLAT-user	Difference Between Predicted and User Values
S1MARSHWL	Actual Water Level

***MarshOutput* worksheet—Continued**

Color Explanation	
Actual (historical) data	
Predicted (predicted using actual flow conditions)	
Difference (predicted actual – predicted user)	
User (predicted using user flow conditions or EFDC deltas)	

Column heading	Heading description
S1MARSHWL-predactual	Predicted Water Level Using Actual Flow
dS1MARSHWL(pred-user)	Predicted Water Level Using User Set Flow
S1MARSHWL-user	Difference Between Predicted and User Values
S2CANALWL	Actual Water Level
S2CANALWL-predactual	Predicted Water Level Using Actual Flow
dS2CANALWL(pred-user)	Predicted Water Level Using User Set Flow
S2CANALWL-user	Difference Between Predicted and User Values
S2MARSHWL	Actual Water Level
S2MARSHWL-predactual	Predicted Water Level Using Actual Flow
dS2MARSHWL(pred-user)	Predicted Water Level Using User Set Flow
S2MARSHWL-user	Difference Between Predicted and User Values
S3CANALWL	Actual Water Level
S3CANALWL-predactual	Predicted Water Level Using Actual Flow
dS3CANALWL(pred-user)	Predicted Water Level Using User Set Flow
S3CANALWL-user	Difference Between Predicted and User Values
S3MARSHWL	Actual Water Level
S3MARSHWL-predactual	Predicted Water Level Using Actual Flow
dS3MARSHWL(pred-user)	Predicted Water Level Using User Set Flow
S3MARSHWL-user	Difference Between Predicted and User Values
S4CANALWL	Actual Water Level
S4CANALWL-predactual	Predicted Water Level Using Actual Flow
dS4CANALWL(pred-user)	Predicted Water Level Using User Set Flow
S4CANALWL-user	Difference Between Predicted and User Values
S4MARSHWL	Actual Water Level
S4MARSHWL-predactual	Predicted Water Level Using Actual Flow
dS4MARSHWL(pred-user)	Predicted Water Level Using User Set Flow
S4MARSHWL-user	Difference Between Predicted and User Values
S5CANALWL	Actual Water Level
S5CANALWL-predactual	Predicted Water Level Using Actual Flow
dS5CANALWL(pred-user)	Predicted Water Level Using User Set Flow
S5CANALWL-user	Difference Between Predicted and User Values
S5MARSHWL	Actual Water Level
S5MARSHWL-predactual	Predicted Water Level Using Actual Flow
dS5MARSHWL(pred-user)	Predicted Water Level Using User Set Flow

***MarshOutput* worksheet—Continued**

Color Explanation	
Actual (historical) data	
Predicted (predicted using actual flow conditions)	
Difference (predicted actual – predicted user)	
User (predicted using user flow conditions or EFDC deltas)	

Column heading	Heading description
S5MARSHWL-user	Difference Between Predicted and User Values
S6CANALWL	Actual Water Level
S6CANALWL-predactual	Predicted Water Level Using Actual Flow
dS6CANALWL(pred-user)	Predicted Water Level Using User Set Flow
S6CANALWL-user	Difference Between Predicted and User Values
S6MARSHWL	Actual Water Level
S6MARSHWL-predactual	Predicted Water Level Using Actual Flow
dS6MARSHWL(pred-user)	Predicted Water Level Using User Set Flow
S6MARSHWL-user	Difference Between Predicted and User Values
S6MARSHWLAT	Actual Water Level
S6MARSHWLAT-predactual	Predicted Water Level Using Actual Flow
dS6MARSHWLAT(pred-user)	Predicted Water Level Using User Set Flow
S6MARSHWLAT-user	Difference Between Predicted and User Values
S7CANALWL	Actual Water Level
S7CANALWL-predactual	Predicted Water Level Using Actual Flow
dS7CANALWL(pred-user)	Predicted Water Level Using User Set Flow
S7CANALWL-user	Difference Between Predicted and User Values
S7MARSHWL	Actual Water Level
S7MARSHWL-predactual	Predicted Water Level Using Actual Flow
dS7MARSHWL(pred-user)	Predicted Water Level Using User Set Flow
S7MARSHWL-user	Difference Between Predicted and User Values
S8CANALWL	Actual Water Level
S8CANALWL-predactual	Predicted Water Level Using Actual Flow
dS8CANALWL(pred-user)	Predicted Water Level Using User Set Flow
S8CANALWL-user	Difference Between Predicted and User Values
S9CANALWL	Actual Water Level
S9CANALWL-predactual	Predicted Water Level Using Actual Flow
dS9CANALWL(pred-user)	Predicted Water Level Using User Set Flow
S9CANALWL-user	Difference Between Predicted and User Values
S9MARSHWL	Actual Water Level
S9MARSHWL-predactual	Predicted Water Level Using Actual Flow
dS9MARSHWL(pred-user)	Predicted Water Level Using User Set Flow
S9MARSHWL-user	Difference Between Predicted and User Values
S10CANALWL	Actual Water Level

***MarshOutput* worksheet—Continued**

Color Explanation	
Actual (historical) data	
Predicted (predicted using actual flow conditions)	
Difference (predicted actual – predicted user)	
User (predicted using user flow conditions or EFDC deltas)	

Column heading	Heading description
S10CANALWL-predactual	Predicted Water Level Using Actual Flow
dS10CANALWL(pred-user)	Predicted Water Level Using User Set Flow
S10CANALWL-user	Difference Between Predicted and User Values
S10MARSHWL	Actual Water Level
S10MARSHWL-predactual	Predicted Water Level Using Actual Flow
dS10MARSHWL(pred-user)	Predicted Water Level Using User Set Flow
S10MARSHWL-user	Difference Between Predicted and User Values
S1CANALSC	Actual Salinity
S1CANALSC-predactual	Predicted Salinity Using Actual Flow
dS1CANALSC(pred-user)	Difference Between Predicted and User Values
S1CANALSC-user	Predicted Salinity Using User Set Flow
S1MARSHSC	Actual Salinity
S1MARSHSC-predactual	Predicted Salinity Using Actual Flow
dS1MARSHSC(pred-user)	Difference Between Predicted and User Values
S1MARSHSC-user	Predicted Salinity Using User Set Flow
S2CANALSC	Actual Salinity
S2CANALSC-predactual	Predicted Salinity Using Actual Flow
dS2CANALSC(pred-user)	Difference Between Predicted and User Values
S2CANALSC-user	Predicted Salinity Using User Set Flow
S2MARSHSC	Actual Salinity
S2MARSHSC-predactual	Predicted Salinity Using Actual Flow
dS2MARSHSC(pred-user)	Difference Between Predicted and User Values
S2MARSHSC-user	Predicted Salinity Using User Set Flow
S3CANALSC	Actual Salinity
S3CANALSC-predactual	Predicted Salinity Using Actual Flow
dS3CANALSC(pred-user)	Difference Between Predicted and User Values
S3CANALSC-user	Predicted Salinity Using User Set Flow
S3MARSHSC	Actual Salinity
S3MARSHSC-predactual	Predicted Salinity Using Actual Flow
dS3MARSHSC(pred-user)	Difference Between Predicted and User Values
S3MARSHSC-user	Predicted Salinity Using User Set Flow
S4CANALSC	Actual Salinity
S4CANALSC-predactual	Predicted Salinity Using Actual Flow
dS4CANALSC(pred-user)	Difference Between Predicted and User Values

***MarshOutput* worksheet—Continued**

Color Explanation	
Actual (historical) data	
Predicted (predicted using actual flow conditions)	
Difference (predicted actual – predicted user)	
User (predicted using user flow conditions or EFDC deltas)	

Column heading	Heading description
S4CANALSC-user	Predicted Salinity Using User Set Flow
S4MARSHSC	Actual Salinity
S4MARSHSC-predactual	Predicted Salinity Using Actual Flow
dS4MARSHSC(pred-user)	Difference Between Predicted and User Values
S4MARSHSC-user	Predicted Salinity Using User Set Flow
S5CANALSC	Actual Salinity
S5CANALSC-predactual	Predicted Salinity Using Actual Flow
dS5CANALSC(pred-user)	Difference Between Predicted and User Values
S5CANALSC-user	Predicted Salinity Using User Set Flow
S5MARSHSC	Actual Salinity
S5MARSHSC-predactual	Predicted Salinity Using Actual Flow
dS5MARSHSC(pred-user)	Difference Between Predicted and User Values
S5MARSHSC-user	Predicted Salinity Using User Set Flow
S6CANALSC	Actual Salinity
S6CANALSC-predactual	Predicted Salinity Using Actual Flow
dS6CANALSC(pred-user)	Difference Between Predicted and User Values
S6CANALSC-user	Predicted Salinity Using User Set Flow
S6MARSHSC	Actual Salinity
S6MARSHSC-predactual	Predicted Salinity Using Actual Flow
dS6MARSHSC(pred-user)	Difference Between Predicted and User Values
S6MARSHSC-user	Predicted Salinity Using User Set Flow
S7CANALSC	Actual Salinity
S7CANALSC-predactual	Predicted Salinity Using Actual Flow
dS7CANALSC(pred-user)	Difference Between Predicted and User Values
S7CANALSC-user	Predicted Salinity Using User Set Flow
S7MARSHSC	Actual Salinity
S7MARSHSC-predactual	Predicted Salinity Using Actual Flow
dS7MARSHSC(pred-user)	Difference Between Predicted and User Values
S7MARSHSC-user	Predicted Salinity Using User Set Flow
S7MARSHPWSC	Actual Salinity
S7MARSHPWSC-predactual	Predicted Salinity Using Actual Flow
dS7MARSHPWSC(pred-user)	Difference Between Predicted and User Values
S7MARSHPWSC-user	Predicted Salinity Using User Set Flow
S8CANALSC	Actual Salinity

***MarshOutput* worksheet—Continued**

Color Explanation	
Actual (historical) data	
Predicted (predicted using actual flow conditions)	
Difference (predicted actual – predicted user)	
User (predicted using user flow conditions or EFDC deltas)	

Column heading	Heading description
S8CANALSC-predactual	Predicted Salinity Using Actual Flow
dS8CANALSC(pred-user)	Difference Between Predicted and User Values
S8CANALSC-user	Predicted Salinity Using User Set Flow
S9CANALSC	Actual Salinity
S9CANALSC-predactual	Predicted Salinity Using Actual Flow
dS9CANALSC(pred-user)	Difference Between Predicted and User Values
S9CANALSC-user	Predicted Salinity Using User Set Flow
S9MARSHSWSC	Actual Salinity
S9MARSHSWSC-predactual	Predicted Salinity Using Actual Flow
dS9MARSHSWSC(pred-user)	Difference Between Predicted and User Values
S9MARSHSWSC-user	Predicted Salinity Using User Set Flow
S9MARSHPWSC	Actual Salinity
S9MARSHPWSC-predactual	Predicted Salinity Using Actual Flow
dS9MARSHPWSC(pred-user)	Difference Between Predicted and User Values
S9MARSHPWSC-user	Predicted Salinity Using User Set Flow
S10MARSHSWSC	Actual Salinity
S10MARSHSWSC-predactual	Predicted Salinity Using Actual Flow
dS10MARSHSWSC(pred-user)	Difference Between Predicted and User Values
S10MARSHSWSC-user	Predicted Salinity Using User Set Flow
S10MARSHPWSC	Actual Salinity
S10MARSHPWSC-predactual	Predicted Salinity Using Actual Flow
dS10MARSHPWSC(pred-user)	Difference Between Predicted and User Values
S10MARSHPWSC-user	Predicted Salinity Using User Set Flow
B1MWL	Actual Water Level
B1MWL-predactual	Predicted Water Level Using Actual Flow
dB1MWL(pred-user)	Predicted Water Level Using User Set Flow
B1MWL-user	Difference Between Predicted and User Values
B2MWL	Actual Water Level
B2MWL-predactual	Predicted Water Level Using Actual Flow
dB2MWL(pred-user)	Predicted Water Level Using User Set Flow
B2MWL-user	Difference Between Predicted and User Values
B3MWL	Actual Water Level
B3MWL-predactual	Predicted Water Level Using Actual Flow
dB3MWL(pred-user)	Predicted Water Level Using User Set Flow

***MarshOutput* worksheet—Continued**

Color Explanation	
Actual (historical) data	
Predicted (predicted using actual flow conditions)	
Difference (predicted actual – predicted user)	
User (predicted using user flow conditions or EFDC deltas)	

Column heading	Heading description
B3MWL-user	Difference Between Predicted and User Values
B4MWL	Actual Water Level
B4MWL-predactual	Predicted Water Level Using Actual Flow
dB4MWL(pred-user)	Predicted Water Level Using User Set Flow
B4MWL-user	Difference Between Predicted and User Values
F1MWL	Actual Water Level
F1MWL-predactual	Predicted Water Level Using Actual Flow
dF1MWL(pred-user)	Predicted Water Level Using User Set Flow
F1MWL-user	Difference Between Predicted and User Values
M1MWL	Actual Water Level
M1MWL-predactual	Predicted Water Level Using Actual Flow
dM1MWL(pred-user)	Predicted Water Level Using User Set Flow
M1MWL-user	Difference Between Predicted and User Values
M2MWL	Actual Water Level
M2MWL-predactual	Predicted Water Level Using Actual Flow
dM2MWL(pred-user)	Predicted Water Level Using User Set Flow
M2MWL-user	Difference Between Predicted and User Values
B1MSC	Actual Salinity
B1MSC-predactual	Predicted Salinity Using Actual Flow
dB1MSC(pred-user)	Difference Between Predicted and User Values
B1MSC-user	Predicted Salinity Using User Set Flow
B2MSC	Actual Salinity
B2MSC-predactual	Predicted Salinity Using Actual Flow
dB2MSC(pred-user)	Difference Between Predicted and User Values
B2MSC-user	Predicted Salinity Using User Set Flow
B3MSC	Actual Salinity
B3MSC-predactual	Predicted Salinity Using Actual Flow
dB3MSC(pred-user)	Difference Between Predicted and User Values
B3MSC-user	Predicted Salinity Using User Set Flow
B4MSC	Actual Salinity
B4MSC-predactual	Predicted Salinity Using Actual Flow
dB4MSC(pred-user)	Difference Between Predicted and User Values
B4MSC-user	Predicted Salinity Using User Set Flow
F1MSC	Actual Salinity

***MarshOutput* worksheet—Continued**

Color Explanation	
Actual (historical) data	
Predicted (predicted using actual flow conditions)	
Difference (predicted actual – predicted user)	
User (predicted using user flow conditions or EFDC deltas)	

Column heading	Heading description
F1MSC-predactual	Predicted Salinity Using Actual Flow
dF1MSC(pred-user)	Difference Between Predicted and User Values
F1MSC-user	Predicted Salinity Using User Set Flow
M1MSC	Actual Salinity
M1MSC-predactual	Predicted Salinity Using Actual Flow
dM1MSC(pred-user)	Difference Between Predicted and User Values
M1MSC-user	Predicted Salinity Using User Set Flow
M2MSC	Actual Salinity
M2MSC-predactual	Predicted Salinity Using Actual Flow
dM2MSC(pred-user)	Difference Between Predicted and User Values
M2MSC-user	Predicted Salinity Using User Set Flow